THE UNIVERSITY OF WARWICK

Library Declaration and Deposit Agreement

1. STUDENT DETAILS

Please complete the following:

Full name: ……

University ID number: ……

2. THESIS DEPOSIT

2.1 Under your registration at the University, you are required to deposit your thesis with the University in BOTH hard copy and in digital format. The digital copy should normally be saved as a single pdf file.

2.2 The hard copy will be housed in the University Library. The digital copy will be deposited in the University's Institutional Repository (WRAP). Unless otherwise indicated (see 2.6 below), this will be made immediately openly accessible on the Internet and will be supplied to the British Library to be made available online via its Electronic Theses Online Service (EThOS) service.
[At present, theses submitted for a Master's degree by Research (MA, MSc, LLM, MS or MMedSci) are not being deposited in WRAP and not being made available via EthOS. This may change in future.]

2.3 In exceptional circumstances, the Chair of the Board of Graduate Studies may grant permission for an embargo to be placed on public access to the thesis **in excess of two years**. This must be applied for when submitting the thesis for examination (further information is available in the *Guide to Examinations for Higher Degrees by Research*.)

2.4 If you are depositing a thesis for a Master's degree by Research, the options below only relate to the hard copy thesis.

2.5 If your thesis contains material protected by third party copyright, you should consult with your department, and if appropriate, deposit an abridged hard and/or digital copy thesis.

2.6 Please tick one of the following options for the availability of your thesis (guidance is available in the *Guide to Examinations for Higher Degrees by Research)***:**

☐ Both the hard and digital copy thesis can be made publicly available immediately

☐ The hard copy thesis can be made publicly available immediately and the digital copy thesis can be made publicly available after a period of two years (*should you subsequently wish to reduce the embargo period please inform the Library*)

☐ Both the hard and digital copy thesis can be made publicly available after a period of two years (*should you subsequently wish to reduce the embargo period please inform the Library*)

☐ Both the hard copy and digital copy thesis can be made publicly available after _____ (insert time period in excess of two years). **This option requires the prior approval of the Chair of the Board of Graduate Studies (see 2.3 above)**

The University encourages users of the Library to utilise theses as much as possible, and unless indicated below users will be able to photocopy your thesis.

☐ I **do not** wish for my thesis to be photocopied

3. GRANTING OF NON-EXCLUSIVE RIGHTS

Whether I deposit my Work personally or through an assistant or other agent, I agree to the following:

- Rights granted to the University of Warwick and the British Library and the user of the thesis through this agreement are non-exclusive. I retain all rights in the thesis in its present version or future versions. I agree that the institutional repository administrators and the British Library or their agents may, without changing content, digitise and migrate the thesis to any medium or format for the purpose of future preservation and accessibility.

4. DECLARATIONS

I DECLARE THAT:

- I am the author and owner of the copyright in the thesis and/or I have the authority of the authors and owners of the copyright in the thesis to make this agreement. Reproduction of any part of this thesis for teaching or in academic or other forms of publication is subject to the normal limitations on the use of copyrighted materials and to the proper and full acknowledgement of its source.

- The digital version of the thesis I am supplying is either the same version as the final, hard-bound copy submitted in completion of my degree once any minor corrections have been completed, or is an abridged version (see 2.5 above).

- I have exercised reasonable care to ensure that the thesis is original, and does not to the best of my knowledge break any UK law or other Intellectual Property Right, or contain any confidential material.

- I understand that, through the medium of the Internet, files will be available to automated agents, and may be searched and copied by, for example, text mining and plagiarism detection software.

- At such time that my thesis will be made publically available digitally (see 2.6 above), I grant the University of Warwick and the British Library a licence to make available on the Internet the thesis in digitised format through the Institutional Repository and through the British Library via the EThOS service.

- If my thesis does include any substantial subsidiary material owned by third-party copyright holders, I have sought and obtained permission to include it in any version of my thesis available in digital format and that this permission encompasses the rights that I have granted to the University of Warwick and to the British Library.

5. LEGAL INFRINGEMENTS

I understand that neither the University of Warwick nor the British Library have any obligation to take legal action on behalf of myself, or other rights holders, in the event of infringement of intellectual property rights, breach of contract or of any other right, in the thesis.

Please sign this agreement and ensure it is bound into the final hard bound copy of your thesis, which should be submitted to Student Reception, Senate House.

Student's signature: .....…… Date: .....

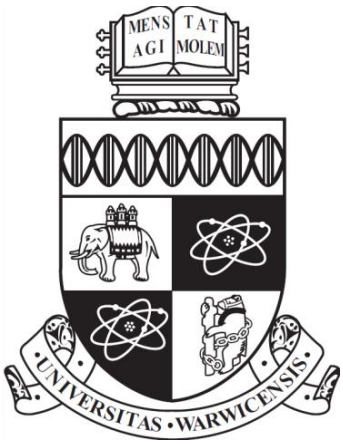

Experimental Characterisation of Jumping and Bobbing Actions for Individuals and Small Groups

Madison Grace McDonald

Thesis Submitted to the University of Warwick

for the degree of Doctor of Philosophy

School of Engineering

University of Warwick

September 2015

Summary

Stadia and structures which host crowd events often experience dynamic crowd loading. Of greatest concern is the loading from the actions of jumping and bobbing, especially if the action is regulated by an external stimulus. Gathered crowds of individuals will often synchronise their actions with one another exacerbating the jumping and bobbing load. Crowd and individual jumping and bobbing models are used to predict the dynamic forces experienced by a structure, however there is a lack of in-situ forces and experimental data from groups. To further the advancement of current crowd and individual models, this thesis provides an in depth study into the actions of jumping and bobbing.

Experiments with eight test subjects (TS) and a range of activity frequencies were first conducted to study the loads generated by individuals. The properties of both actions were characterised and the variation within each TS's ground reaction force (GRF) known as intra-subject variability, and inter-subject variability (between TSs) was quantified. Weight, gender and height affected the jumping GRFs. For jumping a significant portion of the properties were found to have the largest inter-subject variation at a frequency of 2Hz, suggesting high diversity of jumping properties between TSs. Overall there was more inter and intra-subject variation in the activity of bobbing than jumping.

A novel indirect force measurement method was sought to aid the data collection of in-situ individual and group jumping and bobbing GRFs, by monitoring a single point on individual's bodies. It was found that the best monitoring point was the C7th Vertebrae which provided reliable force data for the 1^{st} and 2^{nd} harmonics of jumping and bobbing.

Having verified the single body point methodology for force measurement, group experiments with 2, 4 and 8 TSs were conducted. Metronome, music and visual stimuli were used to dictate the target frequency which ranged between 1.5 and 3.5Hz. A large database comprising of 4,794 individual GRFs was collected. The degree of individual and group synchronisation with the beat and with one another was quantified for the first two harmonics. Group size, stimulus, and stimulus frequency were found to affect synchronisation. Charts detailing the expected levels of synchronisation were produced.

The responses of simulated single degree of freedom (SDOF) systems to the group GRFs were examined and compared to responses from a periodic signal. For resonance responses there is potential for crowd loads to be modelled as a half-sine periodic force. Structural responses from forces measured on rigid surfaces were compared to responses from forces measured on flexible surfaces and found to be larger, especially at resonance. Charts are presented detailing the likely levels of structural resonance response for each stimulus and group size.

Table of Contents

List of Tables

List of Figures

Abbreviations and Notations

Abbreviations	Definition	Abbreviations	Definition
A	Acceleration	IESV	Inter-subject variation
AD	Anderson-Darling	IR	Infra-red
ASD	Auto spectral density	LH1, LH2	Left hip markers labelled 1-2
B1-B6	Back markers labelled 1-6	LLSM	Linear least squares method
BMI	Body mass index	MTVV	Maximum transient vibration value (peak 1s RMS)
C7th	7^{th} Cervical vertebrae	PD	Percentage difference
COM	Centre of mass	PSD	Power spectral density
CoV	Coefficient of variation	RH1, RH2	Right hip markers labelled 1-2
DIC	Digital image correlation	RMS	Root mean squared
DLF	Dynamic load factor	SDOF	Single degree of freedom
EIASV	Inter-intra-subject variation	SEK	Standard error of kurtosis
F.P	Force plate	SES	Standard error of skewness
F1-F7	Front markers labelled 1-7	STD	Standard deviation
f-domain	Force frequency spectra	t-domain	Force time history
GLF	Generated load factors	TS	Test subject
GRF	Ground reaction force	V	Velocity
HSI	Human structure interaction	W	Weight
IASV	Intra-subject variation		

Symbol	Definition	Symbol	Definition
A	Steady state accelerations (ms^{-2})	m	Body mass (kg)
a_{CoM}	CoM acceleration (ms^{-2})	m_f	mass factor
a_i	Acceleration of the $_i{}^{th}$ body segment (ms^{-2})	m_i	mass of the $_i{}^{th}$ body segment (kg)
$a_{Indirect,i}$	Accelerations of the $_i{}^{th}$ marker (ms^{-2})	N	No. of people
C	Coordination factors	n	Harmonic no.
F_{GR}	Dynamic part of the GRF (N)	R^2	Coefficient of determination
$F_{Indirect,i}$	GRF from the $_i{}^{th}$ marker (N)	r_A	Response ratio
F_{direct}	GRF from the forceplate (N)	r_F	Force ratio
$\overline{F_{direct}}$	Average value of direct force (N)	SS_{err}	Residual sum of squares
f_B	Bobbing frequency (Hz)	SS_{tot}	Total sum of squares
f_J	Jumping frequency (Hz)	$T\ or\ T_p$	Period (s)
f_n	Structural natural frequency (Hz)	t	Time (s)
$F_{p,max}$	Peak force (jumping or bobbing)	t_f	Jump flight time (s)
g	acceleration due to gravity (ms^{-2})	t_P	Contact time (s)
k	Structural stiffness (Nm^{-1})	W	TS weight (N)
K_P	Dynamic impact factor $F_{p,max}$/W	α	Contact ratio $\alpha=t_P/T$
M	Structural modal mass (kg)	ζ	Damping ratio (%)

Subscript	Definition	Subscript	Definition
$1st$	1st harmonic	$harmonic$	Relating to a harmonic
$2nd$	2nd harmonic	I	Impulse
$3rd$	3rd harmonic	$indirect$	Relating to the indirect force
B	Relating to bobbing	ith	ith body segment or ith marker
CoM	Centre of Mass	J	Relating to jumping
CoV	Coefficient of variation	n	Harmonic no.
CR,J	Contact ratio of jumping	O	Overall value considering all TSs
D	Displacement	sim	Line of best fit
$direct$	Relating to the indirect force	t	Relating to the t-domain
DLF	DLF	TS	Variable specific to TSs
F	Force	Δ	Difference
f	Relating to the f-domain	μ	Mean
$Peak$	Peak force	σ	STD

Acknowledgements

I would like to express my extreme gratitude to my supervisor Dr Stana Zivanovic for her guidance, patience, and liberal red pen throughout this project. I really appreciate the tireless discussions, suggestions, reading and other help offered during my Ph.D study. I would also like to thank my second supervisor Prof Toby Mottram for his encouragement.

I would like to thank the Engineering and Physical Sciences Research Council (EPSRC) who funded my research. My thanks also to Birmingham Science City and Advantage West Midlands for allowing me use of the Gait lab.

I am grateful for access to the experimental data acquired on the Valladolid Science Museum Bridge in Spain by Dr Zivanovic, Dr Ivan Munoz Diaz of Universidad Politécnica de Madrid, and Dr Antolín Lorenzana of Universidad de Valladolid and his team at Cartif.

Many thanks to Ian Poole who assisted during the synchronisation experiments and those individuals willing to jump and bob for hours at a time. In total 63 different people volunteered for the experiments detailed in this thesis. I am extremely grateful to them all.

Many thanks to my Ph.D friends for advising, listening, commiserating and sometimes just telling me get on with it. I'd also like to thank my friends in the Warwick Canoe Polo and Ultimate Frisbee teams, the Leamington Lemmings and the Ranger girls for their love, friendship and necessary distractions.

I am very grateful to my family, particularly my parents and my sister who have been very supportive and encouraging throughout this period. I would especially like to thank my wonderful husband Andrew Clough for his tireless love and support throughout. His help has been invaluable, whether it be in the form of proof reading tedious chapters, jumping for hours in the lab or a glass of wine, you are a star, thank you.

Declaration

This thesis is submitted to the University of Warwick in support of my application for the degree of Doctor of Philosophy. It has been composed by myself and has not been submitted in any previous application for any degree.

The work presented (including data generated and data analysis) was carried out by the author.

List of data provided by collaborators:

> Access was provided to experimental data acquired on the Valladolid Science Museum Bridge in Spain by Dr Zivanovic, Dr Ivan Munoz Diaz of Universidad Politécnica de Madrid, and Dr Antolín Lorenzana of Universidad de Valladolid and his team at Cartif.

Parts of this thesis have been published by the author:

> MCDONALD, M. G. & ZIVANOVIC, S. 2013. Measuring Dynamic Force of a Jumping Person by Monitoring their Body Kinematics. *RASD 2013.* Pisa: University of Southampton OCS (beta).
>
> ZIVANOVIC, S., MCDONALD, M. G. & DANG, H. V. 2016. Characterising randomness in human actions on civil engineering structures *IMAC 2016.*

1 Introduction

1.1 Research Problem

Crowd activity on structures can lead to large dynamic loads. To ensure safe yet economical design of event space, understanding of individual and crowd actions is required to allow adequate provision of the expected loading. Of special concern is the dynamic load from jumping and bobbing activities, especially when the action is regulated by an external stimulus such as music or a visual cue. The problem is exacerbated if other individuals join in, creating a dynamic group load. Inclusion within a group can further increase the motivation for action, the external stimulus and the dynamic load.

There is a lack of in-situ jumping and bobbing force measurements from individuals and groups which limits the modelling capabilities of the force. Of particular concern is the shortage of group loads, which are limited by data collection difficulties especially outside of a laboratory environment. Conventional direct measurement techniques require a device such as a force plate to measure each individual's ground reaction forces (GRF) (Sim, 2006; Ebrahimpour and Fitts, 1996). However for several individuals equipment constraints make this unfeasible. Indirect methods include measuring the structural response and back calculating the group dynamic load factors (DLFs) (Kasperski and Niemann, 1993; Ellis and Ji, 2002) however quantification of the group synchronisation is often neglected. Other indirect methods using motion capture are capable of accurately measuring the force but are limited to small numbers of individuals by the number of observation points required (Racic et al., 2010). A robust and simple indirect force measurement method is needed to quantity group forces, with the potential to be used in-situ on flexible real event structures.

To advance the understanding and modelling of jumping and bobbing forces, more focus on the action's properties is required. Consideration of the relationships between the properties,

and how they vary between individuals and within an individual's GRF will improve current force models.

Furthermore group interaction has not been studied on real crowds in enough depth, with sufficient thought to the synchronisation of individuals to one another and to a beat. The extrapolation of individual force time histories, or those from pairs forms a significant portion of the basis of current knowledge (Sim, 2006; Parkhouse and Ewins, 2006). Little thought is currently given to the type of stimuli present and the effect on individual and group synchronisation.

1.2 Research Objectives and Thesis Scope

The objectives of this research are outlined below:

- To characterise the relationships and variation in the properties of jumping and bobbing activities. This will increase understanding and facilitate future stochastic force models.
- To develop a novel indirect force measurement method using one monitoring point to enable the GRF measurement of groups whilst jumping and bobbing.
- The quantification of individual and group synchronisation with a beat and one another, for groups of 2, 4 and 8 TSs for different target frequencies and stimuli.
- To investigate the influence of synchronisation in groups on the structural response.

The previous literature and investigations into jumping and bobbing forces of individuals and groups are examined in Chapter 2. The focus of the chapter is factors affecting individual and group synchronisation, such as external cues and crowd environments. Reviews of jumping and bobbing modelling techniques of both individuals and crowds are presented in Chapter 3. Models of varying complexity and focus are examined and compared.

Jumping and bobbing force time histories are studied in Chapter 4. The purpose is to investigate the relationships between different characteristics of jumping and bobbing loads.

In addition the variation between test subjects (TS) known as the inter-subject variation (IESV), and the individual TS variation within their time history, known as the intra-subject variation (IASV) are observed for different properties of jumping and bobbing. This addresses the shortage of IASV knowledge in current literature. The properties which are the focus of the jumping study are frequency, peak force, dynamic load factor (DLF), impulse, contact ratio and displacement. Within the bobbing study the frequency, peak force, DLF and displacement are examined, in addition the variation between different styles of bobbing are studied and characterised (Zivanovic et al., 2016).

To combat the lack of in-situ data, and the shortage of group loads, a novel indirect technique is proposed in Chapter 5 to measure the GRFs from the body kinematics of individuals and groups jumping. This technique is then expanded to the activity of bobbing in Chapter 6. The motion capture method detailed by previous authors (Racic et al., 2010) is adapted to require only one monitoring point per TS. Experiments using both this technique and a conventional force plate are conducted and the results compared. The development of this methodology is partially reported in a conference publication (McDonald and Zivanovic, 2013). The use of the indirect force technique is verified for both jumping and bobbing activities.

Having established a technique which enables the simultaneous force measurements of multiple individuals this technique is utilised in Chapter 7 to measure the GRFs from groups of 2, 4, and 8 TSs. Different activity frequencies are investigated and conveyed using a variety of audial and visual stimuli. A large database of GRFs are collected amounting to 1,275 trials and 4,794 individual GRFs. This is the most extensive database of individual GRFs and group GRFs in response to different stimuli and group sizes. The database addresses the lack of real small and medium sized group loads in response to varied stimuli. To combat the limited knowledge regarding the achievable group and individual synchronisation, the synchronisation of individuals and groups with a beat and each other, for each stimulus is examined and quantified. The response of simulated single degree of freedom (SDOF) systems to the group

GRFs are examined and compared to responses from periodic signals. In addition structural responses from forces measured on a rigid surface are compared to responses from forces measured on a flexible surface. Charts are presented detailing the possible levels of structural resonance response for each stimulus and group size.

The conclusions from this work and recommendations for further work are presented in Chapter 8.

2 Dynamic Crowd Activities

2.1 Introduction

When designing a building, one of the most challenging loads to design against are those induced by humans. Unlike furnishings, utilities and equipment, human occupants have the ability to move around and generate dynamic forces that are up to seven times larger than their body weight (Bachmann and Ammann, 1987). These dynamic loads are a result of a range of movements performed by humans such as: walking, running, rising up from sitting, sitting down from standing, swaying, jumping and bobbing. The review detailed here focuses on the vertical component of jumping and bobbing loads as they are considered the most critical for venue design (Jones et al., 2011).

Psychological and physiological differences between individuals diversify the range of movements and applied forces for any particular human activity. The array and variation of activities can lead to difficulties adequately accounting for the dynamic loading within the design process. Tackling limited understanding of dynamic loads with unnecessarily conservative and uneconomical designs is no longer acceptable in the age of performance-based design and minimised use of natural resources.

One-off activities, such as a single jump, can produce a significant force, and they are introduced in the first part of Section 2.2. The presence of a beat or other stimulus encourages sustained rhythmic activity coordinated to the beat, inducing cyclic loading upon the structure. Rhythmic activities are repetitive and therefore steady state vibrations can arise (Tuan and Saul, 1985; Ebrahimpour and Sack, 1989). The resulting vibrations may increase in magnitude if the dynamic loading matches a natural frequency of the structure, causing resonance. Therefore the most critical cases are rhythmic activities such as jumping and bobbing which are reviewed in the second part of Section 2.2 and Section 2.3, respectively.

To fully understand the dynamic loads generated by jumping and bobbing, the effects of various factors on the loading pattern must be investigated. One of the most important factors is the ability of individuals to synchronise to externally generated cues of different frequencies, and to other individuals. The influences of the crowd environment and various stimuli such as visual, tactile and proximity to others, on coordination, is discussed in Section 2.4. The findings of this review are summarised in Section 2.5.

2.2 Jumping

Jumping, which is characterised as 'Launching one's self in the vertical direction, removing the entire body from contact with the ground' (Jones et al., 2011), is regarded as the most severe load case (Ellis and Ji, 1994; Tuan and Saul, 1985). Due to its high impact nature, the applied dynamic force is often several times larger than the weight of the individual.

Standing vertical jumps are the most common form of jumping seen within a crowd, and they are therefore the focus of this section. There are several variations of standing vertical jumps such as squat, countermotion and rhythmic jumps. When participating in a squat jump, the subject's initial position originates from a squat posture, with knees bent and the body centre of mass (CoM) lowered (Linthorne, 2001). This form of jumping is not regularly seen at public events and it is unlikely to be viewed within typical crowds. A countermotion jump initiates from an upright posture, followed by the bending of the knees, lowering of the body and an upwards launch. It is a common form of single jump. Rhythmic jumping is defined as jumping consecutively to a beat or rhythm for multiple jumping cycles, and is common crowd behaviour. Therefore countermotion and rhythmic jumping will be considered in this study, both the kinematics and kinetics will be analysed.

2.2.1 Single Jump

The most common single vertical standing jump is the countermotion jump. The subject's initial stance is upright, the body is then lowered into a squat position and the leg muscles are

engaged (Linthorne, 2001). The legs are used to push the subject upwards, resulting in loss of contact with the ground.

The dynamic loading from a single countermotion jump results in a peak force that is up to six times larger than the person's weight, and potentially up to seven times for extremely high jumping (Bachmann and Ammann, 1987). A single countermotion jump is an one off activity that generates transient structural vibrations that die out shortly after the initial excitation (Racic, 2009).

The phases of human motion during a countermotion jump and the corresponding force, displacement, velocity and acceleration time histories of the CoM are shown in Figure 2.1. The subject is initially at rest (point **a** in Figure 2.1) and the ground reaction force (GRF) is equal to the weight of the subject (750N in this case). As the subject lowers their body into the countermotion, the downwards acceleration acts as an upward force. The resultant force is less than the body weight. This is known as the unweighting phase (Linthorne, 2001) and it can be observed between points **a** and **c** on Figure 2.1b. The maximum take-off force is witnessed just after the lowest position in the counter-motion (point **d**), as the subject pushes off from the ground in preparation to take off at point **f**. During the flight phase there is no contact between the subject and the ground and therefore the GRF is zero (**f**-**h**). Upon landing (point **h**) the subject generates an impact force which is the largest GRF during the jump. As the subject regains their original position (**h**-**k**), the CoM reaches rest and the GRF is equivalent to the subject's weight once more. A more detailed description of jumping phases is presented in Table 2.1.

A single jump can produce a significant force, but the resulting vibrations are transient and die out relatively quickly. Rhythmic jumping is of more interest in structural engineering and is presented in the next section.

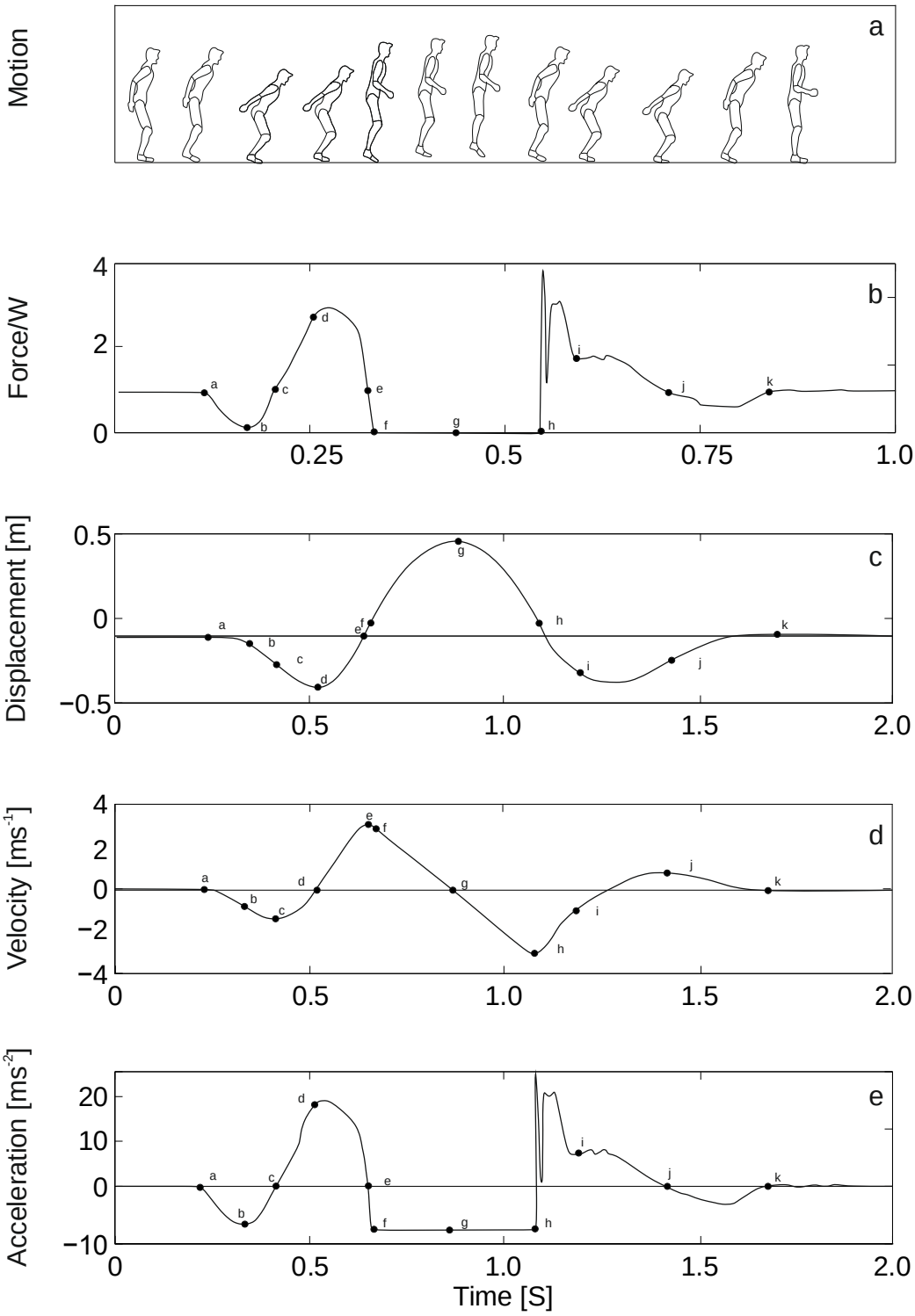

Figure 2.1 Countermotion jumping profile corresponding to a) phases of motion b) force, c) displacement, d) velocity and e) acceleration (adapted from Meghdari and Aryanpour, 2003).

Table 2.1 The description of a countermotion jump, corresponding to Figure 2.1 (after Meghdari and Aryanpour, 2003; Sakka and Yokoi, 2005; Linthorne, 2001; Cross, 1999).

Points Figure 2.1	Jump Phase	Description of jumping GRFs, kinematics and human actions
a	Initial position	The test subject (TS) is at rest, maintaining an upright posture. The CoM is stationary. GRF=Weight (W).
a-b	Unweighting phase (GRF<W), the counter motion before the jump	TS lowers the body CoM and flexes knees and hips. The downwards acceleration acts as an upwards force, GRF < W.
b		Maximum downwards acceleration (A) of CoM as the body moves down.
b-c		COM's downwards acceleration reduces, the resultant force is downwards. The muscles in the legs are increasingly activated.
c		The resultant force on the TS is zero as GRF= W. A=0, the maximum downwards velocity (V) occurs.
c-d	The push off phase, the jumper rises out of the squat	Resultant force and acceleration upwards, displacement is downwards.
d		CoM at lowest position, V=0, jumper at rest, leg muscles strongly activated. GRF close to maximum.
d-e		TS moves upwards, extends knees and hips, upwards velocity. Maximum GRF occurs during push off after squat in countermotion.
e		GRF= W, resultant force=0, A=0, maximum upwards velocity occurs prior to take off.
e-f		GRF < W, resultant force and acceleration downwards.
f	Take off	Instant of take-off, GRF=0, A=-9.81ms^{-2}, CoM is higher at take off than rest as ankle joints are extended.
f-g	Ascent	TS projectile in free flight, CoM moves upwards, A=-9.81ms^{-2}.
g		Peak height of jump, body CoM at rest.
g-h	Descent	Descent, CoM and velocity downwards, A=-9.81ms^{-2}.
h	Landing uncontrolled deceleration	Sharp impact force peak, as the TS lands. CoM higher than initial position as TS lands on toes.
h-i		Large downwards acceleration as the TS is no longer in free flight. Double force peak as the toes hit the ground, the TS's knees bend, then heels hit the ground. The TS's CoM drops below standing height as knees continue to bend.
i	Controlled deceleration	The TS's muscles control the fall, the CoM displacement and velocity is downwards, acceleration is upwards and decreasing, GRF> W.
i-j		Initially the TS's CoM is at the lowest position in the landing squat, the TS is at rest. V=0, GRF is constant, acceleration is upwards. The TS rises out of squat with increasing upwards velocity.
j	Returning to original position	TS rises from squat, maximum upwards velocity, A=0, GRF= W.
j-k		TS's CoM returns through the start position, TS rises on to toes. Velocity is upwards, acceleration is downwards, resulting in GRF< W.
k	Initial position	The TS brings their heels down, CoM returns to original position. The TS is at rest; V=0, A=0, GRF= W.

2.2.2 Rhythmic Jumping

Rhythmic jumping is the process of consecutive jumping that could produce steady state vibrations of the supporting structure, usually leading to a larger vibration response compared to that induced by a single jump (Tuan and Saul, 1985; Ebrahimpour and Sack, 1989).

It is suggested that rhythmic jumping (Figure 2.2a) can be performed at frequencies between 1.2-2.8Hz (Ginty et al., 2001) and it is often aided by a beat. The number of jumping cycles in a second is referred to as the jumping frequency f_j. The reciprocal value of f_j is the jumping period T (Figure 2.2b). Rhythmic jumping most often occurs in the presence of music or at events where crowds are encouraged to participate by moving, clapping or dancing. Music can motivate individuals to jump, and through its audio beat encourages a specific jumping rhythm. Due to this music led rhythmic jumping, dynamic loading at the frequency of the music can arise with potential for large structural vibrations (Parkhouse and Ewins, 2006; Littler, 2002). Sports venues hosting one off concerts are often most vulnerable to this (BBC, 1999; ManchesterEveningNews, 2007).

In design guidelines music was considered the only stimuli likely to cause crowd synchronisation and extreme dynamic loads (BSI, 1996). Recent case studies have shown that synchronised crowd movement can occur without music. For example, remedial work was required due to excessive stand movement caused by synchronised foot stamping in the absence of music at the Liverpool football ground Anfield (Rogers and Thompson, 2000). Vibrations at the CenturyLink Field in Seattle from fans celebrating a touchdown was registered as a magnitude 1-2 earthquake by the Pacific Northwest Seismic Network (BBC, 2013). It is now acknowledged that other stimuli, such as foot stamping and chanting, can prompt synchronised movement and rhythmic jumping (Ginty et al., 2001). In addition, stadium managers and performers often encourage spectator participation by the use of visual cues (Salyards and Hanagan, 2007; Littler, 2002). Furthermore, recent experiments report some group synchronisation without any stimuli (Noormohammadi et al., 2011). Therefore, even venues which do not host events accompanied by music should be aware of the potential for synchronised crowd movement and jumping.

If the crowd's dynamic load matches a natural frequency of the structure resonance can ensue. This can lead to a large acceleration response. Vertical accelerations of 50%g, where g

is the acceleration due to gravity, have been recorded at a football stadium in Germany (Kasperski and Niemann, 1993).

The phases of motion and resulting GRFs and body's CoM displacement, velocity and accelerations from an individual rhythmically jumping at 2Hz are shown in Figure 2.2a-e. The Jumping GRF is normalised by the individual's weight, typical values of normalised GRF are between 2.5* W and 4.5* W (Figure 2.2b). The peak to peak displacement of the CoM ranges between 10cm and 30cm. Peak velocities are generally between 0.8ms^{-1} and 1.70ms^{-1} and accelerations between 15ms^{-2} and 35ms^{-2}.

The ratio of the peak force $F_{p,max}$ and the subject's weight W, is referred to as the dynamic impact factor K_P (Figure 2.2b). Comparing Figure 2.2 with Figure 2.1, it can be noticed that the take-off and landing impulses have merged and the profiles of the GRF and kinematic quantities are smoother. For both a single jump and rhythmic jumping, the mean value of the force time history is equal to the weight of the subject (Tuan and Saul, 1985).

The jumping period T can be divided into the contact time t_P when the TS is in contact with the structure, and flight time t_f (Figure 2.2b). The proportion of contact time to jump duration is called the contact ratio $\alpha = t_P/T$.

As well as characterising rhythmic jumping within the time domain, the frequency domain representation also can be used. The force spectrum in Figure 2.2f shows energy leaks around the main harmonics, signifying that jumping is a narrow band random process (Brownjohn et al., 2004; Racic, 2009). The main forcing harmonics are composed of a phase amplitude which is normalised by the subject's weight and known as the dynamic load factors (DLFs) r_n, and a phase lag ϕ_r.

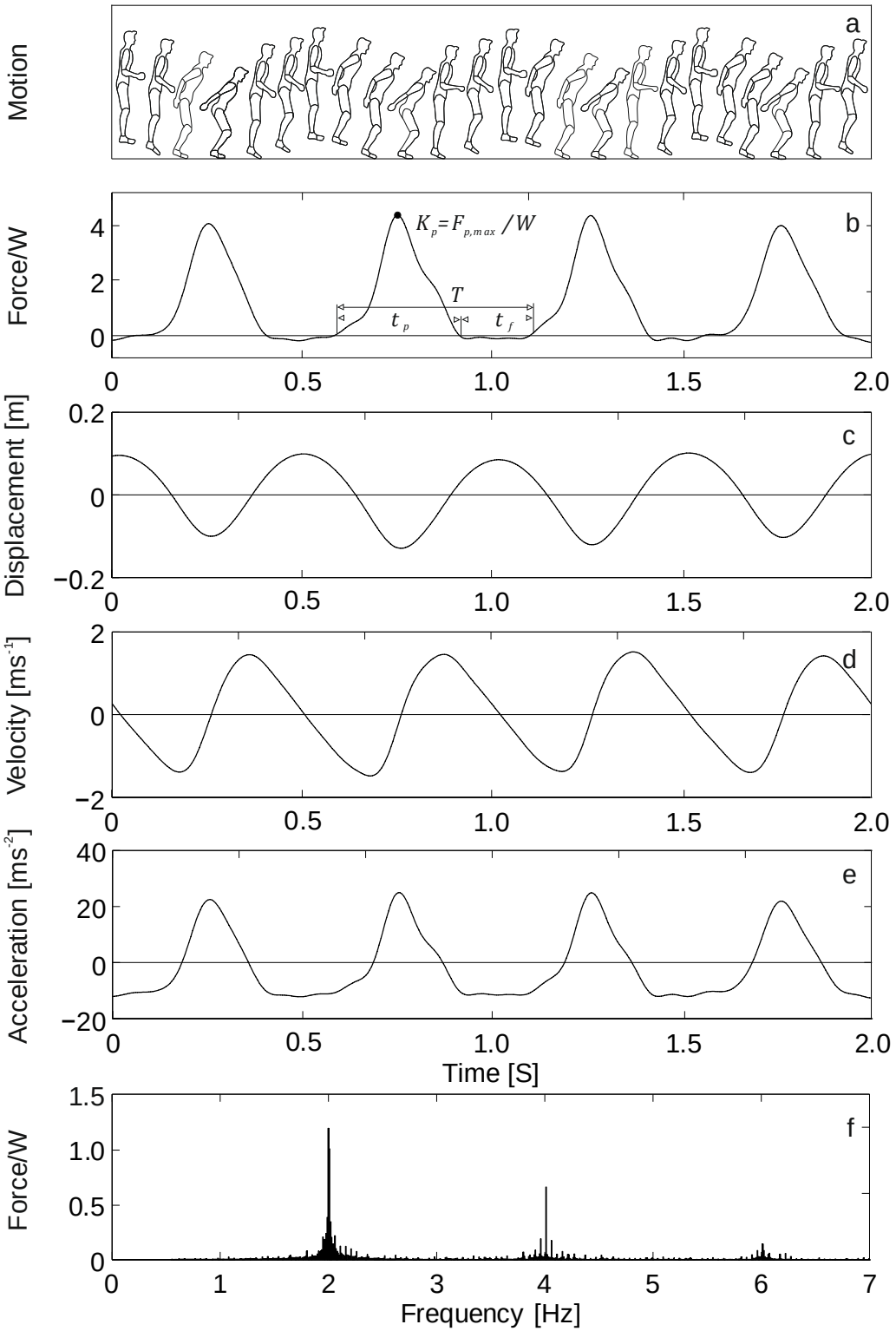

Figure 2.2 a) Phases of jumping motion b) normalised force, c) displacement, d) velocity and e) acceleration of the CoM for rhythmic jumping, f) normalised force spectrum.

Figure 2.3 shows that DLFs have typical values of between 1.2-1.8 for the 1st harmonic, for the frequency range of 1.2Hz to 4Hz (Pernica, 1990; Rainer et al., 1988). The maximum DLFs are for the 1st harmonic, and are typically around 1.75 and occur for jumping frequencies between 2 and 3Hz (Rainer et al., 1988). The range of values of DLF for the 1st harmonic are marked by the error bars (Pernica, 1990) on Figure 2.3. The range in DLF values is narrowest at mid-jumping frequencies (2-3Hz). The DLFs decrease at higher harmonics, with the maximum values occurring at frequencies corresponding to multiples of the maximum 1st harmonic DLFs.

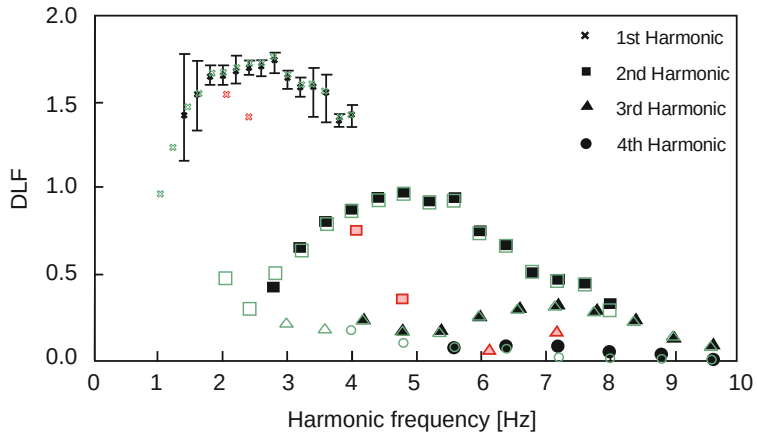

Figure 2.3 The DLFs for the first four harmonics established from experimental work, for a range of jumping frequencies. The solid black markers are data from Pernica (1990), where the smallest and largest DLFs are noted by the accompanying error bars. The hollow markers are from Rainer et al. (1988) and solid grey from Ellis and Ji (1994) and Ji and Ellis (1994).

The contribution of the 1st and 2nd harmonic to a jumping signal is shown in Figure 2.4. The number of harmonic components required to reproduce the jumping time history increases with decreasing contact ratio, though 3-6 components are generally sufficient (Ji and Ellis, 1994). However, this does not necessarily equate to a reliable frequency spectrum as non-dominant spectral components, which have the potential to cause resonance, can be overlooked.

The shape of the jumping force profile is frequency dependant, and potentially asymmetric, as demonstrated by the waveforms of the normalised dynamic load in Figure 2.5. Low frequency jumping (1Hz) has a similar force profile and action to countermotion jumping. Due to the slow nature, each jump is a separate action and the subject is briefly at rest in between jumps. This

causes two distinct landing and launching peaks, and a 'stationary interval' where the jumper pauses between the motions (Nhleko et al., 2008; Sim et al., 2005). The force spectrum is dominated by the 2nd forcing harmonic due to the two force peaks when jumping slowly (Yao et al., 2006). This is demonstrated in Figure 2.6 where 2Hz is the dominant harmonic for jumping at 1Hz.

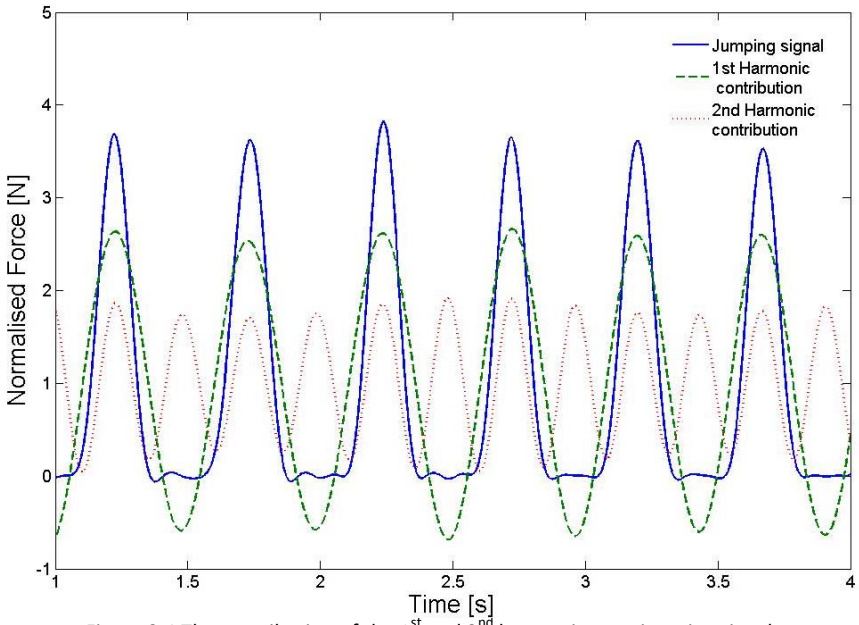

Figure 2.4 The contribution of the 1st and 2nd harmonics to a jumping signal.

When jumping at higher frequencies (i.e. at or above 2Hz) the motion becomes quicker. The subject lands on their toes, and without pause or heel contact with the ground, re-launches into the next jump. Increasing the frequency encourages the two impulse peaks to merge into one peak, hence the 1st harmonic dominates the spectrum (Figure 2.6). Observing Figure 2.5 for jumping at 1.5Hz, the peaks are shifted closer and the dominance is split between the 1st and 2nd harmonic for different subjects (Figure 2.6). Potentially the split in dominance occurs as the target frequency is between the two distinct jumping patterns and subjects may favour either of the jumping actions. This is consistent with the difficulty often expressed by subjects when jumping at mid frequencies, such as 1.5Hz (Yao et al., 2006).

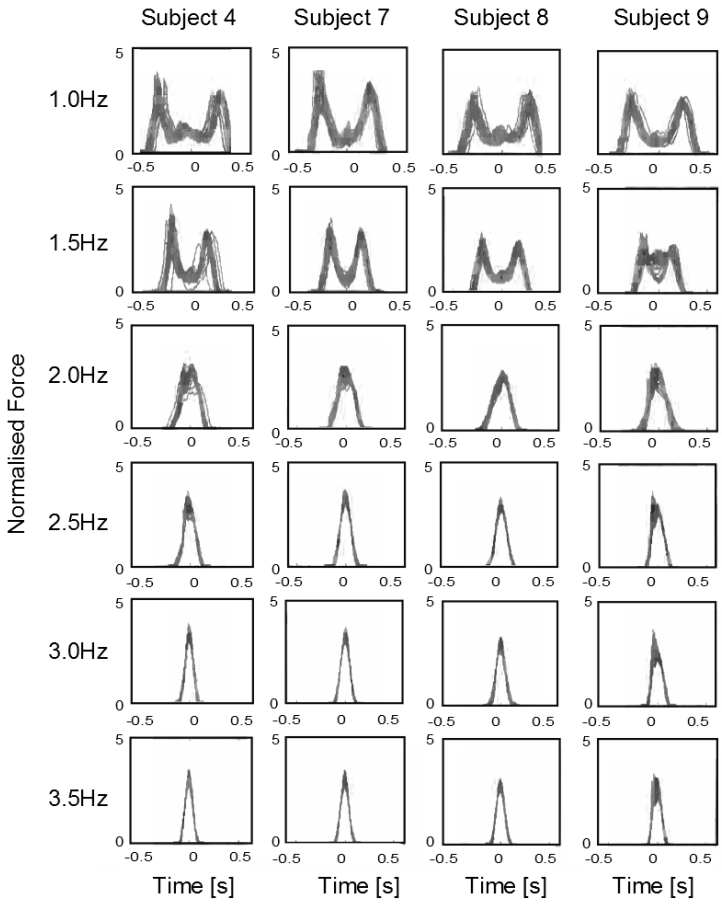

Figure 2.5 Variation in jumping profiles, at six different frequencies by four individuals (after Sim et al., 2005).

Comparison between the subjects' force profiles (inter-subject variability) in Figure 2.5 shows that the waveforms follow a similar trend. However there were more differences between the force profiles at lower frequencies than high frequencies. Inter-subject variation is smaller for rhythmic jumping than for single jumping. It has been demonstrated that the introduction of a beat reduces the variability in DLFs. A beat, to some extent, dictates the contact time, resulting in more uniform jumping amongst individuals (Parkhouse and Ewins, 2004).

Figure 2.5 also demonstrates the intra-subject variation in the jumping cycles by overlaying individual cycles from the time history. Intra-subject variation causes the frequency (and period) to change on a jump-by-jump basis. Less variation suggests that the subject can repeat the action more consistently. It appears the force patterns become more consistent at higher jumping frequencies (Figure 2.5).

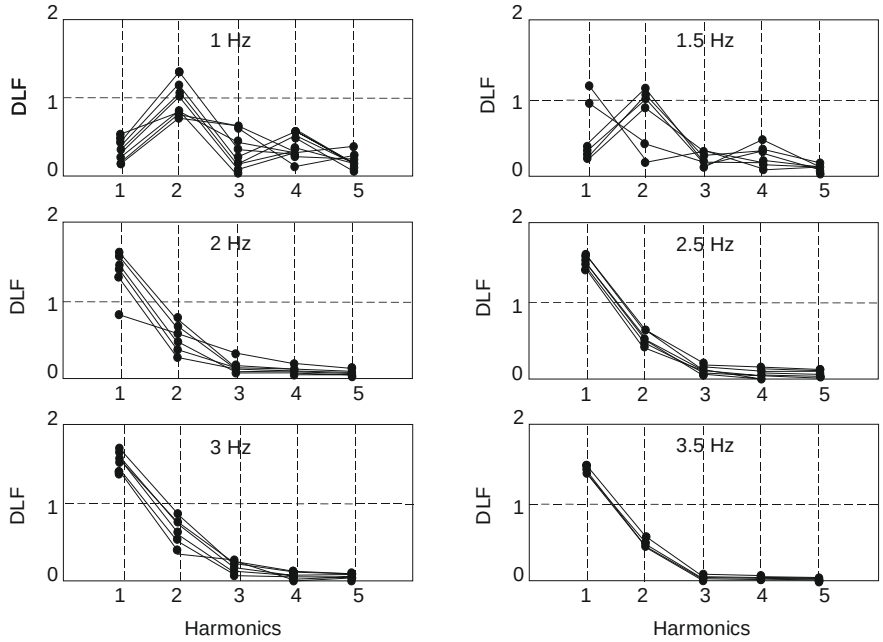

Figure 2.6 The average DLF values for 4-10 subjects corresponding to the jumping profiles shown in Figure 2.5 (after Sim et al., 2005).

2.3 Bobbing

Bobbing is defined as "attempting to jump whilst the feet maintain contact with the ground" (Jones et al., 2011). It is more common at events than jumping as it requires less energy to be maintained (Racic et al., 2013; Dougill et al., 2006). A single bob is rare and the expected impact force is small only 1.5 to 3 times the subject's weight (Yao, 2004), less than expected from a single jump. Hence only rhythmic bobbing will be introduced in this section.

An example of bobbing motion at 2Hz and the corresponding GRFs and CoM kinematic profiles are shown in Figure 2.7a-e. Figure 2.7f shows the spectrum of the force, which, similar to jumping, demonstrates that bobbing is a narrow band activity (Racic, 2009).

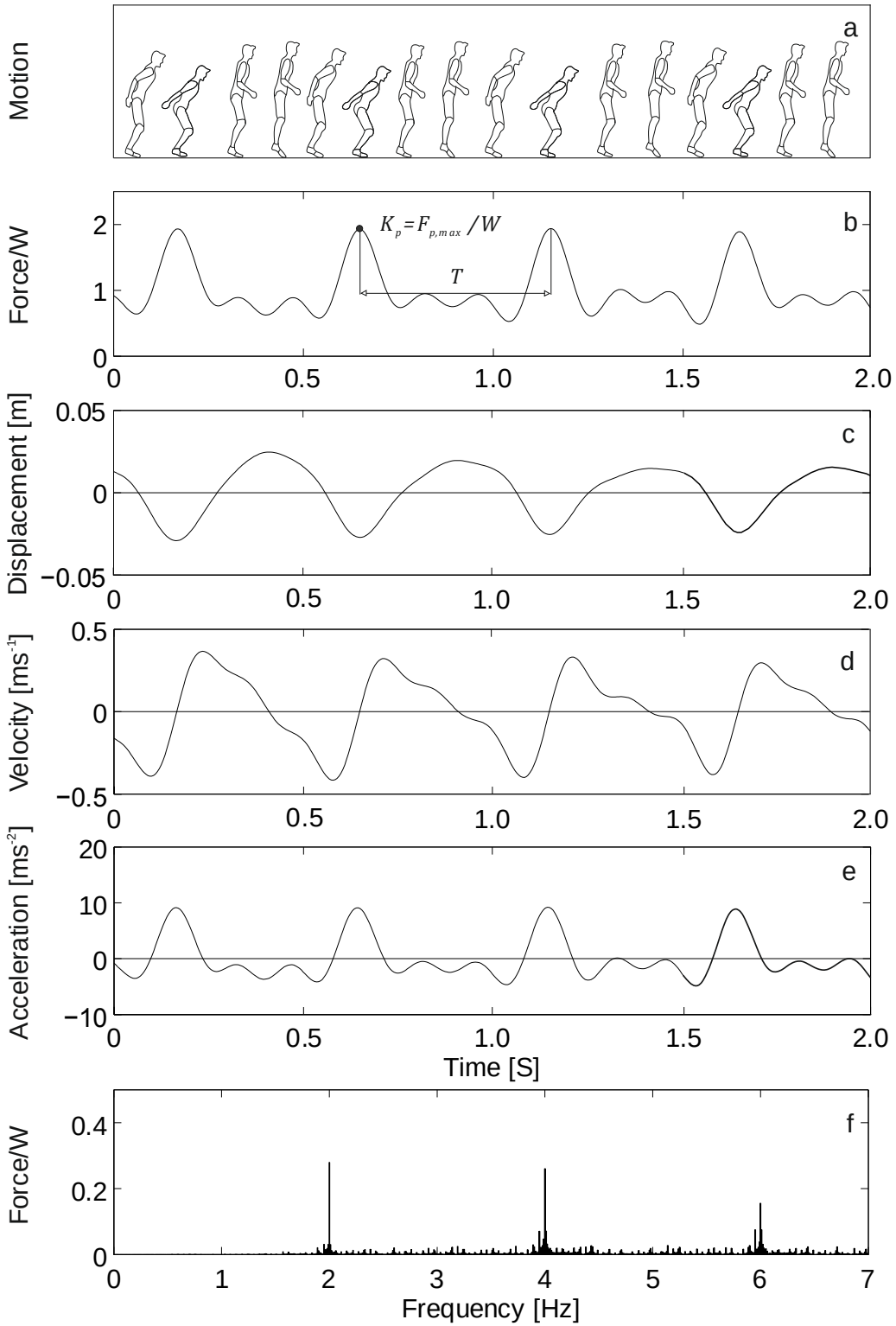

Figure 2.7 a) Phases of bobbing motion b) normalised force, c) displacement, d) velocity and e) acceleration of the CoM for rhythmic bobbing, f) normalised force spectrum.

A typical bobbing force is presented in Figure 2.7b. Compared to rhythmic jumping, bobbing is characterised by smaller peak forces $F_{p,max}$. In Figure 2.7b the bobbing peak force is approximately 2*W, half that of the jumping example (Figure 2.2b). The GRF never drops to zero during bobbing, as contact with the structure is continuously maintained. The shape of the bobbing GRF is more irregular as the action is more complex than jumping, involving the raising and lowering of the CoM, whilst maintaining contact with the floor. The mean value of the force time history, as with jumping, is equal to the weight of the subject (Tuan and Saul, 1985). The CoM displacements, velocities and accelerations are reduced compared to jumping. A peak to peak displacement of approximately 5cm is seen in Figure 2.7c, compared to approximately 20cm whilst jumping (Figure 2.2c). Likewise the peak velocity and accelerations in Figure 2.7d and e are approximately 0.4ms^{-1} and 10ms^{-2} compared to approximately 2ms^{-1} and 30ms^{-2} in Figure 2.2d and e. These diminished values are due to the continuous contact with the floor, which restricts the height of the movement, and reduces the launching and landing forces as overcoming gravity is unnecessary.

While a bobbing individual generates on average smaller forces than a jumping individual, a larger activity frequency range is possible. Bobbing frequencies as high as 6Hz are achievable, whilst the upper limit on comfortable bobbing is stated to be 4.5-5Hz (Yao et al., 2004). Therefore the harmonics of bobbing have the potential to excite resonance in a wider range of structures than jumping. In addition, continuous contact with the structure during bobbing allows the active person to feel the structural movement, and adjust their actions to match it. This feedback effect may increase the likelihood of resonance (Yao et al., 2004).

Distinctions are often made between two different styles of bobbing known as bouncing and jouncing. Heel contact is maintained with the ground when bouncing, resulting in a more controlled motion. The majority of the movement is from the subject bending their knees (Sim et al., 2005). The more energetic alternative is referred to as jouncing, where the subject rises to their toes, breaking contact between their heels and the floor (Jones et al., 2011). It is

thought that the action of jouncing is more complex than bouncing. It is suggested that multiple muscles and joints, in addition to the knees, are required for body balance whilst the subject rises on to their toes.

Examples of GRFs of different styles of bobbing are shown in Figure 2.8, where subjects seven and ten bounced while the other four jounced. Similarly to jumping, the shapes of the force profiles for bobbing are frequency dependant. At lower frequencies the force profiles of the bouncing subjects favour two peaks, merging into one peak at frequencies of 3Hz and above. At lower frequencies the jouncing subjects exhibit 2-3 peaks in their force profile, before merging into one peak at higher frequencies. Sim et al. (2005) reported that for slow bobbing, i.e. 1-1.5Hz, the force spectra were not dominated by a specific harmonic (Figure 2.9). At higher rates of bobbing (3-3.5Hz) the 1st harmonic was dominant (Figure 2.9), while at 2 and 2.5Hz both cases were possible, depending on the subject. Interestingly, this phenomenon was not noted by Yao et al. (2004) during their bouncing experiments over 1-3.5Hz, where the 1st harmonic reportedly dominated the response. Yao et al's experiments took place upon a flexible structure, rather than rigid ground, which may explain the discrepancies with Sim et al's work. This observation highlights the importance of characterising bobbing (and in general, jumping) on surfaces of different flexibility.

As in the case of jumping, Figure 2.8 demonstrates that the inter- and intra-subject variabilities are reduced at higher bobbing frequencies. Due to different bobbing styles the inter-subject variation in the GRF profiles and the DLFs are greater than for jumping (Sim et al., 2005). The range of possible bobbing DLFs are between 0 and 1 (Figure 2.9). As a consequence of the subject variability and the continuous contact with the floor, the lower bobbing DLF limit can approach zero. In theory to avoid lifting off from the ground, an upper DLF limit of one exists (Parkhouse and Ewins, 2004). In reality, however, enthusiastic bobbing can produce values slightly higher than one as demonstrated in Figure 2.9.

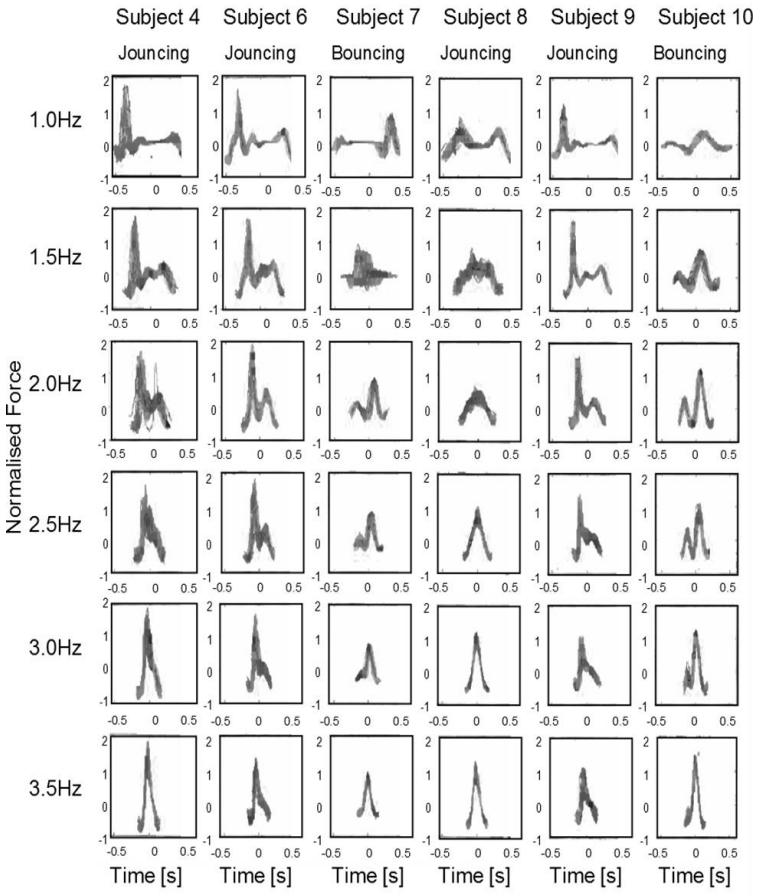

Figure 2.8 Variation in bobbing force profiles, between different frequencies and individuals. Subjects 7 and 10 bounced, the remaining subjects jounced (after Sim et al., 2005).

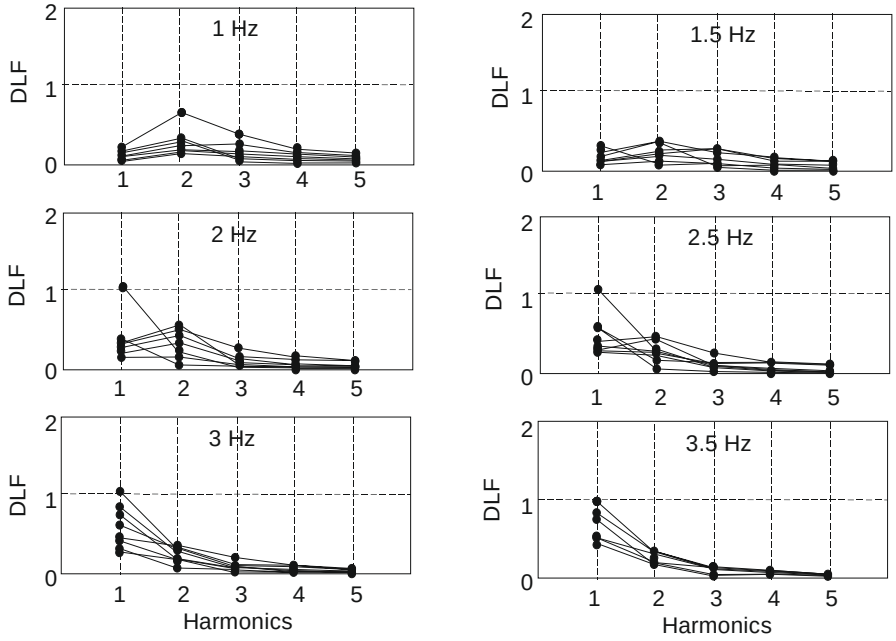

Figure 2.9 DLFs for the first five harmonics of bobbing subjects (after Sim et al., 2005).

2.4 Synchronisation

At events where large groups of people assemble, it is common for their movements and actions to become coordinated with one another. This occurrence is exacerbated in the presence of a beat (especially music), which can act as a catalyst to synchronised jumping, bobbing and dancing. In this section, the ability of bobbing or jumping individuals to synchronise to external stimuli will be examined. Then the ability of individuals to synchronise within a group will be considered.

2.4.1 Synchronisation with External Stimuli

Knowledge of individuals' coordination potential with an external cue is required for performing numerical simulations of human loading, necessary for reliable structural designs. The external cues considered in this section include aural, visual and tactile stimuli as well as the presence of another individual.

2.4.1.1 Aural Stimuli

Aural cues are the most common form of stimuli that individuals might encounter. The stimulus can be in the form of a metronome beat, music, or crowd initiated beats such as chanting, stamping and clapping (Rogers and Thompson, 2000; Parkhouse and Ewins, 2006).

The synchronisation of subjects with a metronome beat at frequencies of 1.50, 2.00, 2.67 and 3.50 Hz, was investigated for 40 participants jumping and bobbing individually on a force plate (Parkhouse and Ewins, 2004). The standard deviation (STD) of the phase lag between each jump or bob, and the beat, has been used to characterise the synchronisation with the beat. A subject having a STD of above 60° was deemed unsynchronised with the beat. The criterion was chosen as some jumping cycles would be separated by 180°. These cycles would therefore be out of phase with one another and cancel each other out (Parkhouse and Ewins, 2004). A phase angle STD of 60° corresponds to a time lag of 16.6% of the period. For jumping at 2.0Hz this is 0.083s.

The results are shown in Figure 2.10, the highest number of synchronised jumping individuals were recorded for 2.00Hz, where 33 out of 40 subjects had a STD below 60˚. The second highest was 28 synchronised individuals jumping at 2.67Hz. For bobbing the highest number of subjects synchronised with the beat were at frequencies of 1.50, 2.00 and 2.67Hz (35, 36 and 29 individuals respectively). The greatest number of unsynchronised subjects was apparent for activity at 3.50Hz for both jumping and bobbing. In general, better synchronisation was achieved whilst bobbing.

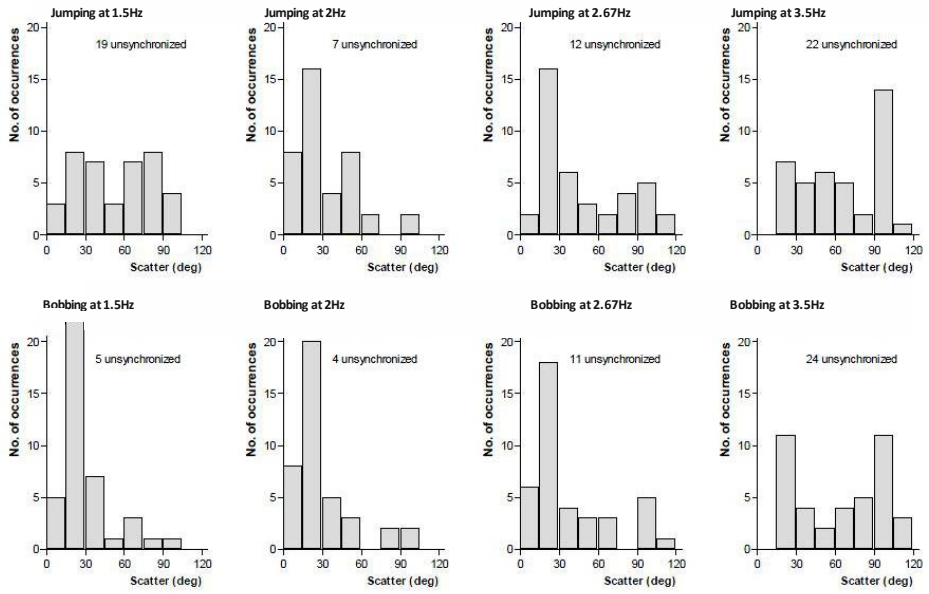

Figure 2.10 The ability of individuals to synchronise with a beat using the phase angle STD as a measure of synchronisation. The numbers of unsynchronised subjects are stated for each frequency (after Parkhouse and Ewins, 2004).

In similar work, the capabilities of ten individuals to jump and bob to a metronome beat over the frequency range of 1.0-3.5Hz were experimentally examined (Sim et al., 2005). Synchronisation was characterised by the jump deficit, i.e. the disparity between the number of jumps/bobs and number of beats. A large jump deficit was associated with unsynchronised activity. Table 2.2 shows that on average 65% of the test subjects were able to synchronise with the beat whilst jumping and 80% when bobbing. Four test subjects consistently achieved a jump deficit of zero whilst jumping, compared to six subjects when bobbing. This reveals that test subjects found it easier to control bobbing activity and synchronise it to a specific beat.

The force profiles of the test subjects able to consistently synchronise with the beat can be seen in Figure 2.5 for jumping and Figure 2.8 for bobbing.

Table 2.2 The number of synchronised TSs (jumping defict=zero) at each activity frequency (after Sim et al., 2005).

	Jumping frequency (Hz)							Bobbing frequency (Hz)						
	1	1.5	2	2.5	3	3.5	Ave	1	1.5	2	2.5	3	3.5	Ave
Synchronised TSs	9	6	7	6	7	4	6.5	10	8	8	8	8	6	8

The results of Sim et al's work suggest that the majority of people can synchronise their actions with a beat at certain frequencies. Synchronisation occurs within the range of 1.0-3.0Hz for jumping, and 1.0-3.5Hz for bobbing. The frequency of 1.0Hz was the easiest to synchronise with, while the frequency of 3.5Hz was the most difficult. The latter conclusion agrees with findings by Parkhouse and Ewins (2004). The difficulty in synchronising at 3.5Hz is probably caused by lack of control when performing an activity at such a fast speed.

Due to the larger sample size of 40, Parkhouse and Ewins's work is likely to be a better reflection on the abilities of the population in general. However Parkhouse and Ewins (2004) did not conduct experiments at frequencies below 1.50Hz, nor at 3.00Hz, preventing comparison with Sim et al's conclusions at these frequencies.

Both studies suggest that coordination with a beat is easier to maintain when bobbing than when jumping (Parkhouse and Ewins, 2004; Sim et al., 2005). A possible explanation is the continuous contact with the ground whilst bobbing allows the subjects to control their movements better, therefore matching the beat more consistently. As mentioned in the previous section, in Figure 2.8 subjects seven and ten 'bounced' whilst the remaining subjects 'jounced'. The bouncing subjects synchronised with the beat throughout each test frequency. Therefore, synchronisation with a beat is potentially easier when bouncing than jouncing, although further experiments are required before a firm conclusion can be drawn.

To investigate the frequency ranges of aural stimuli likely to be present at music events, the beat frequency of a selection of pop songs from the 1960s to the 1990s were analysed (Ginty

et al., 2001). As presented in Table 2.3 an increase of 0.12Hz was observed in the average song beat between each decade. If the trend of increasing music frequency continued to the present time, the average tempo of current pop songs would be 2.31Hz. High frequency songs are likely to continue becoming more relevant in the future.

Table 2.3 Average music beat frequency of pop songs over each decade (after Ginty et al., 2001).

Decade	**1960s**	**1970s**	**1980s**	**1990s**
Frequency (Hz)	1.72	1.84	1.96	2.07

Of the songs investigated 96% have a frequency between 1.0 and 2.8Hz, deeming this the common frequency range. A small number of songs (2.9%) had a beat greater than 2.8Hz and 83% of these high-frequency songs were composed in the 90s. This again highlights the increased prominence and relevance of high frequency songs in recent times. Of the songs investigated 3.3% were slower than 1Hz, these low frequency songs are unlikely to stimulate people to jump (Ginty et al., 2001).

The selection of songs were used to investigate the ability of individuals to jump to a beat (Ginty et al., 2001). Two individuals jumped together to different samples of music in the range of 0.6-3.1Hz. To characterise an individual's synchronisation with the beat, the coordination between both individuals whilst jumping was observed. The ease of synchronisation between the individuals was quantified, where 1 was denoted as easy to synchronise, 2 moderately easy, 3 difficult and 4 very difficult (Table 2.4). Unfortunately the method used for this classification was not described and therefore cannot be evaluated.

It was proposed that an individual jumping independently could coordinate to a greater range of frequencies than two individuals jumping together (Ginty et al., 2001). This was reasoned as synchronisation was only required with the beat and not the other person's actions. Therefore it was suggested that individual beat synchronisation was possible for synchronisation scores greater or equal to 3. A frequency range of 1.2-2.8Hz (Table 2.4) was identified as potentially dangerous for individuals rhythmically jumping (Ginty et al., 2001). This assumption that

frequencies with a score of 3 facilitate coordinated activity is questionable. Furthermore the applicability of these findings to a wider population is limited as only two test subjects were used.

Table 2.4 Ease of synchronisation between two individuals (1 easy, 2 moderate, 3 difficult, and 4 very difficult) (after Ginty et al., 2001).

Freq (Hz)	**0.6**	**0.8**	**1.0**	**1.1**	**1.2**	**1.3**	**1.4**	**1.5**	**1.6**	**1.7**	**1.8**	**1.9**	**2.0**	**2.1**	**2.2**	**2.3**	**2.4**	**2.5**	**2.6**	**2.7**	**2.8**	**3.0**	**3.1**
Score	4	4	4	4	3	3	3	2	2	2	1	1	1	1	1	1	2	2	3	3	3	4	4

There are discrepancies between Ginty et al's work and the findings of Sim et al. (2005), where a high degree of synchronisation was observed at 1Hz and 3Hz. The likelihood of crowds jumping at low frequencies downgrades the concern of the high synchronisation potential at 1Hz. However, the conclusion that synchronisation is not possible at 3Hz (synchronisation score of 4) directly contradicts the good synchronisation seen from 70% of Sim et al.'s test subjects. In addition, the trend of increasing song frequency suggests that high frequency songs will become more popular. Therefore, the proposed jumping synchronisation range is too low.

The discrepancies between authors may also originate from the difference in stimulus. The results from individuals (Sim et al., 2005) and two test subjects (Ginty et al., 2001) may not be comparible, as the presence of another person may have acted as an additional stimulus. Within the two test subject experiments no consideration was given to the effect of the other person, and no one test subject trials were conducted to quantify this effect.

A further difference in the stimuli between the two experiments is the use of music (Ginty et al., 2001) instead of a metronome beat (Sim et al., 2005). As music is not purely a beat like a metronome, individuals may struggle to detect the beat, or may jump at a comfortable harmonic of the beat (Littler, 2003). As music is a more common stimulus at events, further research into the synchronisation due to music is required.

2.4.1.2 Other Stimuli

In addition to aural beats, visual and tactile stimuli can influence an individual's ability to jump or bob consistently. Furthermore, as mentioned in the previous section the presence of another person may act as an additional stimulus. The effect of these stimuli on synchronisation with a beat will be examined in the following section.

To investigate an individual's ability to synchronise with a visual stimulus, experiments were conducted using an image in simple harmonic motion (Parkhouse and Ewins, 2006). Within the experiments 30 people jumped and bobbed individually upon a force plate. The aim was to investigate the ability of individuals to synchronise their action's with the movement of the image. A subject having a phase angle STD equal or greater than 60° was deemed unsynchronised, while subjects were considered synchronised if their STD was less than 60˚. A comparison with similar experiments using an audio metronome showed that individuals were less synchronised when reacting to purely visual cues. An exception was seen at 1.5Hz.

In comparison other experiments found that people were more synchronised when jumping in a pair, indicating visual cues in the form of another person may be significant (Ebrahimpour and Fitts, 1996). Experiments were conducted using a metronome and pairs of individuals in different orientations on two force plates. The synchronisation was characterised as the time lag between the peak forces of the active pair. Better synchronisation was observed in pairs when jumping facing one another than back to back. The minimum phase angles, indicating the best synchronisation, occurred when subjects could both see and hear one another, the angles were smallest at 2Hz. When the subjects were exposed to only aural cues, the synchronisation between the individuals decreased with increasing tempo.

This research was expanded to explore how jumping and bobbing in pairs was influenced by aural, visual and tactile stimuli, as well as the absence of stimuli (Noormohammadi et al., 2011). A sample population of two pairs were used. Pair 1 contained individuals a and b, and

pair 2 individuals c and d. Nominally the same experiments were conducted with each pair. Each individual within the pair performed jumping and bobbing on a separate force plate. A metronome beat, a flashing LED light box, and a solenoid actuator providing a shock to the thumb, were used as the aural, visual and tactile stimuli, respectively. Although these stimuli are unrepresentative of real events, the results can be used as an indication of the effect.

The coordination between the individuals and the beat was characterised by a synchronisation factor. The synchronisation factor was defined as the ratio of the power of the force component coordinated with the beat $P_{Synchronised,}$ and the power of the entire signal P_{Total} (Parkhouse and Ewins, 2006); where P_{Total} was calculated as the area under the power spectral density (PSD) curve around the relevant harmonic, with a frequency bandwidth equal to the target frequency. The $P_{Synchronised}$ component corresponds to the area of the PSD at the activity frequency, as demonstrated in Figure 2.11. In addition to the synchronisation between the individuals and the beat, the synchronisation between the two individuals was investigated. For the purpose of this review, the synchronisation between the individuals within the pairs has been characterised by the absolute difference in phase angle between them $|\Delta\varphi|$.

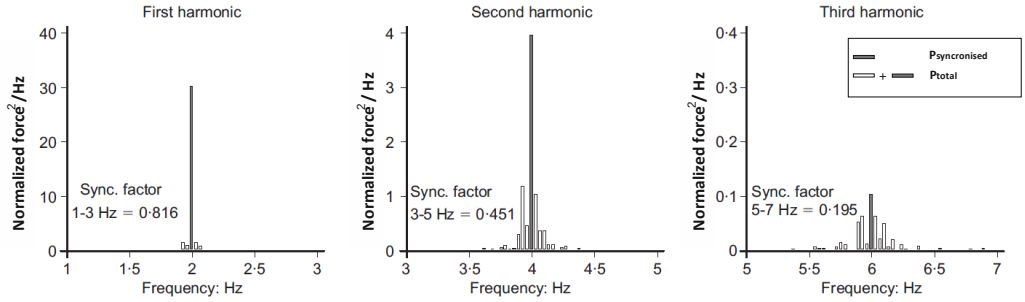

Figure 2.11 The calculation of synchronisation factor for the first three harmonics (after Parkhouse and Ewins, 2006).

The results from jumping at 2Hz are shown in Table 2.5. An average synchronisation factor of 0.942 was seen at the 1st harmonic due to the aural stimulus. It was deemed the most effective cue for individuals synchronising with a beat. The best synchronisation between the pairs occurred when cued by the visual stimulus, differences in phase angle of 0.2° and 6.1° were

seen for pair 1 and pair 2. Likewise the differences in phase angles were small when the pairs coordinate their actions by watching one another, without an external cue. These trials indicate that visual cues have the potential to be as significant as aural stimuli. Some degree of synchronisation was seen for each type of stimulus, however the worst synchronisation occurred when using a purely tactile cue.

Table 2.5 Pair and individual syncronisation when jumping at 2Hz (adapted from Noormohammadi et al., 2011).

Stimulus	Pair	1st Harmonic		2nd Harmonic	
		Phase (˚)	Sync factor	Phase (˚)	Sync factor
	1a	18.5	0.922	-147.0	0.793
	1b	8.3	0.950	-171.6	0.916
	|Δϕ|	10.2		24.6	
Aural	2c	5.5	0.935	173.8	0.797
	2d	17.6	0.962	-151.2	0.871
	|Δϕ|	12.1		35	
	Ave sync factor		0.942		0.844
	1a	21.9	0.767	-144.8	0.36
	1b	106.1	0.308	-176.0	0.237
	|Δϕ|	84.2		31.2	
Tactile	2c	-41.9	0.387	147.4	0.263
	2d	-45.6	0.579	55.6	0.257
	|Δϕ|	3.7		91.8	
	Ave sync factor		0.510		0.279
	1a	-89.6	0.599	119.5	0.225
	1b	-89.4	0.617	90.6	0.301
	|Δϕ|	0.2		28.9	
Visual	2c	-86.5	0.681	119.0	0.237
	2d	-80.4	0.730	12.3	0.337
	|Δϕ|	6.1		106.7	
	Ave sync factor		0.657		0.275
	1a	-44.7	0.831	83.0	0.526
	1b	-41.2	0.876	88.7	0.592
	|Δϕ|	3.5		5.7	
None	2c	-68.4	0.767	161.9	0.299
	2d	-75.6	0.707	162.5	0.316
	|Δϕ|	7.2		0.6	
	Ave sync factor		0.795		0.433

The difference in the phase angle between the pairs varied considerably for different trials (Table 2.5). When using the tactile stimulus pair 1 exhibited a phase angle difference of 84.2°, whereas pair 2 achieved a difference of 3.7°. The large variation in the results highlights the presence of inter-pair variability, and the need for a larger sample size.

Smaller synchronisation factors at the 2nd harmonic were seen for the majority of trials (Table 2.5). The best 2nd harmonic synchronisation occurred when using an aural stimulus (average

synchronisation factor 0.844). The smallest differences in phase angle at the 2nd harmonic (5.7˚ and 0.6˚) indicating good synchronisation between test subjects occurred when jumping without an external stimulus. Pair 2's individual synchronisation factors were small, 0.299 and 0.316, without an external stimulus. Therefore the individuals were not jumping at a consistent frequency, just consistently with one another, suggesting group synchronisation is more dominant than beat synchronisation.

Further experiments that were more representative of real situations were conducted by Racic et al. (2013). Bobbing subjects were encouraged to interact together providing a rhythmic stimulus. Aural, visual and tactile cues, and the effect of subject proximity on coordination was investigated. The synchronisation factor β was quantified by summing the time lags Δ_i of n cycles between the subjects on a cycle-by-cycle basis:

$$\boldsymbol{\beta} = \frac{\sum_{i=1}^{n}|\Delta_i|}{\boldsymbol{nT}} = \frac{\boldsymbol{f}}{\boldsymbol{n}}\sum_{i=1}^{n}|\Delta_i| \qquad 2.1$$

Values of β closest to zero indicate the best synchronisation. Figure 2.12 shows that individuals were most in-sync when all the stimuli were included (i.e. bobbing to the metronome beat, whilst facing each other and holding hands). Furthermore the poorest synchronisation was observed when subjects stood back to back, not touching, with only the metronome to guide them. It was also noted that when individuals were sideways on to one another the synchronisation increased with proximity. The effect of proximity reduced when individuals were facing one another, as the additional visual cues compensated for the distance between them. The best synchronisation was seen between the subjects at the highest bobbing frequencies investigated 2.0Hz and 2.7Hz.

It can be concluded from this section that aural, visual and tactile cues, as well as the presence of other people, affect the degree of synchronisation. An aural beat is considered to have the greatest effect on synchronisation, followed by visual and then tactile stimuli. It is therefore necessary, when designing against human induced rhythmic loading, to consider the increased

coordination due to these stimuli. The variation in the results between different authors highlights the need for more experimental tests, allowing the full extent of the synchronisation potential in different circumstances to be understood.

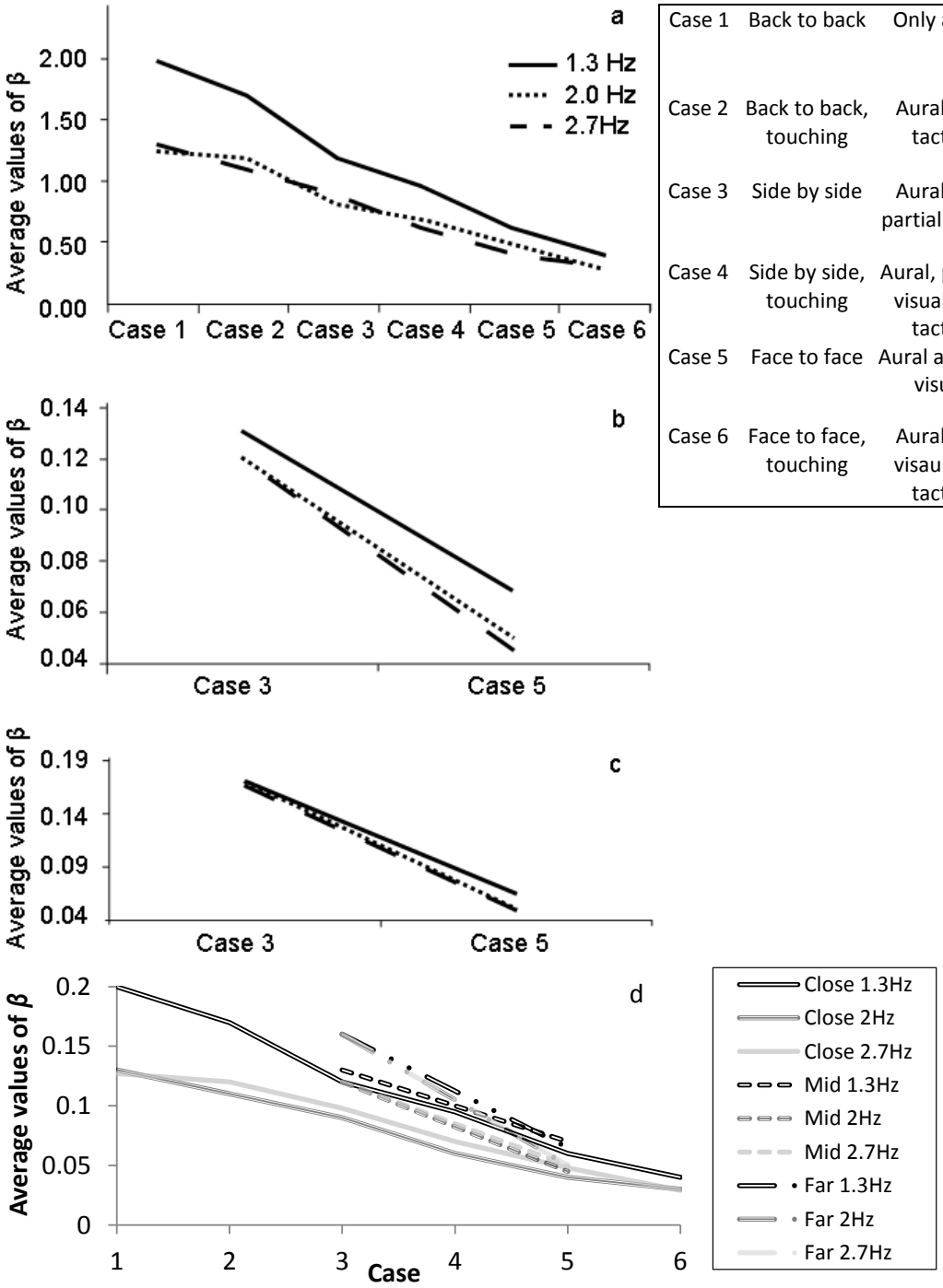

Case 1	Back to back	Only aural
Case 2	Back to back, touching	Aural and tactile
Case 3	Side by side	Aural and partial visual
Case 4	Side by side, touching	Aural, partial visual and tactile
Case 5	Face to face	Aural and full visual
Case 6	Face to face, touching	Aural, full visaul and tactile

Figure 2.12 The β values between subjects when a) at close proximity, b) at medium distance c) at far distance and d) all scenarios (adapted from Racic et al., 2013).

2.4.2 Group Synchronisation

Large dynamic forces and excessive structural vibrations are a potential consequence of a group of individuals accurately coordinating their motions. The BS 6399 (BSI, 1996) recommends a potential synchronisation frequency range of 1.5-2.8Hz for large groups. Ginty et al. (2001) quotes synchronised frequency ranges of 1.5-2.5Hz for small groups and 1.8-2.3Hz for large groups. Due to natural variations in human physiology and rhythmic ability, it is highly unlikely that perfect synchronisation could be achieved across a group of individuals. Designing a structure to withstand a dynamic load from a fully synchronised crowd therefore is a too conservative and expensive approach. Hence a knowledge base of the degrees of synchronisation possible for different group sizes, stimuli and at different events is required.

Few experiments involving groups of individuals have been conducted due to limitations in equipment, space for testing and availability of subjects. As stated in Section 2.4.1.2 the presence of other individuals has an effect on the achieved degree of synchronisation. Therefore, it would be desirable to experimentally quantify synchronisation between multiple individuals.

Ebrahimpour and his co-authors discovered experimentally that people are better synchronised with an aural beat when acting together, than when they are on their own (Section 2.4.1.2) (Ebrahimpour and Fitts, 1996; Ebrahimpour and Sack, 1989). Recent jumping experiments confirmed this finding for groups of up to 15 people (Comer et al., 2007). The mean phase delay which represents the average timing of an individual's jump relative to the aural cue, was used as a measure of beat synchronisation. A 33% reduction in the STD of the mean phase delay was apparent for subjects when jumping in a group, compared to jumping alone. It was concluded that people jumping within a group are more capable of synchronising their actions to one another, than an individual to a metronome beat. It was also suggested that visual stimuli was of more importance than aural, when considering short-term crowd synchronisation.

Parkhouse and Ewins (2006) dismissed the dangers of increased synchronisation due to crowds observing one another. They reasoned that as the phase lags varied between individuals, using another subject as a cue was likely to propagate the phase lags reducing the synchronisation. This reasoning, however, has not been verified experimentally.

The largest laboratory investigations into the effect of crowd size on the structural response included 75 different groups of up to 64 individuals (Ellis and Ji, 2002). The experiments were conducted on two different floors of known dynamic properties. The subjects jumped to music of a specified beat and the responses of the floors were measured. The DLFs for the first three forcing harmonics were back calculated. Figure 2.13 shows that the DLFs decrease with increasing crowd size. A large scatter in the DLFs was observed for all group sizes. This indicates large variations of the force even within groups of the same size. It is therefore suggested that further experimental work with different group sizes is undertaken.

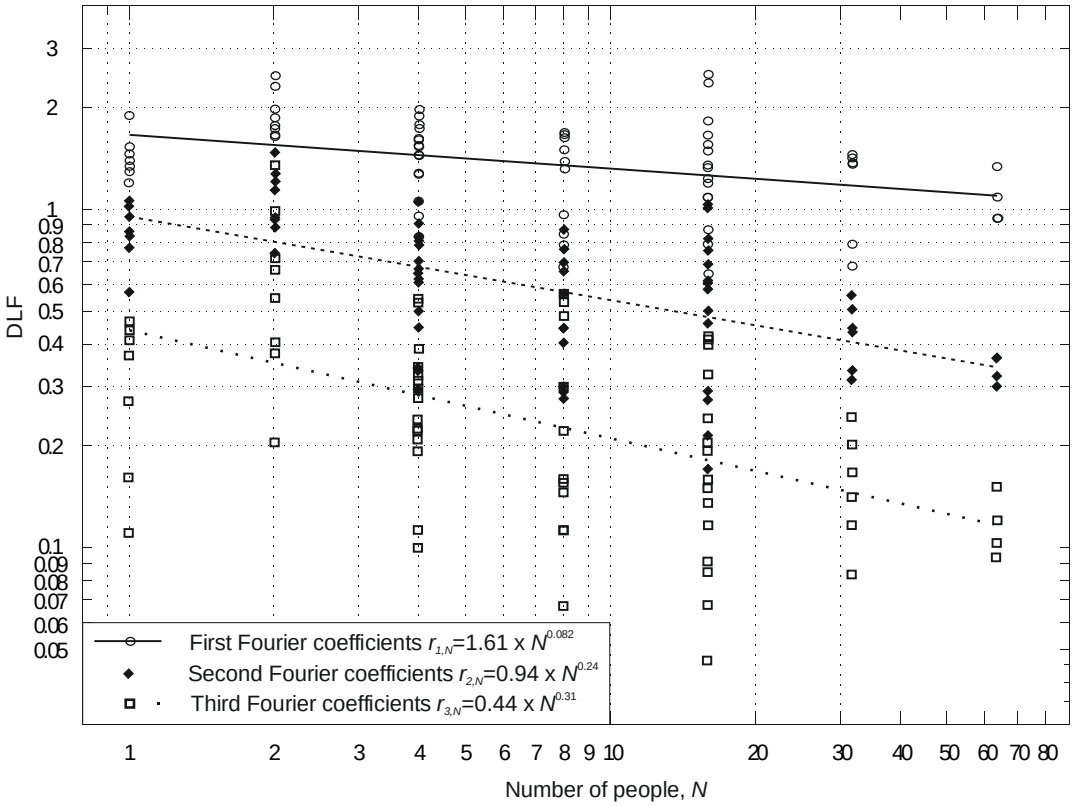

Figure 2.13 The DLFs of the first three harmonics for different sized groups jumping (after Ellis and Ji, 2002).

The previous investigations took place within a lab environment which may not have recreated the ambiance of a pop concert. To overcome this issue insitu experiments were conducted by Kasperski and Niemann (1993) and Littler (2003).

The accelerations and deflections of a stand due to 5-70 individuals jumping to music were measured (Kasperski and Niemann, 1993). For groups with less than 20 individuals little decrease in coordination was observed. For groups of more than 20 individuals a linear decrease in coordination (coordination factor) with increasing crowd size was identified (Figure 2.14). For groups larger than 70 individuals, the coordination factor was assumed to approach a maximum reduction of 50% of the dynamic load. The authors also noted the importance of motivation in maintaining coordination between the group. It was observed during some tests, that the groups of older, less enthusiastic individuals, were poorly coordinated, and low structural vibrations were recorded. On the other hand, groups of younger enthusiastic individuals caused larger vibrations. However a large scatter of response data was recorded between nominally identical tests performed by the same group. This indicates the wide range of possible loading situations and the need for a statistical modelling approach.

Figure 2.14 Coordination factors (adapted from Kasperski and Niemann, 1993).

The responses of 15 stands to crowd movements were monitored over 18 different concerts (Littler, 2003). It was observed that crowd activity depended on the tempo and the song. Individuals often chose not to jump at the beat of the music, but at half or double the beat,

whichever was comfortable. It was also apparent that people changed their jumping rhythm once tired, or at the chorus of a song. Consequentially, awareness of the common song frequencies may not be sufficient to predict the reaction of a crowd. A variety of factors may influence their movements. It was noted on several occasions that a crowd were able to coordinate their movements to songs with a tempo greater than 2.8Hz. As a result recommendations were made to raise the upper limit of comfortable jumping from 2.8Hz (BSI, 1996) to 3.0-3.5Hz (Littler, 2003). An increased limit has now been adopted by ISO (2007).

The variations in the results presented by different authors demonstrate the need for more experiments with groups of individuals that are exposed to different stimuli. In particular, it is necessary to quantify the importance of visual stimuli, for which contradictory observations currently exist. Despite previous work very little is known about actual crowd behaviour. The motions and actions of crowds are of great interest. The design of stadia and other high capacity venues would benefit from more crowd observations.

2.5 Conclusion

Having examined literature which reviewed jumping and bobbing activities, it is accepted that rhythmic jumping is the most severe human induced dynamic load. Amplitudes of dynamic force, up to seven times the weight of the individual can occur (Bachmann and Ammann, 1987). However it is generally thought that as bobbing requires less energy, it is the more common of the two activities. It is worth noting that a greater degree of synchronisation, both with the beat and between individuals, has been seen for rhythmic bobbing. Furthermore, a higher activity frequency range is achievable whilst bobbing. Therefore, both activities should be considered during the design process.

Many authors have deliberated and proposed frequency limits, which individuals can effectively synchronise with. Earlier work disregarded the ability of individuals to synchronise at frequencies above 2.8Hz (Ginty et al., 2001). Other experiments saw good synchronisation

at 3Hz for jumping and up to 3.5Hz for bobbing (Sim et al., 2005). These findings were consistent with insitu stadium tests, where an increase in the comfortable jumping limit to 3-3.5Hz was recommended (Littler, 2003). Observing the work of these authors and the variation in results, there is a need for further jumping and bobbing experiments at a variety of frequencies, specifically using music as an aural cue.

It was generally thought that an aural beat was required for synchronisation and that other cues and the effect of crowd interaction were of little importance (Parkhouse and Ewins, 2004; BSI, 1996). The effects of tactile and visual stimuli were investigated and it was found that both increased coordination (Noormohammadi et al., 2011; Racic et al., 2013). Experiments demonstrated individuals synchronised with a beat better when within a group (Ebrahimpour and Fitts, 1996; Comer et al., 2007). However, discrepancies between authors indicate the need for more experiments investigating beat synchronisation within a group of individuals.

Synchronisation within a group was investigated, in general coordination and DLFs decreased with crowd size (Kasperski and Niemann, 1993; Ellis and Ji, 2002). For crowds greater than 70 individuals this tended towards a 50% reduction in the dynamic load (Kasperski and Niemann, 1993). However, larger variations in the results were seen within the same experimental setup for the same group. This indicates the wide range of crowd responses possible, and the need for more synchronisation experiments with groups, especially within stadium environments.

Examining the contents of this review, it is apparent that multiple subject GRF experiments investigating group synchronisation and the effect of various stimuli, especially music, should be conducted. These experiments, and more observations of real crowds, would better allow the incorporation of crowd-interaction into the structural design process. The effect of inclusion within a group and the additional visual and tactile stimuli should be considered when accounting for dynamic loads. This shortage is addressed in Chapter 7 where the results from varying stimuli group experiments are reported.

3 Review of Jumping and Bobbing Models

As detailed in the previous section, jumping and bobbing activities are the most relevant human induced load cases for structures where crowds assemble. These venues include stadiums, concert halls and grandstands. The dynamic forces applied to the structure may vary between venue type and between different regions and countries (Jones et al., 2011a).

The actions and forces associated with jumping and bobbing vary between individuals which can lead to difficulties adequately accounting for the dynamic loading within the design process. Large structural accelerations are often a consequence of excessive dynamic loading and numerous problems can arise. These include damage to non-structural components, unwanted noise, discomfort or panic of the occupants and overstressing of the structure. In extreme cases large vibrations may compromise the structural integrity. Dynamic loads therefore require adequate consideration within the design process without reverting to unnecessarily conservative and uneconomical design.

In the following section various approaches to model the vertical component of jumping and bobbing forces, first for individuals (Section 3.1) and then for crowds (Section 3.2) are critically examined. Sophisticated models that include dynamic features of both the human body and structure are also covered. The findings of this literature review are summarised in Section 3.3.

3.1 Mathematical Models for Individuals' Forces

To account for and predict the dynamic loading likely to be inflicted upon a structure by an individual jumping or bobbing, various load models have been developed. The methods of modelling individuals' bobbing and jumping will be reviewed, starting with equivalent static models, progressing to periodic and near periodic models. These models are developed with reference to ground reaction forces (GRF) recorded on rigid surfaces. Single jumps or bobs will not be considered due to their transient nature.

3.1.1 Equivalent Static Loads

The earliest method of accounting for human induced dynamic loads in structural design involved replacing them with an equivalent static load. In the 19th century the accepted practice was to allow an equivalent static load of 100 lbft^{-2} (equivalent to 4.8kNm^{-2}) for a dense crowd (Tilden, 1913). However, this design value was not consistent with experimental work (Moreland, 1905) and observations of structures (Tilden, 1913). Equivalent static loads were used in structural design over a large part of the 20th century, with suggested values between 2.15 and 8.14 kNm^{-2}, as shown in Table 3.1. A static load representing the dynamic force is insufficient to meet the structural vibration serviceability criteria. Dynamic forces are present at the harmonics of the applied force, which, if matching a natural frequency of the structure can cause resonance. In consideration of this, from the 1980s onwards more sophisticated dynamic load models were proposed.

Table 3.1 Equivalent static dynamic loads by various authors, assuming the average seating area per person is 0.7m by 0.5m (adapted from Jones et al., 2011b).

	Jones et al. (2011b)	**Tuan and Saul (1985)**	**Ebrahimpour et al. (1986)**	**Moreland (1905)**	**Tilden (1913)**
Action	Static	Rhythmic jumping	Periodic jumping	Jumping	'Jouncing'
Frequency	N/A	2.2 Hz	3 Hz	Unknown	N/A
Participants	1	1	1	90	1
Load Observed	0.75 kN/person	4.50 kNm^{-2}	2.85 kN/person	1.13 kN/person	2.04 kN/person
Equivalent static load (kNm^{-2})	2.15	4.50	8.14	3.23	5.83

3.1.2 Periodic Models

To imitate the repetitive nature of rhythmic activities, many authors proposed periodic load models. The semi-sine model (Bachmann and Ammann, 1987) was one of the first dynamic load models for jumping forces (Figure 3.1):

$$F(t) = \begin{matrix} K_P \cdot W \cdot \sin(\pi \cdot t/t_P) & for \quad t \le t_P \\ 0 & for \quad t_P < t \le T_P \end{matrix} \qquad 3.1$$

where K_P is the impact factor, while W, T_P and t_P, represent the test subject's weight, period and contact time, respectively.

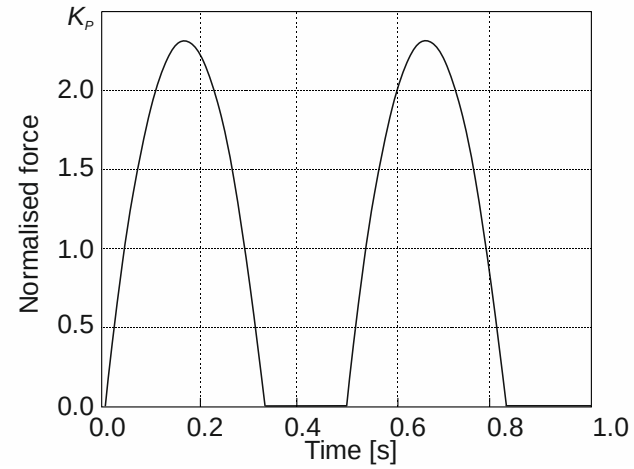

Figure 3.1 Force time history of the semi-sine model (after Bachmann and Ammann, 1987).

A Fourier series is used to describe the semi-sine profile and incorporate the harmonic components of the jumping force. The force spectra of the semi-sine model showing the DLFs of each harmonic for various contact ratios are shown in Figure 3.2. This can be written analytically (Ji and Ellis, 1994; Ji and Wang, 2001):

$$\boldsymbol{a_0 = \frac{2K_P\alpha}{\pi} = 1.0} \tag{3.2}$$

$$\boldsymbol{F(t) = W\left[1.0 + \sum_{n=1}^{\infty} r_n \sin\left(\frac{2n\pi}{T_P}t + \phi_n\right)\right]} \tag{3.3}$$

where

$$\boldsymbol{r_n = \sqrt{a_n^2 + b_n^2}}$$

when:

$$\boldsymbol{2n\alpha = 1, \quad then \ldots \qquad a_n = 0 \qquad b_n = \frac{\pi}{2}}$$

else:

$$\boldsymbol{a_n = 0.5\left[\frac{\cos(2n\alpha - 1)\pi - 1}{2n\alpha - 1} - \frac{\cos(2n\alpha + 1)\pi - 1}{2n\alpha + 1}\right]} \tag{3.4}$$

$$\boldsymbol{b_n = 0.5\left[\frac{\sin(2n\alpha - 1)\pi}{2n\alpha - 1} - \frac{\sin(2n\alpha + 1)\pi}{2n\alpha + 1}\right]} \tag{3.5}$$

where α is the contact ratio, r_n is the DLF and ϕ_n is the phase angle. The mean value of the signal is a_o, and a_n and b_n are the Fourier coefficients associated with the n^{th} harmonic.

Contact ratio dependent DLFs and phase angles for the first six harmonics of jumping are shown in Table 3.2. As the harmonic number and the contact ratio increases, the DLF magnitude decreases. The number of harmonic components used will alter the dynamic load and the structural response. Figure 3.3 compares two force profiles using one and six harmonic

components of the semi-sine model (Table 3.2). However, a visually acceptable reconstruction of the force time history does not necessarily equate to a reliable force spectrum.

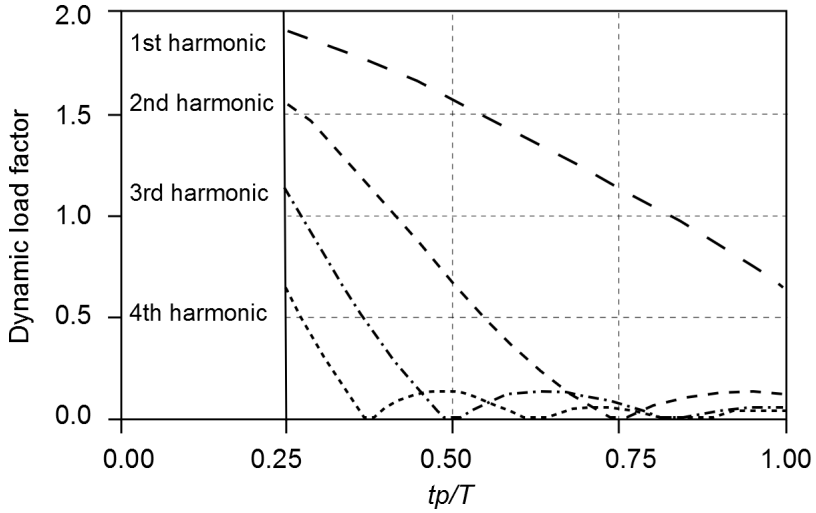

Figure 3.2. Harmonics load amplitudes from the semi-sine model (after Bachmann and Ammann, 1987).

Table 3.2 DLFs factors for different contact ratios for up to the 6th harmonic (after BRE, 2004).

Contact Ratio		Harmonic number					
		***n*=1**	***n*=2**	***n*=3**	***n*=4**	***n*=5**	***n*=6**
***α*=2/3**	r_n	9/7	9/55	2/15	9/247	9/391	2/63
	φ_n	-π/6	-5π/6	-π/2	-π/6	-5π/6	-π/2
***α*=1/2**	r_n	π/2	2/3	0	2/15	0	2/35
	φ_n	0	-π/2	0	-π/2	0	-π/2
***α*=1/3**	r_n	9/5	9/7	2/3	9/55	9/91	2/15
	φ_n	π/6	-π/6	-π/2	-5π/6	-π/6	-π/2

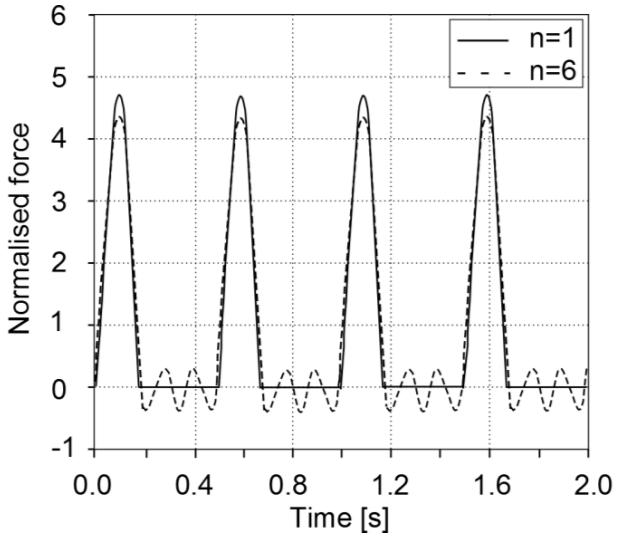

Figure 3.3 The effect of the number of Fourier components on the semi-sine model (after BRE, 1997).

The number of harmonics recommended by various researchers vary between two and six (Allen et al., 1985; Rainer et al., 1988; Pernica, 1990; Allen, 1990; Ellis and Ji, 1994; BSI, 1996; Reid et al., 1997). To design against resonance at the assumed jumping frequency f_J at the lowest structural frequency f_n, the inclusion of harmonic components to the nearest integer value of $n = f_n/f_J$ is recommended (BRE, 2004; Ellis and Ji, 1994). This method suggests that the number of harmonic components depends on the structure. Therefore a very stiff structure would require a high number of components for adequate consideration of the response. However, it is unlikely that an individual will jump with enough precision to stimulate resonance at the corresponding harmonic. Energy dissipates around the higher harmonics reducing their influence unless a very precise jumping rhythm is maintained. Therefore, very stiff structures are unlikely to be in danger. In general, to adequately reconstruct the force time history three or four harmonic components are recommended (Ellis and Ji, 2002).

As seen in Figure 3.2 and Table 3.2 the DLFs and the impact factors decrease with increasing contact duration, due to the conservation of energy (Bachmann and Ammann, 1987). As the contact ratio of the jump decreases, the jumper is airborne for longer and lands with greater force increasing the impact factor. Figure 3.4 shows the relationship between the contact ratio and impact factor when the force profile takes the shape of the theoretical semi-sine model (Bachmann and Ammann, 1987). In practise it was demonstrated that this relationship is not always satisfied (Sim et al., 2008). It was shown that the force profiles of some test subjects had strong correlation between the contact ratio and impact factor, whereas others had little. The correlation reduced further at higher frequencies. This is likely due to differences in jumping styles, for example it is possible to jump whilst maintaining a flat footed style, although it is more common to rise and land on the toes. These and other personal preferences are likely to alter the GRF profile and the correlation between contact ratio and impact factor.

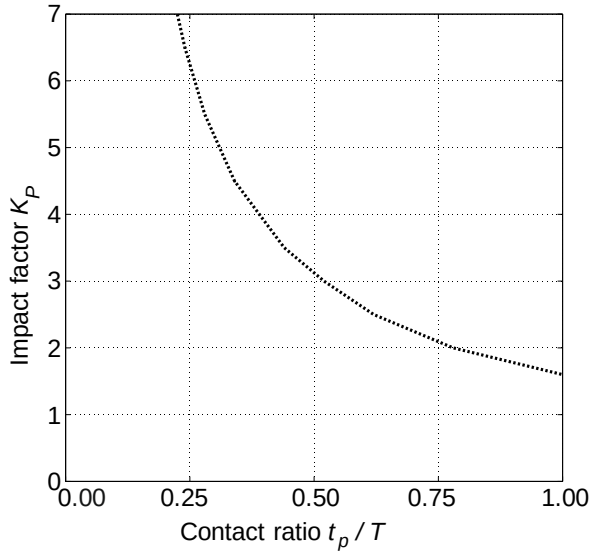

Figure 3.4 Contact ratio dependant impact factors (after Bachmann and Ammann, 1987).

Previously the contact ratios in Table 3.2 were used to distinguish between high impact and low impact jumps. To allow the jumping frequency to be specified with the model, a relationship was sought between the contact ratio and the jumping frequency (Bachmann and Ammann, 1987). Contact ratios between 0.25 and 0.6 were found experimentally at a variety of jumping frequencies (Bachmann and Ammann, 1987; Ji and Ellis, 1994). It was observed that a range of contact ratios were possible for each jumping frequency due to variability in the jumping style and height (Bachmann and Ammann, 1987). However, the lower contact ratio boundary is dictated by the limits of muscular strength and human discomfort (Wyatt, 1985). The contact time is unlikely to fall below 0.15s for jumping (Bachmann and Ammann, 1987), therefore overall the minimum contact ratio can be calculated as:

$$\boldsymbol{\alpha = \frac{t_p}{T_P} = 0.15 \cdot f_J} \tag{3.6}$$

However, after experiments over a range of frequencies, a frequency dependent lower limit for contact time was observed (Baumann and Bachmann, 1987; Wilford, 2001) shown by the medium dashed line in Figure 3.5. Once contact ratios are established from t_p x f_j where t_p is sourced from Figure 3.5, Figure 3.2 and Figure 3.4 can be utilised to find the maximum DLFs and impact factors. The predicted DLFs (dashed and dotted lines) have been compared to

experimental DLFs found using a force platform (Pernica, 1990), and from measured responses of beams of known dynamic properties (Ji and Ellis, 1994) in Figure 3.6.

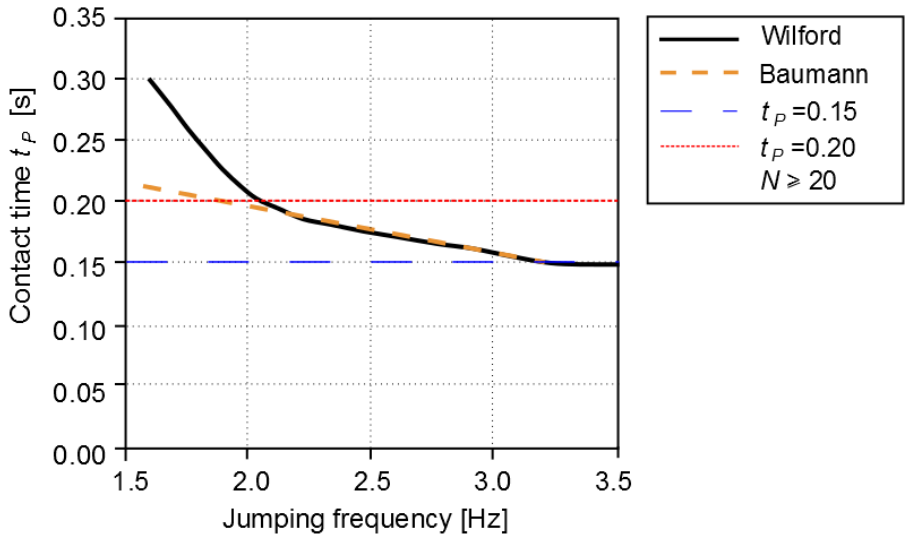

Figure 3.5 Contact times as a function of jumping frequency (adapted from Wilford, 2001).

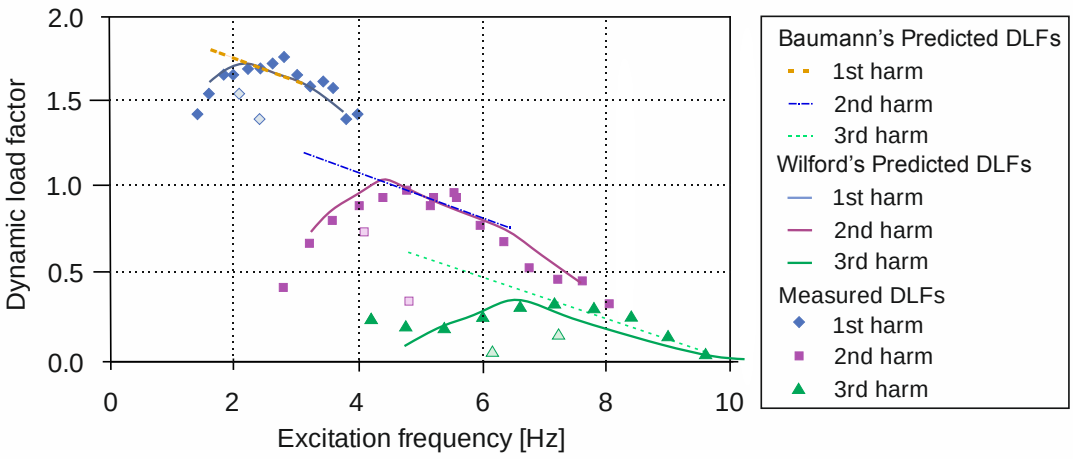

Figure 3.6 Frequency varying DLFs for a jumping person using the minimum observed contact ratios (Baumann and Bachmann, 1987), and the revised minimum contact ratios (Wilford, 2001), compared to experimental DLFs (filled markers (Pernica, 1990), hollow markers (Ellis and Ji 1994; Ji and Ellis, 1994)) (adapted from Wilford, 2001).

The predicted DLFs from the semi-sine model compare well at higher frequencies to the measured data. However, at lower frequencies the DLFs are overestimated. The discrepancy between the measured and predicted data at low frequencies suggests that the theoretical model does not perform well in this frequency region, and that the minimum contact ratios are too small. As larger contact ratios values (0.4-0.75) have been found in some experimental

studies (Yao et al., 2002, 2006; Sim et al., 2008), the conservative values of minimum contact times were revised by Wilford (2001). The DLFs from the amended minimum contact times (Figure 3.5) compare better with the experimental data as seen by the solid lines in Figure 3.6. However, there is little experimental evidence to suggest that jumping frequency dictates a unique contact ratio. From recent experimental work on a flexible surface contact ratios of 0.5-0.7 were observed for jumping at 2Hz (Yao et al., 2002). The GRFs increased with surface stiffness suggesting the contact ratios varied with the natural frequency of the surface. During resonance and near resonance conditions the contact ratio values increased further to 0.75-0.95. It was suggested that individuals subconsciously altered their contact ratio to track the surface movement (Yao et al., 2002).

The semi-sine model is a simple way of modelling the jumping GRF and a good basic representation can be achieved. However, the jumping frequency is used to establish a frequency specific contact ratio which is inconsistent with experimental findings (Yao et al., 2002). This deterministic model does not account for intra and inter-subject variability. In addition, the shape of the force profile is unable to replicate the asymmetric and double peaked profiles seen at low frequencies discussed in Chapter 2.

3.1.3 Near Periodic and Shape Varying Models

Modelling jumping and other human forces as a periodic function provides a general representation of the force. However, due to human inability to perfectly repeat actions, the loading is rarely periodic. Recent studies described human motion as occurring over a narrow band of frequencies instead of at a specific frequency (Brownjohn et al., 2004). Accordingly, human loading is referred to as near-periodic to accommodate both its cyclic nature and its inevitable variability (Racic, 2009). A repercussion of using a periodic model is a force spectrum consisting of discrete spectral lines at the jumping frequency and its integer multiples. Real dynamic forces are characterised by the energy leakage around these main harmonics. This spectral leakage increases at higher harmonics and therefore a periodic model may cause

overestimations of the structural response at higher harmonics (Racic, 2009). There is also potential for smaller non-dominant spectral lines with resonance potential to be missed.

Jumping can be modelled by a normalised experimental force history from an individual, this can be extrapolated to represent a crowd (Sazak et al., 2011). This method intrinsically allows for the inclusion of some intra-subject variation. There is a lack of inter-subject variability as the force history profiles and the jump timings are identical for each individual simulated, which is an unrealistic representation (Sim et al., 2005, 2006, 2008).

An near periodic model (Sim et al., 2008) which incorporates both intra and inter-subject variation using five independent parameters is described in Figure 3.7. This five parameter model is based on an experimental database of individuals jumping on a force plate (Parkhouse and Ewins, 2006, 2004). Beta parameters (Figure 3.7) are found from the experimental data and used in Beta distributions which model the variation in the parameters between individuals. Three of the parameters represent the intra-subject variation in the jump timing. These include an auto-regression timing coefficient, to mimic the subject's conscious effort to realign to the beat with reference to the previous jump. In addition, the mean phase delay of the jumps is included, and human error in the jump timing is incorporated using the STD of the random timing errors.

The final two parameters are the STD and mean values of the contact ratio which vary between individuals (Sim et al., 2008). This variation is modelled using another beta distribution based on the experimental data.

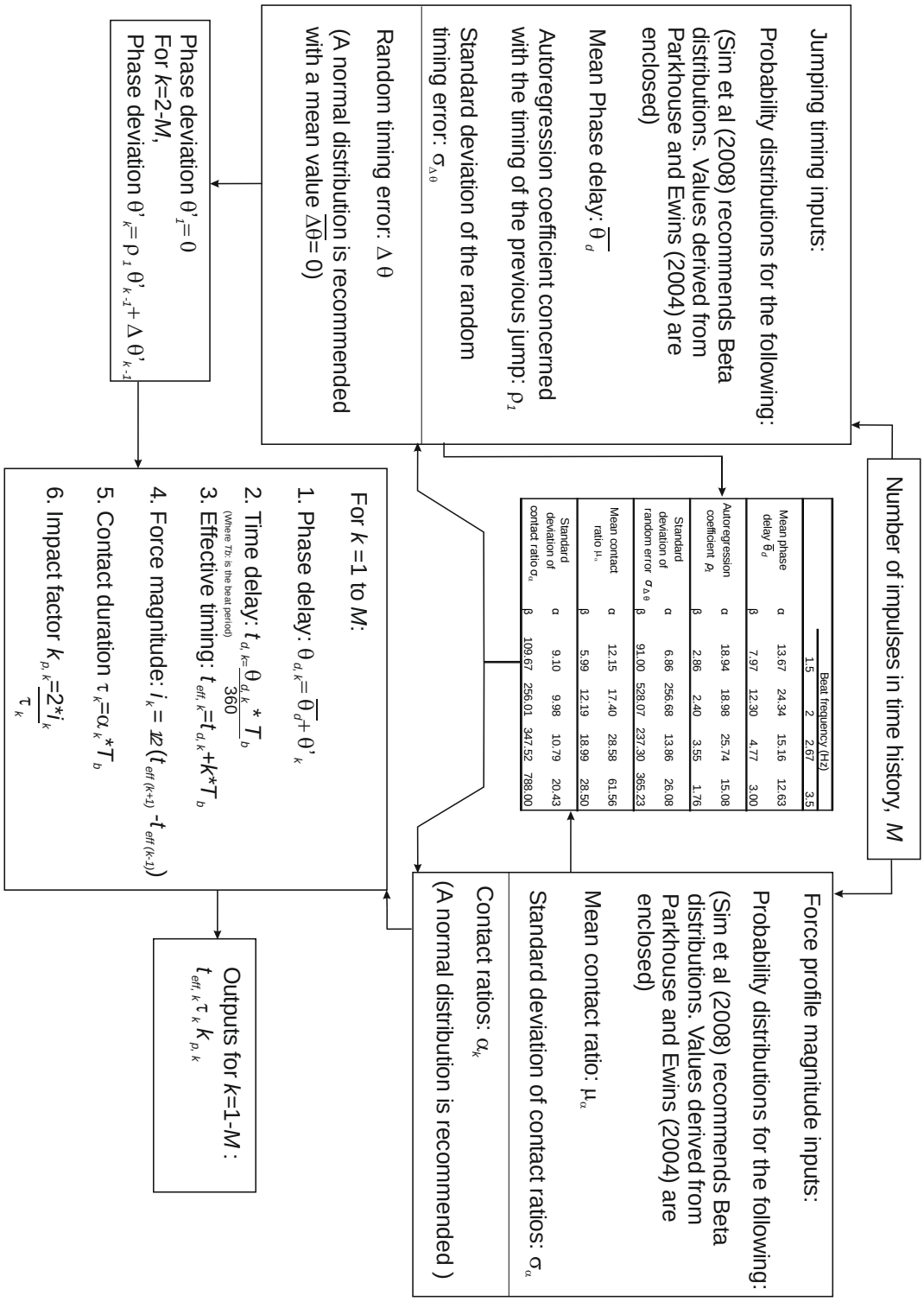

		Beat frequency (Hz)				
		1.5	2	2.67	3	3.5
Mean phase delay $\overline{\theta_d}$	α	13.67	24.34	15.16	12.63	
	β	7.97	12.30	4.77	3.00	
Autoregression coefficient ρ_1	α	18.94	18.98	25.74	15.08	
	β	2.86	2.40	3.55	1.76	
Standard deviation of random error $\sigma_{\Delta\theta}$	α	6.86	256.68	13.86	26.08	
	β	91.00	528.07	237.30	365.23	
Mean contact ratio μ_α	α	12.15	17.40	28.58	61.56	
	β	5.99	12.19	18.99	28.50	
Standard deviation of contact ratio σ_α	α	9.10	9.98	10.79	20.43	
	β	109.67	256.01	347.52	788.00	

Figure 3.7 A flow chart for the use of the near periodic model (adapted from Sim et al., 2008).

To further refine the five parameter model, a relationship was devised between force magnitude i_k and the timing of the previous and upcoming jumps. Finally a semi-cosine-squared function was adopted to represent the shape of each jump, providing a better fit to experimental data than a semi-sine profile. Monte Carlo simulations can then be used to accumulate individual jumping forces to model an entire crowd. However, as the data were collected from individuals, the greater synchronisation often seen within crowds (Section 2.4.2) is not considered. Therefore the resulting crowd DLFs are likely to underestimate the dynamic load and therefore this model may be unreliable for crowd simulations.

The five parameter model is complex, requiring distributions for a significant number of parameters, however the end user is considered and several flow charts to aid calculation are presented. A further advantage is the inclusion of the beta distribution parameters collected from jumping experiments which allow the user to model the various distributions of each jumping parameter. Hence if experimental reference data is unavailable these distributions can be used within the model, but the option for using alternative reference data exists.

Within the five parameter model a linear relationship between the timing of the jump and the size of the impulse is assumed. Later authors have observed a lack of correlation between these two variables (Racic and Pavic, 2010).

The model is based upon test subjects without a jump deficit (Sim et al., 2005). Subsequently only 75% of participants jumping at 2Hz were included despite this frequency being considered as easy to jump at. The inclusion rate decreased further at higher frequencies dropping to only 41% at 3.5Hz. This selective inclusion favours an unrealistic worst-case scenario where individuals are able to maintain rhythmic jumping to a high level of accuracy.

A further shortfall of this model is the use of the centroid of the force profile to define the jump timings. This technique is perhaps appropriate for jumping frequencies over 2Hz, where the force profiles tend towards a symmetrical arc. At lower frequencies a range of profile

shapes are seen (Section 2.2.2), due to this variation the centroid may be inappropriate to identify the timings of each jump. This also highlights that a half-cosine-squared function is unrepresentative of the force profile at low frequencies.

The most detailed narrow band jumping model is a many Gaussian model (Racic, 2009). An extensive database of experimental jumping forces was compiled, consisting of 825 force profiles generated by 38 males and 17 females. Using characteristics from a pre-existing jumping force history from this database the model replicates the average shape and amplitude of the force profile. This was accomplished using a closed loop trajectory, $Z_i(t)$, in 3D space (x,y,z) around a circle with a radius of one in the plane of (x, y), demonstrated in Figure 3.8. Gaussian exponentials are summed together to create the profile shape, allowing for the possibility of asymmetric jumping profiles.

The jumping periods of the modelled force were simulated from the mean jumping period of a pre-collected trial, summed with a period variation value. The auto spectral density (ASD) of the trial period variations were used to simulate period variations with the same standard deviation and ASD as the original trial. A linear relationship between the jumping periods and the weight normalised impulses was observed, and utilised to create synthetic impulses which correspond to the synthetic periods.

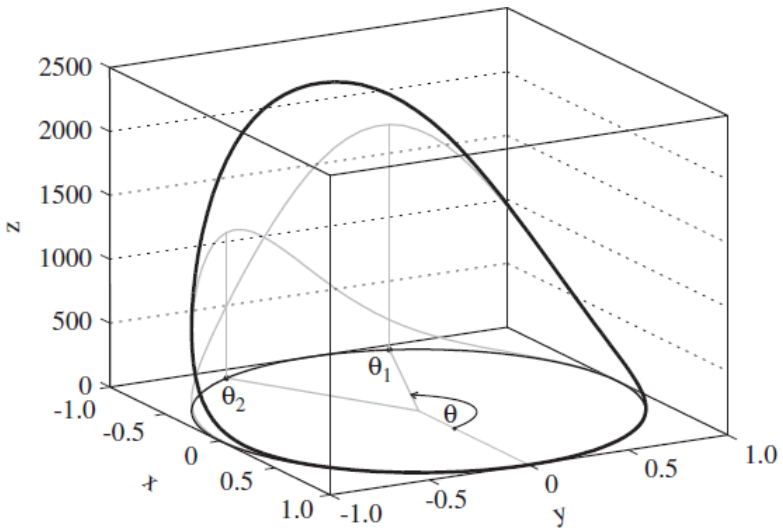

Figure 3.8 Trajectories $Z_i(t)$ of jumping, displayed in a 3D form (after Racic and Pavic, 2010).

The many Gaussian model is currently the best available model for representing individual forces on rigid ground. Consideration to intra-subject variation is a major benefit. The jump characteristics are modelled with reference to real forces, and therefore reflect real jumping time histories. The major benefit over the five parameter model is the ability to change the profile shape to produce an asymmetric profile akin to low frequency jumping. However, the modelling process is complex and significant processing is required. Furthermore, the synthesised force time histories are created using force characteristics from an experimental database. Currently the model is used in conjunction with a large database of forces, which is not publically available.

Both the many Gaussian and the five parameter models are based upon GRFs collected on rigid ground, and therefore there may be limited applicability of these models upon other surfaces.

3.2 Crowd Models

At stadium events multiple people move within a crowd, applying a dynamic crowd load to the structure (Jones et al., 2011b). Models which account for the dynamic load due to crowds jumping and bobbing are discussed within this section. Often individuals within crowds will attempt to synchronise their actions with one another. The inclusion of a component to reflect the degree of crowd synchronisation is necessary for realistic crowd models. Modelling approaches to crowd synchronisation are discussed in Section 3.2.1.

Human occupants can affect the dynamic properties of the structure through a phenomenon known as human structure interaction (HSI). HSI is introduced in Section 3.2.2 and its inclusion within crowd modelling is presented in Section 3.2.3. The consideration, or lack thereof, of HSI within stadium guidance is discussed. Thought is also given to the effect of ground flexibility on the GRFs.

3.2.1 Synchronisation

During stadium events crowds of people are likely to be active and attempt to coordinate their movements with one another. Due to the differences in physiology and human nature a variety of movements, not restricted to rhythmic jumping or bobbing, will occur. A particular beat may be prominent amongst the movements, prompted by aural or other stimuli. However, due to different coordination abilities, other frequencies of movement will be present (BRE, 1997), and will reduce the potency of the dominant harmonic. The synchronisation of the crowd, or lack thereof, can be described by the phase lags between the individuals. Two methods have been used to account for these phase lags. The cumulative effects of the phase lags within the crowd can be considered by applying an overall coordination factor to the crowd load or including it within the DLFs. An alternative method is to apply phase lags of a specified distribution to force profiles which are then used within Monte Carlo simulations of the crowd loading. The synchronisation and participation of the crowd will be affected by various factors (Section 2.4). The implementation of these methods and the consideration of the factors which affect synchronisation are presented within this section.

Originally crowds were represented by static equivalent multiples of individual loads as discussed in section 3.1.1. At times these models included a factor to reflect the likelihood of an extreme loading case, or to demonstrate the lack of coordination within a crowd (Tilden, 1913; Moreland, 1905). The American Standards Association (ASA) found that the size of the crowd affected the degree of synchronisation (Homan et al., 1932). This “group effect” was observed when comparing the horizontal forces on a platform for groups of three and nine men. The groups of three were more synchronised and consequentially the ASA recommended that the total applied force should be multiplied by a factor of 0.75 (Homan et al., 1932; Saul and Tuan, 1986). The recognition that perfect group synchronisation is rarely seen in large crowds is a significant development towards modern crowd models.

Many modern crowd models are developed based on summations of experimental or analytical individual force time histories. A crowd adapted version of the semi-sine model reflects the reduced coordination as an increased minimum contact duration of 0.2s (Baumann and Bachmann, 1987) for groups larger than 20 (Figure 3.5). The extended duration acts to increase the contact ratios, reducing the impact factors and DLFs. This results in a 10% reduction in the dynamic load for jumping at 2.45Hz.

Coordination factors C can also be used with the semi-sine and other models to account for imperfect synchronisation. Coordination factors may incorporate the influence of variables, such as, number of people, frequency of stimuli, harmonic number, type of event and number of events occurring within the structure's lifetime. Examples of Coordination factors which reflect the decreased synchronisation with increasing group size N, are demonstrated in Figure 3.9, Figure 3.10 and Figure 3.11. The decreased synchronisation is due to the spread of jumping abilities and enthusiasm as the sample sizes increases. For groups larger than approximately 50 the coordination factor tends to a constant value (Parkhouse and Ewins, 2004; Kasperski and Niemann, 1993), potentially rendering a size dependant coordination factor unnecessary in the design of large event venues (Figure 3.9).

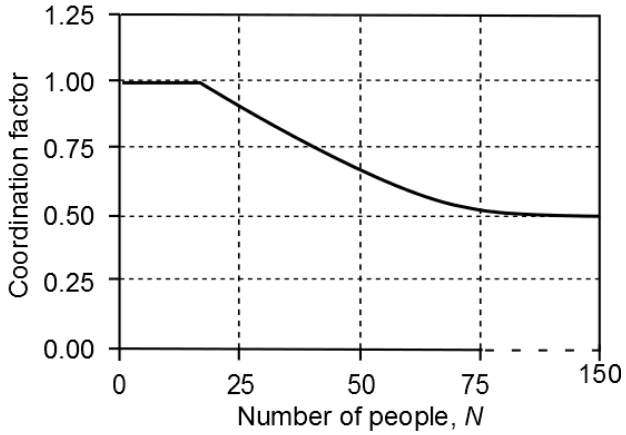

Figure 3.9 Coordination factors (after Kasperski and Niemann, 1993).

A further effect of group size is the reduced influence of the higher harmonic components, which is reflected in the coordination factors shown in Figure 3.10 and Figure 3.11.

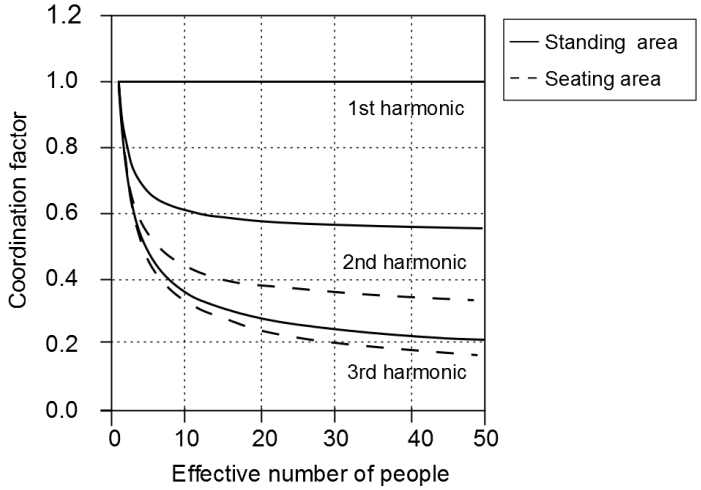

Figure 3.10 Coordination factors for free and restricted movement (after Hansen and Sørensen, 2002).

The coordination factors in both Figure 3.9 and Figure 3.10 are based upon crowd experiments on grandstand structures. Hansen and Sørensen (2002) observed a relatively small reduction in the response at the 1st harmonic for group sizes between 1 and 10. They therefore recommended a 1st harmonic coordination factor of one for all values of N (Figure 3.10). Kasperski and Niemann (1993) observed crowds of up to 70 people and saw a decrease in coordination for groups larger than 20 (Figure 3.9). This would therefore suggest that a 1st harmonic coordination factor of one, for all group sizes is over-conservative.

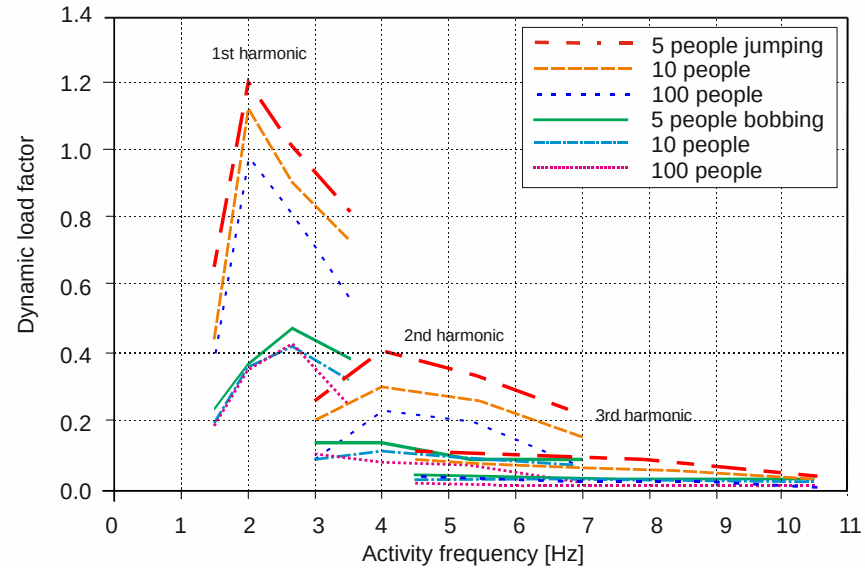

Figure 3.11 DLFs for group size, harmonic, activity and activity frequency (after Parkhouse and Ewins, 2004).

Frequency dependent coordination factors are seen in Figure 3.11 and Figure 3.12. As discussed previously, some frequencies are more common, or easier to coordinate with (Ginty et al., 2001). Frequency dependent coordination factors provide an awareness of the frequencies likely to provoke a severe structural response. In addition, the natural frequencies of the structure can be checked for potential vulnerabilities and the design altered or proactive remedial measures invoked.

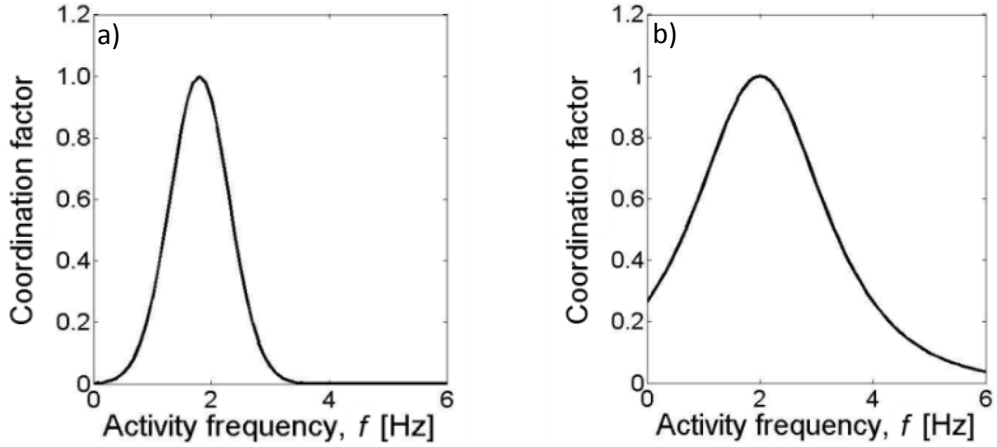

Figure 3.12 Coordination factors a) for mild loading (Scenarios 2 and 3) and b) extreme loading (Scenario 4) (after UK Working Group, 2008).

Parkhouse and Ewins (2004) found DLFs which reflected the varying degrees of coordination due to group size, activity, activity frequency, and harmonic. They measured individuals' GRFs and modelled crowds by aligning the individual trials with the original beat. By looping each force history and starting at a different jumping cycle, dictated by a random number, the simulation of groups larger than the subject pool was possible. This approach made it unlikely that two identical force time histories would feature within a crowd. The synchronisation within these simulated groups was quantified using the STD of the mean phase lags of each individual to the beat. The highest level of crowd synchronisation occurred at 1.5Hz and 2Hz for jumping, and at 1.5Hz and 3.5Hz for bobbing (Parkhouse and Ewins, 2004). From the simulations DLFs for jumping and bobbing groups of various sizes, which reflect the frequency and harmonic were found (Figure 3.11). Constant DLFs were observed for crowd sizes greater

than 100 indicating that there is a lower limit on poor synchronisation. However, these results are based on individual's GRFs and therefore crowd influences are not included.

The coordination factors in Figure 3.10 reflect differences in stadium seating conditions, (standing, solid line or seated, dashed line), as these may affect movement, reducing crowd activity and synchronisation (Hansen and Sørensen, 2002). This allows a basic assessment of the dynamic load based on the stadium layout.

In the previous coordination factors the nature of the event, which may influence crowd synchronisation, is not considered. The UK stadium recommendations (UK Working Group, 2008) consider four event scenarios involving large crowds and their effect on synchronisation (Table 3.3). The events considered include low profile sporting events, classical concerts, medium-tempo pop concerts and high energy rock events. Figure 3.12 shows the coordination factors which vary with activity frequency for Scenarios 2-4. Scenario 1 events are thought to have minimal crowd activity and therefore little influence on the structure. This method allows stadia to be designed in consideration of their end use.

Table 3.3 Event scenarios (adapted from UK Working Group, 2008 and Parkhouse and Ward, 2010).

Scenario 1	Scenario 2	Scenario 3	Scenario 4
'A low profile sporting event', 'less than maximum attendance'.	'Classical concert and typical well attended sporting event' with the 'audience seated with only a few exceptions – 'potentially excitable crowd with minor excitation'.	'High profile sporting events and concerts with medium tempo music', 'pop concerts with cross generation appeal' with a crowd participation.'	'More extreme events including high energy concerts with periods of high intensity music' featuring a young excited crowd, mostly standing/bobbing and jumping, vigorous participation.

The use of questionnaires alongside experimental GRFs is another method to reflect the audience and event within the coordination factor. Questionnaires have been used to characterise the subjects' rhythmic aptitude and likelihood of attendance at events (Parkhouse and Ewins, 2006). This allows the GRFs that correspond to a certain group, for example concert going subjects, to be selected from an experimental database. To compile this database, the GRFs of individuals jumping to a metronome beat were collected. The total dynamic force of an individual upon a structure was found to be comprised of a synchronised and stochastic

component. The component synchronised is the mean cycle of the force history (solid line, Figure 3.13). The stochastic component is comprised of the portions of the force history with a different phase angle to the synchronised component. An equivalent synchronised load can be created by applying the power of the total force history to the mean cycle of the force history (Figure 3.13, dashed line). The equivalent synchronised load can represent the force history of a jumping individual via a half-cosine model with three harmonics.

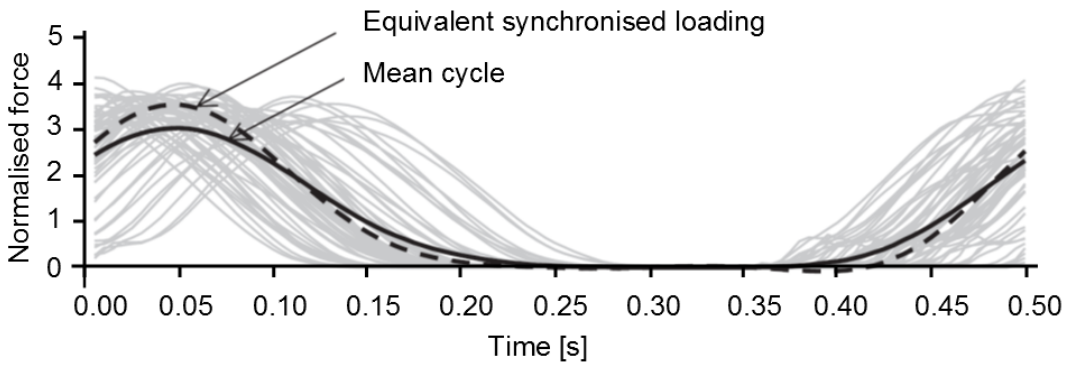

Figure 3.13 A half-cosine model representing the equivalent synchronised loading component, and the mean GRF compared to individual jumping GRFs (after Parkhouse and Ewins, 2006).

In Figure 3.13 the equivalent synchronised loading better accounts for potential peak loads than the mean force history. Nevertheless, peak loads over those encompassed by the equivalent synchronised load can still occur and the neglect of these may cause the underestimation of the structural response. It is more likely however that the removal of intra-subject variability will cause the load to be overestimated.

By the modelling and summation of specific GRFs various crowds can be simulated. When extrapolating this model to a crowd, the synchronised component was found to be dominant and proportional to the size of the crowd. The stochastic component was proportional to the square root of crowd size, thereby decreasing in significance in comparision to the synchronised component for larger crowds. Crowds ranging in size between 5-200 individuals, of various dispositions were simulated 1000 times. DLFs, which reflect the coordination of the groups for varying conditions were calculated (Figure 3.14). Figure 3.15 demonstrates the

variation in the DLFs between simulations. The DLFs in Figure 3.15 match experimental data well (Pernica, 1990; Ellis and Ji, 2004), except for large groups at the third harmonic. The least DLF variation is seen for large crowds and the first harmonics.

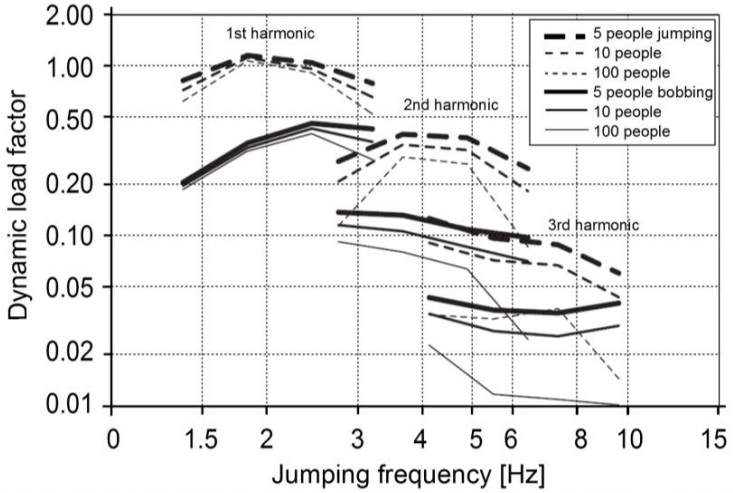

Figure 3.14 DLFs for group size, harmonic, activity and activity frequency (after Parkhouse and Ewins, 2006).

Crowd models which summed audio aligned individual force times histories were shown to underestimate the force, as crowd interaction was not included (Comer et al., 2013). Caution should be used when using models which are based on the extrapolation of individual forces.

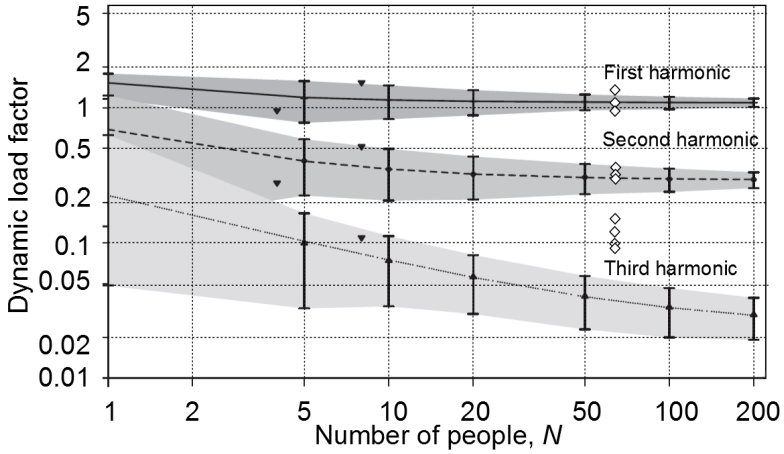

Figure 3.15 The variation in DLFs for different group sizes, *N*, jumping at 2Hz, compared with experimental DLFs from Pernica (1990) (solid) and Ellis and Ji (2004) (hollow) (after Parkhouse and Ewins, 2006).

An alternative method of incorporating coordination factors into crowd models is by considering the number of dynamic events k which are likely to occur within a structure's

lifetime (Kasperski and Agu, 2005). If the structure is hosting a large number of dynamic events, there is a higher risk that several events will result in high dynamic loads. Experiments were conducted using 70 individuals jumping alone for 30 seconds on a force plate, to measure the DLFs and phase angles (Kasperski and Agu, 2005). No clear pattern of frequency change between jumps was observed and therefore it was assumed that the variation between each jump was statistically independent. The force time histories of the subjects were categorised to reflect the ability of the individuals to match a beat. The subjects were accordingly divided into 'good', 'medium', 'bad (slow)' and 'bad (fast)' subgroups. This approach provided the opportunity, as in previous models, for various rhythmic abilities to be incorporated into the model, enabling the reflection of a variety of crowds. 'Good' jumpers had normally distributed root mean squared (RMS) values and reduced variates, y_i, of the 1st harmonic load amplitudes; where the reduced variate is:

$$\boldsymbol{y_i} = \frac{\boldsymbol{r_{i,\ n}} - \overline{\boldsymbol{r_n}}}{\boldsymbol{r_{i,\ n,\ RMS}}} \tag{3.7}$$

where $r_{i,n}$ is the DLF of the i^{th} jump, of the n^{th} harmonic, $\overline{r_n}$ is the average DLF value of the n^{th} harmonic and $r_{n,RMS}$ is the RMS value.

The variations in individuals' weights were incorporated into the model using a distribution found by the Robert-Koch-Institut in Berlin. By including these three distributions in the semi-sine model (Bachmann and Ammann, 1987), a 'normal' crowd of various group sizes can be simulated. The coordination factor was defined as the maximum structural acceleration from N people jumping, divided by the maximum acceleration of one 'good' male jumping.

A non-exceedance probability approach, favoured by the Eurocodes, was applied to the above model. The purpose was to prevent structural accelerations exceeding the serviceability limits over the lifetimes' of 95% of structures. The number of dynamic crowd events within the lifetime of the structure is estimated. The coordination factor is then determined to reflect the number of dynamic events as demonstrated in Figure 3.16 and Table 3.4.

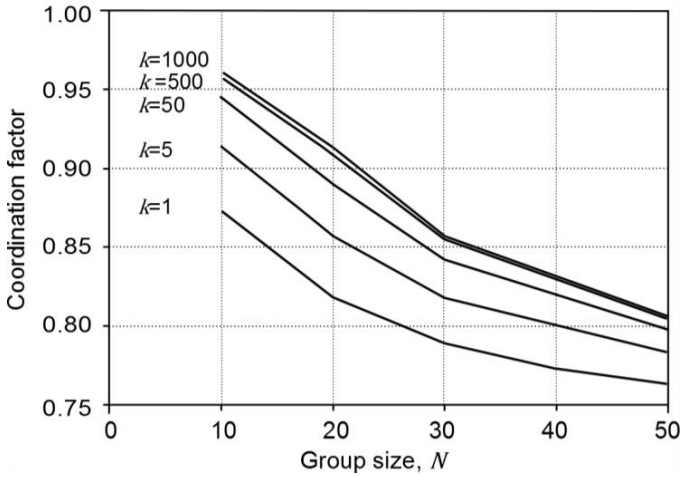

Figure 3.16 Crowd coordination factor based on number of dynamic events, k (after Kasperski and Agu, 2005).

The crowd dynamic force is calculated thus:

$$\boldsymbol{F(t) = NC(N, n, k) Wr_n \cdot \sin(\frac{2\pi n}{T} \cdot t)} \quad 3.8$$

where C is dependent on the group size N, the harmonic number n, and the number of dynamic events k.

Table 3.4 Event dependant coordination factors C for N=10 (after Kasperski and Agu, 2005).

	Coordination factors C				
Number of events k	**1**	**5**	**50**	**500**	**1000**
n=1	0.87	0.91	0.95	0.96	0.96
n=2	0.69	0.78	0.84	0.87	0.87
n=3	0.62	0.71	0.78	0.82	0.83

It is shown in Figure 3.16 and Table 3.4 that as group size increases, the coordination decreases in agreement with previous models. In addition, as the number of events increases above 500, the coordination factor tends to a constant value at each harmonic. This model was used within ISO (2007) alongside the semi-sine model and the Fourier coefficients in Table 3.5, to calculate the worst case loads.

The majority of coordination factors are based on data from individuals or small groups jumping and bobbing. In general the coordination factors and DLFs found with reference to group experiments are higher than those using individual forces. However, most of the group experiments rely upon extrapolation to draw conclusions for larger crowds. Further

experiments with different group sizes are required to observe and realistically incorporate crowd behaviour into coordination factors. Furthermore, rigid GRFs formed the basis for most of the models and knowledge of the effect of surface stiffness, and an awareness of the transferability of the models to different environments is recommended.

Table 3.5 The DLFs used in ISO (2007) (adapted from ISO, 2007).

	Fourier coefficients DLFs r_n		
Activity	**1st Harm**	**2nd Harm**	**3rd Harm**
Vertical action, seated audience	0.5	0.25	0.15
Coordinated jumping (areas without seats)	1.7 or 2.1-0.15f_j	1.0 or 1.9-0.17*(2f_j)	0.4 or 1.25-0.11*(3f_j)

Coordination factors account for the cumulative effects of the time lags between individuals, an alternative approach is to apply a time lag of a specified distribution to each force time history. To investigate the distribution of phase lags groups of two and four individuals, from a subject pool of 20 males and 15 females, jumped on a force plate (Ebrahimpour and Sack, 1989). It was observed that the phase lags followed an exponential distribution, suggesting that people tended to jump in phase. Monte Carlo simulations were used to define a load model for groups of up to 50 individuals jumping at a range of frequencies (Ebrahimpour and Sack, 1989). The results were used to define 'load intensity amplitudes' per unit area. Figure 3.17 shows that for large groups the load amplitude tends toward 3.35 kNm^{-2}. The standard seating allowance of modern stadia is $0.4m^2$ per person, thus a dynamic addition of 536N per person is recommended. This loading is approximately a multiplication factor of 1.80 to the static load (Ebrahimpour and Sack, 1989; Racic, 2009). For a large crowd jumping at 2Hz this is equivalent to a coordination factor of 0.80, comparable to Kasperski and Agu's values and smaller than the UK recommendations (UK Working Group, 2008). The phase lags in this model were sourced from individuals jumping together and therefore considered human-human interaction. However, extrapolation to larger groups is likely to overestimate the coordination achievable in crowds. Further experimental work is desirable, to decide whether the empirical phase lags from a small number of individuals are valid for larger crowds.

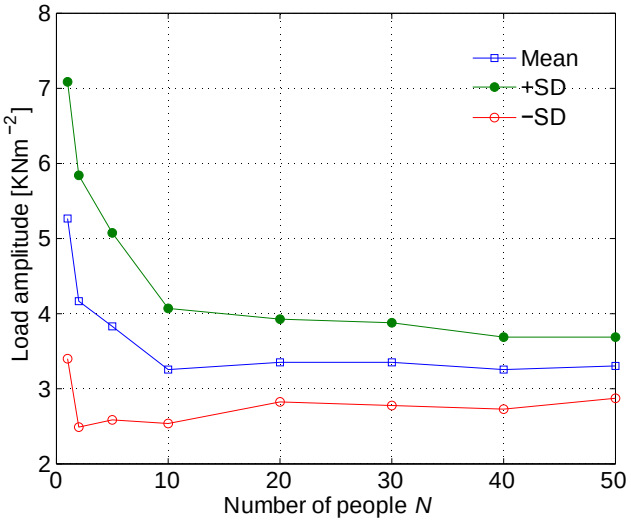

Figure 3.17 Load intensity amplitudes for 2Hz jumping for varying crowd sizes (after Ebrahimpour and Sack, 1989).

Wilford (2001) used Monte Carlo simulations to model crowd loads using a normally distributed time delay with a standard deviation of 0.14 T, where T is the period. The predicted crowd DLFs are displayed in Figure 3.18, and are compared to those measured from groups of 8-25 people (Pernica, 1990). The predicted DLFs closely match the experimental values for the 1st and 3rd harmonic for mid-frequency jumping (2-3Hz). However, the predictions of the 2nd harmonic were not as successful and overestimated the DLFs. By increasing the standard deviation of the period to 0.2 T for jumping at 4Hz, a better correspondence at higher frequencies was possible (Wilford, 2001). A larger standard deviation reflects the increased difficultly of synchronising with a beat at high frequencies, as seen in previous experimental work (Parkhouse and Ewins, 2004).

The normally distributed phase lag model, relies on matching simulated data to previous experimental work (Pernica, 1990) without actually observing the phase lags. Therefore a normal distribution may not be the most appropriate method for describing phase lags.

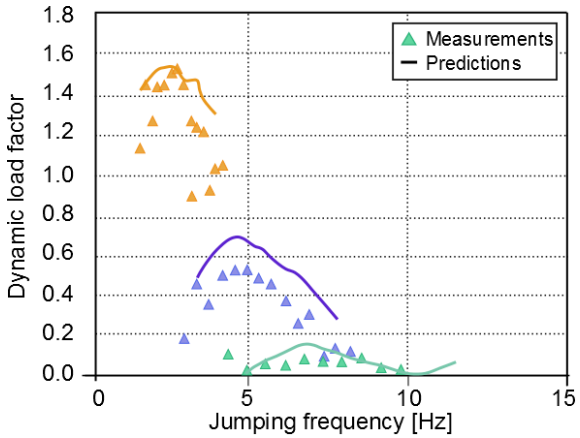

Figure 3.18 Predicted DLFs for 10 people compared to experimental DLFs from 8-25 people jumping (Pernica, 1990) (after Wilford, 2001).

There is disagreement between several authors as to the distribution of phase lags. Furthermore, in some experimental work no obvious distributions of phase lags were found (Kasperski and Agu, 2005). Therefore, more experiments to observe phase lags within large groups are recommended.

3.2.2 Human Structure Interaction

The majority of the previous models use GRFs from rigid surfaces and therefore do not consider the interaction between the occupants and the structure. The presence of humans upon a structure can alter the dynamic properties. In addition, the response of the structure can affect the movement and forces of the inhabitants. Until the late 1990s, the spectators on a structure were modelled only as an external mass in structural engineering applications. A study at the rugby union ground at Twickenham, however, revealed that people are dynamic entities that interact with the structural dynamics (Ellis and Ji, 1997). The response to impact excitation was measured whilst the stadium was empty and during a full capacity varsity match in 1991 (Figure 3.19).

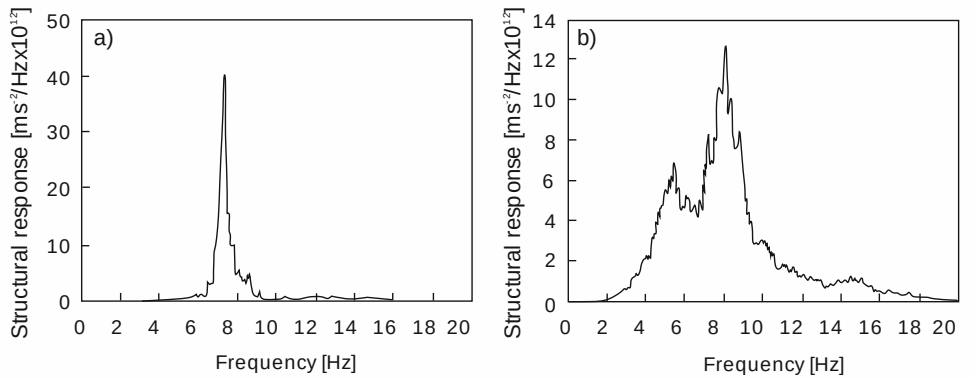

Figure 3.19 An auto-spectra of the structural response at Twickenham stadium when a) empty and b) occupied (after Ellis and Ji, 1997).

As shown in Figure 3.19 the presence of the crowd changed the single mode of the empty structure into a system with two modes. The two modal frequencies of the occupied stand lay either side of the natural frequency of the empty stand. The response magnitudes of the occupied stand were reduced, implying a higher damping ratio. It has been suggested that spectators have the potential to increase the overall damping ratio of a structure from a typical value of 2% to a value as high as 25% (Parkhouse and Ward, 2010).

Sim (2006) simulated the response of a cantilever stand to passive crowds. For low natural frequency structures the passive crowd acted as additional mass increasing the structural response. The passive crowd on structures with higher natural frequencies acted as a damper, reducing the structural response. The frequency and structural response reduction factors are presented in Figure 3.20 for a seated passive crowd.

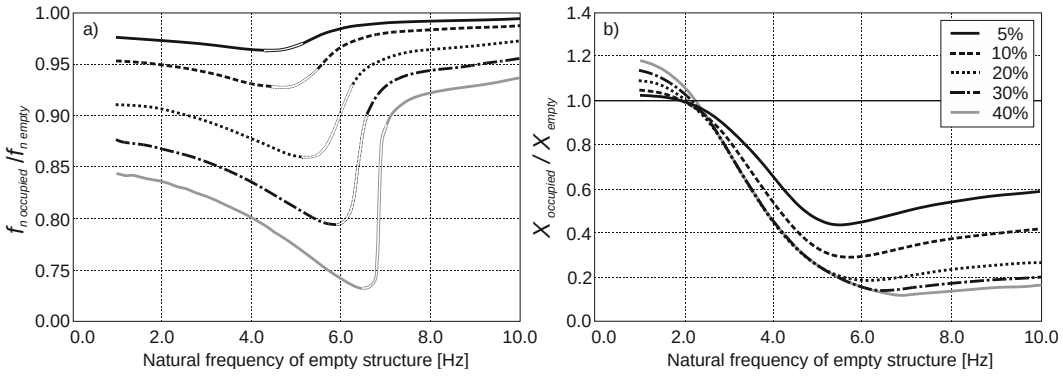

Figure 3.20 a) The natural frequency reduction factor and the b) structural response reduction factor for different modal ratios and structural natural frequencies, where X is the maximum structural displacement.

Investigations into the dynamic properties of individuals (Sachse et al., 2002) confirmed that passive humans could not simply be modelled as an additional mass (Ellis and Ji, 1997). This is because the human body is a dynamic system with its own natural frequency and damping. The data in Table 3.6 demonstrates that the dynamic properties of passive crowds vary dramatically and are affected by posture. The presence of a passive crowd alters the structural properties. However, due to variation in the modal parameters between passive subjects (Wei and Griffin, 1998) the development of statistical approaches for modelling human-structural properties are required.

Table 3.6 Variation in body properties between men and women and different postures (after Sim, 2006).

	Undamped natural frequency (Hz)				**Damping ratio (%)**			
	f_1		f_2		ζ_1		ζ_2	
	Mean	STD	Mean	STD	Mean	STD	Mean	STD
Seated men	5.1	0.58	9.3	2.01	31.1	10.11	43.7	43.41
Seated women	5.3	1.06	9.2	2.85	38.5	14.90	31.7	11.63
Seated children	5.2	5.16	15.9	24.20	37.5	39.23	31.2	36.35
Standing men	5.8	0.54	12.6	2.34	33.1	7.21	45.9	17.21

Ellis and Ji (1997) performed impact tests on a simple beam whilst an individual either stood, sat, walked or jumped upon it. Differing from the passive cases (standing or sitting), they found that an active subject, (i.e. a person walking or jumping) did not alter the dynamic properties (natural frequency and damping ratio) of the structure and therefore only acted as external exciter. This conclusion was however based on one subject on a flexible beam. In this configuration, there were instances when the person was not in contact with the structure and therefore could not affect the structure's properties at those times. It is possible that the periods of contact between the subject and the structure were too short to affect the structural properties. In a crowd environment it is unlikely that at any instant in time the entire crowd will be airborne. Therefore an active crowd may cause the human-structure system's properties to differ from those of the empty stand.

A further concern is how the structural movement will affect the forces of the occupants. Modern stadia often feature cantilever stands, which are flexible and have the capacity to

affect GRFs (Dougill et al., 2006; Yao et al., 2006). In addition, it has been stated that the most severe loading cases occur when jumping on rigid ground (Kasperski and Niemann, 1993). To investigate the effect of surface stiffness experiments consisting of individuals jumping or bobbing on a flexible beam of varying frequency were conducted (Yao et al., 2006). It was observed that subjects struggled to coordinate their activity with the natural frequency of the structure when it was undergoing significant motion. As a consequence, the GRFs decreased significantly, this was referred to as force drop out. It was reasoned that force drop out was caused by the inability of the subjects to push off the structure due to its movement and the psychological fear that they would be flung from the structure.

Harrison et al. (2008) recommended the use of V-notch curves for a given mass and damping ratio to reduce the DLFs of rigid GRFs at resonance frequencies (Figure 3.21).

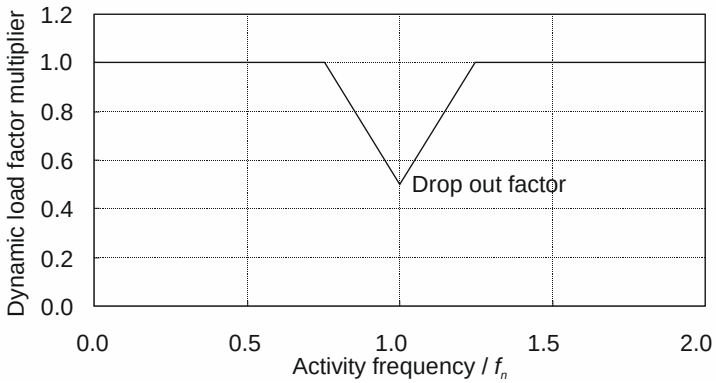

Figure 3.21 V-notch multiplication factor for the DLF to include the force drop out around resonance, for a specific mass and damping ratio (after Harrison et al., 2008)

Experimental crowd DLFs from bobbing on flexible and rigid surfaces (Comer et al., 2013) are compared to those predicted using a model based on rigid GRFs (Figure 3.22). The rigid half cosine model (Parkhouse and Ewins, 2006) tends to underestimate the experimental DLFs as no crowd interaction is considered. The DLFs from rigid surfaces are greater than the equivalent flexible DLFs at the 2nd and 3rd harmonic, however both sets of DLFs are similar at the 1st harmonic. Force drop out cannot be investigated by this work, as the range of bobbing frequencies does not extend to the natural frequency of the empty structure. It is worth

emphasising that these are bobbing DLFs and are smaller, less likely to excite large structural responses which affect the subjects, than equivalent jumping DLFs.

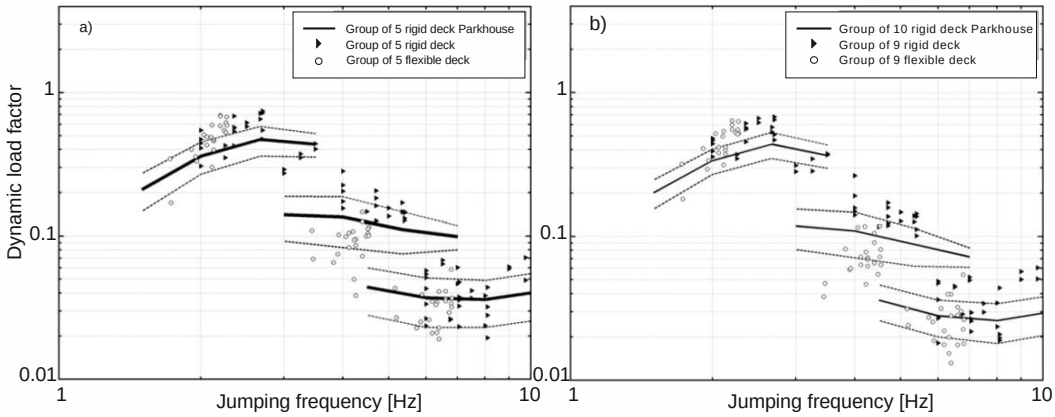

Figure 3.22 Measured DLFs for groups of a)5 and b) 9 people bobbing on rigid and flexible surfaces, compared to predicted DLFs (Parkhouse and Ewins, 2006) (after Comer et al., 2013).

These experiments demonstrate that human behaviour and contact forces on perceivably moving structures are not directly comparable with those on rigid surfaces. Therefore consideration of the HSI is necessary to predict the vibration response of flexible structures accurately.

The mass ratio of the crowd and structure affects the extent of HSI and the response of the structure (Harrison et al., 2008). Lighter, flexible structures occupied by a large crowd are often characterised by a high mass ratio. In this case, the structure is more vulnerable to the movements of the occupants and may vibrate excessively. Figure 3.23 shows that the contact forces differ with regard to mass ratio (Dougill et al., 2006). It can be seen that the DLFs measured on a rigid surface can both over and under-estimate the contact forces occurring on a flexible structure. The most extreme differences occur for crowds with a high human to structure mass ratio. The mass ratio and acceleration response do not increase at the same rate. It has been demonstrated that a 100 times increase in mass ratio corresponds to a 30 times increase in acceleration (Dougill et al., 2006). From this it can be deduced that a perfectly synchronised crowd of N individuals would be unable to excite a response which is N times greater than the response from one individual. Previously, lack of crowd coordination

was credited with the un-proportional structural response to corresponding crowd size, however the response is also affected and limited by the mass ratio.

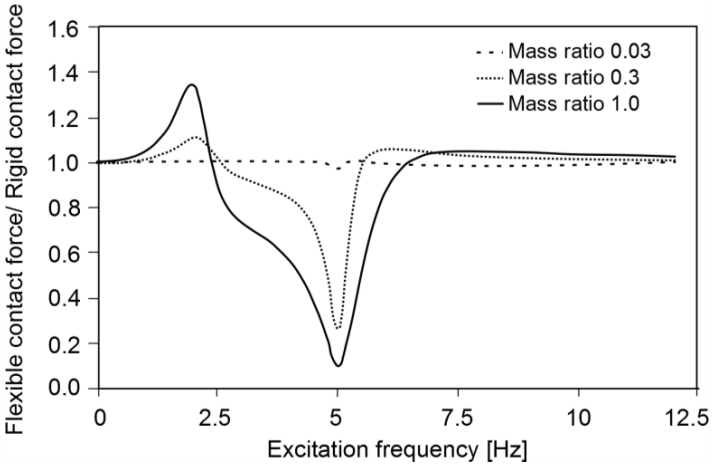

Figure 3.23 The ratio of flexible contact forces to rigid contact forces (after Dougil et al., 2006).

3.2.3 Combination Models

As previously discussed the original method of modelling a crowd was as an external load upon a structure. With the increased understanding of HSI more authors are considering the effects of the human and structural movements upon one another. One of the shortfalls of the models presented in Section 3.2.1 is their reliance upon experimental GRFs collected using a force plate. A force plate is comprised of stiff, thin platform dynamometers or stiff, simple structural elements, and is therefore a rigid base, designed not to vibrate in reaction to human movements (Dougill et al., 2006). The data collected as the basis for these force models adopts the assumption that GRFs from rigid and flexible surface are equivalent, which is not always the case (Dougill et al., 2006; Yao et al., 2006). As a consequence new models that utilise GRFs measured on flexible surfaces, or that model human body dynamics directly are emerging.

Comer et al. (2013) carried out crowd simulations using the time histories from groups of 5 to 15 people bobbing on flexible and rigid surfaces. The model was based on the half-cosine model (Parkhouse and Ewins, 2006) reviewed in Section 3.2.1, however they included the power from the synchronised and stochastic components of crowd time histories (Figure 3.24).

When compared to measured crowd loads (white lines) Comer et al.'s synthesised load (solid black) was more conservative than the equivalent synchronised loading using crowd force time histories (dashed line). However, the synthesised load still underestimated the force for a significant number of cycles. As surface specific GRFs were used the model is a better reflection of real dynamic forces. Crowd interaction is included as the force time histories are from groups of people bobbing together.

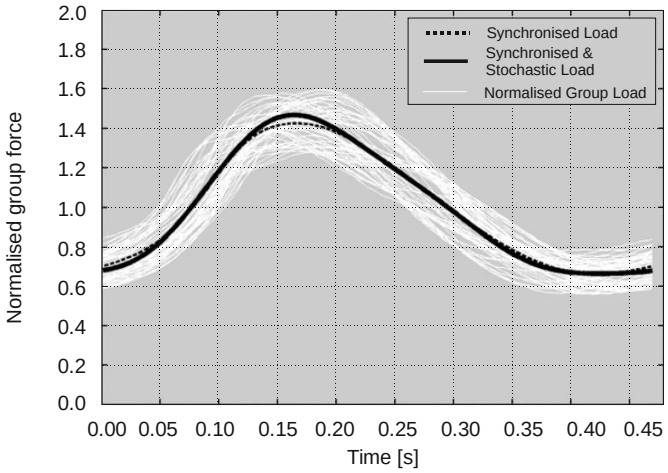

Figure 3.24 The normalised group loading of a bobbing crowd modelled using the equivalent synchronised load and both the synchronised and stochastic components, compared to normalised cycles of crowd load (after Comer et al., 2013).

Another proposed approach is a combined SDOF structure-jumper model with a varying mass (Nhleko et al., 2008), shown in Figure 3.25. The mass variation is dictated by a semi-sine function representing the impact and flight phases of the jumping subject. The methodology is an improvement on a previous step-function varying mass model (Ebrahimpour and Sack, 1992). The latter approach is problematic as it implies that the mass transfer of the jumper onto the structure is instantaneous.

At lower jumping frequencies large contact ratios and a variety of different shaped GRF profiles occur (Nhleko et al., 2008; Sim et al., 2008). To model jumping at low frequencies Nhleko et al. (2008) introduced, impulse shape factors λ_1 and λ_2.

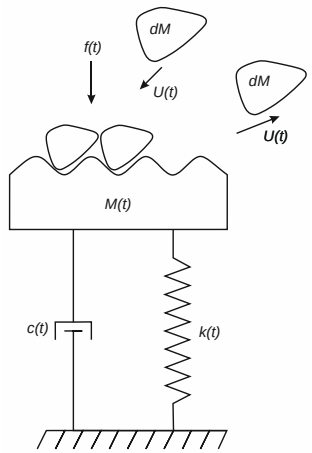

Figure 3.25 Combined SDOF structure-jumper model with a varying mass, where $c(t)$ is the structural damping coefficient, $k(t)$ the structural stiffness and $M(t)$ is the structural mass, all as functions of time. dM is a mass element of the jumper and $U(t)$ is the velocity it is added to, or leaves the system. The input force in the system is $f(t)$ (after Nhleko et al., 2008).

They identified the impulse shape factors by fitting the model to experimental force profiles of five individuals jumping at different frequencies on a flexible beam (Nhleko et al., 2008). The shape factors are used alongside a specified contact ratio to determine the waveform of the GRF profile. Figure 3.26 shows that it is possible to achieve diverse shapes to better account for the GRF variation with regards to jumping frequency. However, within Section 2.2.2 it was demonstrated that the shape of the GRF when jumping at 1.5Hz is changeable between individuals (Sim et al., 2005). Therefore, one set of frequency dependant impulse shape factors is insufficient to represent the general population when jumping at a specific frequency. Further work to establish the distribution of λ_1 and λ_2 is required, this would account for inter-subject variability.

When using this model to predict dynamic loads underestimations of the experimental loads occurred. However, it should be noted that the factors are based on experimental studies on a flexible surface allowing consideration of the HSI.

Another class of HSI models assumes that a person can be modelled as a DOF system within a combined human-structure model (Figure 3.27). The model allows the human and structural

properties to be modelled separately and combined to account for their interaction on each other (Sachse et al., 2002).

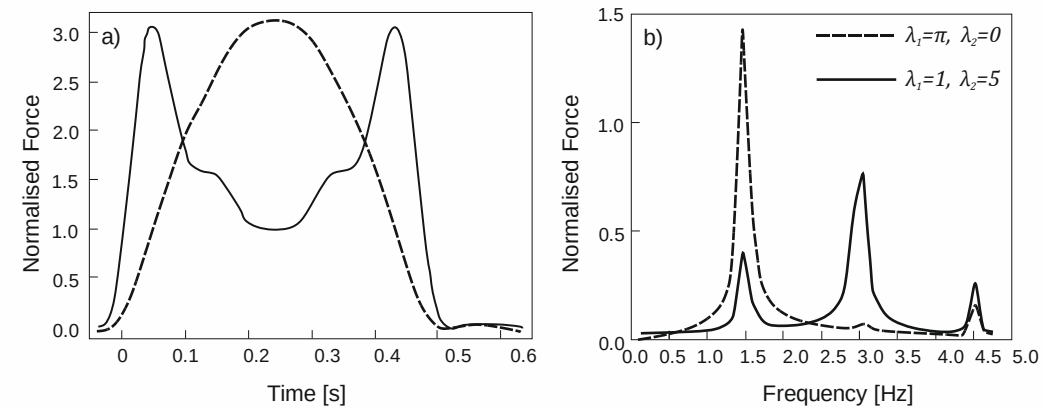

Figure 3.26 The effect of impulse shape factors (λ_1 and λ_2) on the a) force profile and b) its dominant harmonic for a given jumping frequency (f=1.5 Hz) and a contact ratio (α=0.725) (after Nhleko et al., 2008).

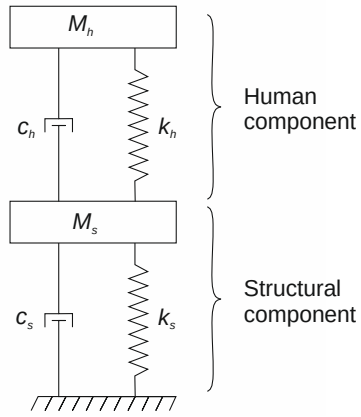

Figure 3.27 A 2DOF human ($_h$) structure ($_s$) model (after Sachse et al., 2002).

Sim (2006) adapted 2DOF passive models of individuals sitting and standing (Wei and Griffin, 1998) and a 1DOF cantilever stand model to form a combined 5DOF crowd and stadium model. The crowd properties used were based on experimental observations of individuals subjected to vibrations (Wei and Griffin, 1998). Feedback loops were used to reflect the effect of the structural movements on the crowd forces and vice versa. Natural frequency and response reduction charts (Figure 3.20) were created from the simulations and can be used to aid quantification of structural responses.

For structures with natural frequencies up to 4Hz it was found that a SDOF system with altered Human-Structure properties was able to reproduce the natural frequencies and response reduction values, found using the 5DOF model (Sim, 2006). Above 4Hz a 3DOF model, including SDOF systems to represent the standing and sitting crowds and the stand provided a good fit. The 3DOF passive model can be used in conjunction with Monte Carlo simulations of the active crowd using the five parameter model described in Section 3.1.3 to form a complete crowd model.

Dividing the crowd in this manner facilitates the application of different body properties to the active and passive crowd portions (Jones et al., 2011b). The overall damping coefficient benefits from the influence of the passive crowd, without ignoring the negative effects of the active crowd. However, it is worth noting that the simulated jumping forces are based on force time histories from individuals jumping on a rigid force plate, therefore no crowd interaction or HSI is included. Furthermore only individuals synchronised to the beat were considered in the pre-model analysis therefore representing a worst case high synchronisation scenario.

A similar approach (Figure 3.28) is used in the current UK recommendations for stadium design (UK Working Group, 2008). A more detailed representation of the model for crowd bobbing is shown in Figure 3.29. The crowd induced bobbing forces are modelled as an internal driver that causes the body and structural motion, and is consequentially influenced by both structural and human vibration. Dougill et al. (2006) derived a relationship between the normalised internal (sinusoidal) driving force $G(t)$ and the normalised contact force $F(t)$. The relationship reflected the modal mass of the system. The internal (driver) force was calibrated using GRFs collected from rigid surfaces (Parkhouse and Ewins, 2004, 2006). The natural frequency of the body unit was determined by assuming the peak contact and internal force ratio occurred when bobbing at the body's natural frequency (Figure 3.30). The mean natural frequency and damping of individuals bobbing was found as 2.3Hz and 25%.

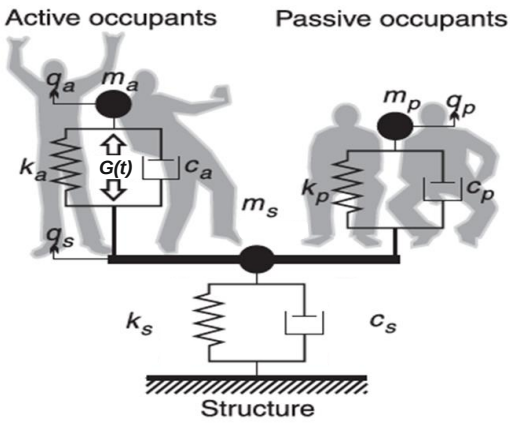

Figure 3.28 A 3DOF model representing passive ($_p$) and active ($_a$) occupants and the structure ($_s$), where *q* represents displacement and *G(t)* the internal driving force (adapted from Jones et al., 2011b).

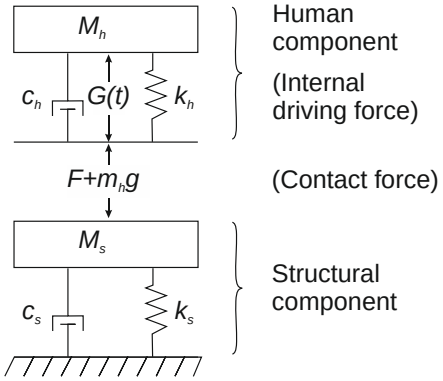

Figure 3.29 2DOF crowd model (after Dougill et al., 2006).

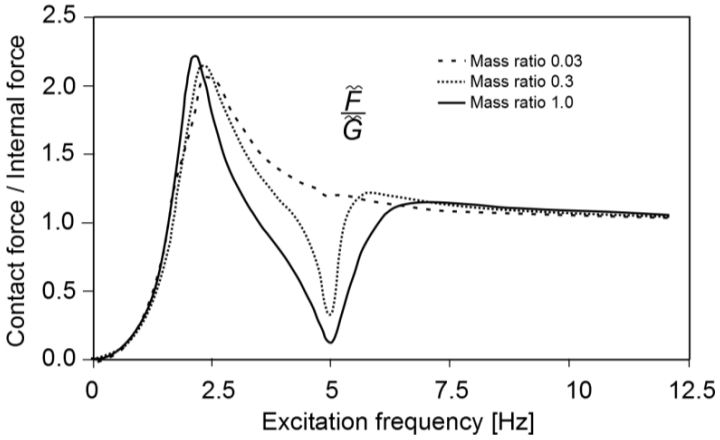

Figure 3.30 The relation between contact and internal force for different mass ratios (after Dougill et al., 2006).

The internal force was assumed to be independent of surface. As both the internal and the contact forces are periodic they can be described using the Fourier series. The frequency

independent Fourier coefficients G_n that describe the internal force are known as Generated Load Factors (GLFs) and are essentially DLFs which consider the HSI (Table 3.7).

Table 3.7 The GLF of the internal driver forces, where the human body properties are f_n = 2.3Hz and ζ=25% (after Dougill et al., 2006).

Group size N	GLFs G_n 1st harmonic	2nd harmonic	3rd harmonic
5	0.286	0.095	0.033
10	0.242	0.075	0.024
20	0.217	0.064	0.018
50	0.199	0.057	0.013
100	0.194	0.055	0.010
200	0.191	0.054	0.008

Experimental contact forces from bobbing on flexible surfaces are compared to those predicted using the GLFs and the internal and contact force relationship in Figure 3.31. In general a good fit is seen, however the peak DLFs are overestimated for one person bobbing Figure 3.31a) and underestimated for groups bobbing Figure 3.31b) and c). It is likely the group DLFs are underestimated as the GLFs are based on individual force time histories, without group interaction. Force drop out can be seen in Figure 3.31a) at the 2nd harmonic. The DLFs of the 2nd harmonic approaching the natural frequency of the system are underestimated, however at the natural frequency and above it good DLF predictions are seen. Further comparisons between real GRFs would best identify whether the GRFs in Figure 3.31 are typical and amendments to the model are required.

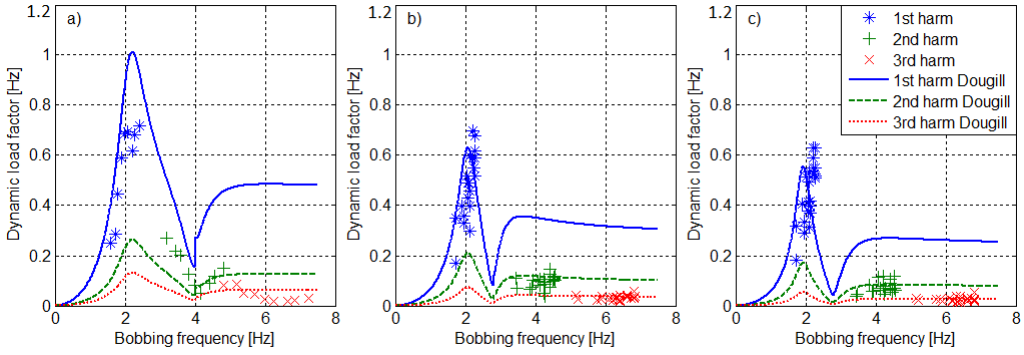

Figure 3.31 The predicted contact force DLFs (Dougill et al., 2006) compared to experimental DLFs from flexible surfaces for a) 1 person on a beam where f_n=4Hz, ζ=4%, mass ratio (μ)=0.2 (Yao et al., 2006) b) 5 people on a flexible stadium simulator where f_n=2.8Hz, ζ=3%, μ=0.22 (Comer et al., 2013) and c) 9 people on a flexible stadium simulator where f_n=2.8Hz, ζ=3%, μ=0.4 (Comer et al., 2013).

This model is used in the latest UK recommendations (UK Working Group, 2008) to model the dynamic loads on structures where the lowest relevant natural frequency is below 6Hz. The UK recommendations do not consider structures with a natural frequency above 6Hz to be at risk from human induced dynamic loads. The scenarios presented in Table 3.3 are included in the recommendations to allow a variety of audience responses to be examined. The allowable response accelerations and displacements differ depending on the scenario (Table 3.8). The variations in audience response are predominantly due to the nature of the event, such as a classical concert, or a heavy metal gig. The procedure allows venues to be designed with consideration to the end use, improving on the 'one size fits all' approach seen in previous guidance. To further improve the accuracy of the model, additional crowd units of different properties, as seen in Table 3.8, can be added to represent a variety of crowd behaviours. This allows both passive and active portions of the crowd to be accounted for (Wei and Griffin, 1998; Matsumoto and Griffin, 2003). Crowd units encompass all the individuals within the stands, the load from the crowd and the active crowd members are assumed to be uniformly distributed within each crowd unit.

Table 3.8 The body mass properties for different scenarios from the Working Group's UK recommendations for groups of 50 people, and the allowable RMS values for each scenario (adapted from UK Working Group, 2008 and Parkhouse and Ward, 2010).

Crowd	Event Scenario	Allowable RMS value	f_n (Hz)	ζ(%)	GLFs		
					n=1	n=2	n=3
Seated	Scenario 1		5	40%			
Mostly Seated	Scenario 2	3%g	5	40%	0.12	0.015	0
Active, mostly standing	Scenario 3	7.5%g	2.3	25%	0.188	0.047	0.013
Active, mostly standing	Scenario 4	20%g, 7mm displacement	2.3	25%	0.375	0.095	0.026

When using the crowd units, the body mass m is assumed to be 80kg per person, the stiffness of the unit k is therefore given by:

$$\boldsymbol{k = 4\pi^2 f_n^2 mN} \qquad 3.9$$

where N is the number of individuals contained within the body unit. To reflect the lack of crowd synchronisation a coordination factor, C, is used as a multiplier to the periodic loading.

The factors used within the UK recommendations (UK Working Group, 2008) are frequency dependent and relate to the event scenario (Figure 3.12).

To improve the internal driver model additional research should address the activity of jumping. The model would further benefit from the use of GRFs from individuals within a crowd. Additional GRF experiments upon flexible surfaces are required as limited force profiles are available. Inconsistencies occurred between the GRFs from the same bobbing individuals (Dougill et al., 2006), this highlights the variability in GRF and the necessity for the range and distribution of forces to be found.

Jones et al. (2011a) aimed to verify the applicability of the UK recommendations (UK Working Group, 2008) by using them to calculate the response of a stand and comparing it to the empirical response. They found that the model reproduced the response at the middle of the stand well, while it underestimated the response at other locations (Figure 3.32). In the example considered the dominant mode was antisymmetric. Subsequently the maximum response occurred at the quarter-span points of the stand, resulting in an underestimation by the internal driver model.

The presence of antisymmetric modes suggests the assumption of uniform crowd loading is not always invalid. It was observed from crowds within stadia that the people closest to the source of the music reacted before those in the middle of the stand, and the people at the back of the stand reacted last. The phase shifts between the audience were consistent with the time taken for the music to reach the various sections of the stand (Littler, 2002). The UK recommendations (UK Working Group, 2008) present the lack of coordination as a blanket factor, reducing the overall force magnitude. When this coincides with an antisymmetric mode, the modal forces may cancel out, preventing the simulated antisymmetric mode from excitation.

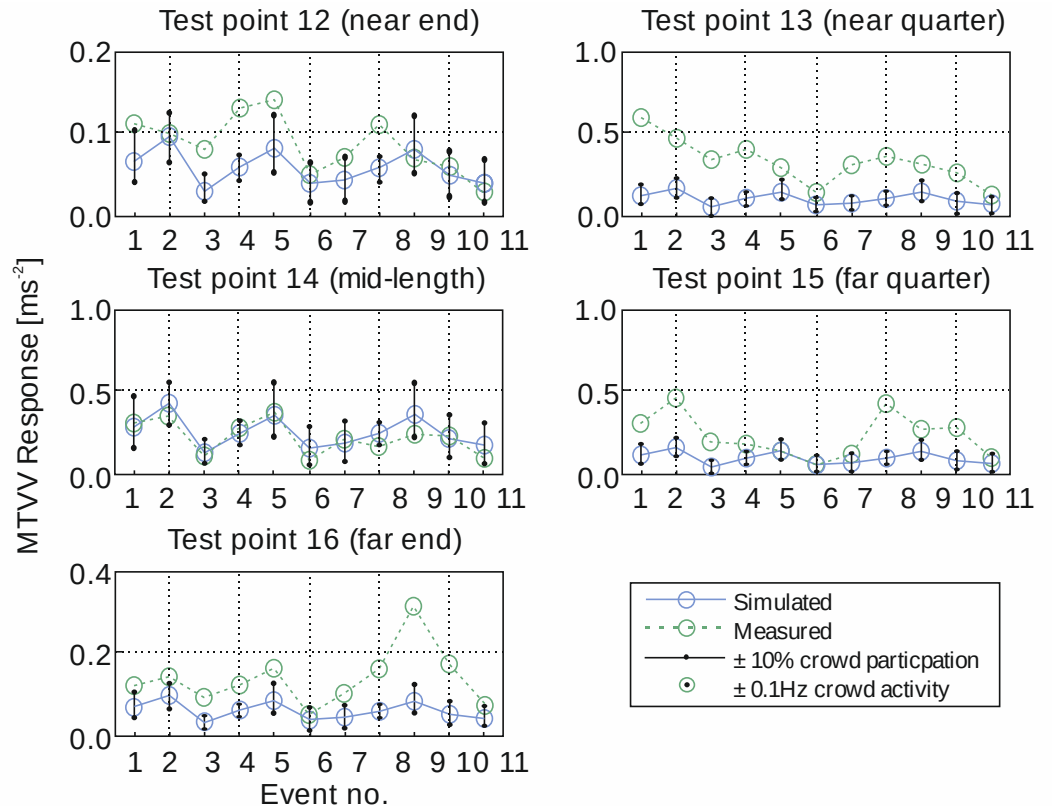

Figure 3.32 Measured and calculated responses using accelerometers and the UK Working Group (2008) model upon the City of Manchester Stadium during sporting events and concerts. MTVV is the maximum transient vibration value, calculated as peak 1 s RMS (after Jones et al., 2011a).

The approaches of the other major stadia guidelines towards HSI are briefly reviewed, and their predicted responses compared to measured values. The Canadian Commentaries (NRC, 2006) assume that low energy activities are typical for stadium environments as groups are unlikely to partake in prolonged coordinated jumping. Reduced load coefficients are utilised to incorporate the low energy activities, the lack of inter-subject coordination and HSI. The recommended DLFs (Table 3.9) are smaller than those of other guidelines and authors. In addition, a damping ratio of 6-12% is suggested to reflect the increased damping due to human occupation. Within this method the human-structure system is not directly modelled but its effects are taken into consideration through the DLFs and damping ratios. The low DLFs and high damping coefficients, published by the NRC, predict structural responses that are similar to the responses measured by Jones et al. (2011a) (Figure 3.33). This guidance also encourages stadia and grandstands design to avoid structural natural frequencies below 6Hz.

Table 3.9 The Canadian Code's recommended loading functions (after NRC,2006).

	Lively concert with seating (0.5m^2/person)	Lively concert no seating
r_1	0.25	0.40
r_2	0.05	0.15
r_3	0.00	0.00

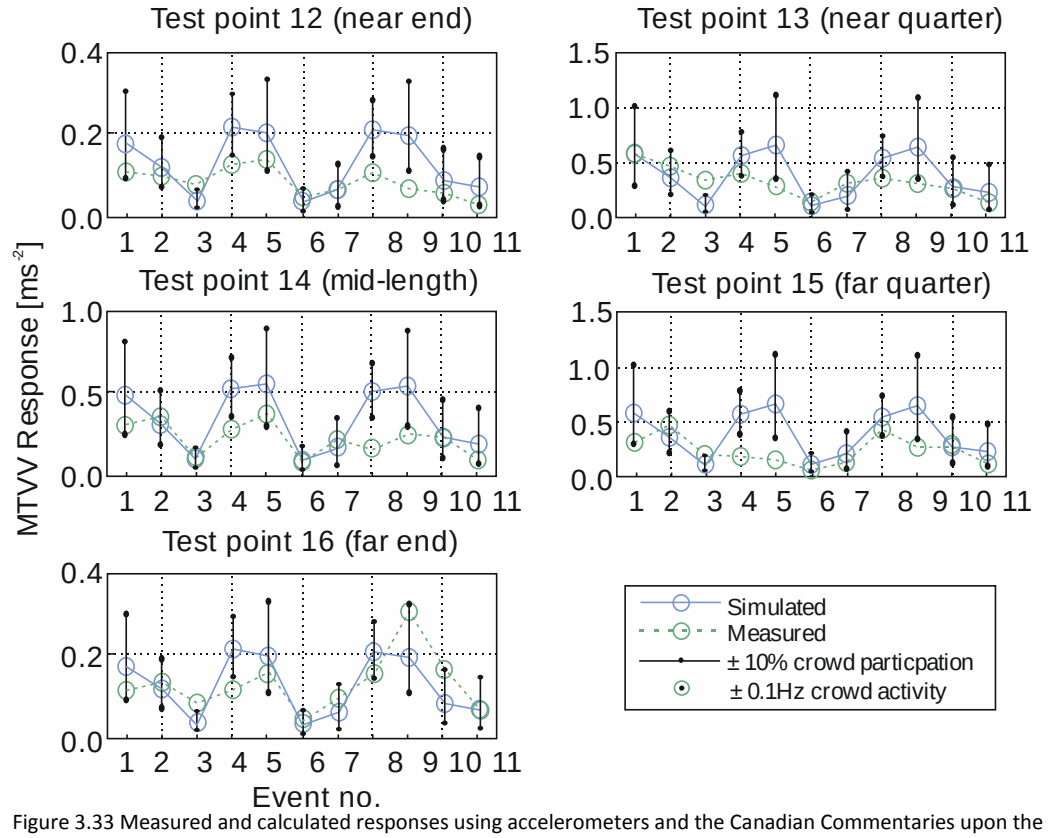

Figure 3.33 Measured and calculated responses using accelerometers and the Canadian Commentaries upon the City of Manchester Stadium during sporting events and concerts. MTVV is the maximum transient vibration value, calculated as peak 1 s RMS (after Jones et al., 2011a).

The ISO (2007) guidance does not take HSI into account, as it aims to represent the worst case loading scenarios. The guidance predicts responses that are unlikely to be observed, but may occur once during the structures lifetime. The calculated structural responses in comparison to those measured by Jones et al. (2011a) are shown in Figure 3.34 and demonstrate this overestimation of loads.

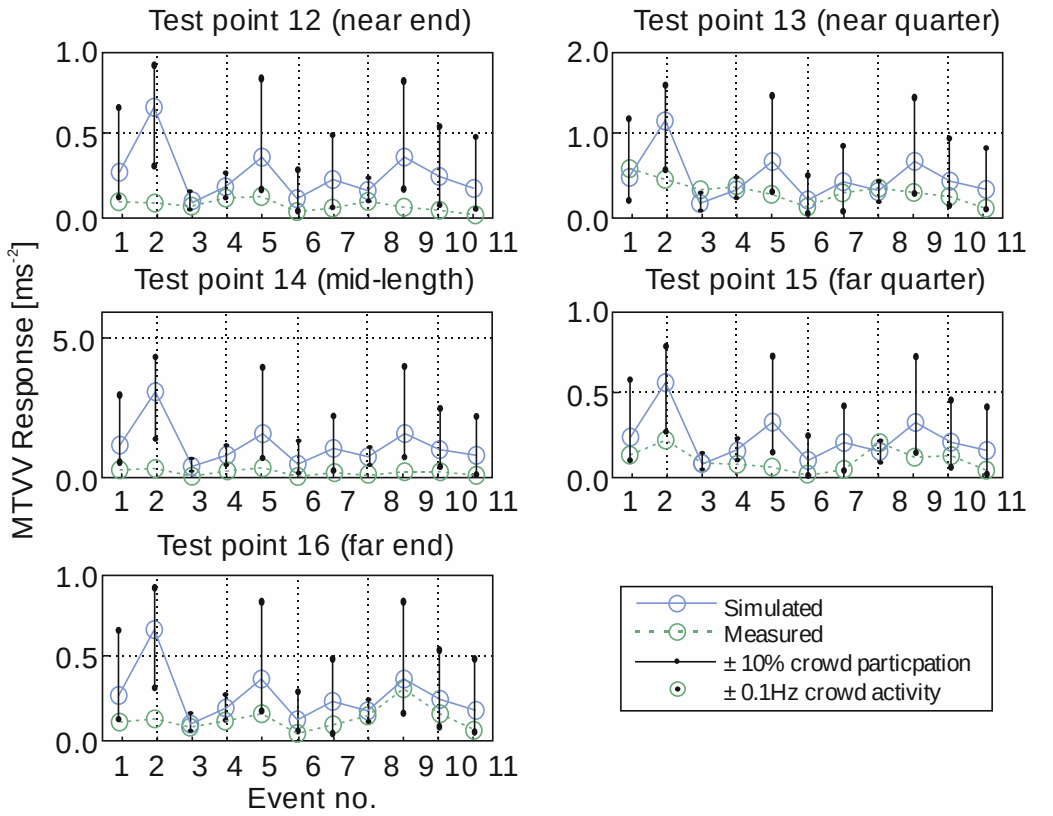

Figure 3.34 Measured and calculated responses using accelerometers and the ISO 2007 approach upon the City of Manchester Stadium during sporting events and concerts. MTVV is the maximum transient vibration value, calculated as peak 1 s RMS (after Jones et al., 2011a).

The guidelines which best reproduce in-situ crowds forces are the Canadian guidance and the UK recommendations. Both encourage the building of stadia with natural frequencies above 6Hz. This recognises that higher harmonic components become less significant within a crowd, and that crowds are unlikely to synchronise at high frequencies. The Canadian guidance provides a simple and effective way of predicting the magnitude of the response, and was able to reproduce the force well in most sections of the stand studied by Jones et al. (2011a). However, the results are sensitive to the frequency of the stadia and the crowd mass which can reduce the precision. The UK recommendations are less sensitive to the input conditions and well replicate the forces in the middle of the stand. However, the process is more complicated than the Canadian guidance and the recommendations were unable to predict the response well at other locations on the stand. These checks were completed upon a single stand, therefore generalisation of conclusions should be made after further verification only.

3.3 Conclusion

In this chapter, different approaches to model dynamic loading from jumping and bobbing crowds and individuals have been reviewed. A semi-sine model is a simple and effective way of representing the general features of the loading (Bachmann and Ammann, 1987). The model was utilised as a basis for representing crowds by many authors. Some incorporated a coordination factor to allow for non-perfect synchronisation between individuals (Hansen and Sørensen, 2002; Kasperski and Agu, 2005). The assumption of uniform loading and a blanket coordination factor simplifies the calculation of the crowd load. However, an alternative method should be sought to allow the various crowd distributions and differences in coordination to be considered. This would prevent antisymmetic modes being over looked.

Other authors incorporated a phase lag between each individual's GRF, to account for inter-subject variability (Wilford, 2001; Ebrahimpour and Sack, 1989). Discrepencies were found in the literature with regard to the statistical distribution of the phase lags. Experiments using small groups were conducted to find the phase lags, then extrapolated to model a crowd. Experiments to determine the phase lags between individuals within larger groups, would better inform the engineering community.

One of the main shortfalls of the semi-sine model is its periodic nature which assumes no intra-subject variability. A possible consequence of this assumption is the over or under estimation of the DLFs. The model is a good representation of jumping at mid to high frequencies (2-3.5Hz). A large variety of GRF shapes are seen at low frequency jumping, rendering the semi-sine representation inappropriate at certain frequencies.

Attempts were made to adjust the shape of the GRF profile for different jumping frequencies (Nhleko et al., 2008; Racic, 2009). An intra-subject variability component was included in some models to tackle the variability of jumping frequency (Sim et al., 2008; Racic, 2009). The most successful method of recreating an individual jumping GRF is the many Gaussian model as

intra-subject variability is thoroughly considered. Unfortunately the model requires a pre-prepared database of jumping GRFs which is currently unavailable in the public domain. Adapting the model to consider flexible surfaces or jumping within a group would be difficult, as a further database of GRFs would be required.

Further efforts to models human loading were attempted using DOF systems. The integration of HSI and combined human-structure dynamic properties was seen within some models (Dougill et al., 2006).

The current UK recommendations utilise a bobbing internal driver model (Dougill et al., 2006) that incorporates an internal force to account for the actions of the crowd on the structure. The model considers the human to structure mass ratio, and therefore allows the GRFs upon structures of varying flexibilities to be modelled. Crowd coordination factors can be incorporated to expand this model for crowd use. This approach addresses the deficit of flexible surface crowd models, but further work to validate the GRFs on flexible surfaces is required. In addition the model does not reflect the interaction between people and a uniform load distribution is assumed. Within the UK recommendations (UK Working Group, 2008) the crowd coordination factor is applied universally to the internal driver model, causing antisymmetic modes to be overlooked.

Examining the contents of this review, it is apparent that experiments investigating the synchronisation within groups of people are required. This shortage is addressed in Chapter 7 where the synchronisation from groups of 2, 4 and 8 subjects is quantified.

More observations of real crowds would better allow the incorporation of human-to-human interaction into the structural design process. In addition more experiments upon on flexible surfaces would increase the understanding of the effect of surface and allow its incorporation within jumping models. To aid these goals a novel indirect group force measurement technique is proposed in Chapters 5 and 6.

Incorporating the intra-subject variability within force models should be more accessible. Studying the GRFs of different individuals and monitoring how the force time histories vary in Chapter 4, will improve understanding of intra-subject variation and its incorporation within models.

4 Characterising the Activities of Jumping and Bobbing

The purpose of this chapter is to investigate the relationships between different characteristics of jumping and bobbing loads. Ground reaction forces (GRF) collected from a force plate are analysed to observe any patterns or trends. In addition the variation between test subjects (TS) known as the inter-subject variation (IESV), and the variation of a TS with themselves, known as the intra-subject variation (IASV) are observed for different properties of jumping and bobbing. A main focus of this Chapter is quantifying the IASV across a group of TSs as the IASV has often been over looked by previous authors and in force models. This insight will allow future models to reflect the realistic characteristics of individuals jumping or bobbing. This work will be partly published in a 2016 conference publication (Zivanovic et al., 2016).

4.1 Experimental Procedure

Eight test subjects (TS), four males and four females (Table 4.1), jumped and bobbed individually on an AMTI Biomechanics Force Platform OR6 (AMTI, 2007) which measured the GRF at a sampling rate of 1000Hz. A metronome was used to dictate the target jumping frequencies, 1, 2 and 3Hz for jumping and 1, 2, 3 and 4Hz for bobbing. The length of each trial was 20s, hence the minimum number of cycles recorded was approximately 20. In total 24 trials of jumping and 32 trials of bobbing were recorded. In addition, the TSs' displacements were recorded using a marker placed on the C7th vertebra (Figure 4.1 and Chapter 5), which was monitored at 200Hz using a VICON motion capture system (Oxford Metrics Group, 2007). The C7th vertebra was chosen as it was thought likely to track the holistic body movement well, without the additional localised movements which may be introduced if monitoring the head. Both the GRFs and the trajectories were filtered using a 5^{th} order Butterworth filter. The cut-off frequency of the filter was 1Hz above the frequency of the 3^{rd} forcing harmonic or 7Hz, whichever was the larger.

Table 4.1 TS physiological data.

TS	1	2	3	4	5	6	7	8
Sex	M	F	M	F	F	M	M	F
Body mass (Kg)	83	70	83	65	66	85	73	68
Height (m)	1.85	1.82	1.80	1.76	1.74	1.71	1.76	1.66
BMI (Kgm^{-2})	24.4	21.1	25.8	21.0	21.8	29.1	23.6	24.8

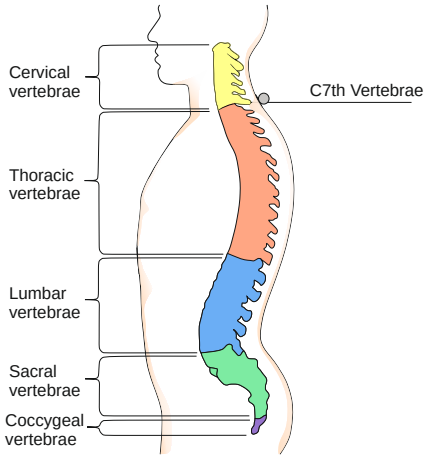

Figure 4.1 The human spine and vertebrae and the motion capture marker placement.

4.2 Jumping Characterisation

Within this section variations in the jumping frequency f_J, peak forces $F_{J,Peak}$, dynamic load factors (DLFs), impulses and the contact ratios CR_J of the jumping GRFs are discussed. The intra-subject variation (IASV), and the variation between the TSs (inter-subject variation IESV) are considered. In addition, the inter-intra-subject variation (EIASV) which is the variation of the IASV between the TSs is investigated. Physiological factors which may affect the peak forces are considered. The displacements of the jumps are analysed to investigate TS variation and the relationships between displacements and peak forces and TS height. If a variable is specific to a TS the subscript $_{TS}$ is used, the subscript $_O$ is used to denote an overall value considering all the TSs. To ensure comparable peak forces between the TSs, the GRFs within this chapter are normalised by the TS's weight.

4.2.1 Variations in Jumping Frequency

The average frequency and the frequency of each jump, calculated as the reciprocal value of the time elapsed between the points of zero force at the flight stage (Figure 4.2), were found. In Figure 4.3a the average TS jumping frequencies are plotted against target frequency. The overall mean jumping frequency and the mean ± 1 standard deviation (STD) from the population of 8TSs are plotted by square and circular marker respectively, this representation will be used throughout the chapter.

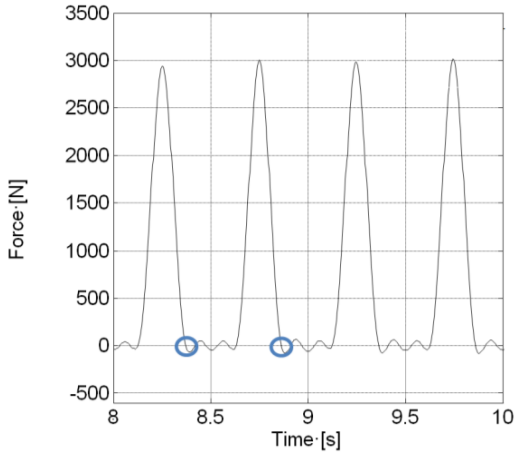

Figure 4.2 A measured GRF from jumping with a single jumping cycle marked.

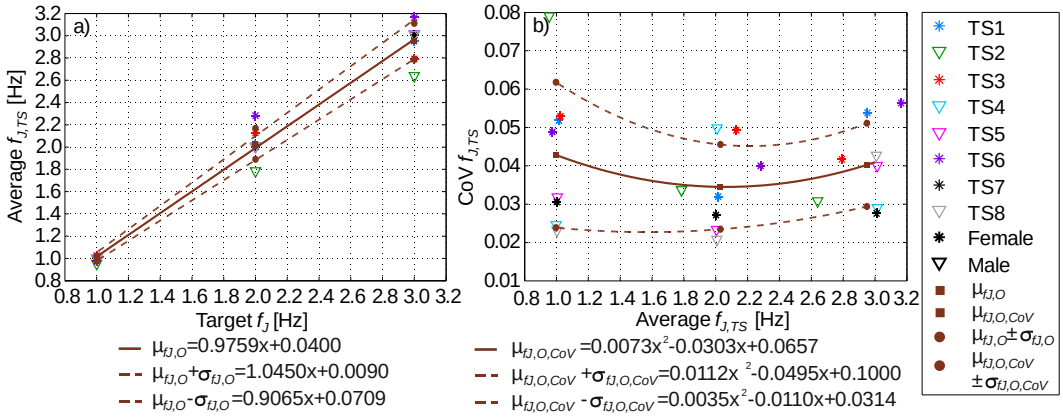

Figure 4.3 a) The average TS jumping frequency and target frequency, the mean $f_{J,O}$ ($\mu_{fJ,O}$) and the mean ± 1STD ($\mu_{fJ,O}\pm\sigma_{fJ,O}$) are approximated and the equations listed. b) The CoV of $f_{J,TS}$ and average $f_{J,TS}$, the relationships between f_J and the mean CoV values ($\mu_{fJ,O,CoV}$) and the mean ± 1STD ($\mu_{fJ,O,CoV}\pm\sigma_{fJ,O,CoV}$) are aproximated.

The distribution of the cycle-by-cycle jumping frequencies of each TS were investigated for each target frequency. The Anderson-Darling (AD) test was used to test for normality. 79.2% of the trials passed the 5% significance level of the test and therefore the majority of $f_{J,TS}$ data can

be considered as normally distributed. The skewness and excess kurtosis of the distributions were investigated. For a normal distribution both values equal zero (Press et al., 1996), however the skewness and kurtosis of a distribution of size N is only considered significant if the value is twice as large as the standard error of skewness (SES) or the standard error of kurtosis (SEK) respectively (Lomax and Hahs-Vaughn, 2013):

$$\boldsymbol{SES} = \sqrt{\frac{\boldsymbol{6N(N-1)}}{\boldsymbol{(N-2)(N+1)(N+3)}}} \quad 4.1$$

$$\boldsymbol{SEK} = \boldsymbol{2(SES)}\sqrt{\frac{\boldsymbol{N^2-1}}{\boldsymbol{(N-3)(N+5)}}} \quad 4.2$$

87.5% of the trials had skewness values below 2*SES and 95.8% of trials had a kurtosis value less than 2*SEK. The low skewness and kurtosis values from the majority of trials are consistent with normally distributed data.

The coefficient of variation (CoV) is a measure of each TS's IASV and is calculated for each individual by normalising the STD of the data set by the average value (Figure 4.3b). The CoV facilitates the comparison of the data spread irrespective of the average value of the data set, therefore allowing trials of different jumping frequencies to be compared. The $f_{J,TS}$ CoV values for each TS and target frequency are displayed in Table 4.2. The frequencies at which the largest and smallest CoV values occur vary between TSs, therefore there is not one target frequency which is solely responsible for the worst or best IASV. In general 1Hz and 3Hz have the highest IASV values, suggesting a lot of TS frequency variation. The lower CoV values at 2Hz suggest more consistency.

The EIASV quantifies the range of IASV at each frequency, using the mean and the STD of the $f_{J,TS}$ CoV values (Table 4.2). Both variables are needed to address the magnitude of the variation and the differences in variation between TSs. In Figure 4.3b the relationship between the EIASV and jumping frequency has been approximated by three 2nd order polynomials found using the linear least squares method (LLSM). On average the most TS variation (mean of $f_{J,TS}$ CoV =0.043, Table 4.2) and the largest differences in EIASV between TSs occurred at 1Hz

(STD of $f_{j,TS}$ CoV =0.019). Hence some TSs were able to perform the activity relatively consistently (CoV (IASV)=0.023) and others demonstrated more significant frequency variation between jumps (CoV (IASV)=0.079). On average the TSs' jump frequencies were most consistent at 2Hz (mean of $f_{j,TS}$ CoV =0.035, Table 4.2). At 2 and 3Hz the variation demonstrated by each TSs was most consistent with one another (STD of $f_{j,TS}$ CoV =0.011, Table 4.2).

Table 4.2 The average, STD and COV values of the $f_{j,TS}$. The EIASV (hatched background) and IESV (highlighted) are marked. The markers denote gender (* male, ▽ female).

	1Hz			2Hz			3Hz		
TS	**Ave (Hz)**	**STD (Hz)**	**COV (IASV)**	**Ave (Hz)**	**STD (Hz)**	**COV (IASV)**	**Ave (Hz)**	**STD (Hz)**	**COV (IASV)**
1 *	1.02	0.053	0.052	2.02	0.064	0.032	2.95	0.159	0.054
2 ▽	0.95	0.075	0.079	1.79	0.060	0.034	2.64	0.081	0.031
3 *	1.03	0.054	0.053	2.13	0.105	0.049	2.79	0.116	0.042
4 ▽	1.00	0.025	0.025	2.01	0.100	0.050	3.01	0.088	0.029
5 ▽	1.00	0.032	0.032	2.00	0.047	0.023	3.01	0.121	0.040
6 *	0.97	0.048	0.049	2.28	0.091	0.040	3.16	0.178	0.056
7 *	1.00	0.031	0.031	2.00	0.054	0.027	3.01	0.083	0.028
8 ▽	1.00	0.023	0.023	2.01	0.042	0.021	3.01	0.129	0.043
Mean (Hz)	1.00	0.043	0.043	2.03	0.070	0.035	2.95	0.119	0.040
STD (Hz)	0.03	0.018	0.019	0.14	0.025	0.011	0.16	0.036	0.011
CoV	0.03	0.421	0.440	0.07	0.351	0.321	0.05	0.299	0.266
Single f_j	Lowest (Hz)	Largest (Hz)	Range (%f_j)	Lowest (Hz)	Largest (Hz)	Range (%f_j)	Lowest (Hz)	Largest (Hz)	Range (%f_j)
	0.83	1.14	31%	1.67	2.43	38%	2.43	3.52	36%

The IESV was measured using the CoV of the average $f_{j,TS}$ values. The IESV was smallest at 1Hz (0.03, Table 4.2) therefore, although the most EIASV occurred, the average jumping frequencies of the TSs were most consistent with one another. The greatest IESV occurred at 2Hz (0.07, Table 4.2). The TSs were able to maintaining their jumping frequency well, however were targeting slightly different frequencies from one another hence the large average frequency variations between TSs.

At 1Hz all TSs were on average within 5% of the target frequency, consistent with previous authors who observed the greatest TS synchronisation at 1Hz (Sim et al., 2005). The number of TSs achieving the target frequency ± 5% reduced to 5/8 at both 2 and 3Hz (Table 4.2). The TSs whose frequencies were within ±5% were mostly consistent between the different target frequencies. This indicates that TSs are likely to be consistently poor or consistently good at

synchronising with a beat. Of those TSs with average frequencies outside of 5% more TSs underestimated the target frequency at 3Hz (2/8), whereas more overestimations were seen at 2Hz (2/8). There was little consistency of TSs over or underestimating the frequency. It is worth noting that the number of TSs achieving the exact target frequency reduced with increasing frequency. The implications from these observations are that jumping at the target frequency is more achievable at 1Hz. Synchronisation with the target beat is as likely at 3Hz as it is at 2Hz, consistent with Sim et al. (2005). Furthermore, frequency overestimations are more likely at 2Hz, and underestimations more common at 3Hz.

The TSs' jumping frequencies were analysed by gender in Table 4.3. The STDs from the female TSs were on average smaller, suggesting greater ability in maintaining a specific jumping frequency. At 1 and 2Hz male TSs tended to jump faster than the target frequency, whereas on average female TSs were slower (Table 4.3). At 3Hz both genders on average jumped below the target frequency.

Table 4.3 The mean and STD of the frequency normalised by target frequency comparing male and female TSs

	1Hz		2Hz		3Hz	
	Mean normalised average	**Mean normalised STD**	**Mean normalised average**	**Mean normalised STD**	**Mean normalised average**	**Mean normalised STD**
Mean	1.00	0.043	1.02	0.035	0.98	0.040
Mean Male	1.01	0.047	1.05	0.039	0.99	0.045
Mean Female	0.99	0.039	0.98	0.031	0.97	0.035

4.2.2 Variations in the Peak Force

The average peak forces for each TS are shown in Figure 4.4a. On average the smallest peak forces occur at 1Hz and the largest at 2Hz. The lines of best fit were approximated using a 2nd order polynomial and LLSM.

An AD test revealed that the peak forces from 83% of the trials were normally distributed. All the trials had skewness values below 2*SES, consistent with normally distributed data. However, only 45.8% of trials had an excess kurtosis value less than 2*SEK. The kurtosis is not

the most reliable test for normality (Press et al., 1996) and is sensitive to sample size which may have influenced the values.

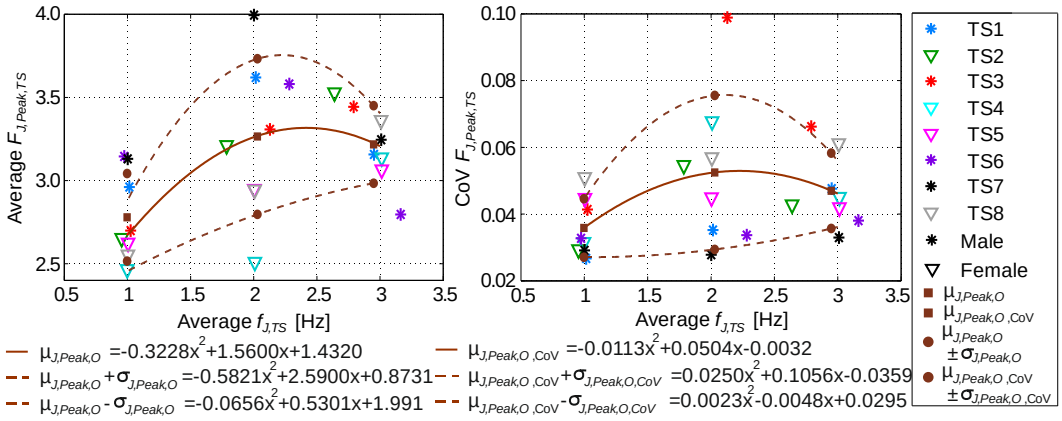

Figure 4.4 a) The average peak forces and jumping frequency, the mean $F_{J,Peak,O}$ ($\mu_{J,Peak,O}$) and the mean ± 1STD ($\mu_{J,Peak,O} \pm \sigma_{J,Peak,O}$) are approximated and the equations listed. b) The CoV of $F_{J,Peak,TS}$ and average $f_{J,TS}$, the relationships between f_J and the mean CoV values ($\mu_{J,Peak,O,CoV}$) and the mean ± 1STD ($\mu_{J,Peak,O,CoV} \pm \sigma_{J,Peak,O,CoV}$) are aproximated.

The smallest values of IASV (CoV of $F_{J,Peak,TS}$) occurred at 1Hz, indicating consistent TS peak forces. The largest values were split between 2 and 3Hz suggesting more jump-by-jump peak variation at these frequencies. On average the most peak force EIASV (mean of $F_{J,Peak,TS}$ CoV =0.052, Table 4.4) and the largest differences in EIASV between TSs (STD of $F_{J,Peak,TS}$ CoV =0.023) occurred at 2Hz. The spread of TS peak forces can be visualised by the range of CoV values in Figure 4.4b. The smallest EIASV occurred at 1Hz, the mean and STD of the $F_{J,Peak,TS}$ CoV values were 0.036 and 0.009 respectively. The TSs maintained consistent peak forces within their own jumping trials, and this variation was consistent between TSs.

The IESV was assessed using the CoV of the average $F_{J,Peak,TS}$. The least IESV occurred at 3Hz (0.07, Table 4.4), indicating the most consistent average peak forces between TSs. The largest IESV, 0.14, occurred at 2Hz, double the value seen at 3Hz. In addition a wider range of peak forces (2.07) at 2Hz was seen. These factors both demonstrate a greater spread of peak forces between TSs at 2Hz, a frequency deemed easy to jump at (Ginty et al., 2001). This is likely because 2Hz is a mid-frequency and a range of jumping actions, and therefore peak forces are

possible. There is enough time allocated for each jump for some degree of personal preference to affect the force time history. TSs have the ability to perform both high and low force jumps.

Table 4.4 The average, STD and COV values of the $F_{J,Peak,TS}$. The EIASV (hatched background) and IESV (highlighted) are marked. The markers denote gender (* male, ▽ female).

	1Hz			2Hz			3Hz		
TS	**Ave**	**STD**	**COV (IASV)**	**Ave**	**STD**	**COV (IASV)**	**Ave**	**STD**	**COV (IASV)**
1 *	2.96	0.079	0.027	3.62	0.127	0.035	3.16	0.150	0.048
2 ▽	2.65	0.078	0.029	3.21	0.175	0.055	3.53	0.151	0.043
3 *	2.70	0.112	0.041	3.31	0.327	0.099	3.44	0.228	0.066
4 ▽	2.47	0.078	0.032	2.51	0.170	0.068	3.14	0.141	0.045
5 ▽	2.63	0.118	0.045	2.95	0.133	0.045	3.07	0.129	0.042
6 *	3.14	0.103	0.033	3.58	0.121	0.034	2.80	0.106	0.038
7 *	3.13	0.091	0.029	3.99	0.111	0.028	3.25	0.107	0.033
8 ▽	2.55	0.130	0.051	2.94	0.168	0.057	3.36	0.206	0.061
Mean	2.78	0.099	0.036	3.26	0.166	0.052	3.22	0.152	0.047
STD	0.26	0.020	0.009	0.47	0.069	0.023	0.23	0.044	0.011
CoV	0.09	0.205	0.245	0.14	0.417	0.440	0.07	0.288	0.241
Peak	Lowest	Largest	Δ	Lowest	Largest	Δ	Lowest	Largest	Δ
force	2.30	3.31	1.01	2.15	4.22	2.07	2.58	3.88	1.30

At 1 and 2Hz larger peak forces were seen from the male TSs (*) than from the female TSs (▽) (Figure 4.4a). This is potentially due to physiological gender differences, as men are typically larger and more muscular. At 1Hz the mean value of the peak force from female TSs was 2.57 compared to 2.98 from male TSs (Table 4.5). The discrepancies were greatest at 2Hz where the female and male mean peak values were 2.90 and 3.63 respectively. However, there was little gender based distinction between the peak forces at the highest jumping frequency of 3Hz. There was no obvious link between consistency of peak force and gender (Table 4.5).

Table 4.5 The means and STDs for the normalised peak forces comparing male and female TSs.

	1Hz		2Hz		3Hz	
	Mean	**STD**	**Mean**	**STD**	**Mean**	**STD**
Mean	2.78	0.099	3.26	0.166	3.22	0.152
Mean Male	2.98	0.096	3.63	0.172	3.16	0.148
Mean Female	2.57	0.101	2.90	0.161	3.27	0.157

These findings indicate that the magnitudes of the peak forces are not solely the product of TS weight, differences in physiology can affect them.

4.2.3 Other Physiological Factors

Physiological factors that may affect the peak forces such as gender, weight and height are investigated within this section. Figure 4.5a, b and c shows the relationship between the average peak force and TS weight at each target frequency. At 1 and 2Hz there is a suggestion of a weak positive correlation between the TSs' weight and $F_{J,Peak,TS}$. If the correlation holds true for a larger sample size it is likely that heavier TSs have higher normalised peak forces due to larger and stronger leg muscles facilitating greater push off forces. However, this may only be the case in healthy and not obese TSs. At 3Hz there is potentially a positive correlation amongst the female TS, the correlation is strongest amongst the female test population at all frequencies. It is also worth noting that the weight range of the female TSs was considerably smaller (65kg-70kg) than that of the male TSs (73kg-85kg).

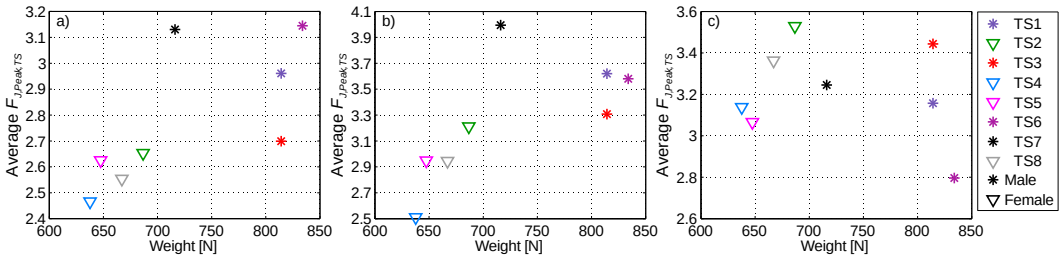

Figure 4.5 Average peak jumping force against TS weight at a)1Hz, b) 2Hz and c) 3Hz.

The TSs' heights are compared to the average peak forces in Figure 4.6a, b, c. At 1 and 2Hz (Figure 4.6a and b) there is no obvious correlation, however at 3Hz the correlation appears positive (Figure 4.6c). Therefore, at 3Hz taller TSs may naturally jump higher and consequentially generate larger landing forces. At lower jumping frequencies personal choice is likely to influence the jumping characteristics. The reduced jump consideration time at 3Hz may have increased the significance of the TS height.

It would appear that weight influences the peak forces at 1 and 2Hz, whereas at 3Hz TS height is the dominant factor. The peak forces of women are more affected by TS weight, even at 3Hz. To understand why the effect of TS weight is more significant amongst females, and to

confirm the correlation between peak force and weight and height, further experiments with larger sample sizes are recommended.

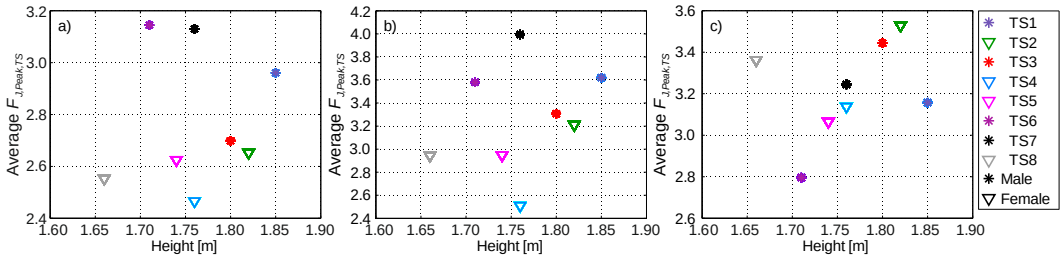

Figure 4.6 Average peak jumping force against TS height at a)1Hz, b) 2Hz and c) 3Hz.

4.2.4 DLFs from Jumping

The DLFs were calculated for harmonic frequencies up to the larger of 6Hz or three harmonics. A 5th order band-pass Butterworth filter was used to extract each harmonic between the average harmonic frequency ± 3STD or $f_J \pm 0.5f_J$, which ever was smaller. The low and high cut-off frequencies were set to ensure that 99.7% of the frequency components contributing to the DLF at each harmonic were included, but also to prevent the overlap of harmonic components. The peak forces were found from the filtered force time histories and used to calculate the jump-by-jump DLFs. The average DLFs and the overall mean and mean ± 1STD are shown in Figure 4.7 a and b respectively.

The largest DLF values occurred at the 1st harmonics of 2 and 3Hz jumping (1.27-1.63). The DLFs from the 1st harmonic of 1Hz jumping are smaller, due to the separate landing and launching impulses (Section 2.2.2), which caused the 2nd harmonic (2Hz) to dominant. As a result the even harmonic DLFs tend to be larger than the odd, except at 6Hz. By separating the force spectra into the odd and even constituents, separate relationships (dashed lines) between the harmonics of 1Hz can be observed in Figure 4.7a. The DLF values at the harmonics of 2 and 3Hz were very similar and decreased with increasing harmonic number (Figure 4.7b).

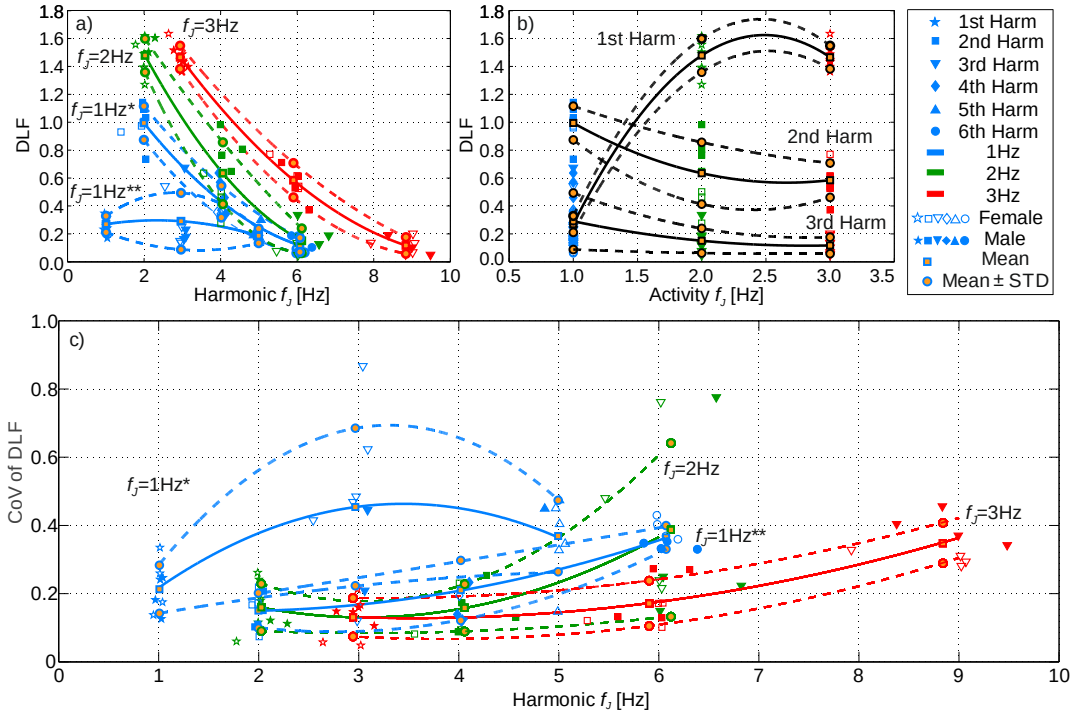

Figure 4.7 a) The DLFs values b) The DLFs of the harmonics and the mean and ± 1STD at each activity frequency. c) The CoV of the DLF, the relationships between f_J and the mean CoV values ($\mu_{J,DLF,O,CoV}$) and the mean ± 1STD ($\mu_{J,DLF,O,CoV} \pm \sigma_{J,DLF,O,CoV}$) are aproximated. *The even harmonics of 1Hz, ** the odd harmonics of 1Hz.

On a jump-by-jump basis only 25% of the DLFs from the 1st harmonic of the trials passed a 5% AD test for normality. Considering all the included harmonics 20.8% of the trials passed the AD test. 23.9% of the harmonically split trials had a skewness value less than 2*SES, 43.5% had an excess kurtosis value below 2*SEK. All these factors indicate that the jump-by-jump DLFs of the included harmonics are not normally distributed.

The values of DLF IASV (CoV of DLF) were plotted on Figure 4.7c. The CoV values tended to increase with harmonic number. The smallest values of IASV were seen at the 1st and 2nd harmonics of the trials (Table 4.6). The largest values indicating decreased individual DLF consistency occurred at the 3rd harmonic of 1 and 2Hz jumping, demonstrated by the wide data spread on Figure 4.7c. The most EIASV of DLF (mean of DLF CoV =0.454) occurred at the 3rd harmonic of 1Hz, hence the TSs exhibited a wide range of DLF values. The largest differences in EIASV between TSs occurred at the 3rd harmonic of 2Hz (STD of DLF CoV =0.255), where the range of DLF values varied most between TSs. The smallest EIASV was at 1st

harmonic of 3Hz (mean of DLF CoV =0.131), the TSs' EIASV were most similar to one another at the 2nd harmonic of 1Hz (STD of DLF CoV =0.051).

Table 4.6 The average, STD and COV values of the DLFs from jumping. The EIASV (hatched background) and IESV (highlighted) are marked. The markers denote gender (* male, ▽ female).

1Hz	1st Harmonic			2nd Harmonic			3rd Harmonic			4th Harmonic			5th Harmonic			6th Harmonic		
TS	Ave	STD	COV (IASV)	Ave	STD	COV (IASV)	Ave	STD	COV (IASV)	Ave	STD	COV (IASV)	Ave	STD	COV (IASV)	Ave	STD	COV (IASV)
1*	0.31	0.039	0.126	1.03	0.156	0.151	0.18	0.080	0.445	0.46	0.107	0.233	0.18	0.079	0.451	0.10	0.034	0.330
2▽	0.23	0.032	0.137	0.97	0.162	0.167	0.54	0.225	0.415	0.36	0.089	0.250	0.16	0.063	0.404	0.07	0.024	0.359
3*	0.17	0.042	0.247	0.74	0.153	0.208	0.67	0.141	0.209	0.34	0.131	0.382	0.30	0.106	0.354	0.19	0.065	0.348
4▽	0.24	0.042	0.175	0.96	0.071	0.074	0.25	0.030	0.120	0.34	0.067	0.194	0.21	0.031	0.147	0.06	0.027	0.429
5▽	0.26	0.067	0.260	1.01	0.221	0.219	0.14	0.066	0.485	0.37	0.044	0.120	0.14	0.044	0.327	0.07	0.026	0.368
6*	0.35	0.063	0.182	1.14	0.117	0.102	0.23	0.144	0.623	0.64	0.151	0.237	0.19	0.086	0.449	0.19	0.062	0.332
7*	0.33	0.080	0.241	1.09	0.121	0.110	0.16	0.141	0.867	0.57	0.079	0.139	0.17	0.082	0.474	0.17	0.060	0.352
8▽	0.27	0.089	0.335	1.01	0.175	0.173	0.15	0.070	0.469	0.37	0.045	0.123	0.15	0.051	0.346	0.09	0.037	0.403
Ave	0.27	0.06	0.213	0.99	0.15	0.150	0.29	0.11	0.454	0.43	0.09	0.210	0.19	0.07	0.369	0.12	0.04	0.365
STD	0.06	0.02	0.070	0.12	0.04	0.051	0.20	0.06	0.231	0.11	0.04	0.088	0.05	0.03	0.105	0.06	0.02	0.035
CoV	0.22	0.370	0.331	0.12	0.304	0.342	0.70	0.554	0.509	0.26	0.433	0.417	0.28	0.368	0.284	0.47	0.421	0.095

2Hz	1st Harmonic			2nd Harmonic			3rd Harmonic		
TS	Ave	STD	COV (IASV)	Ave	STD	COV (IASV)	Ave	STD	COV (IASV)
1 *	1.49	0.360	0.241	0.76	0.132	0.173	0.18	0.045	0.250
2 ▽	1.56	0.093	0.060	0.63	0.052	0.081	0.08	0.037	0.480
3 *	1.50	0.182	0.121	0.65	0.164	0.253	0.13	0.098	0.776
4 ▽	1.27	0.236	0.186	0.28	0.064	0.231	0.12	0.025	0.216
5 ▽	1.39	0.161	0.115	0.46	0.100	0.215	0.05	0.037	0.762
6 *	1.60	0.180	0.112	0.81	0.105	0.130	0.19	0.042	0.223
7 *	1.62	0.289	0.179	0.98	0.086	0.088	0.34	0.050	0.149
8 ▽	1.39	0.364	0.261	0.50	0.047	0.094	0.13	0.032	0.239
Ave	1.48	0.233	0.159	0.63	0.094	0.158	0.15	0.046	0.387
STD	0.12	0.097	0.069	0.22	0.040	0.069	0.09	0.023	0.255
CoV	0.08	0.418	0.435	0.35	0.432	0.437	0.58	0.492	0.658

3Hz	1st Harmonic			2nd Harmonic			3rd Harmonic		
TS	Ave	STD	COV (IASV)	Ave	STD	COV (IASV)	Ave	STD	COV (IASV)
1 *	1.45	0.212	0.146	0.53	0.145	0.273	0.05	0.024	0.456
2 ▽	1.63	0.094	0.057	0.77	0.093	0.121	0.14	0.045	0.328
3 *	1.52	0.225	0.148	0.71	0.094	0.132	0.19	0.077	0.404
4 ▽	1.43	0.069	0.048	0.54	0.093	0.172	0.13	0.039	0.294
5 ▽	1.36	0.290	0.213	0.53	0.053	0.101	0.07	0.021	0.311
6 *	1.40	0.148	0.106	0.37	0.101	0.271	0.05	0.017	0.342
7 *	1.49	0.237	0.159	0.61	0.079	0.129	0.10	0.038	0.370
8 ▽	1.44	0.241	0.167	0.62	0.106	0.171	0.20	0.057	0.281
Ave	1.47	0.189	0.131	0.59	0.096	0.171	0.12	0.040	0.348
STD	0.08	0.078	0.056	0.12	0.026	0.066	0.06	0.020	0.059
CoV	0.06	0.410	0.431	0.21	0.268	0.388	0.50	0.502	0.170

Average DLFs	1st harmonic all frequencies			2nd harmonic all frequencies			3rd harmonic all frequencies		
	Lowest	Largest	Range	Lowest	Largest	Range	Lowest	Largest	Range
	0.17	1.63	1.46	0.28	1.14	0.87	0.05	0.67	0.63

The DLF IESV between TSs was least at the 1st harmonics of 2 and 3Hz, the CoV values of the average TS DLFs were 0.076 and 0.053 respectively (Table 4.6). The largest variation occurred at the 3rd harmonic of 1Hz (0.652) where two TSs had significantly greater DLFs (above 0.5) than the other TSs. In general, the IESV increased with harmonic number, except at 1Hz. Variations in jumping frequency were more influential on the magnitude of the DLFs at the higher harmonics.

The DLFs from males TSs at the harmonics of 1 and 2Hz tend to be larger than those from their female counterparts (Table 4.7). At 3Hz there is no obvious gender distinction. The larger DLFs are consistent with the higher peak forces associated with male TSs (Table 4.5).

Table 4.7 The means and STDs of the 1st harmonic DLFs comparing male and female TSs

	1Hz Mean	1Hz STD	2Hz Mean	2Hz STD	3Hz Mean	3Hz STD
Mean	0.270	0.057	1.478	0.233	1.465	0.189
Mean Male	0.290	0.056	1.553	0.253	1.463	0.205
Mean Female	0.249	0.058	1.403	0.213	1.468	0.173

4.2.5 Variations in Contact Ratios

Contact ratios are used by some authors as a key input in defining the jumping frequency and force, as described in Section 2.2.2 (Bachmann and Ammann, 1987; BRE, 2004). Therefore to critically evaluate these approaches the relationships between contact ratio and jumping frequency and peak force is investigated.

The peak force and corresponding contact ratio of each jump were plotted in Figure 4.8 a-c. The correlation between the variables is negative indicating that small contact ratios correspond to large peak forces. This is consistent with the conservation of energy whilst jumping (Bachmann and Ammann, 1987) described in Section 2.2.2. The correlation is strongest at 1 and 2Hz. At 3Hz the gradient is shallower and the spread is greater (Figure 4.8c), consistent with the reduced correlation observed at higher frequencies (Sim et al., 2008).

At 1 and 2Hz from Figure 4.8 a and b, women typically have larger contact ratios than men. This finding agrees with the lower forces from female TSs (Figure 4.4a). This gender distinction is lost at 3Hz.

The mean peak forces and the mean ± 1STD were plotted for each contact ratio in steps of 0.02 (dash-dot line, and dashed line respectively). The mean STD was 0.175, the greatest STDs occurred between contact ratios of 0.63 and 0.78. A 2nd order polynomial line of best fit ($\mu_{J,Peak,O,sim}$) was plotted between the two variables (Figure 4.8d). The line of best fit matches the data well especially the maximum peak forces seen at low contact ratios. Some peak forces between contact ratios of 0.700 and 0.775 were underestimated, fortunately these were not the most severe.

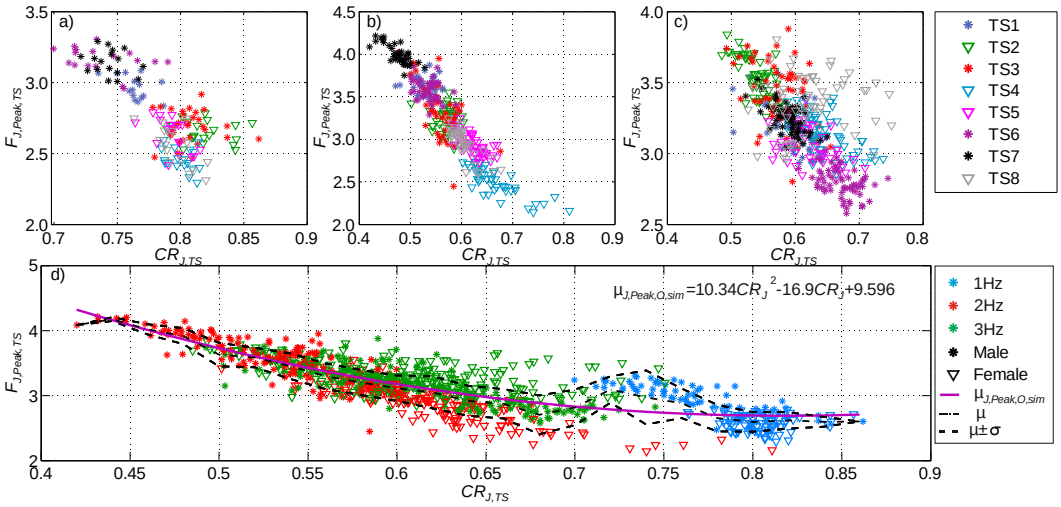

Figure 4.8 The contact ratio of each jump against the peak jumping force for a) 1Hz, b) 2Hz, c) 3Hz d) all frequencies. The mean $F_{Peak,O}$ and the mean ± 1STD at each contact ratio in steps of 0.02 are plotted via the dash-dot line and dashed lines respectively. The mean $F_{J,Peak,O}$ is aproximated by a 2nd order polynomial fit $\mu_{J,Peak,O,sim}$.

In Figure 4.9a the average TS contact ratios were plotted against the average jumping frequencies. The overall mean contact ratio and the mean ± 1STD were plotted for each frequency and approximated by lines of best fit. The contact ratios at 1Hz were higher than at 2 and 3Hz, where similar values are seen. The similarities at 2 and 3Hz suggest that contrary to the work of Bachmann and Ammann (1987) the jumping frequency does not necessarily dictate the contact ratio.

The contact ratios from 70.8% of the trials passed the AD test for normality. 75% of the trials had a skewness value below 2*SES and 95.8% of the trials had an excess kurtosis value less than 2*SEK. These findings suggest the contact ratios of individuals are normally distributed, which is consistent with the approach of Sim et al. (2008).

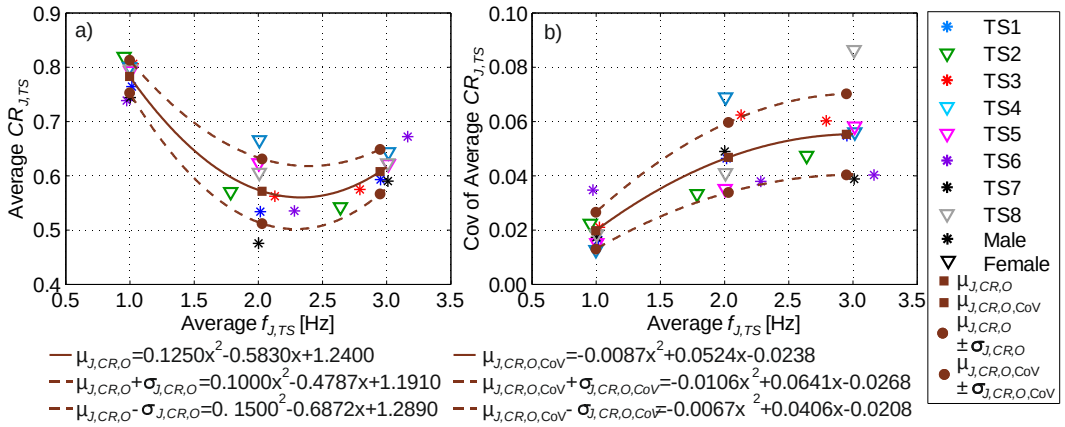

Figure 4.9a) The average contact ratios and jumping frequency, the mean $CR_{J,O}$ ($\mu_{J,CR,O}$) and the mean ± 1STD ($\mu_{J,CR,O} \pm \sigma_{J,CR,O}$) are approximated and the equations listed. b) The CoV of $CR_{J,TS}$ and average $f_{J,TS}$, the relationships between f_J and the mean CoV values ($\mu_{J,CR,O,CoV}$) and the mean ± 1STD ($\mu_{J,CR,O,CoV} \pm \sigma_{J,CR,O,CoV}$) are aproximated.

The CoV of the contact ratios tends to increase with target frequency and are plotted on Figure 4.9b. The smallest values of each TS occurred at 1Hz and hence the minimum IASV. The largest CoV values were split between 2 and 3Hz at a ratio of 3:5. Consistent with the low values of IASV, the magnitude and range of EIASV was significantly smaller at 1Hz than at the other frequencies (mean of $CR_{J,TS}$ CoV =0.020, STD of $CR_{J,TS}$ CoV =0.007, Table 4.8). Hence, at 1Hz the TSs' contact ratios were most consistent, and each TS showed a similar amount of variation. From Figure 4.9b the EIASV was greatest at 3Hz, the contact ratios of the TSs were inconsistent, and the amount of TS variation fluctuated (mean of $CR_{J,TS}$ CoV =0.055, STD of $CR_{J,TS}$ CoV =0.015).

The IESV was assessed using the CoV of the average $CR_{J,TS}$ from each TS. The smallest value 0.038 (Table 4.8) occurred at 1Hz, indicating that the TSs were most consistent with one another at this frequency. Significantly more variation between TSs occurred at 2Hz (IESV=0.104). The contact ratios at 2Hz range from 0.420 to 0.811, indicating the diversity

possible when jumping at this frequency. The lowest contact ratios occur at 2Hz, consistent with the largest peak forces seen.

Table 4.8 The average, STD and COV values of the contact ratios. The EIASV (hatched background) and IESV (highlighted) are marked. The markers denote gender (* male, ▽ female).

TS	1Hz Ave	1Hz STD	1Hz COV (IASV)	2Hz Ave	2Hz STD	2Hz COV (IASV)	3Hz Ave	3Hz STD	3Hz COV (IASV)
1 *	0.764	0.013	0.016	0.534	0.025	0.046	0.593	0.033	0.055
2 ▽	0.820	0.018	0.022	0.571	0.019	0.033	0.543	0.026	0.047
3 *	0.806	0.017	0.021	0.563	0.035	0.062	0.575	0.035	0.060
4 ▽	0.801	0.010	0.013	0.666	0.046	0.069	0.644	0.036	0.056
5 ▽	0.793	0.012	0.015	0.624	0.022	0.035	0.622	0.036	0.058
6 *	0.739	0.026	0.035	0.535	0.020	0.038	0.672	0.027	0.040
7 *	0.744	0.013	0.017	0.476	0.023	0.049	0.590	0.023	0.039
8 ▽	0.796	0.015	0.019	0.606	0.025	0.041	0.623	0.054	0.086
Mean	0.783	0.015	0.020	0.572	0.027	0.047	0.608	0.034	0.055
STD	0.030	0.005	0.007	0.060	0.009	0.013	0.041	0.010	0.015
CoV	0.038	0.319	0.342	0.104	0.338	0.276	0.067	0.285	0.270
Contact ratio	Lowest 0.700	largest 0.862	Δ 0.162	Lowest 0.420	largest 0.811	Δ 0.391	Lowest 0.485	largest 0.751	Δ 0.265
95th Percentiles	2.5% 0.717	97.5% 0.843	Δ 0.127	2.5% 0.461	97.5% 0.699	Δ 0.238	2.5% 0.511	97.5% 0.717	Δ 0.207

All the contact ratios observed were above 0.4 (Table 4.8), and 95.2% were above 0.5, similar to previous findings (Sim et al., 2008; Yao et al., 2002). The 95th percentiles for each frequency are displayed in Table 4.8. 97.5% of the 1Hz contact ratios are above 0.717, this value reduces to 0.461 at 2Hz and 0.511 at 3Hz. Hence very low contact ratios only occur at frequencies around 2Hz. These experiments therefore support Sim et al.'s statement that the contact ratios (0.25-0.67) featured in BSI (1996) are too low.

It can be concluded that there is an inverse relationship between contact ratio and peak force, which varies with jumping frequency. Contact ratios are not necessarily specific to a jumping frequency. However, very high contact ratios are mostly associated with low frequency jumping, and very low contact ratios with jumping at frequencies around 2Hz.

4.2.6 Force Impulse

The relationship between the contact ratios and peak forces mean it is likely that the jump frequency influences the area under the force peak (impulse). Figure 4.10a-c shows the weight

and frequency normalised impulse against the frequency of each jump for each target frequency. As the jumping frequency increases the normalised impulse decreases.

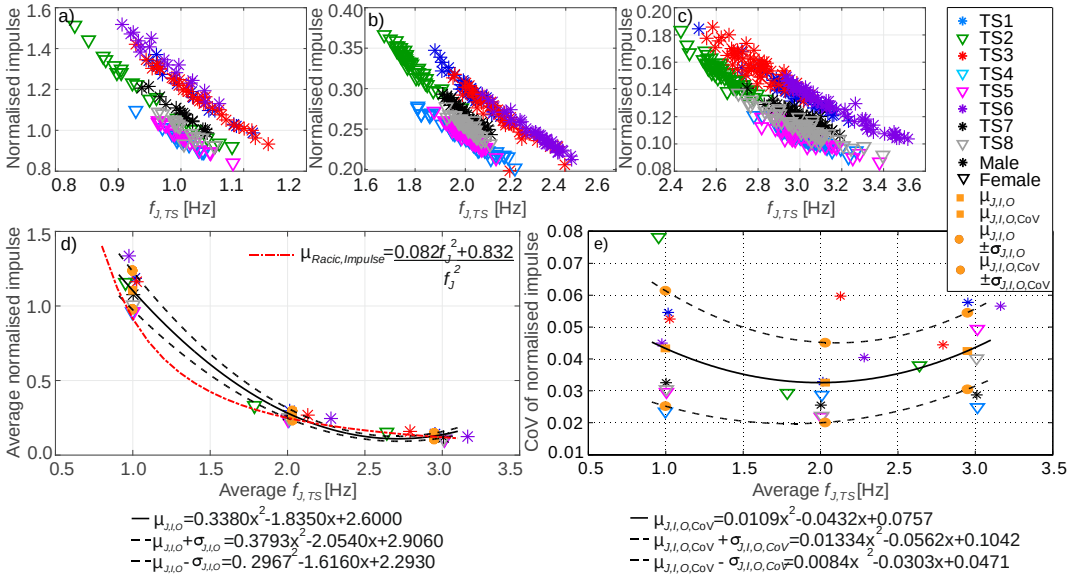

Figure 4.10 The normalised impulse against the jump frequency a) 1Hz, b) 2Hz, c) 3Hz. d) The average TSs normalised impulse and average jumping frequency, the overall mean normalised impulse ($\mu_{J,I,O}$) and the mean ± 1STD ($\mu_{J,I,O} \pm\sigma_{J,I,O}$) are approximated and the equations listed. e) The CoV of the normalised impulses and average $f_{J,TS}$, the relationship between f_J and the mean CoV values ($\mu_{J,I,O,CoV}$), the mean ± 1STD ($\mu_{J,I,O,CoV} \pm\sigma_{J,I,O,CoV}$) are aproximated.

In Figure 4.10 a-c there is a clear TS specific negative trend at each frequency. This is consistent with the positive linear relationship between the weight normalised impulse and the period found by Racic and Pavic (2010). Their equivalent jumping frequency, and frequency normalised impulse relationship has been plotted (dashed dot line) on Figure 4.10d. As a comparison the average normalised impulses and the mean ± 1STD are plotted and approximated by 2nd order polynomial lines of best fit (solid and dashed respectively). Racic and Pavic's relationship accounts well for the normalised impulses at 2 and 3Hz, however at 1Hz the impulses are underestimated.

The normality of the distribution of the jump-by jump impulses was investigated, 70.8% of trials passed a 5% AD test. Furthermore 87.5% of trials had a skewness value below 2*SES, and 91.6% had an excess kurtosis value less than 2*KES. These factors all indicate that the jumping impulses are distributed normally.

Table 4.9 The average, STD and COV values of the normalised impulses. The EIASV (hatched background) and IESV (highlighted) are marked. The markers denote gender (* male, ▽ female).

	1Hz			2Hz			3Hz		
TS	**Ave**	**STD**	**COV (IASV)**	**Ave**	**STD**	**COV (IASV)**	**Ave**	**STD**	**COV (IASV)**
1 *	1.19	0.123	0.104	0.30	0.019	0.063	0.14	0.016	0.117
2 ▽	1.17	0.183	0.156	0.33	0.020	0.060	0.15	0.010	0.066
3 *	1.17	0.121	0.103	0.27	0.027	0.100	0.16	0.012	0.076
4 ▽	0.96	0.047	0.049	0.24	0.019	0.078	0.11	0.005	0.052
5 ▽	0.96	0.058	0.060	0.24	0.011	0.044	0.11	0.008	0.078
6 *	1.34	0.120	0.090	0.24	0.020	0.081	0.13	0.014	0.108
7 *	1.08	0.069	0.064	0.27	0.014	0.052	0.12	0.006	0.053
8 ▽	1.01	0.051	0.050	0.25	0.010	0.040	0.11	0.009	0.079
Mean	1.11	0.096	0.084	0.27	0.017	0.065	0.13	0.010	0.079
STD	0.132	0.048	0.036	0.032	0.006	0.020	0.020	0.004	0.024
CoV	0.118	0.498	0.432	0.120	0.321	0.316	0.156	0.367	0.300
Impulse	Lowest	Largest	Δ	Lowest	Largest	Δ	Lowest	Largest	Δ
	0.908	1.382	0.474	0.431	0.652	0.221	0.292	0.508	0.216

The IASV of the impulses (CoV of impulses) are plotted on Figure 4.10e. The smallest values and therefore the most TS consistency was seen at 2Hz (Table 4.9). The largest values indicating a wider range of TS impulses occurred at 1 and 3Hz jumping. The most impulse EIASV (mean of the CoV of the impulses =0.084) and the greatest TS variation in EIASV (STD of the CoV of the impulses =0.036) occurred at 1Hz. Hence most TS exhibited a wide range of impulse values, and the spread of values differed between TSs (Figure 4.10e). The smallest values of EIASV occurred at 2Hz.

The greatest IESV was seen at the jumping frequency of 3Hz (CoV of the average impulses =0.156, Table 4.9), the average impulses values differed most between the individuals. The least IESV occurred at 1Hz (0.118), therefore although each TSs values varied, the values were similar amongst TSs.

The impulses from female TSs tended to be smaller than those from males at the same frequency. This is consistent with the smaller normalised peak forces and larger contact ratios from female TSs. There is less distinction in the impulses of each TSs, and between genders at 3Hz. However differences in impulse still occur between men and women unlike the gender-based discrepancies at 3Hz in peak force and contact ratio. Impulse is a function of both peak

force and flight time, the continued discrepancies suggest subtle differences in the variables based on gender, which are emphasised in the impulse calculation.

4.2.7 The Peak Displacements

The vertical displacements of the TS's body were monitored using a motion capture system (Oxford Metrics Group, 2007) to track a marker on the C7th vertebra (Figure 4.1). The maximum jump displacements were calculated on a jump-by-jump basis as the maximum elevation of the marker above the elevation of the marker when standing. The jump-by-jump peak force and maximum displacement of each TS are plotted in Figure 4.11a, the average peak forces and maximum displacements are plotted in Figure 4.11b. There is a positive correlation between the variables at 1 and 3Hz, the peak forces increase with maximum displacement. At 2Hz the spread of peak forces is greater and there is no obvious correlation. The reduced correlation at 2Hz indicates that the maximum displacement is less influential on the peak force at this frequency.

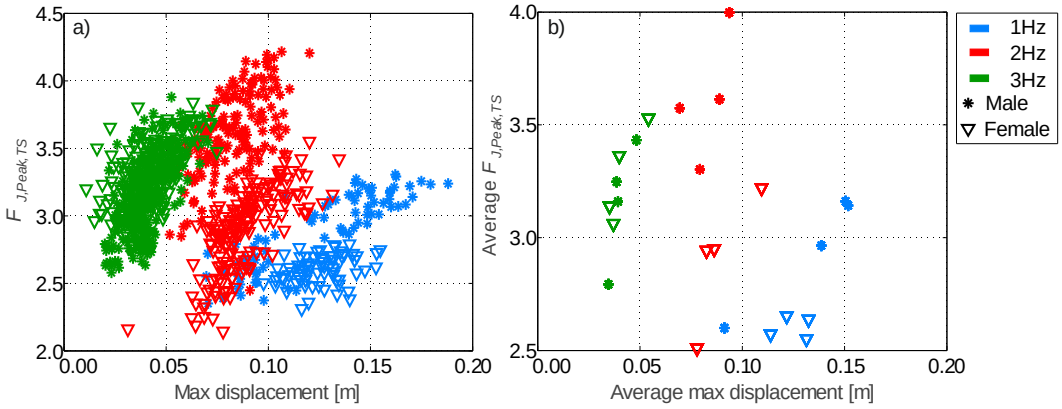

Figure 4.11 a) The jump-by-jump peak force and maximum displacement, b) the average peak force against the avergae maximum displacement for each TSs

Although the trend at 1 and 3Hz is positive, no correlation is obvious when considering all frequencies (Figure 4.11b). However, the displacements decrease with increasing jumping frequency (Figure 4.12a). Hence, a large maximum displacement does not necessarily equate to a large force, jumping frequency has a greater influence on the peak force.

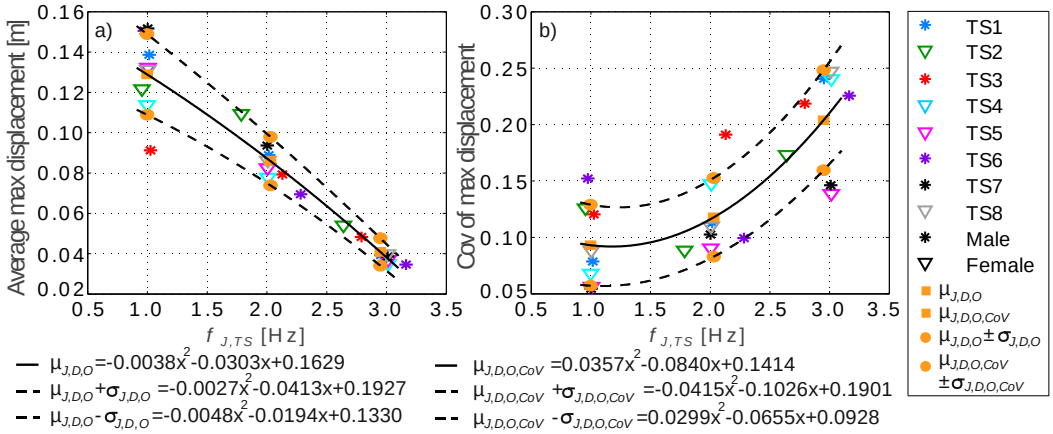

Figure 4.12 a) The average maximum displacement and jumping frequency, the mean maximum displacement ($\mu_{J,D,O}$) and the mean ± 1STD ($\mu_{J,D,O} \pm \sigma_{J,D,O}$) are approximated and the equations listed. b) The CoV of the maximum displacements and average $f_{J,TS}$, the relationship between f_J and the mean CoV values ($\mu_{J,D,O,CoV}$) and the mean ± 1STD ($\mu_{J,D,O,CoV} \pm \sigma_{J,D,O,CoV}$) are aproximated.

70% of the trials had jump-by-jump displacements which passed the 5% AD test. Furthermore 91.6% of trials had a skewness value less than 2*SES and the excess kurtosis value was less than 2*SEK in 91.6% of cases. Considering these tests it is likely that the maximum displacements of the jumps are normally distributed.

The IASV, calculated as the CoV of the displacements, were plotted on Figure 4.12b. The CoV values increase with jumping frequency. Therefore, the smallest CoV values and hence most consistent TS displacements were seen at 1Hz, the largest values occurred at 3Hz. Overall the least EIASV (mean CoV of the displacements =0.093, Table 4.10) occurred at 1Hz. However, the EIASV values were most similar to one another at 2Hz (STD CoV of the displacements =0.035). From Figure 4.12b the most EIASV and the most variability in EIASV between TSs was seen at 3Hz (mean and STD of CoV of the displacements, 0.204 and 0.044 respectfully). The TSs varied their maximum displacements between jumps, and the spread of displacements differed between TSs.

The average values of TS maximum displacement were most consistent between TSs at 2Hz (CoV average displacement (IESV)=0.140, Table 4.10). The greatest variation between TSs was seen at 3Hz (IESV=0.167). The range of maximum displacements decreased with increased

jumping frequency. The values were between 0.068m and 0.188m at 1Hz (a difference Δ of 0.12), 0.051m and 0.135m at 2Hz (Δ=0.084) , and 0.010 and 0.075 at 3Hz (Δ=0.65).

Table 4.10 The average, STD and COV values of the maximum displacements. The EIASV (hatched background) and IESV (highlighted) are marked. The markers denote gender (* male, ▽ female).

	1Hz			2Hz			3Hz		
TS	**Ave (m)**	**STD (m)**	**COV (IASV)**	**Ave (m)**	**STD (m)**	**COV (IASV)**	**Ave (m)**	**STD (m)**	**COV (IASV)**
1 *	0.14	0.011	0.079	0.09	0.010	0.113	0.04	0.009	0.241
2 ▽	0.12	0.015	0.126	0.11	0.010	0.089	0.05	0.009	0.173
3 *	0.09	0.011	0.120	0.08	0.015	0.191	0.05	0.011	0.219
4 ▽	0.11	0.008	0.068	0.08	0.011	0.147	0.04	0.008	0.240
5 ▽	0.13	0.007	0.056	0.08	0.007	0.091	0.04	0.005	0.139
6 *	0.15	0.023	0.152	0.07	0.007	0.099	0.03	0.008	0.226
7 *	0.15	0.008	0.054	0.09	0.010	0.103	0.04	0.006	0.146
8 ▽	0.13	0.012	0.088	0.09	0.009	0.110	0.04	0.010	0.247
Mean (m)	0.13	0.012	0.093	0.09	0.010	0.118	0.04	0.008	0.204
STD (m)	0.020	0.005	0.036	0.012	0.003	0.035	0.007	0.002	0.044
CoV	0.155	0.432	0.386	0.140	0.255	0.296	0.167	0.238	0.217
Max mean displacement (m)	Lowest (m)	Largest (m)	Δ (m)	Lowest (m)	Largest (m)	Δ (m)	Lowest (m)	Largest (m)	Δ (m)
	0.09	0.15	0.06	0.07	0.11	0.04	0.03	0.05	0.02

The TS height was observed to influence the peak force at 3Hz (Section 4.2.3). The relationship between the maximum displacement and TS height was investigated. At 1Hz there was no correlation (Figure 4.13a). A slight positive correlation existed at 2 and 3Hz, suggesting that taller TSs performed higher jumps, consistent with the hypothesis in Section 4.2.3. The correlation was strongest at 3Hz, supporting the positive relationship between the peak force and the TS height in Figure 4.6.

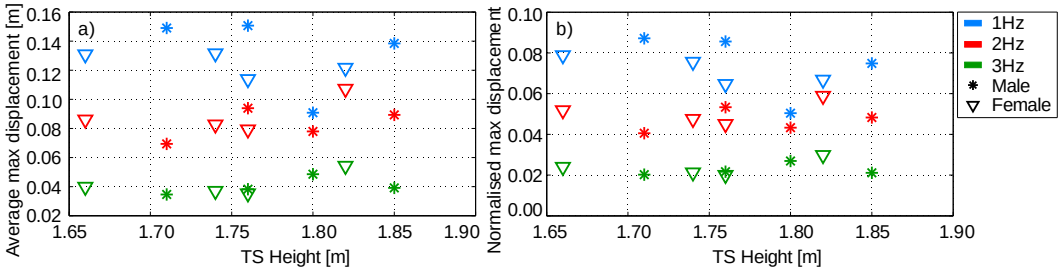

Figure 4.13 a)The avergae maximum displacement and b) the normalised average maximum displacement against TS height for each frequency.

The average maximum displacements were further normalised by the TSs' height to investigate whether they were proportional (Figure 4.13b). At 1Hz there is little correlation indicating that height does not influence the maximum displacement at this frequency. At 1Hz

the TSs have more time between jumps and hence the freedom to alter their jump displacement. A wider range of displacements are seen, which are likely due to TS preference and not necessarily their physiology. At 2Hz and 3Hz the average normalised maximum displacements oscillate around 5% and 2% of the TSs' height, respectfully. It would appear at these frequencies the displacements are approximately proportional to the TSs' height.

4.2.8 Conclusions

The characteristics of jumping with specific thought to the IASV, EIASV and IESV have been observed and analysed within this section.

The distribution of the jumping frequencies of each individual was observed, 79.2% of the trials passed an AD test for normality. The greatest amount of EIASV occurred at the target frequency of 1Hz, the least at 2Hz. The IESV was greatest at 2Hz, suggesting that although TSs demonstrated high consistency, a considerable amount of variation occurred between the TSs. The least IESV occurred at 1Hz.

All TSs on average achieved the target frequency ±5% at 1Hz, however only 5/8 TSs were able to do this for 2 and 3Hz. More frequency overestimations were seen at 2Hz and more underestimations at 3Hz. TSs in general either consistently achieved the target frequency or were consistently unable to do so.

The peak forces of the TSs were normally distributed in 83.3% of trials. The EIASV was smallest at 1Hz and greatest at 2Hz. The IESV was also largest at 2Hz. The TSs were most consistent with one another at 3Hz. It was observed that male TSs had larger peak forces than female TSs, however this distinction was lost at 3Hz. TS weight influenced the peak forces at 1 to 2Hz, however at 3Hz height was the dominant influence. The peak forces of the female TSs were still strongly affected by weight at 3Hz.

The jump-by-jump DLFs of the individuals were not normally distributed. The DLFs were greatest at the 1st harmonic of 2 and 3Hz. A negative correlation was observed between the

DLFs and the harmonic number for each jumping frequency. At 1 and 2Hz the DLFs from male TSs tended to be larger. The most EIASV occurred at the 3rd harmonic of 1Hz, the least at the 1st harmonic of 3Hz. The IESV generally increased with harmonic number.

A frequency dependant inverse relationship was discovered between the peak forces and the contact ratios of jumping. A good approximation of the relationship was achieved (Figure 4.8). It was observed that at lower frequencies (1-2Hz) women tended to have larger contact ratios, consistent with the smaller peak forces witnessed.

The relationship between jumping frequency and contact ratio was investigated. It was found that jumping frequency does not necessarily dictate the contact ratio, however larger contact ratios were primarily associated with 1Hz jumping, and small contact ratios with 2Hz. Consistent with the work of Sim et al. (2008) and Yao et al. (2002) the contact ratios were greater than 0.4, and 95.2% of the contact ratios were above 0.5, this reconfirms that the contact ratios in BSI (1996) are too low.

The distribution of the contact ratios was normal in 70.8% of trials. The EIASV was smallest at 1Hz and largest at 3Hz. The least amount of IESV occurred at 1Hz, the largest at 2Hz.

The weight and frequency normalised impulse was calculated for each jump. The results from AD, skewness and excess kurtosis tests on the distributions indicate that the jump-by-jump impulse is normally distributed. A negative relationship was observed between impulse and jumping frequency. The impulse size was affected by jump frequency, gender and a degree of personal preference. The most EIASV occurred at 1Hz, the smallest value was at 2Hz. The IESV was greatest at 2Hz and least at 1Hz. It is worth noting for the majority of the characteristics of jumping the target frequency of 2Hz has the highest levels of IESV. This is likely because 2Hz is a mid-frequency and there is enough time for TSs to have an element of choice in the jumping parameters.

The jump-by-jump maximum displacements were found to be normally distributed. The maximum displacements decreased with increased jumping frequency. At 1 and 3Hz the correlation between peak force and maximum displacement was positive. However, when including all jumping frequencies no correlation was obvious. The jumping frequency has a greater influence on the peak force than the maximum displacement. The least EIASV occurred at 1Hz and the most at 3Hz. The IESV was greatest at 3Hz and the TSs were most consistent to one another at 2Hz.

The effect of TS height on the maximum displacements was investigated to affirm the hypothesis that taller TSs have a greater maximum displacement. The results imply that for the jumping frequencies of 2 and 3Hz the hypothesis is valid. At 1Hz TS height appeared to have little influence on the maximum displacements.

4.3 Characterising Bobbing

Within this section the GRFs from the bobbing TSs are examined. Firstly differences between bouncing and jouncing force profiles will be considered. Then variations in the bobbing frequencies, the normalised peak forces, DLFs and maximum displacements will be investigated. A focus on the IASV, EIASV and the IESV will be adopted during the analysis.

4.3.1 Characterising Bouncing and Jouncing

The variation of the bobbing force profiles is exacerbated by the two possible bobbing styles, bouncing and jouncing, described in Section 2.3. Video footage from the trials showing the TSs' heels was used to determine their bobbing style at each frequency. Few studies have been conducted into the differences in the GRF profiles of the two activities. These differences will be examined in this section.

4.3.1.1 Bouncing and Jouncing at 1Hz

Figure 4.14 shows the force profiles from TSs bouncing at 1Hz, the corresponding jouncing profiles are shown in Figure 4.15. Greater similarities in the shape exist between the bouncing

profiles (Figure 4.14), than between the jouncing profiles (Figure 4.15). The bouncing profiles are comprised of a large and small force peak. The lowest GRFs are approximately 0.6, and the highest values approximately 1.8 (Figure 4.14).

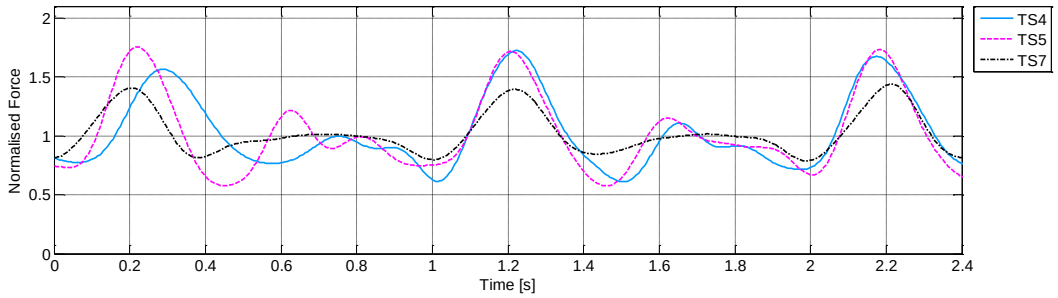

Figure 4.14 The normalised GRF profiles from bouncing at 1Hz.

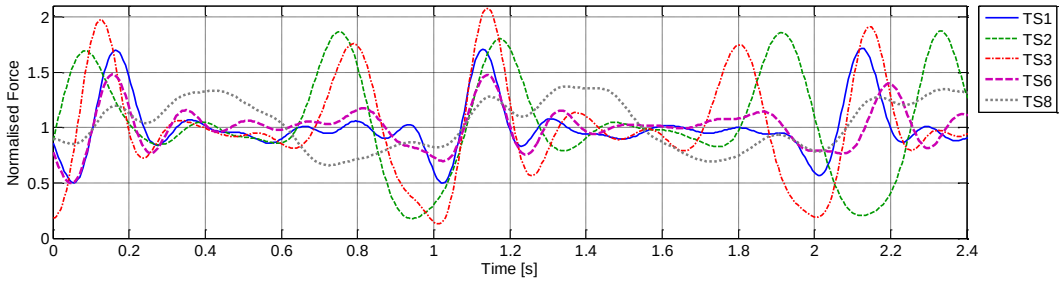

Figure 4.15 The normalised GRF profiles from jouncing at 1Hz.

There are three profile patterns amongst the jouncing TSs. The force profiles of TS1 and TS6 consisted of a force peak, followed by small oscillations around the TS's static force (Figure 4.15). There are two small force peaks in the negative direction either side of the main force peak. The force histories of TS2 and TS3 have a similar pattern; a force peak, followed by oscillations around the TSs' weight, and a force peak in the positive and then negative directions (Figure 4.15). The force magnitudes are greater than those of TS1 and TS6 in both the positive and negative directions, approaching 2 and 0. The additional positive peak may be caused by a heel strike between bobs. It is likely that TS1 and TS6 used their toes to control the action and therefore reduced the heel impact.

TS8's force time history consists of wider dual peaks and dual troughs of smaller force magnitude (Figure 4.15). The profile could be considered as two peaks followed by an oscillating trough, hence containing elements similar to the profiles shapes of TS2 and TS3.

4.3.1.2 Bouncing and Jouncing at 2Hz

There are two force profile patterns from bouncing at 2Hz (Figure 4.16). The 2Hz profiles of TS1 and TS7 are similar to their 1Hz bouncing profiles, except TS1 includes an additional localised peak. The force profile from TS4 consists of a large peak followed by a significantly smaller peak, similar to the other bouncing profiles. However, the magnitude of the peaks and troughs are larger and more reminiscent of jouncing (Figure 4.17).

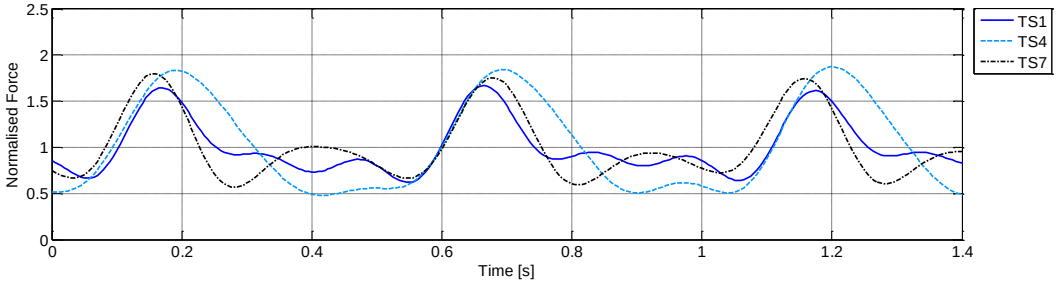

Figure 4.16 The normalised GRF profiles from bouncing at 2Hz.

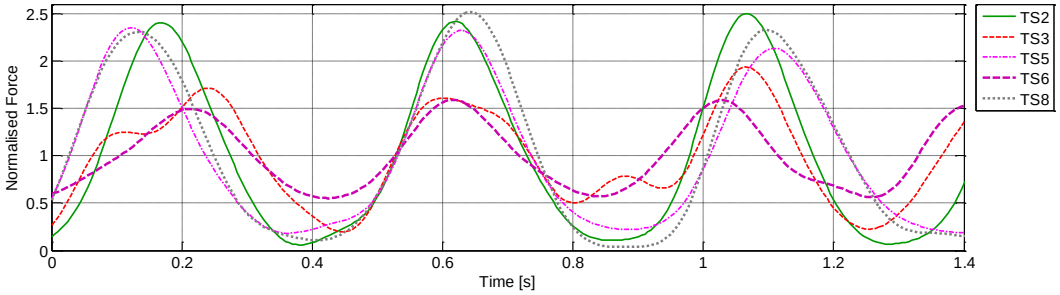

Figure 4.17 The normalised GRF profiles from jouncing at 2Hz.

The 2Hz jouncing profiles in Figure 4.17 have a range of shapes. Three of the profiles approach low magnitude jumping (TS2, TS5 and TS8). The GRFs of these profiles are between 0.0 and 2.5, more extreme than those seen in Figure 4.14 to Figure 4.16. TS6 has a similar profile shape however the force magnitudes are more comparable to bouncing (Figure 4.16). This is an example of low energy jouncing with minimal GRFs. TS3 demonstrates that irregular jouncing

force profiles can occur at 2Hz (Figure 4.17). The dual peaks observed from the TS at 1Hz (Figure 4.15) are merging into one.

4.3.1.3 Bouncing and Jouncing at 3Hz

There are two patterns of bobbing force profile at 3Hz. The profile of TS1 (Figure 4.18) consists of a large peak followed by two smaller peaks akin the 2Hz profile (Figure 4.16), however the large peak and foremost small peak have begun to merge. This implies that TS1 uses the same bobbing action but with increased tempo. The shape and force magnitude of TS4's force profile (Figure 4.18) is very similar to the jouncing profiles in Figure 4.19. The second bouncing peak within the trough at 2Hz (Figure 4.16) has mostly merged with the larger peak.

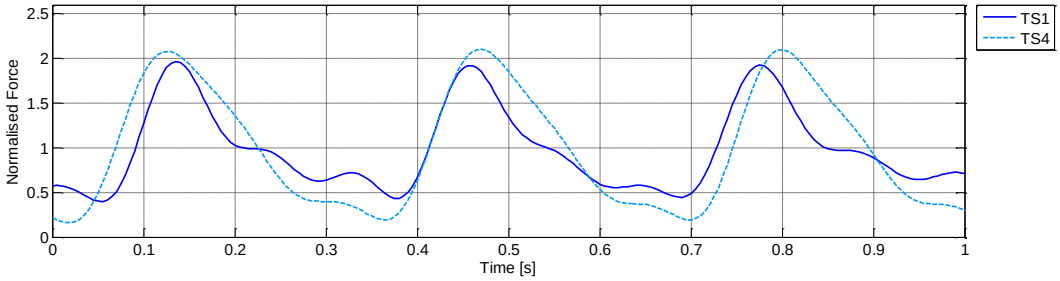

Figure 4.18 The normalised GRF profiles from bouncing at 3Hz.

The jouncing profiles in Figure 4.19 all follow the same pattern. However variation of the force magnitude demonstrates the possibility of large and small jouncing GRFs. Some of the troughs reach zero indicating the occasional jump. At 3Hz jouncing becomes very similar to jumping.

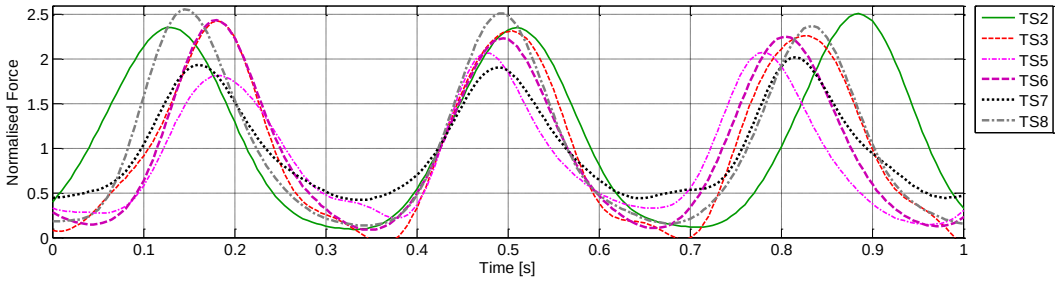

Figure 4.19 The normalised GRF profiles from jouncing at 3Hz.

4.3.1.4 Bouncing and Jouncing at 4Hz

The profiles from the bouncing (Figure 4.20) and jouncing (Figure 4.21) TSs all follow the same single peaked pattern at 4Hz. The bouncing peaks are between 1.5 and 2, the jouncing peaks are slightly larger, the majority of which are between 1.5 and 2.7.

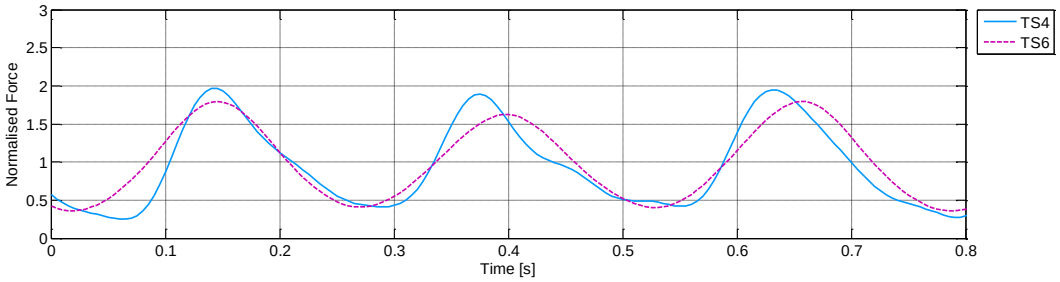

Figure 4.20 The normalised GRF profiles from bouncing at 4Hz.

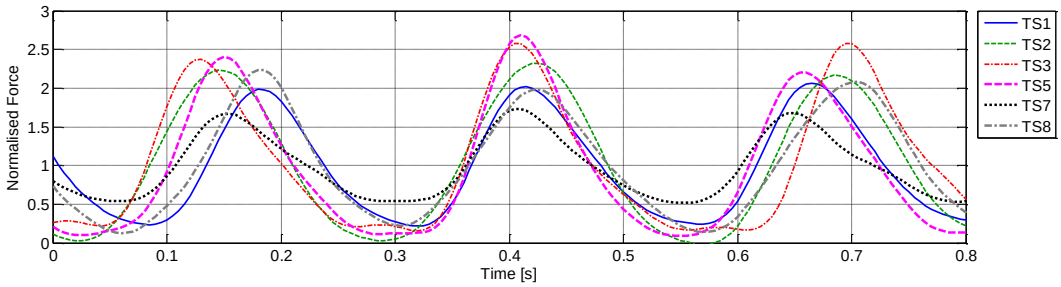

Figure 4.21 The normalised GRF profiles from jouncing at 4Hz.

From these force profiles a variety of patterns are found to be associated with jouncing and bouncing. In general the magnitudes of jouncing forces are larger. However, low energy jouncing and high energy bouncing can occur and the corresponding force magnitudes reflect this. The variety of profile shapes reduces with increasing bobbing frequency. At high frequencies the force profiles of bouncing and jouncing become more similar, tending towards a single force peak comparable to jumping.

4.3.2 Variation in Bobbing Frequency

The frequency of each individual bob f_B for every TS was calculated. The period of a bobbing cycle was measured between points where the force was equal to the average GRF of the trial. The notation $_{TS}$ and $_{O}$ referring to TS and overall values respectively is consistent with the previous section of jumping. The average bobbing frequencies of the TSs at each target

frequency are plotted in Figure 4.22a. Star and triangular markers are used to denote male and female TSs and solid and hollow markers are used to distinguish the jouncing and bouncing TSs. The overall mean values and the mean ± 1STD are approximated by 1st order polynomial line of best fit (solid and dashed lines respectively).

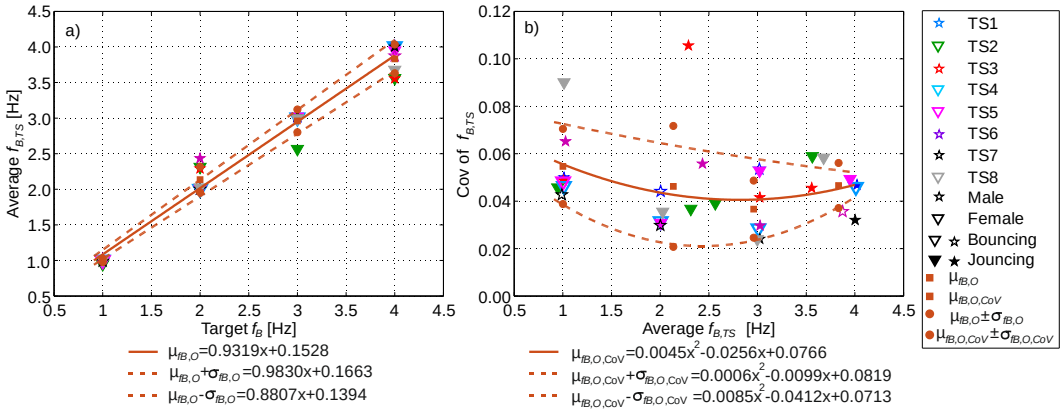

Figure 4.22 a) The average bobbing frequency against target frequency, the mean $f_{B,O}$ ($\mu_{fB,O}$) and the mean ± 1STD ($\mu_{fB,O}\pm\sigma_{fB,O}$) are approximated and the equations listed. b) The CoV of $f_{B,TS}$ against average $f_{B,TS}$, the relationships between f_B and the mean CoV values ($\mu_{fB,O,CoV}$) and the mean ± 1STD ($\mu_{fB,O,CoV}\pm\sigma_{fB,O,CoV}$) are aproximated.

Overall 53.1% of the trials passed an AD test for normality, however 75% of the 1Hz trials passed. The number of successful trials decreased with increasing target frequency. 75% of the trials had a skewness value below 2*SES and 87.5% of trials had an excess kurtosis value less than 2*SEK. However, with reference to the AD test the bob-by-bob frequencies should only be considered normally distributed at 1Hz.

The smallest CoV values of bobbing frequency, and therefore the least IASV occurred at the frequencies of 2 and 3Hz (Figure 4.22b). The largest values and therefore the most TS bobbing frequency variation were at 1Hz. The greatest EIASV of bobbing frequency (mean of $f_{B,TS}$ CoV =0.055, Table 4.11) occurred at 1Hz. This signifies the greatest variation in the TSs' bobbing frequencies, consistent with jumping. However the variation in the TSs' bobbing frequency varied most at 2Hz (STD of $f_{B,TS}$ CoV =0.025). This can be visualised in by the wide range of CoV values in Figure 4.22b. The smallest mean $f_{B,TS}$ CoV value was 0.037 and occurred at 3Hz, hence on average the TSs' bobbing frequencies were most consistent. The smallest STD of $f_{B,TS}$ CoV

0.010 occurred at 4Hz revealing that the variation in the TSs' bobbing frequency was most similar to one another.

Table 4.11 The average, STD and COV values of the $f_{B,TS}$. The EIASV (hatched background) and IESV (highlighted) are marked. The markers denote gender (* male, ▽ female), and font the style (bouncing underlined, jouncing italics).

TS	1Hz Ave (Hz)	1Hz STD (Hz)	1Hz COV (IASV)	2Hz Ave (Hz)	2Hz STD (Hz)	2Hz COV (IASV)	3Hz Ave (Hz)	3Hz STD (Hz)	3Hz COV (IASV)	4Hz Ave (Hz)	4Hz STD (Hz)	4Hz COV (IASV)
1 *	*1.01*	*0.051*	*0.050*	2.00	0.089	0.044	3.02	0.162	0.054	*4.02*	*0.188*	*0.047*
2 ▽	*0.95*	*0.043*	*0.046*	*2.31*	*0.085*	*0.037*	*2.57*	*0.100*	*0.039*	*3.56*	*0.210*	*0.059*
3 *	*1.01*	*0.049*	*0.049*	*2.29*	*0.242*	*0.106*	*3.02*	*0.126*	*0.042*	*3.56*	*0.162*	*0.046*
4 ▽	1.01	0.047	0.046	2.01	0.063	0.032	3.01	0.086	0.028	4.01	0.184	0.046
5 ▽	1.00	0.048	0.048	*2.01*	*0.062*	*0.031*	*3.02*	*0.160*	*0.053*	*3.95*	*0.195*	*0.049*
6 *	*1.03*	*0.067*	*0.065*	*2.44*	*0.136*	*0.056*	*3.03*	*0.090*	*0.030*	3.87	0.138	0.036
7 *	0.99	0.042	0.043	2.00	0.060	0.030	*3.02*	*0.073*	*0.024*	*4.00*	*0.128*	*0.032*
8 ▽	*1.01*	*0.091*	*0.090*	*2.03*	*0.072*	*0.036*	*3.00*	*0.072*	*0.024*	*3.68*	*0.215*	*0.058*
Mean (Hz)	1.00	0.055	0.055	2.14	0.101	0.046	2.96	0.108	0.037	3.83	0.178	0.047
STD (Hz)	0.024	0.017	0.016	0.180	0.062	0.025	0.160	0.036	0.012	0.201	0.032	0.010
CoV	0.024	0.302	0.290	0.084	0.615	0.551	0.054	0.336	0.328	0.053	0.180	0.204
Single bob freq (Hz)	Lowest (Hz) 0.784	Largest (Hz) 1.235	Range (%f_B) 45.1%	Lowest (Hz) 1.770	Largest (Hz) 2.899	Range (%f_B) 56.5%	Lowest (Hz) 2.353	Largest (Hz) 3.390	Range (%f_B) 34.6%	Lowest (Hz) 3.175	Largest (Hz) 5.000	Range (%f_B) 45.6%

The smallest amount of IESV, measured using the CoV of the average $f_{B,TS}$ occurred, at 1Hz (0.024, Table 4.11). Although the TSs' bobbing frequencies were variable, the consistency between TSs was high, comparable with jumping. The largest variation in bobbing frequency between TSs occurred at 2Hz (0.084) consistent with jumping. The target frequency of 2Hz had the largest range of bobbing frequencies (56.5%) as a percentage of the target frequency.

The IASV and EIASV of the jumping TSs (Table 4.2) were generally smaller than those in Table 4.11. This is inconsistent with findings of previous authors where bobbing TSs were better at maintaining a target frequency (Sim et al., 2005). There is little difference in the IESV between the two activities, but on average jumping was slightly smaller.

At 1Hz all TSs were on average within 5% of the target frequency, this is consistent with previous observations of highest TS bobbing synchronisation at 1Hz (Sim et al., 2005). The number of TSs achieving the target frequency ±5% reduced to 7/8 at 3Hz and 5/8 at both 2 and 4Hz (Table 4.11). Overestimations of the bobbing frequency were seen at 2Hz, whereas at 3 and 4Hz only underestimations were seen. It is worth noting that on average across all

frequencies slightly more individuals achieved the average target frequency when bobbing (6.25, Table 4.11) compared to jumping (6, Table 4.2). Although more frequency variation is seen between bobs, on average the TS are slightly more likely to achieve the target frequency than when jumping. This is consistent with other authors (Sim et al., 2005; Parkhouse and Ewins, 2004). However, the previous literature recorded a greater segregation between the number of synchronised TSs when jumping and bobbing.

The TSs were split by bobbing style and gender (Table 4.12). There was no significant gender bias in target frequency proximity, however on average the male TSs were slightly closer. The bouncing TSs were consistently nearer the target frequency. All the TSs who did not on achieve an average target frequency ± 5% were jouncing. Beat synchronisation whilst bouncing appears easier than jouncing. It is possible that the TSs within the experiments conducted by Parkhouse and Ewins (2004) were asked to bounce rather than having the freedom to choose the style. No distinction of the bobbing style was reported within their work. This may explain the segregation between the beat synchronisation of bobbing and jumping TSs within their experiments.

Table 4.12 The mean, STD and CoV of the $f_{B,TS}$ values for bobbing style (bouncing (B)/ Jouncing (J)) and gender.

TS	1Hz			2Hz			3Hz			4Hz		
	Ave (Hz)	STD (Hz)	COV	Ave (Hz)	STD (Hz)	COV	Ave (Hz)	STD (Hz)	COV	Ave (Hz)	STD (Hz)	COV
Mean J (Hz)	1.00	0.060	0.060	2.21	0.119	0.053	2.94	0.103	0.035	3.80	0.183	0.049
STD J (Hz)	0.03	0.019	0.018	0.19	0.074	0.031	0.19	0.034	0.011	0.22	0.033	0.010
CoV J	0.03	0.322	0.308	0.09	0.622	0.585	0.06	0.330	0.324	0.06	0.179	0.204
Mean B (Hz)	1.00	0.046	0.046	2.00	0.070	0.035	3.01	0.124	0.041	3.94	0.161	0.041
STD B (Hz)	0.01	0.003	0.003	0.00	0.016	0.008	0.01	0.054	0.018	0.10	0.033	0.007
CoV B	0.01	0.070	0.062	0.00	0.224	0.223	0.00	0.434	0.432	0.02	0.203	0.179
Mean M (Hz)	1.01	0.052	0.052	2.18	0.131	0.059	3.02	0.112	0.037	3.86	0.154	0.040
STD M (Hz)	0.016	0.011	0.010	0.216	0.080	0.033	0.003	0.040	0.013	0.215	0.027	0.007
CoV M	0.016	0.202	0.185	0.099	0.609	0.560	0.001	0.352	0.353	0.056	0.174	0.183
Mean F (Hz)	0.99	0.057	0.058	2.09	0.071	0.034	2.90	0.104	0.036	3.80	0.201	0.053
STD F (Hz)	0.03	0.023	0.022	0.151	0.011	0.003	0.222	0.039	0.013	0.214	0.014	0.007
CoV F	0.03	0.393	0.376	0.073	0.152	0.087	0.077	0.370	0.356	0.056	0.069	0.122

In general the bouncing TSs demonstrated less EIASV and IESV than the jouncing TSs. There was little difference in variability between the genders. In general female TSs had slightly smaller values of IESV, whereas male TSs had slightly smaller EIASV values.

4.3.3 Variation in Peak Force

The average peak force is plotted against the average bob frequency of each TS in Figure 4.23a. The overall mean peak force and the mean ± 1STD are approximated by 2nd order polynomial lines of best fit. On average the smallest peak forces occur at 1Hz and the largest at 3Hz, however between 2 and 4Hz the peak forces are similar (Figure 4.23a). The peak forces from bobbing were smaller than those from jumping in Table 4.4. The range of bobbing peak forces considering all frequencies is 1.24-2.86, compared to 2.15-4.22 whilst jumping.

Using a 5% AD test the bob-by-bob peak forces of 84.4% of the trials were found to be normally distributed. All the trials passed the 2*SES test for skewness, however only 50% passed the 2*SEK test for excess kurtosis.

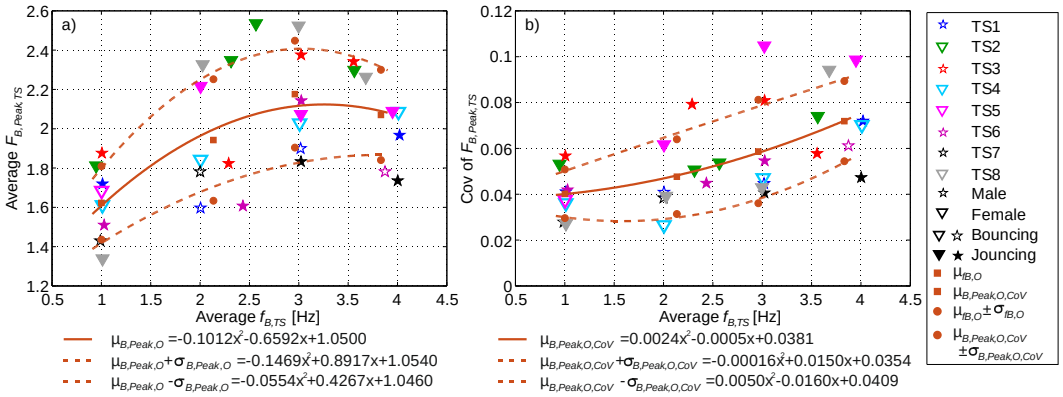

Figure 4.23 a) The average peak forces against average bobbing frequency, the mean $F_{B,Peak,O}$ ($\mu_{B,Peak,O}$) and the mean ± 1STD ($\mu_{B,Peak,O} \pm \sigma_{B,Peak,O}$) are approximated and the equations listed. b) The CoV of $F_{B,Peak,TS}$ against average $f_{B,TS}$, the relationships between f_B and the mean CoV values ($\mu_{B,Peak,OCoV}$) and the mean ± 1STD ($\mu_{B,Peak,O,CoV} \pm \sigma_{B,Peak,O,CoV}$) are aproximated.

The IASV of the peak forces (CoV of $F_{B,Peak,TS}$) increased with bobbing frequency (Figure 4.23a). The majority of the smallest IASV values occurred at 1Hz, and the largest at 4Hz (Table 4.13). The smallest EIASV values occurred at 1Hz (mean and STD of the $F_{B,Peak,TS}$ CoV 0.040, 0.011, respectively), which is consistent with the results from jumping. This indicates that the TSs had

the most consistent peak forces at this frequency, and similar peak force variation between the TSs. The largest EIASV value (mean $F_{B,Peak,TS}$ CoV) was 0.72 at 4Hz, where the TSs' variation was the greatest. The largest STD $F_{B,Peak,TS}$ CoV, representing the greatest differences in force peak variation between TSs was 0.023 at 3Hz.

Table 4.13 The average, STD and COV values of the $F_{B,Peak,TS}$. The EIASV (hatched background) and IESV (highlighted) are marked. The markers denote gender (* male, ▽ female), and font the style (bouncing underlined, jouncing italics).

	1Hz			2Hz			3Hz			4Hz		
TS	**Ave**	**STD**	**COV**	**Ave**	**STD**	**COV**	**Ave**	**STD**	**COV**	**Ave**	**STD**	**COV**
1 *	*1.72*	*0.071*	*0.041*	1.60	0.065	0.041	1.90	0.085	0.045	*1.97*	*0.141*	*0.072*
2 ▽	*1.81*	*0.096*	*0.053*	*2.35*	*0.119*	*0.051*	*2.54*	*0.136*	*0.054*	*2.30*	*0.170*	*0.074*
3 *	*1.88*	*0.106*	*0.057*	*1.82*	*0.145*	*0.079*	*2.38*	*0.192*	*0.081*	*2.34*	*0.135*	*0.058*
4 ▽	1.61	0.058	0.036	1.84	0.049	0.027	2.03	0.095	0.047	2.09	0.147	0.070
5 ▽	1.68	0.063	0.038	*2.22*	*0.137*	*0.062*	*2.07*	*0.217*	*0.105*	*2.09*	*0.206*	*0.099*
6 *	*1.51*	*0.063*	*0.042*	*1.61*	*0.072*	*0.045*	*2.14*	*0.117*	*0.055*	1.78	0.109	0.061
7 *	1.43	0.040	0.028	1.78	0.068	0.038	*1.83*	*0.074*	*0.041*	*1.74*	*0.082*	*0.047*
8 ▽	*1.34*	*0.036*	*0.027*	*2.33*	*0.091*	*0.039*	*2.52*	*0.108*	*0.043*	*2.26*	*0.213*	*0.094*
Mean	1.62	0.067	0.040	1.94	0.093	0.048	2.18	0.128	0.059	2.07	0.150	0.072
STD	0.187	0.025	0.011	0.309	0.036	0.016	0.272	0.051	0.023	0.230	0.045	0.017
CoV	0.115	0.367	0.265	0.159	0.384	0.342	0.125	0.400	0.385	0.111	0.299	0.243
Peak	Lowest	Largest	Δ	Lowest	Largest	Δ	Lowest	Largest	Δ	Lowest	Largest	Δ
forces	1.24	2.08	0.84	1.41	2.53	1.12	1.64	2.86	1.22	1.53	2.74	1.22

The IESV was measured using the CoV of the mean $F_{B,Peak,TS}$ values and was lowest at 4Hz (0.111, Table 4.13), closely followed by 1Hz (0.115). There was good consistency between the TSs at these frequencies. The greatest variation in peak forces between TSs was seen at 2Hz (0.159), consistent with jumping. The values of EIASV and IESV in Table 4.13 are larger than those collected from jumping TSs (Table 4.4). This is likely due to the two distinctive bobbing styles increasing the range of possible peak forces.

The bobbing trials were firstly separated by bobbing style and then gender (Table 4.14). The mean peak forces were larger from jouncing than from bobbing. There was less IESV and EIASV of the peak forces amongst the bouncing TSs, however the sample size was smaller. In general the mean peak forces from female TSs were larger than from male TSs, contrary to jumping. There was no significant difference in the IESV and EIASV amongst male and female TSs.

As with the jumping analysis the effect of various physiological factors upon the peak forces was investigated. However, no obvious correlation was found between peak force and TS

weight or height. It appears physiological features have little effect on the peak forces of bobbing. This is likely due to the continuous contact with the ground.

Table 4.14 The mean, STD and CoV of the peak forces for bobbing style (bouncing/ jouncing) and gender.

	1Hz			2Hz			3Hz			4Hz		
TS	**Ave**	**STD**	**COV**	**Ave**	**STD**	**COV**	**Ave**	**STD**	**COV**	**Ave**	**STD**	**COV**
Mean J	1.652	0.074	0.044	2.066	0.113	0.055	2.247	0.141	0.063	2.117	0.158	0.074
STD J	0.223	0.028	0.012	0.333	0.031	0.016	0.281	0.054	0.025	0.232	0.049	0.020
CoV J	0.135	0.373	0.267	0.161	0.273	0.286	0.125	0.384	0.395	0.109	0.311	0.271
Mean B	1.573	0.054	0.034	1.740	0.061	0.035	1.965	0.090	0.046	1.935	0.128	0.066
STD B	0.129	0.012	0.005	0.125	0.010	0.007	0.092	0.007	0.001	0.219	0.027	0.006
CoV B	0.082	0.225	0.156	0.072	0.168	0.209	0.047	0.079	0.031	0.113	0.210	0.097
Mean M	1.635	0.070	0.042	1.703	0.088	0.051	2.063	0.117	0.056	1.958	0.117	0.060
STD M	0.204	0.027	0.012	0.114	0.038	0.019	0.250	0.053	0.018	0.274	0.027	0.010
CoV M	0.125	0.391	0.282	0.067	0.439	0.375	0.121	0.455	0.324	0.140	0.231	0.173
Mean F	1.610	0.063	0.039	2.185	0.099	0.045	2.290	0.139	0.062	2.185	0.184	0.084
STD F	0.198	0.025	0.011	0.237	0.038	0.015	0.278	0.055	0.029	0.111	0.031	0.014
CoV F	0.123	0.392	0.280	0.108	0.387	0.338	0.121	0.394	0.464	0.051	0.169	0.171

4.3.4 DLFs from Bobbing

The DLFs from bobbing were calculated up to the 3rd harmonic or 6Hz, whichever was the larger following the procedure outlined in Section 4.2.4. The bob-by-bob DLFs were found and used to calculate the average DLFs (Figure 4.24a) and the overall mean DLFs and mean ± 1STD (Figure 4.24b). The bob-by-bob DLFs are not considered normally distributed as only 21.7% of harmonics within the trials passed the 5% AD test. In addition, only 9.5% of the harmonics had skewness values less than 2*SES, 34.8% had an excess kurtosis value less than 2*SEK.

The IASV values (CoV of DLF) were plotted on Figure 4.24 and in general increased with harmonic number. Hence, more TS self-consistency was seen at the 1st harmonics of the bobbing frequencies. The lowest IASV values were seen at 1st harmonic of 3Hz, the highest values occurred at the 3rd harmonic of 4Hz.

Overall the TSs demonstrated least variation (EIASV) at the 1st harmonic of 4Hz (mean DLF CoV =0.131, Table 4.15). The amount the TSs' DLFs varied was also most similar to one another at this harmonic frequency (STD of DLF CoV =0.061). The greatest amount of EIASV occurred at the 3rd harmonic of 4Hz (mean DLF CoV =0.561). The greatest spread in TS variation was at the

6th harmonic of 1Hz (STD of DLF CoV =0.212). In general the IASV and EIASV values from bobbing were greater than from jumping (Table 4.6).

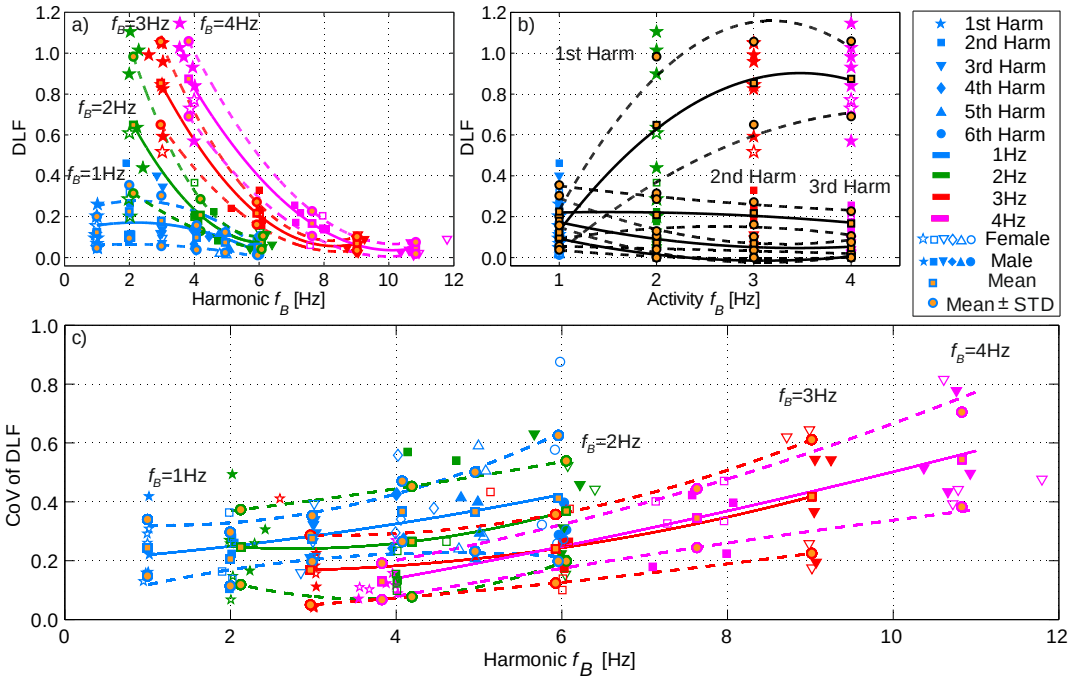

Figure 4.24 a) The DLFs from bobbing, b) The DLFs of the harmonics and the mean and ± 1STD at each activity frequency. c) The CoV of the DLF and the relationship between f_B and the mean CoV values ($\mu_{B,DLF,O,CoV}$) and the mean ± 1STD ($\mu_{B,DLF,O,CoV} \pm \sigma_{B,DLF,O,CoV}$) are aproximated.

The IESV of the DLFs was calculated using the CoV of the average DLFs from each TS, highlighted in Table 4.15. The largest amount of variation between TSs occurred at the 6th harmonic of 1Hz, and the least at the 1st harmonic of 4Hz. In general more IESV was seen at the higher harmonics. Overall the values of IESV were greater than those of jumping. This is likely due to the two styles of bobbing possible. Furthermore, bobbing can vary between enthusiastic borderline bobbing (bobbing which is on the border of jumping (Harrison et al., 2008)) and very low energy bobbing. There is a greater element of TS choice whilst bobbing and therefore the variation between the TSs is greater.

Table 4.15 The average, STD and COV values of the DLFs. The EIASV (hatched background) and the IESV (highlighted) are marked. The markers denote gender (* male, ▽ female), and font the style (bouncing underlined, jouncing italics).

1Hz	1st Harmonic			2nd Harmonic			3rd Harmonic			4th Harmonic			5th Harmonic			6th Harmonic		
TS	Ave	STD	COV	Ave	STD	COV	Ave	STD	COV	Ave	STD	COV	Ave	STD	COV	Ave	STD	COV
1 *	*0.07*	*0.011*	*0.161*	*0.11*	*0.023*	*0.223*	*0.12*	*0.038*	*0.322*	*0.14*	*0.033*	*0.242*	*0.12*	*0.026*	*0.207*	*0.10*	*0.029*	*0.288*
2 ▽	*0.11*	*0.015*	*0.137*	*0.45*	*0.077*	*0.170*	*0.40*	*0.060*	*0.148*	*0.11*	*0.041*	*0.392*	*0.11*	*0.029*	*0.255*	*0.05*	*0.016*	*0.315*
3 *	*0.05*	*0.019*	*0.419*	*0.27*	*0.075*	*0.278*	*0.35*	*0.102*	*0.294*	*0.21*	*0.090*	*0.428*	*0.13*	*0.050*	*0.399*	*0.10*	*0.039*	*0.397*
4 ▽	*0.20*	0.053	0.260	0.26	0.036	0.138	0.10	0.020	0.214	0.04	0.013	0.341	0.01	0.007	0.590	0.01	0.010	0.876
5 ▽	*0.16*	0.045	0.292	0.32	0.036	0.114	0.15	0.039	0.264	0.05	0.029	0.558	0.04	0.020	0.505	0.01	0.009	0.577
6 *	*0.05*	*0.011*	*0.221*	*0.12*	*0.031*	*0.260*	*0.14*	*0.047*	*0.339*	*0.13*	*0.036*	*0.274*	*0.12*	*0.034*	*0.294*	*0.09*	*0.028*	*0.305*
7 *	*0.09*	0.015	0.160	0.18	0.019	0.105	0.12	0.025	0.210	0.04	0.018	0.425	0.02	0.008	0.414	0.01	0.004	0.274
8 ▽	*0.26*	*0.081*	*0.309*	*0.08*	*0.028*	*0.363*	*0.07*	*0.028*	*0.394*	*0.07*	*0.020*	*0.295*	*0.04*	*0.012*	*0.281*	*0.03*	*0.008*	*0.259*
Ave	0.12	0.031	0.245	0.22	0.041	0.206	0.18	0.045	0.273	0.10	0.035	0.369	0.07	0.023	0.368	0.05	0.018	0.411
STD	0.08	0.026	0.095	0.13	0.022	0.091	0.12	0.026	0.080	0.06	0.024	0.103	0.05	0.015	0.133	0.04	0.013	0.214
CoV	0.63	0.818	0.388	0.57	0.553	0.441	0.69	0.587	0.293	0.61	0.693	0.279	0.67	0.629	0.360	0.77	0.718	0.521

2Hz	1st Harmonic			2nd Harmonic			3rd Harmonic		
TS	Ave	STD	COV	Ave	STD	COV	Ave	STD	COV
1 *	0.20	0.099	0.494	0.20	0.031	0.155	0.13	0.039	0.311
2 ▽	*1.01*	*0.263*	*0.259*	*0.22*	*0.059*	*0.264*	*0.06*	*0.028*	*0.443*
3 *	*0.64*	*0.106*	*0.166*	*0.18*	*0.100*	*0.569*	*0.11*	*0.052*	*0.458*
4 ▽	0.61	0.041	0.067	0.20	0.020	0.098	0.05	0.010	0.207
5 ▽	*0.90*	*0.232*	*0.258*	*0.20*	*0.027*	*0.133*	*0.04*	*0.019*	*0.523*
6 *	*0.44*	*0.134*	*0.306*	*0.08*	*0.044*	*0.540*	*0.04*	*0.027*	*0.630*
7 *	0.29	0.077	0.270	0.37	0.046	0.126	0.08	0.018	0.223
8 ▽	*1.10*	*0.163*	*0.147*	*0.21*	*0.049*	*0.233*	*0.07*	*0.010*	*0.153*
Ave	0.65	0.14	0.246	0.21	0.05	0.265	0.07	0.03	0.369
STD	0.33	0.08	0.127	0.08	0.03	0.188	0.03	0.01	0.170
CoV	0.51	0.547	0.518	0.37	0.532	0.708	0.45	0.563	0.462

3Hz	1st Harmonic			2nd Harmonic			3rd Harmonic		
TS	Ave	STD	COV	Ave	STD	COV	Ave	STD	COV
1 *	0.52	0.022	0.043	0.21	0.038	0.178	0.11	0.041	0.367
2 ▽	*0.99*	*0.408*	*0.411*	*0.24*	*0.105*	*0.434*	*0.05*	*0.030*	*0.620*
3 *	*1.05*	*0.192*	*0.183*	*0.23*	*0.061*	*0.262*	*0.09*	*0.049*	*0.542*
4 ▽	0.85	0.034	0.040	0.22	0.030	0.139	0.09	0.016	0.175
5 ▽	*0.83*	*0.129*	*0.156*	*0.18*	*0.068*	*0.376*	*0.03*	*0.017*	*0.644*
6 *	*0.96*	*0.107*	*0.112*	*0.16*	*0.042*	*0.264*	*0.02*	*0.013*	*0.544*
7 *	*0.59*	*0.134*	*0.226*	*0.16*	*0.028*	*0.173*	*0.07*	*0.013*	*0.195*
8 ▽	*1.05*	*0.185*	*0.176*	*0.33*	*0.033*	*0.100*	*0.09*	*0.024*	*0.258*
Ave	0.85	0.15	0.168	0.22	0.05	0.241	0.07	0.03	0.418
STD	0.20	0.12	0.118	0.06	0.03	0.117	0.03	0.01	0.193
CoV	0.24	0.797	0.703	0.25	0.519	0.485	0.48	0.537	0.462

4Hz	1st Harmonic			2nd Harmonic			3rd Harmonic		
TS	Ave	STD	COV	Ave	STD	COV	Ave	STD	COV
1 *	*0.83*	*0.085*	*0.102*	*0.14*	*0.056*	*0.405*	*0.01*	*0.009*	*0.915*
2 ▽	*1.15*	*0.126*	*0.110*	*0.17*	*0.069*	*0.402*	*0.04*	*0.016*	*0.393*
3 *	*1.03*	*0.072*	*0.071*	*0.26*	*0.046*	*0.179*	*0.07*	*0.032*	*0.434*
4 ▽	0.77	0.208	0.269	0.20	0.069	0.335	0.09	0.043	0.477
5 ▽	*0.93*	*0.147*	*0.158*	*0.14*	*0.068*	*0.471*	*0.04*	*0.032*	*0.816*
6 *	0.73	0.090	0.123	0.06	0.026	0.423	0.02	0.011	0.497
7 *	*0.57*	*0.066*	*0.116*	*0.14*	*0.030*	*0.224*	*0.03*	*0.014*	*0.515*
8 ▽	*0.98*	*0.101*	*0.102*	*0.22*	*0.072*	*0.327*	*0.07*	*0.032*	*0.442*
Ave	0.87	0.11	0.131	0.17	0.05	0.346	0.05	0.02	0.561
STD	0.18	0.05	0.061	0.06	0.02	0.101	0.03	0.01	0.194
CoV	0.21	0.422	0.463	0.37	0.340	0.292	0.62	0.537	0.345

Average DLFs	1st harmonic all frequencies			2nd harmonic all frequencies			3rd harmonic all frequencies		
	Lowest	Largest	Range	Lowest	Largest	Range	Lowest	Largest	Range
	0.05	1.15	1.10	0.06	0.45	0.39	0.01	0.40	0.39

From Figure 4.24b, disregarding the 1st harmonic of 1Hz, the mean DLF magnitudes at each harmonic are comparable between the frequencies. The biggest DLFs were seen at the 1st harmonics of 2, 3 and 4Hz bobbing. The largest average value was 1.15 at 4Hz, smaller than the largest average jumping DLF value (1.63 at 3Hz, Table 4.6). Above the 1st harmonic the majority of the DLFs were below 0.4. In theory the bobbing DLFs should be less than one as contact is maintained with the ground (Parkhouse and Ewins, 2004). Six average DLFs from these trials exceed one. Sim et al. (2005) also demonstrated that enthusiastic bobbing can produce DLFs greater than one.

The highest DLFs were produced by the jouncing TSs, marked by solid markers on Figure 4.24a. However, above the 1st harmonics there were no obvious distinctions in the DLFs between the styles. Although larger peak forces are associated with jouncing (Table 4.14), the more consistent bobbing frequency associated with bouncing (Table 4.12) makes the DLFs comparable at higher harmonics. Overall the EIASV values are generally smaller amongst the bouncing TSs, the IESV is similar between the two styles (Table 4.16).

The DLFs from female TSs are larger than those from male TSs (Table 4.16). In general male TSs' have slightly smaller values of EIASV. The IESV is less amongst female TSs.

Table 4.16 The mean, STD and CoV of the 1st harmonic DLF values for bobbing style (bouncing/ Jouncing) and gender.

	1Hz			2Hz			3Hz			4Hz		
TS	**Ave**	**STD**	**COV**	**Ave**	**STD**	**COV**	**Ave**	**STD**	**COV**	**Ave**	**STD**	**COV**
Mean J	0.107	0.027	0.249	0.819	0.180	0.227	0.911	0.192	0.211	0.915	0.100	0.110
STD J	0.090	0.030	0.115	0.276	0.066	0.068	0.177	0.111	0.105	0.198	0.032	0.028
CoV J	0.837	1.091	0.463	0.337	0.368	0.297	0.194	0.575	0.499	0.217	0.317	0.257
Mean B	0.150	0.038	0.237	0.366	0.073	0.277	0.681	0.028	0.042	0.751	0.149	0.196
STD B	0.055	0.020	0.069	0.215	0.029	0.213	0.232	0.008	0.002	0.029	0.083	0.103
CoV B	0.365	0.533	0.291	0.589	0.405	0.770	0.340	0.292	0.050	0.039	0.561	0.528
Mean M	0.064	0.014	0.240	0.391	0.104	0.309	0.779	0.114	0.141	0.790	0.078	0.103
STD M	0.022	0.004	0.122	0.191	0.023	0.137	0.263	0.071	0.080	0.192	0.011	0.023
CoV M	0.335	0.287	0.509	0.489	0.225	0.443	0.338	0.621	0.571	0.243	0.139	0.227
Mean F	0.182	0.048	0.249	0.907	0.175	0.183	0.928	0.189	0.196	0.958	0.145	0.160
STD F	0.064	0.027	0.078	0.216	0.098	0.093	0.111	0.159	0.155	0.154	0.046	0.077
CoV F	0.354	0.555	0.311	0.238	0.563	0.509	0.119	0.840	0.794	0.161	0.315	0.482

Previous literature suggested that there is often not a dominant harmonic for bobbing (Sim et al., 2005). This holds true for most TSs at 1Hz where there is little difference in the harmonic DLFs (Figure 4.24a). At 2, 3 and 4Hz this is not the case for TSs from both bobbing styles.

4.3.5 Bobbing Displacement

As with the jumping experiments the displacements of the TSs' body were monitored and collected. The maximum bob-by-bob displacements were calculated as the maximum elevation of the marker above the rest height of the marker and plotted against the peak force (Figure 4.25a). The average peak force against average maximum displacement for each TS are shown in Figure 4.25b. There is a slight positive correlation between the variables at each frequency (Figure 4.25b). However, likewise to jumping the target frequency has a greater effect on the peak force (Figure 4.11a). Also consistent with jumping, greater maximum displacements were seen at 1 and 2Hz, compared to the higher frequencies. There is little obvious distinction between the average displacements from jouncing and bouncing TSs, however the largest displacements were all from jouncing TSs. The maximum displacements are smaller than those from jumping which can be twice as large. It is worth noting that negative maximum displacements can occur when bobbing (Figure 4.25a). Some TSs bend below their static height when attempting to maintain a continuous stream of bobs at 4Hz.

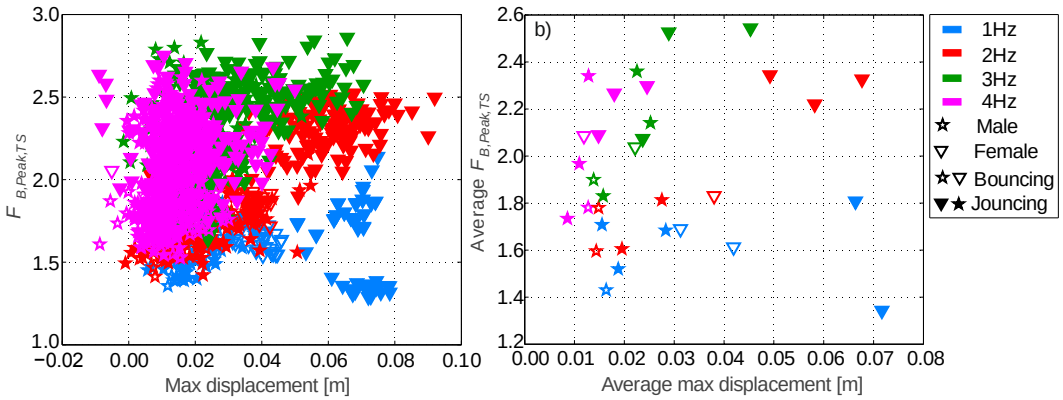

Figure 4.25 a) The bob-by-bob peak force and maximum displacement. b) The average peak force and average maximum displacement for each TS.

The bob-by-bob maximum displacements only passed the 5% AD test in 37.5% of trials, however 75% of the 4Hz trials passed. The skewness value was below 2*SES in 59.4% of cases, all of the 4Hz trials had a value beneath this threshold. 78% of trials had an excess kurtosis less than 2*SEK. Considering these tests it is likely that the maximum displacements can only be considered normally distributed for the bobbing frequency of 4Hz.

The average value of each TS's maximum displacement and bob frequency are plotted in Figure 4.26a. The IASV values calculated as the CoV of the maximum displacements increase with increasing target frequency (Figure 4.26b). The smallest CoV values and hence most consistent TS displacements were seen at 1Hz, the largest values occurred at 4Hz. Overall the least EIASV (mean CoV of displacements =0.202, Table 4.17) occurred at 1Hz. However, the TSs' EIASV of maximum displacements were most similar to one another at 3Hz (STD CoV of displacements =0.115). The greatest EIASV (mean CoV of displacements =0.444) was at 4Hz, highlighting the high variability in each TS's maximum displacement. The greatest spread in TS variation was seen at 2Hz (STD CoV of the displacements =0.162).

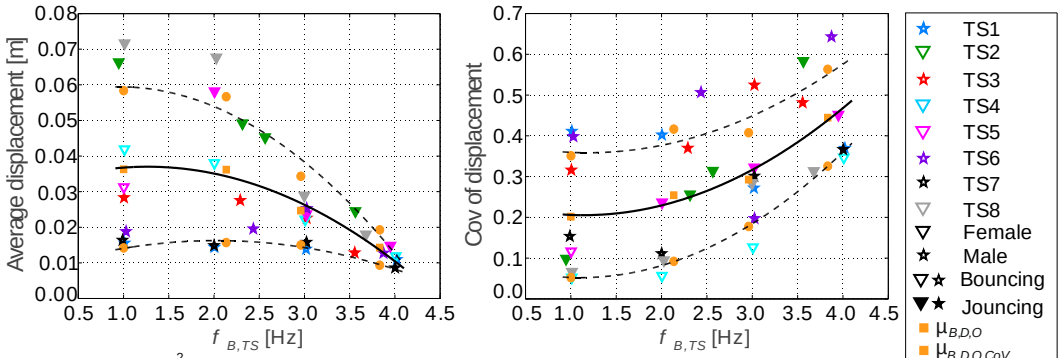

Figure 4.26 a) The average maximum displacement and bobbing frequency, the mean maximum displacement ($\mu_{B,D,O}$) and the mean ± 1STD ($\mu_{B,D,O} \pm \sigma_{B,D,O}$) are approximated and the equations listed. b) The CoV of the maximum displacements and average $f_{B,TS}$, the relationships between f_B and the mean CoV values ($\mu_{B,D,O,CoV}$) and the mean ± 1STD ($\mu_{B,D,O,CoV} \pm \sigma_{BD,O,CoV}$) are aproximated.

The IESV measured as the CoV of the average values of the TSs' maximum displacement was smallest at 4Hz (IESV=0.348, Table 4.17). The greatest average variation between TSs was seen at 1Hz (IESV=0.608) as shown in Figure 4.26a, however the widest range of maximum

displacements occurred at 2Hz (0.092m). Smaller ranges of maximum displacements were seen at the higher bobbing frequencies.

Table 4.17 The average, STD and COV values of the maximum displacements. The EIASV (hatched background) and IESV (highlighted) are marked. The markers denote gender (* male, ▽ female), and font the style (bouncing underlined, jouncing italics).

	1Hz			2Hz			3Hz			4Hz		
TS	**Ave (m)**	**STD (m)**	**COV**	**Ave (m)**	**STD (m)**	**COV**	**Ave (m)**	**STD (m)**	**COV**	**Ave (m)**	**STD (m)**	**COV**
1 *	0.02	0.006	0.411	0.01	0.006	0.402	0.01	0.004	0.272	0.01	0.004	0.369
2 ▽	0.07	0.007	0.098	0.05	0.013	0.256	0.05	0.014	0.314	0.02	0.014	0.584
3 *	0.03	0.009	0.316	0.03	0.010	0.370	0.02	0.012	0.524	0.01	0.006	0.481
4 ▽	0.04	0.002	0.052	0.04	0.002	0.057	0.02	0.003	0.127	0.01	0.004	0.347
5 ▽	0.03	0.004	0.116	0.06	0.014	0.237	0.02	0.008	0.322	0.01	0.007	0.452
6 *	0.02	0.007	0.398	0.02	0.010	0.506	0.03	0.005	0.197	0.01	0.008	0.643
7 *	0.02	0.003	0.153	0.01	0.002	0.111	0.02	0.005	0.301	0.01	0.003	0.366
8 ▽	0.07	0.005	0.067	0.07	0.006	0.095	0.03	0.008	0.284	0.02	0.006	0.313
Mean (m)	0.04	0.005	0.202	0.04	0.008	0.254	0.02	0.007	0.293	0.01	0.007	0.444
STD (m)	0.022	0.002	0.149	0.020	0.005	0.162	0.010	0.004	0.115	0.005	0.004	0.119
CoV	0.608	0.457	0.741	0.566	0.582	0.638	0.391	0.555	0.392	0.348	0.542	0.267
Max disp (m)	Lowest (m)	Largest (m)	Δ (m)	Lowest (m)	Largest (m)	Δ (m)	Lowest (m)	Largest (m)	Δ (m)	Lowest (m)	Largest (m)	Δ (m)
	0.006	0.078	0.072	-0.001	0.092	0.093	-0.002	0.071	0.073	-0.009	0.050	0.059

The EIASV values from the maximum displacements of jumping were smaller, however both activities saw an increase in EIASV with increased frequency. The IESV values from jumping were significantly smaller. In general the TSs maintained a more consistent maximum displacement personally and amongst the other TSs whilst jumping.

The TSs' average maximum displacements were plotted against TS height to determine whether there was a relationship between the variables (Figure 4.27). Little correlation was apparent between the two variables, suggesting that TS height does not affect the maximum bob displacement.

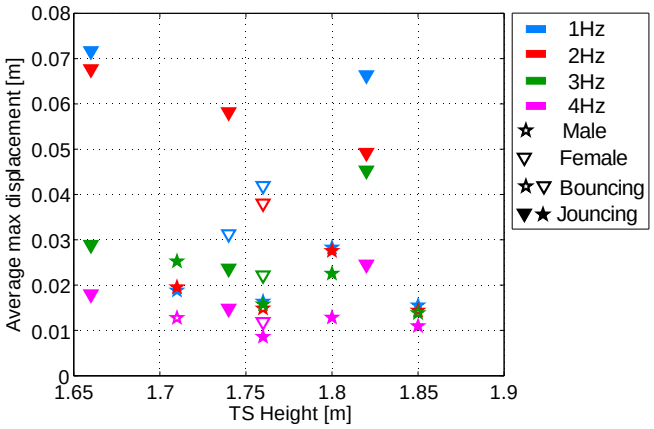

Figure 4.27 The average maximum displacement against TS height.

4.3.6 Conclusions

The force profiles from both bouncing and jouncing TSs have a wide variety of profile shapes. In general the magnitudes of jouncing forces are larger. However, low energy jouncing and high energy bouncing can occur and the corresponding force magnitudes reflect this. The variety of profile shapes reduce with bobbing frequency. At high frequencies the bouncing and jouncing force profiles become more similar, tending towards a single force peak comparable to jumping force profiles. Bouncing and jouncing should be considered as separate activities and both studied further.

For bobbing it was concluded that the frequency of each TS's bobs were not normally distributed (except possibly at 1Hz). The least f_B EIASV was seen at 3 and 4Hz and the greatest f_B EIASV at 1 and 2Hz. Overall the EIASV of bobbing was greater than for jumping. The minimum f_B IESV was at 1Hz where the TSs were most consistent with one another. The greatest f_B IESV occurred at 2Hz, consistent with jumping. The IESV of bobbing and jumping were similar, however on average the IESV from jumping was smaller.

All TSs on average achieved the target frequency ±5% at 1Hz, however only 7/8 TSs were able to do this at 3Hz and 5/8 TSs for 2 and 4Hz. Frequency overestimations were seen at 2Hz and underestimations at 3 and 4Hz. The over and under-estimations were all due to TSs who were

jouncing. The bouncing TSs also had less EIASV and IESV. Beat synchronisation whilst bouncing appears easier than jouncing.

The greatest peak forces from bobbing were at 3Hz, however the values were similar between 2 and 4Hz. Each TS's peak forces were potentially normally distributed. The jouncing TSs had larger peak forces, and greater IESV and EIASV than the bouncing TSs. Contradictory to the observations of jumping, the female TSs on average had larger forces than the male TSs. The least $F_{B,Peak,TS}$ EIASV occurred at 1Hz, which is consistent with the findings from the jumping analysis. The greatest amount of EIASV occurred at 3 and 4Hz. The $F_{B,Peak,TS}$ IESV was lowest at 1 and 4 Hz, and highest at 2Hz, which is consistent with jumping. The values of EIASV and IESV (Table 4.13) were larger than those from jumping (Table 4.4). This is likely due to the two styles of bobbing increasing the range of peak forces. Unlike jumping, the normalised bobbing force is unaffected by TSs weight and height, little correlation was seen between these factors and $F_{B,Peak,TS}$.

The bobbing DLFs were not normally distributed and smaller than those from jumping. In general the DLF's IASV, EIAV and IESV increased with harmonic number and were larger than those from jumping TSs. The largest bobbing DLFs occurred at the 1st harmonic from jouncing TSs at 2, 3 and 4Hz. At 1Hz and the higher harmonics there was little distinction between bouncing and jouncing. It is likely the larger peak forces associated with jouncing are compensated by the more consistent bob frequency of bouncing.

Although bobbing can take place at a higher frequency the DLF values from bobbing are on average between 1.7 and 2.3 times smaller than jumping at the 1st harmonic, and between 2.68 and 4.5 times at the 2nd harmonic. Jumping is the more critical activity and more likely to adversely affect structures.

The bob-by-bob maximum displacements are only normally distributed for the target frequency of 4Hz. The largest maximum displacements were from jouncing TSs and occurred at

1 and 2Hz. The values can be twice as small as the equivalent jumping maximum displacements. There is a slight positive correlation between the maximum displacements and the peak forces, however bob frequency has a greater effect on peak force. No correlation was observed between TS height and maximum displacements. The most EIASV was at 3Hz, however the EIASV values between TSs were similar. The least EIASV occurred at 1Hz. The maximum displacements varied most between TSs (IESV) at 1Hz, and were most consistent with one another at 4Hz. The values of IASV, EIASV and IESV were larger than those from jumping, hence jumping TSs were more consistent with themselves and each other.

It would be of benefit to study the IESV, IASV and EIASV of both bobbing and jumping TSs within groups to observe how inclusion within a group affects TS variation.

5 Measuring Dynamic Force of a Jumping Person by Monitoring their Body Kinematics

5.1 Introduction

Jumping is deemed the most critical human induced dynamic loading that can be applied upon a structure (Ellis and Ji, 1994; Rainer et al., 1988). Jumping forces are tri-directional, however the largest component and the subject of this study is the force in the vertical direction. When jumping, an individual can generate a ground reaction force (GRF) that is up to seven times larger than their static weight (Bachmann and Ammann, 1987). If individuals within a crowd jump in sync with one another, there is potential to produce a large dynamic load which may lead to extreme structural accelerations and displacements. Environmental stimuli such as music, visual cues and other audience members may encourage and increase the coordination. Due to the diverse physiology and psychology of humans, the range of movements and synchronization capabilities vary between individuals. It is therefore difficult to accurately predict the dynamic load capacity of a crowd. Furthermore, within the venues at risk, such as stadiums or concert halls, measuring the dynamic force is challenging.

The current UK recommendations (UK Working Group, 2008) for stadium design predominantly rely on laboratory studies to calculate the likely dynamic forces (Parkhouse and Ewins, 2004; Yao et al., 2006). These studies often observe individuals separately in a lab, and therefore crowd interaction and environmental influences are ignored. In addition, the activities observed within a laboratory may not be consistent with those at a stadium event. Hence, there is a lack of authentic force measurements from crowds, which lead to difficulties predicting the dynamic forces and the corresponding structural response. As a consequence, stadium designs may underestimate the dynamic load, leading to excessive vibrations which can cause crowd panic, and cracking and damage of the structure. Alternatively,

overestimating the force leads to over-conservative and unnecessarily expensive stadia. To further this field of research and ensure safe but economical stadium designs, in-situ observations of crowds on stadia are required.

Within this chapter the current practice and force measurement techniques are discussed. A simple and reliable technique, with in-situ potential, to aid the measuring of dynamic forces from individuals within a crowd is proposed. Experiments using this technique and a force plate to measure the GRFs of jumping subjects are conducted and the results presented and compared to those of previous authors. The results are verified by applying the forces to varying single degree of freedom (SDOF) systems. The contents of this chapter are partially reported in a conference publication (McDonald and Zivanovic, 2013).

5.2 Background

In this section a brief introduction to the current UK stadium guidance is given. This is followed by a discussion of the different methods currently used for measuring the structural response and dynamic forces. These methods include conventional direct measurement methods (such as the use of force plates) and indirect methods (such as the use of accelerometers, marker-based motion capture techniques and marker-less video techniques).

5.2.1 Recommendations for Grandstands

The most recent UK stadium recommendations are provided by the UK Working Group (2008), as detailed in Section 3.2.3. The recommendations include two routes to assess the dynamic response of a structure. The first route advises that if the lowest relevant natural frequency of the structure is 3.5Hz or greater for loading scenarios 1 and 2 (Table 3.3), or 6Hz and above for scenarios 3 and 4 the structure will not be prone to significant crowd excitation. Failing this criterion, the second route for the evaluation of the structural response includes accurate modelling of the structure and the dynamic forces, and the comparison of the calculated response to predefined vibration limits, described in Section 3.2.3. Implementation of this

route requires a good insight into the expected event-specific crowd behaviour and knowledge of the crowd's sensitivity to the vibrations generated.

The current design practice would benefit from in-situ testing of crowds at stadium events, as the majority of the current knowledge is based on laboratory studies. This work would thereby aid further developments and verification of the current force models (Section 3.2.3).

5.2.2 Measuring Dynamic Load

Quantifying the vertical dynamic load due to crowd movements on a structure is challenging. Some existing methods including the evaluation of the structural response, and direct and indirect force measurements are discussed in this section.

A force plate is a direct method of measuring the GRFs (Dougill et al., 2006). Although force plates are able to accurately measure dynamic loads, several limitations are associated with the use of these devices for structural engineering purposes. These restrictions include the limited size of the plate and the potential data bias introduced by a subject targeting a specific landing area. One force plate is required per TS which limits group size. In addition, force plates are often fixed to a location, restricting their use to a particular area of a structure.

Accelerometers can be used as an indirect method to evaluate the dynamic forces via measurements of structural accelerations. Relating the measured response to the applied force is difficult as a range of crowd activities may occur, and the participation levels and distribution, and the synchronisation of the crowd is unknown (Salyards and Hanagan, 2007; Setareh, 2011). In addition the modal properties of the stucture are altered by human occupancy.

A novel indirect GRF measurement system which addresses some of the limitations of force plates and accelerometers was developed by Thornton-Trump and Daher (1975). This approach, originally used in biomedical studies, was introduced into the field of structural

engineering (Harrison, et al., 2006; Racic et al., 2010). Motion-capture systems monitor individual's body movements and use this kinematic data to calculate the GRFs. The dynamic part of the GRF F_{GR} is obtained by subtracting the individual's weight from the total GRF, which is calculated as the product of the body mass m and the acceleration of the centre of mass (CoM) a_{CoM} (positive downwards):

$$\boldsymbol{F_{GR} = ma_{CoM} - mg = m(a_{CoM} - g)} \quad 5.1$$

where g is the acceleration due to gravity (+9.81ms^{-2}). The CoM movement cannot be directly measured as it is within the body for studied jumping postures. An indirect alternative is to theoretically divide the body into rigid segments and apply markers to specific locations on each body segment (Figure 5.1). The setup in Figure 5.1 (Racic et al., 2010) uses nine markers placed on one side of the body, symmetry of segment movement is assumed across the sagittal plane. The marker displacements are tracked via the camera system, and a mass distribution model (De Leva, 1996) is then used to calculate the displacements of each segment's CoM (Racic et al., 2010). Differentiating the segment's CoM displacements twice enables the segment's CoM accelerations to be found. The dynamic GRF is then calculated as the sum of the inertia forces of each segment:

$$\boldsymbol{F_{GR} = \sum_{i=1}^{s} m_i (a_i - g)} \quad 5.2$$

where m_i is the mass and a_i the acceleration of the CoM of the $_i{}^{th}$ body segment. Racic et al. (2010) observed percentage differences of ±2%, ±4% and ±7% over activity frequencies of 1.4-2.8Hz for the 1st, 2nd and 3rd harmonic components respectively, between GRFs measured simultaneously using markers and a force plate. However, it should be noted that the test population in this experiment was limited to two male volunteers. The small sample size prevents the generalisation of the experimental results to the wider population. In addition, the use of nine markers to monitor a subject is impractical when considering multiple subjects. Difficulties will be incurred when identifying the ownership of each marker if using a passive

marker system which relies on external lighting such as VICON (Oxford Metrics Group, 2007). Furthermore, a clear view of each marker is required which is impractical in crowded situations. Tracking nine markers per subject increases the complexity of the experiments and the equipment required.

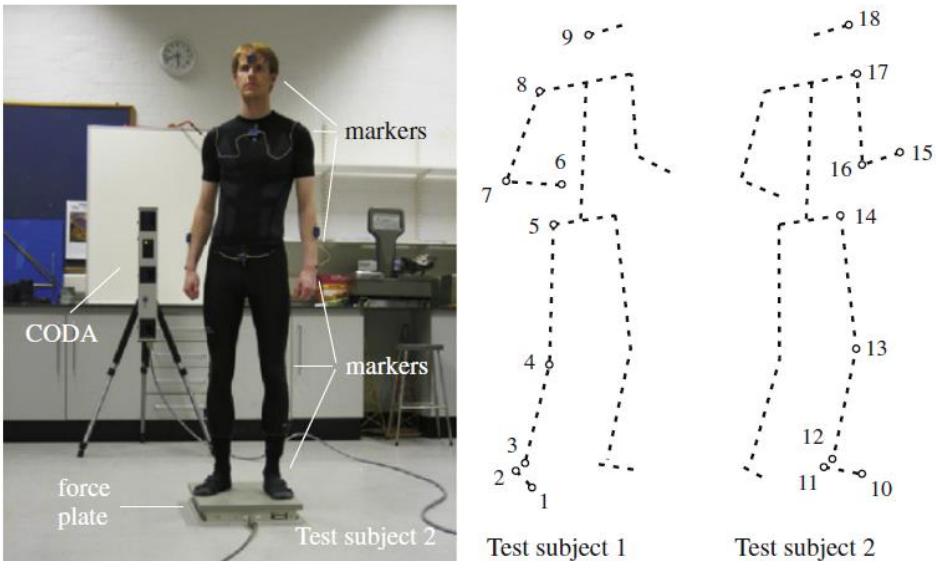

Figure 5.1 Marker positions and experimental setup for motion capture tests (after Racic et al., 2010).

In the previous nine marker work, it was assumed that the body was composed of a series of rigid sections connected by joints (De Leva, 1996; Zatsiorsky et al., 1990). When a subject jumps, the landing impact and corresponding accelerations cause relative movement between the soft body tissue and the underlying "rigid" bone. This movement is called soft tissue artefact and may introduce an error in the calculation of the CoM position of each segment, and therefore the total GRF. The soft tissue artefact can be minimised by placing markers solely on bony landmarks where relative movements are reduced (Racic et al., 2010). Moreover, the frequency of the relative movement is generally higher than the harmonics of interest, in this case the first three, and can be filtered out as background noise using a low pass filter (Racic et al., 2010).

Indirect force measurement has also been attempted using video monitoring (Mazzoleni and Zappa, 2012; Hoath et al., 2007). One such technique uses digital image correlation (DIC)

methods to track the movement of 100 segments (each assumed to have the same mass) per person through each frame of footage (Mazzoleni and Zappa, 2012). The total GRF is calculated as:

$$\boldsymbol{F_{GR}} = \sum_{\boldsymbol{i=1}}^{\boldsymbol{100}} \frac{\boldsymbol{m}}{\boldsymbol{100}} \cdot a_i \qquad 5.3$$

where m is the subject's mass and a_i the acceleration time history of the $_i{}^{th}$ segment. These estimated forces compare well to data collected simultaneously using a force plate. Percentage errors between +3% and -12% for the 1st harmonics of the two force spectra were reported. Although this method was only verified on one subject, a similar approach has been used to estimate the structural response of the Meazza stadium under the loading of up to eight jumping individuals. In this case, the group's average accelerations were calculated by monitoring the accelerations of 1344 segments encompassing the group. However, only 305 segments from the top portion of the subjects, where significant motion was detected, were used to calculate the average accelerations. The average accelerations were multiplied by the total mass of the group to estimate the GRF. The response of the stadium was then estimated and compared to the response measured using accelerometers. It was found that the error relative to the measured response was between +32% and -14%, suggesting that this technology has potential for future developments.

Another video technique, that aimed to distinguish individuals' movements from within a crowd was proposed (Hoath et al., 2007). Individuals' head movements were tracked through frames of video footage and the displacements were compared to GRFs simultaneously measured using a force plate. Correlation was found between the head movements and the GRFs. However, if subjects turned or moved their heads relative to their bodies, the processing software failed to recognise the patch of pixels.

Whilst marker-less video techniques are more convenient, they often consider average crowd movement and the synchronisation between individuals is not prioritised. Increased

percentage errors are seen when compared to the motion capture system technique utilising nine markers (Racic et al., 2010). The aim of this chapter is to investigate a potential method to simplify experimental procedures whilst still achieving accurate measurements of GRFs.

5.3 Experimental Procedure

A large number of markers per person is not suitable for monitoring groups of individuals. Difficulties differentiating between markers on each test subject may arise. Additionally, implementing multiple markers in in-situ conditions is demanding of time and resources. Therefore, a new experimental method, using a single marker to track each individual, is suggested in this study.

The first objective of the experiments is to identify if one marker is sufficient to map the movement of the CoM, and calculate an accurate force profile. The second objective is to investigate the location of the marker which best facilitates the first aim.

A Gait lab facility, equipped with 12 infra-red VICON cameras (Oxford Metrics Group, 2007), two digital video cameras and an AMTI Biomechanics Force Platform OR6 (AMTI, 2007), was used in the experiments. Markers were attached to the Test Subject's (TS) body and cameras recorded their movements. VICON Nexus software (Oxford Metrics Group, 2008) was then utilised to recreate the movements on a computer.

Eight TSs (four male and four female) participated in the experiments. Physiological information regarding the TSs is shown in Table 5.1.

Table 5.1 TS physiological data.

TS	1	2	3	4	5	6	7	8
Sex	M	F	M	F	F	M	M	F
Body mass (Kg)	83	70	83	65	66	85	73	68
Height (m)	1.85	1.82	1.80	1.76	1.74	1.71	1.76	1.66
BMI(Kgm^{-2})	24.4	21.1	25.8	21.0	21.8	29.1	23.6	24.8

The BMI refers to the body mass index calculated as (CDC, 2011):

$$\boldsymbol{BMI} = \frac{\boldsymbol{Body\ mass}}{\boldsymbol{Height^2}} \quad 5.4$$

which is a method of working out the body build of the TSs. If the BMI <18.5 the person is considered to be underweight, for 18.5 ≤ BMI <25 they are considered normal, for 25 ≤ BMI <30 overweight and BMI ≥30 obese (CDC, 2011).

The experimental protocol consisted of a TS jumping on a force plate to the beat of a metronome at frequencies of 1, 2 and 3Hz. The chosen frequency range accommodated extreme jumping frequencies (1Hz, 3Hz) and a frequency deemed easy to jump at (2Hz) (Yao et al., 2006). The frequency of 2Hz is also fairly representative of pop music. For each trial five seconds was allocated to allow the TSs to familiarise themselves with the beat, then 20 seconds of data were recorded.

A total of 17 markers were applied to each TS, as shown in Figure 5.2 and Figure 5.3. The marker positions were at locations with the potential to represent the movement of the CoM well. The markers were divided into three location groups: the back, hips and front of the TSs.

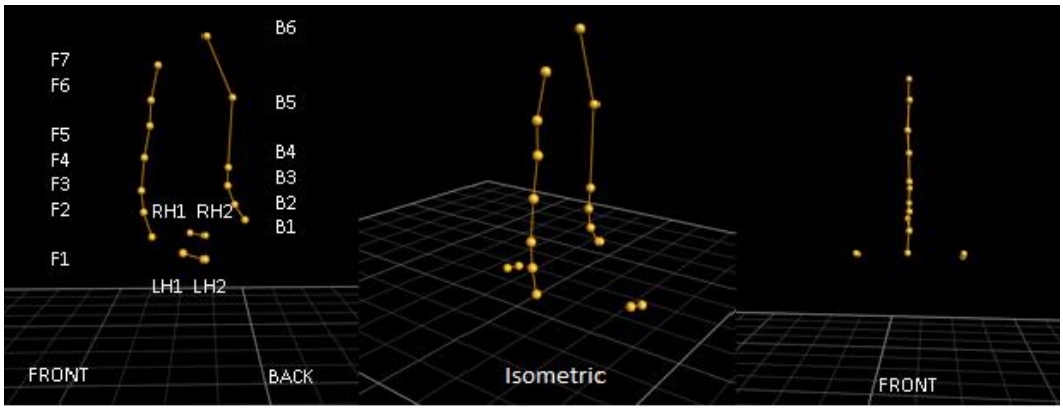

Figure 5.2 From left to right: the side, isometric and frontal views of the 17 markers displayed using Nexus software (Oxford Metrics Group, 2008). B, H and F refer to markers on the back, hips and front of the TS, respectively, where L and R notate left and right, respectively.

Six markers were placed on the TS's back (B1- B6 in Figure 5.2) on the L5th, L3rd and the L1st vertebrae on the lower back, the T11th vertebrae and T6th vertebrae (between the shoulder blades) on the middle back and the C7th vertebrae at the base of the neck (Figure 5.3a). Four

markers were positioned on the hips (RH1 & RH2 on the right hip, and LH1 &LH2 on the left hip, Figure 5.2), on the anterior superior iliac spine and the greater trochanter on both the left and right side of the body. Seven markers were placed on the front of the TS (F1- F7 in Figure 5.2b) positioned evenly up the torso. The majority of the markers were placed on the trunk as the CoM location was expected to be within that region for a jumping posture.

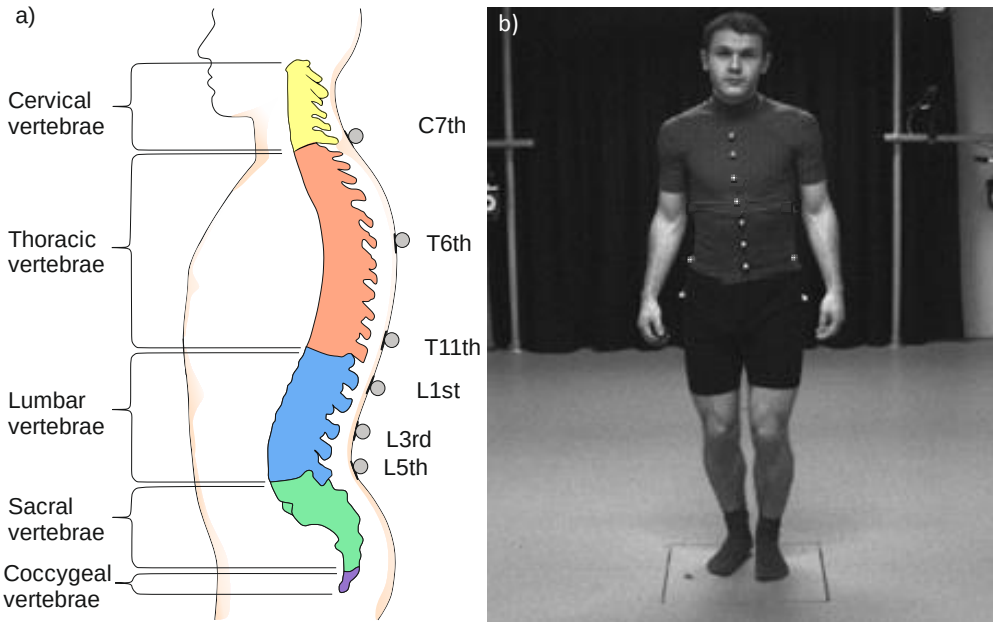

Figure 5.3 a) Vertebrae locations of the back markers. b) Front and hip markers on a TSs.

The displacements from each marker were recorded at 200Hz by the VICON cameras. These were filtered using a 5th order Butterworth filter where the cut-off frequency of the filter was either 1Hz above the frequency of the 3rd forcing harmonic or 7Hz, whichever was the larger. The marker accelerations $a_{Indirect,i}$ of the $_i{}^{th}$ marker were calculated by differentiating the marker displacements twice. The accelerations were re-filtered at the appropriate frequencies, as above. The GRF estimated using the $_i{}^{th}$ marker $F_{Indirect,i}$, hereafter referred to as the indirect force, was calculated as:

$$\boldsymbol{F_{Indirect,i} = m\left(a_{Indirect,i} - g\right)} \quad 5.5$$

For comparison purposes, the benchmark GRF, hereafter referred to as the direct force, was also recorded using the force plate, at a sampling rate of 1000Hz.

As stated in Section 5.2.2, markers placed on soft tissue (which is prevalent around the trunk) are prone to soft tissue artefact. To reduce the relative vibrations of the markers on the trunk a muscle wrap was used around the stomach.

The two force collection methods operate at different sampling frequencies. Before analysis, the direct forces were initially filtered at 100Hz to prevent aliasing (Lynn and Fuerst, 2000) and resampled at 200Hz, the frequency used for measuring the indirect force. Both sets of force data were processed using MATLAB R2011b (MathWorks, 2011). The force spectra were reconstructed between the frequencies of interest to remove the influence of unwanted frequency components. Sine waves of the relevant amplitudes and phase angles at the remaining frequencies were summed together to recreate the force time history. The cut-off frequency was set as previously, either 1Hz above the frequency of the 3rd forcing harmonic or 7Hz, whichever was the larger. The approach allowed the first three harmonics of interest to be fully investigated. In addition the frequency components of the force that could initiate resonance in structures with a vibration mode below 6Hz were included (UK Working Group, 2008).

The experiments were approved by the Biomedical & Scientific Research Ethics Committee at the University of Warwick on 24th September 2012. A risk assessment was completed, alongside TS consent forms and physical readiness questionnaires available in Appendix A.

5.4 Results and Analysis

Within this section the results from the experiments will be presented. The coefficient of determination R^2 (Draper and Smith, 1985) will be used to quantify how well the indirect force agrees with the direct force. R^2 takes values between 0 and 1, where 1 is a perfect fit and 0 shows no correlation. R^2 is calculated as:

$$\boldsymbol{R^2 = 1 - \frac{SS_{err}}{SS_{tot}}} \quad 5.6$$

$$SS_{tot} = \sum_{i=1}^{n} (F_{direct,i} - \overline{F_{direct}})^2 \quad 5.7$$

$$\overline{F_{direct}} = \frac{1}{n} \sum_{i=1}^{n} F_{direct,i} \quad 5.8$$

$$SS_{err} = \sum_{i=1}^{n} (F_{direct,i} - F_{indirect,i})^2 \quad 5.9$$

where *n* is the number of data points, SS_{err} and SS_{tot} are the residual sum of squares and the total sum of squares respectively. $F_{direct,i}$ and $F_{indirect,i}$ represent the directly and indirectly measured force and $\overline{F_{direct}}$ is the average value of directly measured force. The subscripts $_F$, $_t$ and $_f$ will be used to denote the force, and the time- and frequency-domains of the force respectively. If a domain is not specified R^2_F refers to the R^2 values of the force in both domains. Hereafter the time- and frequency-domains will be referred to as the t- and f-domains respectively.

Initially the markers within each location group are examined to identify the markers which consistently measure the jumping force well. Once a stand out marker has been identified the percentage differences between the direct and indirect forces at different harmonics will be examined and compared to results from previous work. To verify the indirect force measurements the direct and indirect forces will be applied to a virtual structure to investigate how the error in the force propagates to the structural response. This study will then be used to establish the likely errors in the structural response for different jumping frequencies and resonance at different harmonics of the force.

5.4.1 Hip Markers

For the hip group as a whole, the mean value and standard deviation (STD) of $R^2_{F,t}$ are 0.945 and 0.027, and for $R^2_{F,f}$ the mean and STD are 0.960 and 0.024 (Table 5.2). High mean values and low STDs suggest that as a group, the hip markers are highly consistent and measure the force successfully. Table 5.3 shows that the RH1 marker (highlighted in the table) is, on average, the best performing hip marker. However, similar values are seen for the LH1 marker

suggesting that the side the marker is positioned on is not significant. The mean R^2_F values for this marker across all TSs and trials in the t- and f-domains are highlighted in Table 5.2, the values are 0.953 and 0.968 respectively, and the STDs are 0.023 and 0.020. The accuracy of the force measurement using the RH1 marker can be seen in Figure 5.4 for each frequency. The indirect force (dashed line) matches the direct force (solid line) well in both the t-and f-domains. The f-domain (Figure 5.4c, f and i) was created from the entire jumping trial.

Table 5.2 The average R^2_F values for the hip markers.

	$R^2_{F,t}$					$R^2_{F,f}$				
	1 Hz	**2 Hz**	**3 Hz**	**Ave**	**STD**	**1 Hz**	**2 Hz**	**3 Hz**	**Ave**	**STD**
RH1	0.969	0.970	0.921	**0.953**	**0.023**	0.981	0.983	0.939	**0.968**	**0.020**
RH2	0.963	0.963	0.904	**0.943**	**0.028**	0.977	0.977	0.929	**0.961**	**0.023**
LH2	0.955	0.956	0.895	**0.935**	**0.028**	0.970	0.970	0.917	**0.952**	**0.025**
LH1	0.965	0.966	0.911	**0.947**	**0.026**	0.979	0.977	0.926	**0.961**	**0.024**
				0.945	**0.027**				**0.960**	**0.024**

Table 5.3 $R^2_{F,t}$ and $R^2_{F,f}$ values for the hip markers.

	TS	**1**	**2**	**3**	**4**	**5**	**6**	**7**	**8**	**Ave**	**STD**
$R^2_{F,t}$											
1Hz	**RH1**	0.968	0.983	0.969	0.982	0.962	0.955	0.959	0.972	**0.969**	**0.009**
	RH2	0.947	0.975	0.963	0.976	0.952	0.959	0.960	0.975	**0.963**	**0.010**
	LH2	0.944	0.980	0.955	0.957	0.926	0.972	0.948	0.958	**0.955**	**0.016**
	LH1	0.956	0.979	0.966	0.983	0.962	0.975	0.942	0.960	**0.965**	**0.013**
2Hz	**RH1**	0.968	0.986	0.960	0.986	0.962	0.970	0.962	0.969	**0.970**	**0.010**
	RH2	0.953	0.979	0.954	0.982	0.947	0.960	0.955	0.971	**0.963**	**0.012**
	LH2	0.960	0.972	0.944	0.959	0.938	0.973	0.947	0.953	**0.956**	**0.012**
	LH1	0.971	0.975	0.959	0.985	0.960	0.979	0.952	0.946	**0.966**	**0.013**
3Hz	**RH1**	0.949	0.952	0.924	0.950	0.853	0.891	0.909	0.947	**0.922**	**0.036**
	RH2	0.929	0.923	0.869	0.943	0.800	0.899	0.908	0.958	**0.904**	**0.047**
	LH2	0.929	0.938	0.861	0.922	0.762	0.929	0.898	0.920	**0.895**	**0.055**
	LH1	0.946	0.946	0.879	0.953	0.795	0.926	0.907	0.933	**0.911**	**0.049**
$R^2_{F,f}$											
1Hz	**RH1**	0.983	0.992	0.989	0.985	0.973	0.974	0.974	0.982	**0.981**	**0.007**
	RH2	0.973	0.988	0.980	0.981	0.963	0.975	0.974	0.984	**0.977**	**0.007**
	LH2	0.976	0.991	0.963	0.965	0.948	0.980	0.967	0.971	**0.970**	**0.012**
	LH1	0.980	0.989	0.976	0.990	0.978	0.985	0.962	0.972	**0.979**	**0.009**
2Hz	**RH1**	0.985	0.996	0.989	0.993	0.973	0.981	0.973	0.976	**0.983**	**0.008**
	RH2	0.976	0.988	0.984	0.989	0.958	0.975	0.971	0.977	**0.977**	**0.009**
	LH2	0.979	0.985	0.962	0.971	0.949	0.984	0.966	0.960	**0.970**	**0.012**
	LH1	0.984	0.988	0.977	0.992	0.970	0.988	0.965	0.953	**0.977**	**0.013**
3Hz	**RH1**	0.965	0.974	0.940	0.979	0.874	0.905	0.913	0.963	**0.939**	**0.038**
	RH2	0.947	0.951	0.916	0.974	0.836	0.917	0.913	0.974	**0.929**	**0.042**
	LH2	0.947	0.967	0.881	0.941	0.790	0.955	0.903	0.952	**0.917**	**0.055**
	LH1	0.961	0.973	0.890	0.963	0.813	0.946	0.910	0.955	**0.926**	**0.050**

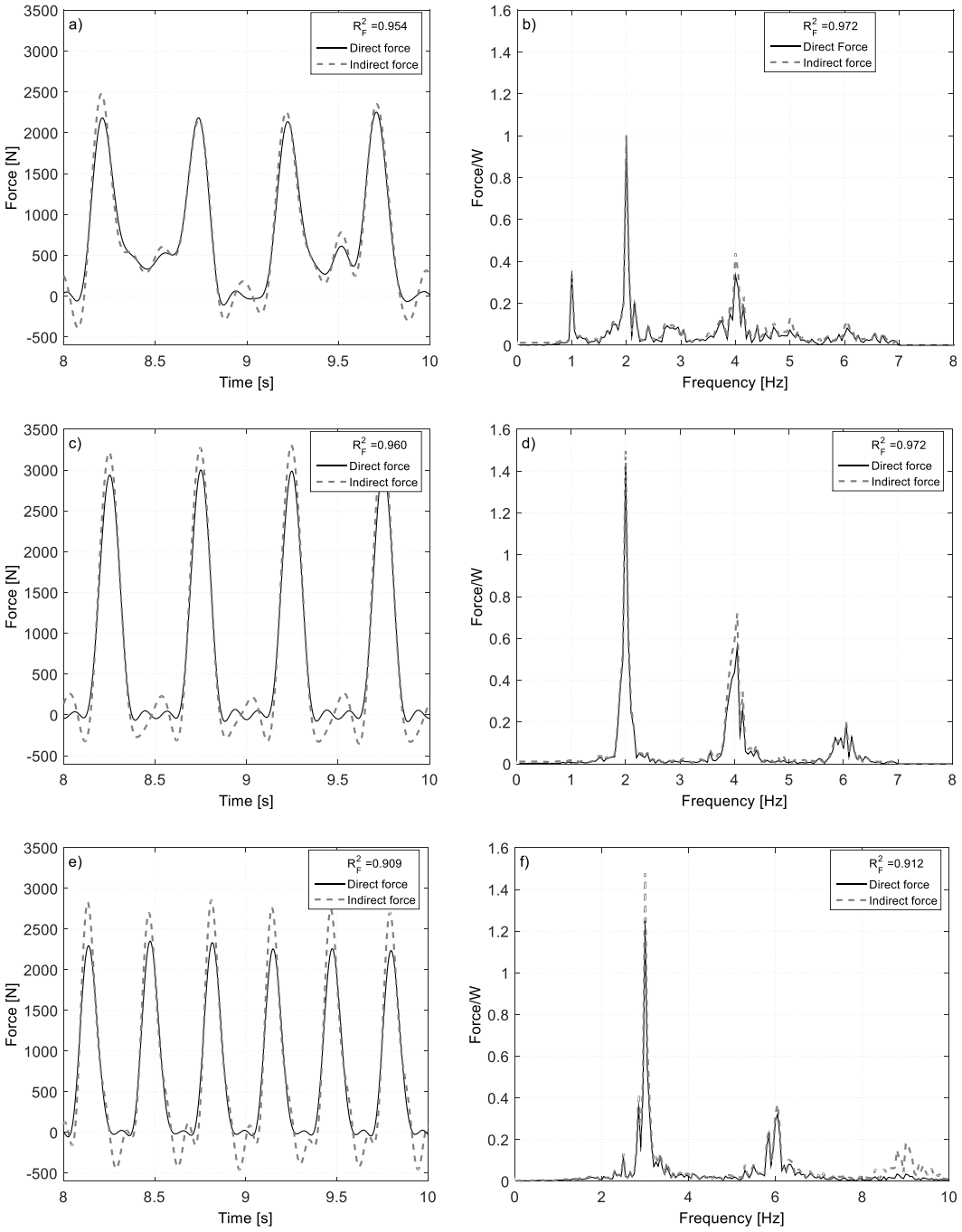

Figure 5.4 Comparing the direct and indirect force using the RH1 marker for jumping at a) 1Hz (t-domain), b) 1Hz (f-domain), c) 2Hz (t-domain), d) 2Hz (f-domain), e) 3Hz (t-domain), f) 3Hz (f-domain).

The range of R^2_F values which contain 95% of the data were investigated. To increase the resolution of the R^2_F distribution each data record was split into three trials and new R^2_F values were calculated for each. The newly split trials were approximately seven seconds in duration. It has been demonstrated that four jumping cycles are required for a stable mean GRF (Racic et

al., 2009), hence a trial duration of seven seconds is adequate. The 95th percentiles were found by calculating the top and bottom 2.5% of R^2_F values within the data set, and hence defining the limits wherein 95% of the data lie. The 95th percentile values of R^2_F for the RH1 marker and the hip group as a whole are calculated in Table 5.4 and shown in Figure 5.5. The percentile ranges across all jumping frequencies and for each jumping frequency are included.

Table 5.4 The average R^2_F and 95% values for the hip markers.

	1Hz				2Hz				3Hz			
	Ave	**95% Min**	**95% Max**	**Range**	**Ave**	**95% Min**	**95% Max**	**Range**	**Ave**	**95% Min**	**95% Max**	**Range**
$R^2_{F,t}$												
RH1	0.962	0.926	0.981	0.055	0.962	0.935	0.984	0.049	0.919	0.800	0.967	0.167
RH2	0.956	0.926	0.977	0.051	0.953	0.921	0.975	0.054	0.903	0.731	0.962	0.231
LH2	0.948	0.903	0.975	0.072	0.947	0.926	0.974	0.048	0.894	0.714	0.955	0.241
LH1	0.958	0.915	0.982	0.067	0.957	0.927	0.977	0.050	0.910	0.787	0.963	0.176
Hip Ave	0.956	0.914	0.981	0.067	0.955	0.926	0.979	0.053	0.906	0.761	0.964	0.203
$R^2_{F,f}$												
RH1	0.977	0.962	0.989	0.027	0.978	0.957	0.994	0.037	0.936	0.825	0.982	0.157
RH2	0.973	0.952	0.983	0.031	0.972	0.948	0.986	0.038	0.926	0.760	0.978	0.218
LH2	0.965	0.930	0.985	0.055	0.966	0.944	0.991	0.047	0.915	0.734	0.985	0.251
LH1	0.974	0.951	0.988	0.037	0.973	0.944	0.993	0.049	0.926	0.806	0.986	0.180
Hip Ave	0.972	0.948	0.988	0.040	0.972	0.945	0.993	0.048	0.926	0.788	0.982	0.194

The majority of the lower percentage limits for both the RH1 marker and the entire hip group in both the t- and f-domain are above 0.90. Limit values less than 0.90 only occur when jumping at 3Hz. However, the range of values at 3Hz in the t-domain is significantly narrower than the range from the front and back markers (analysed later in this chapter). Across all frequencies the lower 95th percentile limit of the RH1 marker in the f-domain is 0.868 and the mean value is 0.948.

Due to the location of the RH1 marker, issues may arise when tracking the marker in a crowd within a stadium environment, as other crowd members are likely to obstruct the marker from camera view.

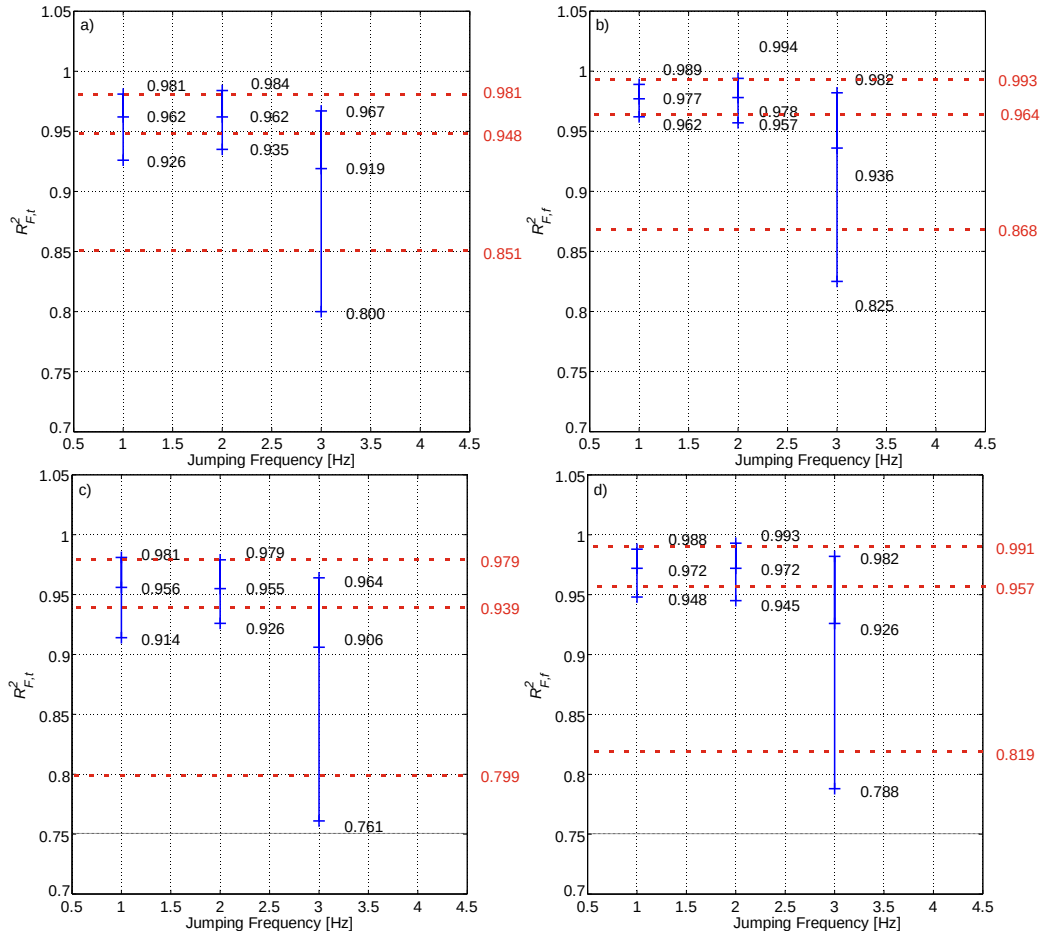

Figure 5.5 Average R^2_F values from the RH1 marker in the a) t-domain and b) f-domain and for the entire hip group in the c) t-domain and d) the f-domain. The mean values and 95th pecentiles for each frequency are marked as crosses, the dashed lines represent the mean and 95th percentile values across all the frequencies.

5.4.2 Front Markers

As a group, the front markers are not as successful at measuring the force as the hip and back markers. The front R^2_F values in Table 5.6 and Table 5.5, which are reduced in comparison to the hip R^2_F values in Table 5.2 and Table 5.3, demonstrate this.

Table 5.5 The average front marker R^2_F values for all TS and frequencies, comparing the direct and indirect forces.

	$R^2_{F,t}$					$R^2_{F,f}$				
	1 Hz	2 Hz	3 Hz	Ave	STD	1 Hz	2 Hz	3 Hz	Ave	STD
F1	0.911	0.920	0.824	0.885	0.043	0.935	0.940	0.846	0.907	0.043
F2	0.885	0.900	0.789	0.858	0.049	0.912	0.921	0.811	0.881	0.050
F3	0.838	0.837	0.684	0.786	0.072	0.866	0.860	0.718	0.815	0.068
F4	0.834	0.842	0.720	0.799	0.056	0.861	0.863	0.750	0.824	0.053
F5	0.830	0.841	0.722	0.798	0.054	0.862	0.865	0.763	0.830	0.047
F6	0.821	0.832	0.749	0.801	0.037	0.864	0.869	0.811	0.848	0.026
F7	0.877	0.902	0.822	0.867	0.033	0.905	0.918	0.861	0.894	0.024
				0.828	0.063				0.857	0.058

Table 5.6 $R^2_{F,t}$ and $R^2_{F,f}$ values for the front markers.

	TS	1	2	3	4	5	6	7	8	Ave	STD
$R^2_{F,t}$											
	F1	0.946	0.940	0.940	0.909	0.968	0.718	0.905	0.964	0.911	0.076
	F2	0.910	0.930	0.924	0.884	0.878	0.681	0.907	0.962	0.885	0.081
	F3	0.905	0.910	0.648	0.876	0.892	0.681	0.872	0.920	0.838	0.102
1Hz	**F4**	0.895	0.888	0.648	0.868	0.850	0.698	0.904	0.923	0.834	0.096
	F5	0.911	0.841	0.645	0.827	0.907	0.718	0.911	0.882	0.830	0.093
	F6	0.898	0.826	0.605	0.839	0.920	0.675	0.908	0.894	0.821	0.110
	F7	0.925	0.936	0.629	0.902	0.934	0.810	0.933	0.951	0.877	0.103
	F1	0.954	0.935	0.946	0.923	0.960	0.783	0.913	0.946	0.920	0.054
	F2	0.928	0.929	0.936	0.897	0.884	0.773	0.915	0.938	0.900	0.051
	F3	0.923	0.910	0.663	0.849	0.900	0.766	0.828	0.854	0.837	0.081
2Hz	**F4**	0.919	0.893	0.649	0.840	0.877	0.791	0.914	0.854	0.842	0.083
	F5	0.945	0.875	0.637	0.814	0.919	0.806	0.933	0.802	0.841	0.095
	F6	0.932	0.834	0.630	0.787	0.947	0.750	0.926	0.852	0.832	0.101
	F7	0.951	0.952	0.673	0.847	0.958	0.946	0.955	0.932	0.902	0.093
	F1	0.894	0.835	0.835	0.795	0.856	0.629	0.796	0.954	0.824	0.089
	F2	0.819	0.826	0.793	0.756	0.679	0.644	0.847	0.945	0.789	0.090
	F3	0.807	0.815	0.396	0.761	0.766	0.628	0.460	0.837	0.684	0.160
3Hz	**F4**	0.804	0.793	0.397	0.720	0.730	0.652	0.834	0.831	0.720	0.135
	F5	0.933	0.794	0.369	0.633	0.784	0.637	0.880	0.746	0.722	0.166
	F6	0.886	0.797	0.393	0.882	0.931	0.439	0.865	0.798	0.749	0.197
	F7	0.914	0.956	0.394	0.944	0.951	0.549	0.929	0.940	0.822	0.207
$R^2_{F,f}$											
	F1	0.959	0.962	0.974	0.919	0.977	0.786	0.925	0.977	0.935	0.060
	F2	0.932	0.952	0.966	0.898	0.897	0.748	0.927	0.975	0.912	0.068
	F3	0.928	0.937	0.690	0.889	0.910	0.746	0.893	0.934	0.866	0.088
1Hz	**F4**	0.914	0.913	0.684	0.882	0.876	0.758	0.923	0.937	0.861	0.085
	F5	0.944	0.887	0.682	0.848	0.924	0.776	0.931	0.902	0.862	0.085
	F6	0.943	0.881	0.662	0.866	0.941	0.755	0.929	0.935	0.864	0.096
	F7	0.951	0.960	0.680	0.917	0.953	0.851	0.955	0.970	0.905	0.092
	F1	0.964	0.949	0.978	0.939	0.971	0.842	0.925	0.955	0.940	0.041
	F2	0.940	0.942	0.967	0.922	0.892	0.833	0.927	0.947	0.921	0.039
	F3	0.934	0.924	0.696	0.879	0.906	0.824	0.846	0.869	0.860	0.071
2Hz	**F4**	0.926	0.906	0.676	0.870	0.884	0.843	0.924	0.871	0.863	0.075
	F5	0.955	0.894	0.665	0.850	0.925	0.864	0.941	0.830	0.865	0.087
	F6	0.952	0.866	0.660	0.839	0.954	0.850	0.936	0.894	0.869	0.090
	F7	0.960	0.960	0.701	0.889	0.965	0.951	0.962	0.953	0.918	0.085
	F1	0.900	0.871	0.865	0.806	0.866	0.689	0.802	0.970	0.846	0.077
	F2	0.831	0.860	0.824	0.769	0.684	0.706	0.851	0.961	0.811	0.084
	F3	0.821	0.849	0.507	0.770	0.770	0.688	0.496	0.846	0.718	0.134
3Hz	**F4**	0.811	0.824	0.509	0.729	0.733	0.709	0.839	0.842	0.750	0.104
	F5	0.945	0.833	0.489	0.655	0.788	0.726	0.889	0.781	0.763	0.134
	F6	0.905	0.833	0.580	0.913	0.952	0.614	0.872	0.816	0.811	0.130
	F7	0.924	0.971	0.577	0.960	0.970	0.600	0.936	0.948	0.861	0.158

The highest R^2_F front marker values in Table 5.6 vary between the F1 and F7 markers. Overall the R^2_F values of the F1 marker are slightly higher (Table 5.5), however the F7 marker is in a better position for crowd observations and will be further analysed. Figure 5.6 demonstrates that the force measurements using the F7 marker for different jumping frequencies are similar

to the direct force measurements. The mean $R^2_{F,t}$ and $R^2_{F,f}$ values for the F7 marker across all TSs and trials, are 0.867 and 0.894, respectively, as highlighted in Table 5.5. The STDs (0.033 and 0.024 in the t- and f-domains) are larger than for the other groups.

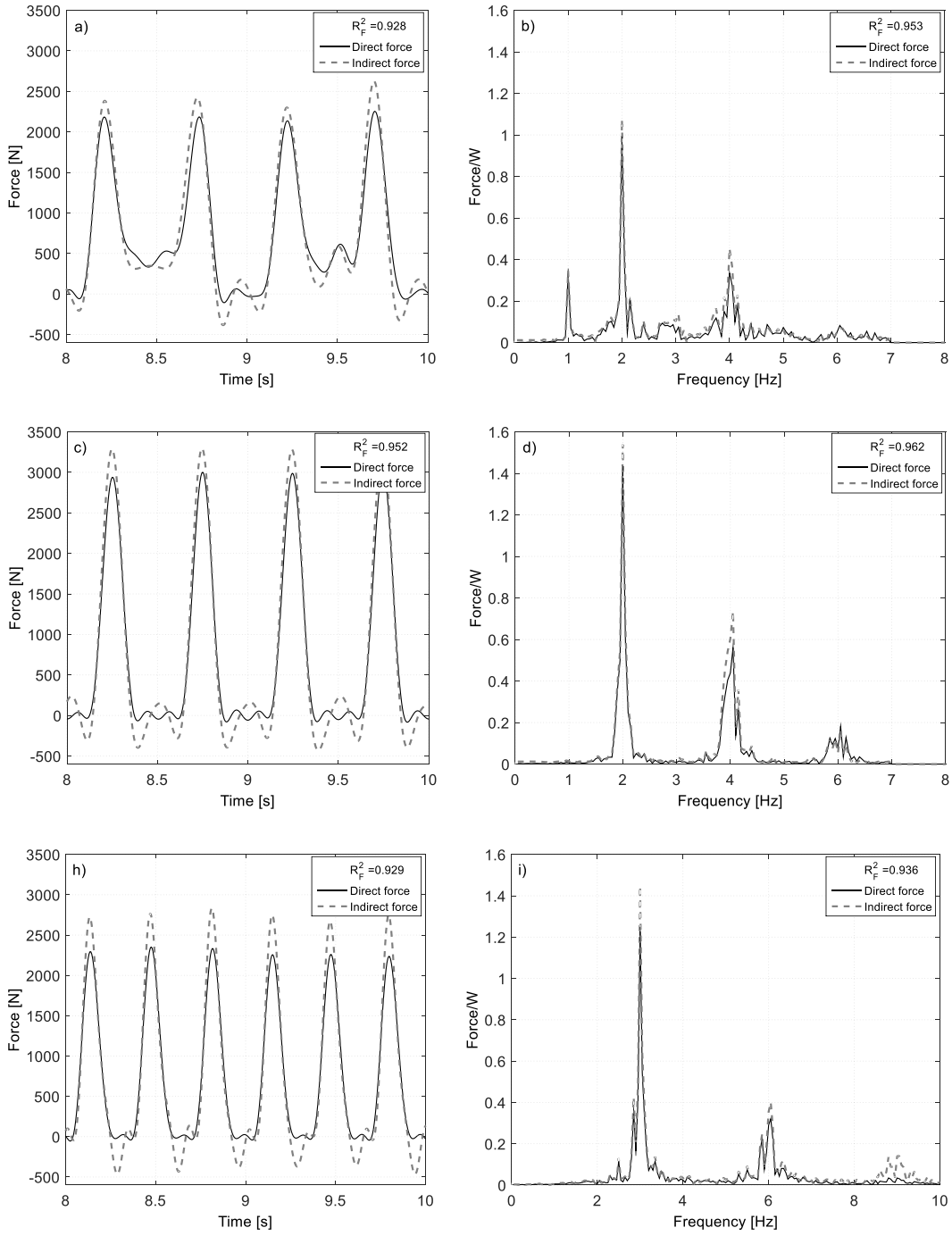

Figure 5.6 Comparing the direct and indirect force using the F7 marker for jumping at a) 1Hz (t-domain), b) 1Hz (f-domain), c) 2Hz (t-domain), d) 2Hz (f-domain), e) 3Hz (t-domain), f) 3Hz (f-domain).

The 95th percentiles of the F7 marker are shown in Figure 5.7 and demonstrate a dramatic increase in variability, compared to the RH1 markers. The range in percentiles (Table 5.7) highlights the lack of consistency associated with the F7 marker.

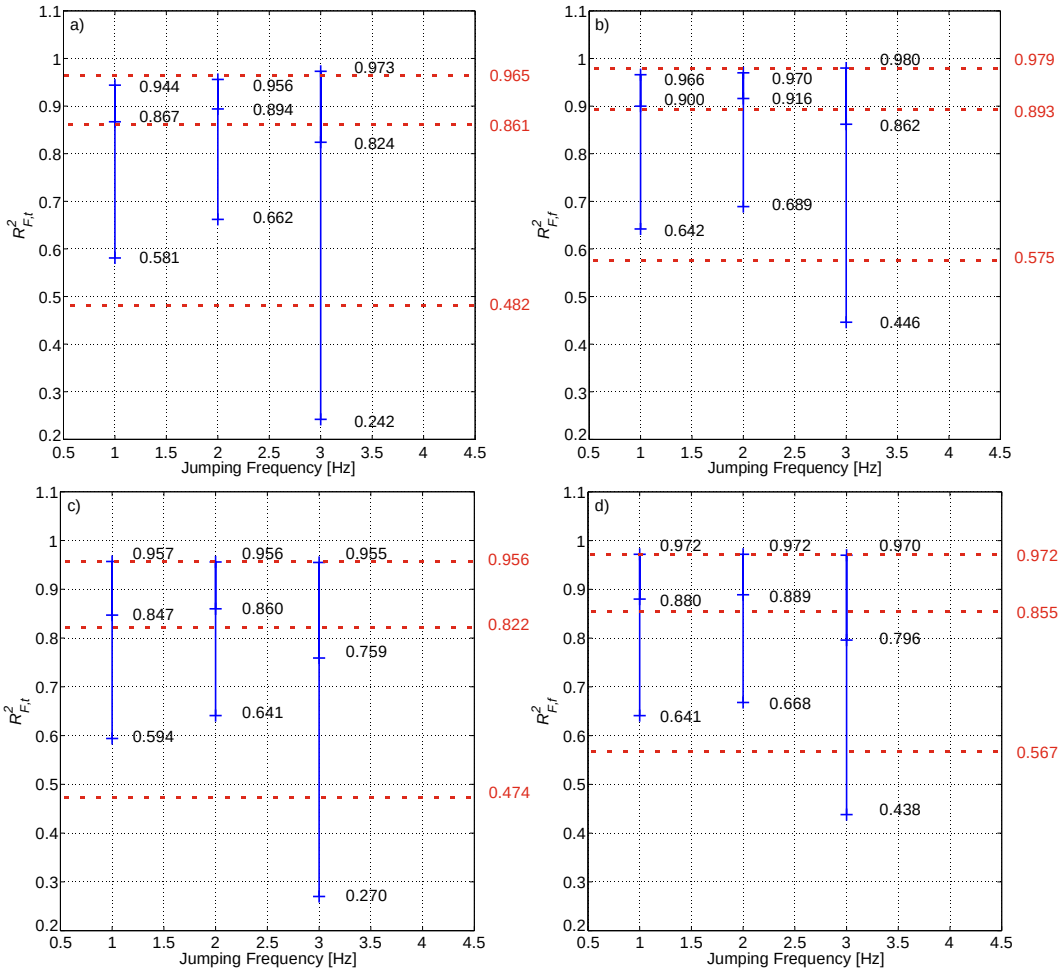

Figure 5.7 Average R^2_F values from the F7 marker in the a) t-domain and b) f-domain and for the entire front group in the c) t-domain and d) the f-domain. The mean values and 95th pecentiles for each frequency are marked as crosses, the dashed lines represent the mean and 95th percentile values across all the frequencies.

The F7 marker is the most visible of the markers analysed thus far. It is situated at the front of the body below the head, and should be visible within the crowded environment typical of grandstands. In addition F7 is located on a bony landmark and therefore measures such as a muscle wrap are unnecessary to combat soft tissue artefact. This marker could be used to calculate the force, but the accuracy of the force will be reduced compared with the RH1

marker. The main discrepancies in the R^2_F values originate from TS3, the removal of this TS significantly increases the average R^2_F values to 0.910 and 0.929 in the t- and f-domains.

Table 5.7 The average R^2_F and 95% values for the front markers.

	1Hz				2Hz				3Hz			
	Ave	95% Min	95% Max	Range	Ave	95% Min	95% Max	Range	Ave	95% Min	95% Max	Range
$R^2_{F,t}$												
F1	0.906	0.670	0.963	0.293	0.913	0.752	0.964	0.212	0.825	0.622	0.957	0.335
F2	0.880	0.631	0.954	0.323	0.891	0.739	0.953	0.214	0.788	0.608	0.950	0.342
F3	0.828	0.592	0.920	0.328	0.830	0.661	0.920	0.259	0.685	0.291	0.850	0.559
F4	0.824	0.602	0.915	0.313	0.835	0.642	0.919	0.277	0.719	0.272	0.841	0.569
F5	0.820	0.604	0.921	0.317	0.833	0.630	0.944	0.314	0.722	0.230	0.941	0.711
F6	0.806	0.549	0.925	0.376	0.823	0.620	0.944	0.324	0.749	0.240	0.939	0.699
F7	0.867	0.581	0.944	0.363	0.894	0.662	0.956	0.294	0.824	0.242	0.973	0.731
Front Ave	0.847	0.594	0.957	0.363	0.860	0.641	0.956	0.315	0.759	0.270	0.955	0.685
$R^2_{F,f}$												
F1	0.929	0.738	0.976	0.238	0.937	0.813	0.982	0.169	0.847	0.694	0.973	0.279
F2	0.904	0.698	0.970	0.272	0.916	0.800	0.973	0.173	0.812	0.643	0.965	0.322
F3	0.860	0.645	0.939	0.294	0.858	0.689	0.936	0.247	0.721	0.410	0.883	0.473
F4	0.855	0.644	0.934	0.290	0.861	0.667	0.930	0.263	0.752	0.407	0.862	0.455
F5	0.857	0.646	0.950	0.304	0.864	0.655	0.954	0.299	0.767	0.374	0.952	0.578
F6	0.857	0.616	0.950	0.334	0.869	0.652	0.956	0.304	0.813	0.457	0.960	0.503
F7	0.900	0.642	0.966	0.324	0.916	0.689	0.970	0.281	0.862	0.446	0.980	0.534
Front Ave	0.880	0.641	0.972	0.331	0.889	0.668	0.972	0.304	0.796	0.438	0.970	0.532

5.4.3 Back Markers

The back group of markers perform well as a whole. The mean value and STD of $R^2_{F,t}$ are 0.944 and 0.040, respectively, and 0.954 and 0.046, respectively, for $R^2_{F,f}$ (Table 5.8). The R^2_F values increase with an increase in marker height on the back of the TS. The most successful marker from this set, having the highest mean R^2_F values across all TSs and trials, is the B6 marker, as highlighted in Table 5.9. The B6 marker additionally scores the highest R^2 values in both domains when compared to the markers from the other two location groups. The t- and f-domains of forces measured using the B6 marker can be observed in Figure 5.8. The figure demonstrates that the B6 marker can be used for successful measurement of the GRF at different jumping frequencies. The mean $R^2_{F,t}$ value for the B6 marker across all TSs for all trials is 0.967 (Table 5.8), likewise the mean of $R^2_{F,f}$ is 0.991 (Table 5.8). Additionally the STDs across all frequencies and TSs for the B6 marker are 0.012 and 0.003 in the t- and f-domains,

respectively (Table 5.8), which are the lowest recorded. These values indicate consistently good performances for all TSs and jumping frequencies.

Table 5.8 The average R^2_F values for the back markers.

	$R^2_{F,t}$					$R^2_{F,f}$				
	1 Hz	**2 Hz**	**3 Hz**	**Ave**	**STD**	**1 Hz**	**2 Hz**	**3 Hz**	**Ave**	**STD**
B1	0.911	0.935	0.777	**0.874**	**0.07**	0.938	0.956	0.823	**0.906**	**0.059**
B2	0.939	0.953	0.843	**0.912**	**0.049**	0.958	0.969	0.880	**0.936**	**0.040**
B3	0.955	0.966	0.857	**0.926**	**0.049**	0.969	0.978	0.875	**0.941**	**0.047**
B4	0.968	0.975	0.923	**0.956**	**0.023**	0.982	0.985	0.938	**0.968**	**0.021**
B5	0.969	0.973	0.934	**0.959**	**0.017**	0.989	0.986	0.968	**0.981**	**0.009**
B6	0.971	0.979	0.95	**0.967**	**0.012**	0.993	0.992	0.987	**0.991**	**0.003**
				0.944	**0.04**				**0.954**	**0.046**

Table 5.9 $R^2_{F,t}$ and $R^2_{F,f}$ values for the back markers.

	TS	**1**	**2**	**3**	**4**	**5**	**6**	**7**	**8**	**Ave**	**STD**
$R^2_{F,t}$											
1Hz	**B1**	0.850	0.972	0.788	0.932	0.898	0.942	0.969	0.935	**0.911**	**0.059**
	B2	0.945	0.978	0.817	0.955	0.935	0.961	0.963	0.960	**0.939**	**0.048**
	B3	0.954	0.974	0.940	0.961	0.944	0.939	0.969	0.960	**0.955**	**0.012**
	B4	0.961	0.973	0.960	0.967	0.976	0.964	0.984	0.962	**0.968**	**0.008**
	B5	0.975	0.978	0.935	0.973	0.977	0.970	0.983	0.965	**0.969**	**0.014**
	B6	0.977	0.978	0.933	0.976	0.975	0.975	0.976	0.975	**0.971**	**0.014**
2Hz	**B1**	0.908	0.984	0.801	0.969	0.910	0.966	0.973	0.966	**0.935**	**0.057**
	B2	0.963	0.986	0.818	0.975	0.958	0.978	0.965	0.981	**0.953**	**0.052**
	B3	0.966	0.983	0.943	0.980	0.966	0.966	0.970	0.958	**0.966**	**0.012**
	B4	0.973	0.980	0.977	0.982	0.981	0.984	0.983	0.942	**0.975**	**0.013**
	B5	0.981	0.981	0.922	0.991	0.979	0.985	0.985	0.961	**0.973**	**0.021**
	B6	0.989	0.984	0.936	0.988	0.986	0.984	0.984	0.979	**0.979**	**0.017**
3Hz	**B1**	0.771	0.950	0.413	0.877	0.500	0.899	0.930	0.873	**0.777**	**0.193**
	B2	0.916	0.941	0.477	0.815	0.909	0.892	0.882	0.910	**0.843**	**0.142**
	B3	0.908	0.916	0.858	0.757	0.817	0.839	0.917	0.842	**0.857**	**0.052**
	B4	0.911	0.907	0.930	0.957	0.946	0.907	0.959	0.867	**0.923**	**0.029**
	B5	0.953	0.933	0.802	0.977	0.951	0.955	0.966	0.938	**0.934**	**0.055**
	B6	0.979	0.942	0.807	0.981	0.975	0.972	0.974	0.973	**0.950**	**0.059**
$R^2_{F,f}$											
1Hz	**B1**	0.912	0.984	0.847	0.940	0.921	0.958	0.985	0.956	**0.938**	**0.042**
	B2	0.974	0.988	0.868	0.960	0.948	0.972	0.976	0.975	**0.958**	**0.036**
	B3	0.977	0.983	0.958	0.965	0.957	0.961	0.983	0.969	**0.969**	**0.010**
	B4	0.980	0.982	0.966	0.988	0.987	0.978	0.996	0.977	**0.982**	**0.008**
	B5	0.992	0.990	0.981	0.995	0.989	0.984	0.996	0.982	**0.989**	**0.005**
	B6	0.995	0.993	0.989	0.994	0.991	0.993	0.995	0.993	**0.993**	**0.002**
2Hz	**B1**	0.946	0.991	0.872	0.979	0.920	0.981	0.985	0.975	**0.956**	**0.039**
	B2	0.980	0.993	0.884	0.984	0.963	0.989	0.976	0.987	**0.969**	**0.034**
	B3	0.980	0.989	0.969	0.985	0.972	0.982	0.982	0.962	**0.978**	**0.009**
	B4	0.984	0.988	0.989	0.990	0.988	0.993	0.993	0.956	**0.985**	**0.011**
	B5	0.996	0.991	0.961	0.998	0.987	0.995	0.994	0.970	**0.986**	**0.013**
	B6	0.999	0.995	0.974	0.994	0.994	0.998	0.996	0.988	**0.992**	**0.008**
3Hz	**B1**	0.784	0.966	0.607	0.906	0.527	0.921	0.941	0.928	**0.823**	**0.157**
	B2	0.927	0.959	0.653	0.835	0.914	0.916	0.885	0.953	**0.880**	**0.094**
	B3	0.917	0.933	0.922	0.772	0.824	0.861	0.922	0.847	**0.875**	**0.054**
	B4	0.919	0.926	0.940	0.967	0.961	0.940	0.967	0.885	**0.938**	**0.026**
	B5	0.972	0.960	0.932	0.996	0.971	0.976	0.976	0.957	**0.968**	**0.018**
	B6	0.997	0.974	0.951	0.997	0.999	0.993	0.994	0.987	**0.987**	**0.016**

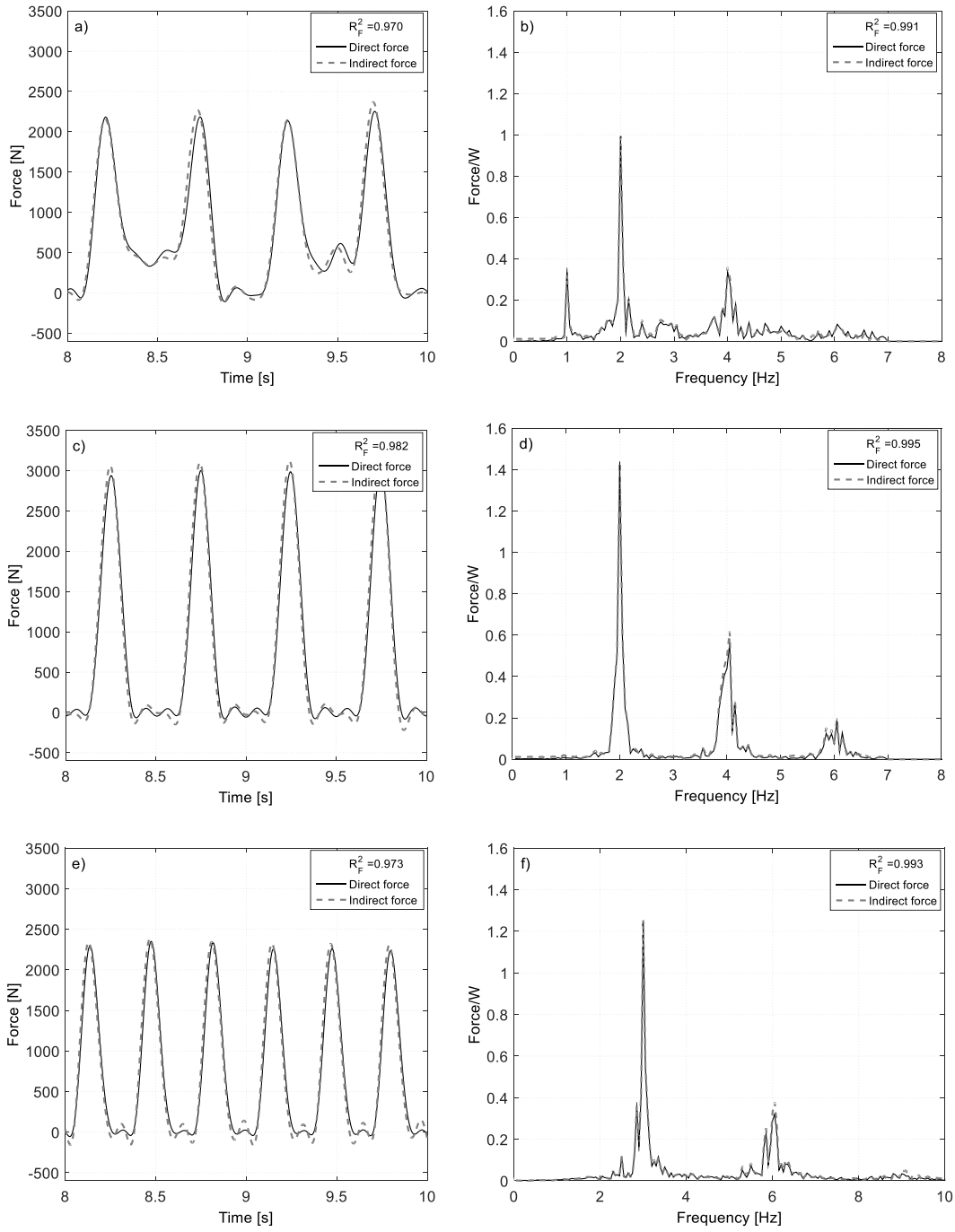

Figure 5.8 Comparing the direct and indirect force using the B6 marker for jumping at a) 1Hz (t-domain), b) 1Hz (f-domain), c) 2Hz (t-domain), d) 2Hz (f-domain), e) 3Hz (t-domain), f) 3Hz (f-domain).

The 95th percentiles of the R^2_F values for the B6 marker and the back group as a whole are demonstrated in Figure 5.9. The $R^2_{F,f}$ lower 95th percentile limits for the B6 marker are all greater than 0.90, being 0.971, 0.965 and 0.919 for 1, 2 and 3Hz jumping, respectively. It

should be noted that the largest range between the percentiles is at 3Hz (Table 5.10). The lower 95th percentiles and average R^2_F values decrease with increasing jumping frequency. This indicates that measurement accuracy reduces with jumping frequency.

To conclude, the B6 marker performs well consistently. The marker is positioned on a bony landmark and therefore is insensitive to soft tissue artefact rendering a muscle wrap unnecessary. However, as the marker is positioned on the back of the TS monitoring the movement may be difficult in actual venues.

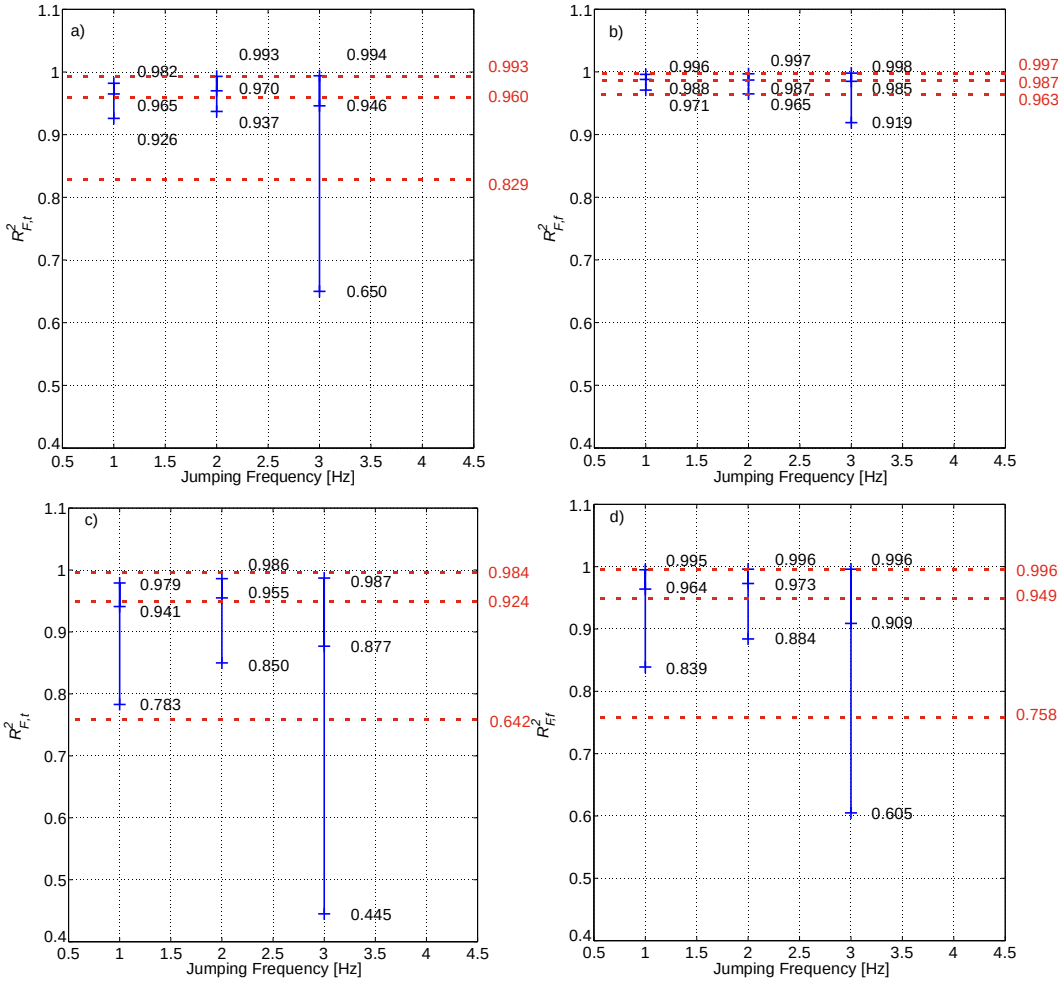

Figure 5.9 Average R^2_F values from the B6 marker a & b) and the entire back group c & d), where a &c) are the t-domain and b &d) the f-domain. The mean values and 95th pecentiles for each frequency are marked as crosses, the dashed lines represent the mean and 95th percentile values across all the frequencies.

Table 5.10 The average R^2_F and 95% values for the back markers.

	1Hz				2Hz				3Hz			
	Ave	**95%Min**	**95%Max**	**Range**	**Ave**	**95%Min**	**95%Max**	**Range**	**Ave**	**95%Min**	**95%Max**	**Range**
$R^2_{F,t}$												
B1	0.901	0.748	0.969	0.221	0.926	0.770	0.978	0.208	0.772	0.335	0.953	0.618
B2	0.912	0.551	0.968	0.417	0.945	0.788	0.983	0.195	0.842	0.429	0.947	0.518
B3	0.946	0.915	0.970	0.055	0.957	0.928	0.981	0.053	0.853	0.738	0.921	0.183
B4	0.960	0.918	0.984	0.066	0.965	0.917	0.984	0.067	0.919	0.856	0.964	0.108
B5	0.963	0.917	0.983	0.066	0.965	0.921	0.986	0.065	0.929	0.676	0.991	0.315
B6	0.965	0.926	0.982	0.056	0.970	0.937	0.993	0.056	0.946	0.650	0.994	0.344
Back Ave	0.941	0.783	0.979	0.196	0.955	0.850	0.986	0.136	0.877	0.445	0.987	0.542
$R^2_{F,f}$												
B1	0.931	0.812	0.986	0.174	0.952	0.860	0.991	0.131	0.819	0.393	0.977	0.584
B2	0.941	0.730	0.979	0.249	0.965	0.871	0.991	0.120	0.880	0.644	0.969	0.325
B3	0.963	0.943	0.986	0.043	0.972	0.951	0.988	0.037	0.873	0.756	0.939	0.183
B4	0.976	0.952	0.995	0.043	0.979	0.943	0.994	0.051	0.935	0.869	0.971	0.102
B5	0.984	0.958	0.996	0.038	0.982	0.953	0.995	0.042	0.965	0.890	0.996	0.106
B6	0.988	0.971	0.996	0.025	0.987	0.965	0.997	0.032	0.985	0.919	0.998	0.079
Back Ave	0.964	0.839	0.995	0.156	0.973	0.884	0.996	0.112	0.909	0.605	0.996	0.391

5.4.4 Percentage Difference

The R^2_Fvalues provide a good overview of the success of the force measurement. However, to further evaluate the quality of the force measurement at each dominant harmonic the percentage difference (PD) of the peak indirect force relative to the peak direct force in the f-domain is calculated. The values of PD at the first three dominant harmonics are discussed and compared to published results. This work is carried out for the B6 marker as it is the best performing marker. In addition, as the F7 marker is the most visible marker the average PDs are also calculated for it.

The force PDs for each jumping frequency and harmonic are plotted in Figure 5.10. The PDs are sorted into two groups comprised of the harmonics where the indirect force overestimated the direct force and those which underestimated it. The mean values of PD are calculated for each group as well as the overall mean and STD for each frequency and harmonic (Table 5.11) and plotted on Figure 5.10.

For the 1st harmonic of the forces, when considering all jumping frequencies, average PDs of +1.96% and -2.85% are seen (Table 5.11). In general this is fairly representative of the values

seen for each jumping frequency. The only exception is the mean underestimated PD of -5.83% for jumping at 1Hz. The 1st harmonic is not dominant at 1Hz which may affect the PD. In addition the harmonic component is smaller, so differences in peak value are exaggerated.

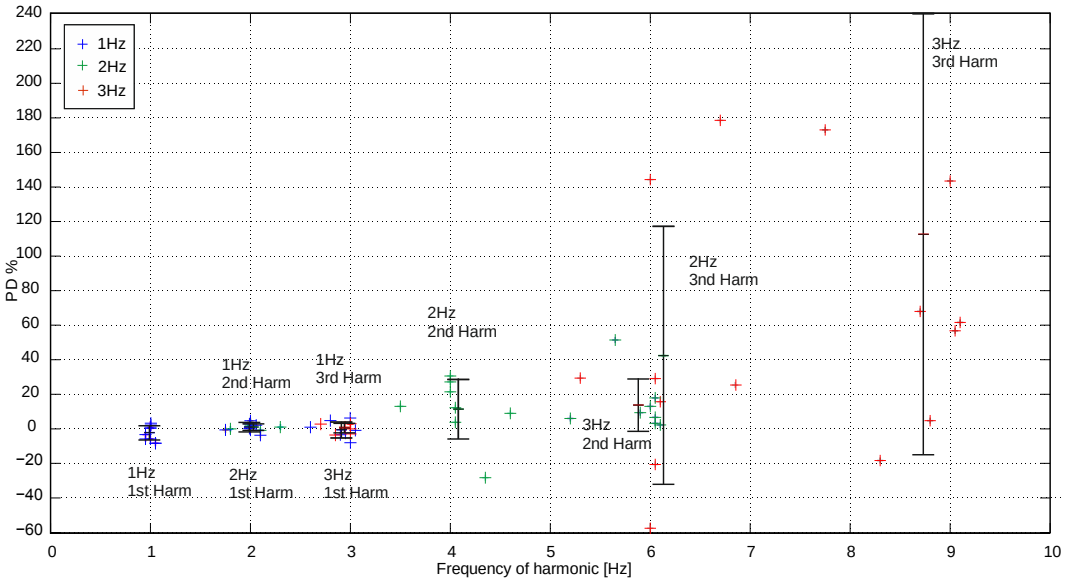

Figure 5.10 The PDs and mean and ±1STDfor each harmonic for each jumping frequency using the B6 marker.

Table 5.11 The PDs of the first three harmonics between the direct and indirect (B6) forces in the f-domain.

Percentage Difference	Jumping Frequency	(+) Average overestimation	(-) Average underestimation	Overall Average	STD
1st Harmonic	1Hz	1.44	-5.83	-2.20	3.90
	2Hz	2.00	-0.49	1.38	1.30
	3Hz	2.46	-2.22	0.70	2.53
	All frequencies	1.96	-2.85	-0.04	3.19
2nd Harmonic	1Hz	2.68	-1.66	1.05	2.53
	2Hz	16.76	-28.31	11.12	17.18
	3Hz	13.73	0.00	13.73	15.05
	3Hz (without TS3)	8.34	0.00	8.34	5.17
	All frequencies	11.05	-9.99	8.63	14.35
	All frequencies (without outliers)	9.26	-9.99	6.84	8.29
3rd Harmonic	1Hz	2.53	-3.72	-0.28	4.26
	2Hz	60.34	-39.08	43.02	74.35
	2Hz (without TS3)	48.76	-39.08	23.66	57.61
	3Hz	114.94	-18.37	112.64	127.81
	3Hz (without TS6)	84.60	-18.37	69.89	63.63
	All frequencies	59.27	-20.39	51.80	97.25
	All frequencies (without outliers)	45.30	-20.39	31.09	26.68
All harmonics ≤ 3Hz		2.34	-3.18	0.13	3.35
2nd Harmonic > 3Hz		12.55	-14.15	9.83	13.11

For all jumping frequencies the average PDs of the 2nd harmonics are +11.05% and -9.99%, as seen in Table 5.11. These values overestimate the error in the 2nd harmonic of 1Hz jumping, where the average PDs are +2.68% and -1.66%. The mean underestimated PD at the 2nd harmonic of 1Hz jumping is closer to zero than the 1st harmonic. The 2nd harmonic, 2Hz, is the dominant frequency when jumping at 1Hz and the magnitude of the harmonic component is greater.

The jumping frequency with the greatest spread in PDs at the 2nd harmonic is 2Hz. Table 5.12 demonstrates the considerable variation in the 2nd harmonic PDs between some of the TSs jumping at 2Hz. This does not conform to the general trend of PD spread increasing with frequency magnitude which can be observed in Figure 5.10. At 2Hz the STD of the 2nd harmonic is 17.18%, which is greater than the STD of its 3Hz counterpart, 15.05% (Table 5.11). High R^2_F values occur at 2Hz, suggesting that the general shape of the force profile is achieved, however the PDs show the measurements of peak values are not as accurate other frequencies.

In contrast, at 3Hz the TSs had similar PDs to one another, however TS3 had a significantly larger average overestimated PD of 51.43% (Table 5.12). Removing this outlier reduces the average PDs for the 2nd harmonic of 3Hz to +13.73% and -0.00%, with a STD of 5.17%. Furthermore the absence TS3 reduces the mean PDs of the 2nd harmonic across all frequencies to below ± 10% (+9.26% and -9.99%).

The 3rd harmonics in Table 5.11 demonstrate an increase in average PDs to +45.30% and -20.39%. This again misrepresents the 3rd harmonic of 1Hz jumping, where mean PDs of +2.53% and -3.72% are recorded. However, these values are representative of the large PDs at the 3rd harmonic of both 2 and 3Hz jumping. After removing the most extreme PDs from 3Hz jumping as outliers, the mean PDs are +60.34% and -39.08% for 2Hz, and 84.60% and -18.37% for 3Hz, which are unacceptably high. The poor PDs at the 3rd harmonics demonstrate the force measurement is not as good at higher frequencies. This is potentially due to the higher noise

to signal ratio at the higher frequencies due to soft tissue artefact. As the frequency of the harmonic increases, in general the range of PDs also increases.

Table 5.12 The PDs at the harmonics for each TS using the B6 marker.

Jumping Freq	TS	1st Harm (%)	2nd Harm (%)	3rd Harm (%)	Freq 1st Harm (Hz)	Freq 2nd Harm (Hz)	Freq 3rd Harm (Hz)
1Hz	**1**	2.73	2.12	0.70	1.00	2.05	2.95
	2	-3.35	-0.61	0.98	0.95	1.75	2.60
	3	-8.34	-3.60	-0.87	1.05	2.10	3.05
	4	-5.83	0.30	-8.01	1.00	2.00	3.00
	5	1.90	4.65	6.24	1.00	2.00	3.00
	6	-5.79	-0.76	4.75	0.95	2.00	2.80
	7	0.83	3.27	-2.62	1.00	2.00	2.95
	8	0.27	3.06	-3.37	1.00	2.00	2.90
	+Ave	1.44	2.68	2.53			
	-Ave	-5.83	-1.66	-3.72			
	Overall Ave	-2.20	1.05	-0.28	0.99	1.99	2.91
	STD	3.90	2.53	4.26	0.03	0.10	0.14
2Hz	**1**	1.63	3.79	15.67	2.00	4.05	6.10
	2	-0.15	13.03	29.37	1.80	3.50	5.30
	3	-0.84	-28.31	178.56	2.10	4.35	6.70
	4	1.70	30.65	-20.61	2.00	4.00	6.05
	5	1.92	21.44	-57.56	2.00	4.00	6.00
	6	1.03	8.99	25.39	2.30	4.60	6.85
	7	2.10	12.25	29.09	2.00	4.05	6.05
	8	3.63	27.14	144.28	2.00	4.00	6.00
	+Ave	2.00	16.76	60.34			
	-Ave	-0.49	-28.31	-39.08			
	Overall Ave	1.38	11.12	43.02	2.03	4.07	6.13
	STD	1.30	17.18	74.35	0.13	0.30	0.44
3Hz	**1**	0.74	9.36	67.96	2.95	5.90	8.70
	2	2.77	5.99	173.05	2.70	5.20	7.75
	3	-3.56	51.43	-18.37	2.85	5.65	8.30
	4	-2.93	6.66	56.74	3.00	6.05	9.05
	5	-0.18	2.23	61.62	3.00	6.10	9.10
	6	2.94	3.19	411.87	3.00	6.05	9.10
	7	2.84	17.92	4.73	3.00	6.05	8.80
	8	2.99	13.04	143.52	3.00	6.00	9.00
	+Ave	2.46	13.73	114.94			
	-Ave	-2.22	0.00	-18.37			
	Overall Ave	0.70	13.73	112.64	2.94	5.88	8.73
	STD	2.53	15.05	127.81	0.10	0.29	0.45

The largest PDs are overestimations of the force, which, although not ideal, are preferable to the component being underestimated. In general the frequencies of the harmonics are more variable at higher jumping frequencies and harmonics. This is demonstrated by the increased width of the data points on Figure 5.10.

The F7 marker is the most visible marker and therefore is potentially the most convenient marker for in-situ testing. The average PDs for the F7 marker are calculated in Table 5.13, where significantly higher PDs are seen compared to those from the B6 marker. For harmonics with a frequency less than or equal to 3Hz, average PDs of +12.50 -23.04 occur. If the magnitude of the 2nd harmonic is greater than 3Hz the average PD is +31.28. It is worth noting that the majority of the PDs are overestimations, therefore if an underestimation is unacceptable the F7 marker may be more appropriate than the B6 marker.

The mean values of 1st harmonic PDs from the B6 marker (+1.96% and -2.85%) recorded in Table 5.11, compare well with the error ± 2% error recorded in the nine marker model (Racic et al., 2010). Furthermore the absolute values of the 1st harmonic PDs are smaller than the -12% to +3% range reported in the video tracking studies (Mazzoleni and Zappa, 2012).

Table 5.13 The PDs of the first three harmonics between the direct and indirect (F7) forces in the f-domain.

Percentage Difference	Jumping Frequency	(+) Average overestimation	(-) Average underestimation	Overall Average	STD
1st Harmonic	1 Hz	12.53	-	12.53	8.66
	1 Hz (without TS3)	9.42	-	9.42	2.84
	2 Hz	15.58	-	15.58	5.64
	2 Hz (without TS3)	13.76	-	13.76	3.15
	3 Hz	20.58	-	20.58	5.51
	All frequencies	16.23	-	16.23	7.53
	All frequencies (without outliers)	14.86	-	14.86	6.20
2nd Harmonic	1 Hz	17.71	-	17.71	6.56
	1 Hz (without TS3)	15.38	-	15.38	2.43
	2 Hz	56.34	-	56.34	39.56
	2 Hz (without TS3 & TS4)	34.51	-	34.51	11.05
	3 Hz	43.42	-	43.42	43.31
	3 Hz (without TS6)	28.51	-	28.51	19.08
	All frequencies	39.16	-	39.16	37.67
	All frequencies (without outliers)	25.72	-	25.72	15.15
3rd Harmonic	1 Hz	28.07	-23.04	8.90	28.12
	1 Hz (without TS5)	21.13	-23.04	2.20	23.33
	2 Hz	141.57	-	141.57	124.08
	2 Hz (without TS5 & TS6)	79.58	-	79.58	71.54
	3 Hz	474.20	-	474.20	674.04
	3Hz (without TS6)	226.26	-	226.26	165.61
	All frequencies	241.26	-23.04	208.22	441.75
	All frequencies (without outliers)	126.23	-23.04	103.84	103.84
	All harmonics ≤ 3Hz	12.50	-23.04	12.50	12.50
	2nd Harmonic >3Hz	31.28	-	31.28	16.17

Comparison between the PDs of the 2nd harmonics from this work and the published nine marker values of ±4%, is less satisfactory for jumping frequencies greater than 1Hz. Average PDs of +2.68% and -1.66% are recorded at the 2nd harmonic of 1Hz, these values increase to +9.26% and -9.99% when the jumping frequencies of 2 and 3Hz are included. However, the mean underestimated PDs are smaller than the 1st harmonic value of -12% from the video tracking studies (Mazzoleni and Zappa, 2012).

For the 3rd harmonic, only the average PDs of 1Hz jumping, +2.53% and -3.72%, are smaller than, and suitably comparable with the nine marker PDs of ±7% (Racic et al., 2010). It should be noted however that the frequency range investigated using the nine marker model is smaller than the frequency range of this study. The large PDs at the 3rd harmonic of 2 and 3Hz are exacerbated as the frequency components at the higher harmonics are small. The inaccuracy of the 3rd harmonic component is not a cause for concern, as for a group load generally only the 1st or 2nd harmonic components are significant (Mazzoleni and Zappa, 2012). When crowds of individuals jump the frequency will vary between each individual. The variability causes leakages of signal energy around the key harmonics; this reduces the peaks and widens the base of the harmonics. As a relatively small amount of energy is associated with the 3rd harmonic of an individual jumping, within a group the amplitude of the 3rd harmonic becomes negligible (Mazzoleni and Zappa, 2012).

The large spread of data at the higher frequency harmonics decreases confidence in the ability to indirectly measure the contribution of higher frequencies. This body of work suggests the first three harmonics can be well reproduced if their frequency is less than, or equal to 3Hz. From Table 5.11 average PDs of +2.34% and -3.18% are expected in this range, the 95th percentiles are +4.79 and -8.02.

Indirect calculation of the 2nd harmonic for harmonic frequencies between 3 and 6Hz is not as satisfactory as below 3Hz. From Table 5.11 average PDs of +12.55% and -14.15% are recorded,

the 95th percentiles are +29.42 and -17.62. Only one data point in this array is negative, demonstrating that the majority of the force peaks are overestimated, this is preferable to underestimations. The 3rd harmonic is unlikely to be reproduced well unless its frequency is less than or equal to 3Hz.

The similarities between the PDs presented here and those calculated in nine marker studies supports the hypothesis that a single marker model is an equally good, but less complex method of calculating the GRF at low frequency harmonics (Racic et al., 2010). When estimating the contribution of harmonics with a frequency greater than 3Hz, the errors in PD using multiple markers were smaller. However, the PDs at the 2nd harmonics using one marker were reasonable. The nine marker study only considers two male test subjects and the lower error achieved in those tests might be unrepresentative of the wider population.

5.4.5 Structural Response

To fully evaluate the success of the indirect force measurement the structural response to both the direct and indirect forces is examined and compared. In this section the structure is modelled as a SDOF system. Resonance responses are investigated and compared to the peak ratios of the applied forces. The relationships between the response ratio and the R^2 value and peak ratio of the force are investigated.

5.4.5.1 SDOF System Implementation

Within this section the implementation of the structural model and the application of the forces will be discussed. The structure is represented as a SDOF system. Both the indirect force from the B6 marker and the direct force are applied for one individual at a time and the structural response due to each force is calculated. To ensure the simulations reflect the likely structural natural frequencies, including the vulnerable frequencies under 6Hz, the frequency of the SDOF system f_n is varied in steps of 0.1Hz from 0.5Hz to 7Hz. In addition three different damping ratios ζ are used, with values of 0.01, 0.02 and 0.03 allowing the consideration of low,

medium and moderately damped structures (Setareh, 2011; Jones et al., 2011b). A modal mass of 10000 kg is assumed for ease of calculation.

A popular stimulus for jumping at events is music. The longest continuous jumping force applied to a structure is therefore likely to coincide with the duration of a song. Since the average duration of current pop songs is four minutes (Foreman and Laser Jock, 2008) the measured force signals are looped for this duration and then applied to the SDOF structure. The steady state resonance response of the SDOF system is of greatest concern from a structural and safety point of view. As the steady state responses of the SDOF systems were achieved within 4 minutes, the numbers of cycles required for steady state resonance response were investigated to speed up processing. An estimate of the number of cycles is given as $1/\zeta$, where ζ is the damping ratio (Anderson and Naeim, 2012). Therefore the highest number of cycles required is 1/0.01 =100 cycles. As 1Hz is the lowest jumping frequency a maximum of 100 seconds is required for resonance steady state response to be reached. Therefore the first 100s of the response are analysed only.

5.4.5.2 Response Magnitude

Within this section the t- and f-domains of the structural responses to both the direct and indirect forces are investigated. This provides an insight into the ability of the indirect force to excite a structural response which matches that of the direct force. The magnitudes of the SDOF system responses are studied to identify high risk structural natural frequencies.

Figure 5.11 demonstrates the resonance response of a structure due to jumping at 1Hz. The t-domain responses from a direct force, and an indirect force, are shown in Figure 5.11a as dashed and solid lines, respectively. It can be seen that the two responses agree well. Good agreement can also be seen in the f-domain (Figure 5.11b), which, in this case includes the contribution of the first five forcing harmonics to the structural response.

In the simulations, each SDOF system is exposed to the forces generated at the three jumping frequencies. Figure 5.12 demonstrates the peak structural acceleration responses of the systems to the direct forces for the given range of natural frequencies, when ζ is 0.01. The purpose is to highlight the maximum structural accelerations likely, and to observe the natural frequency these occur at.

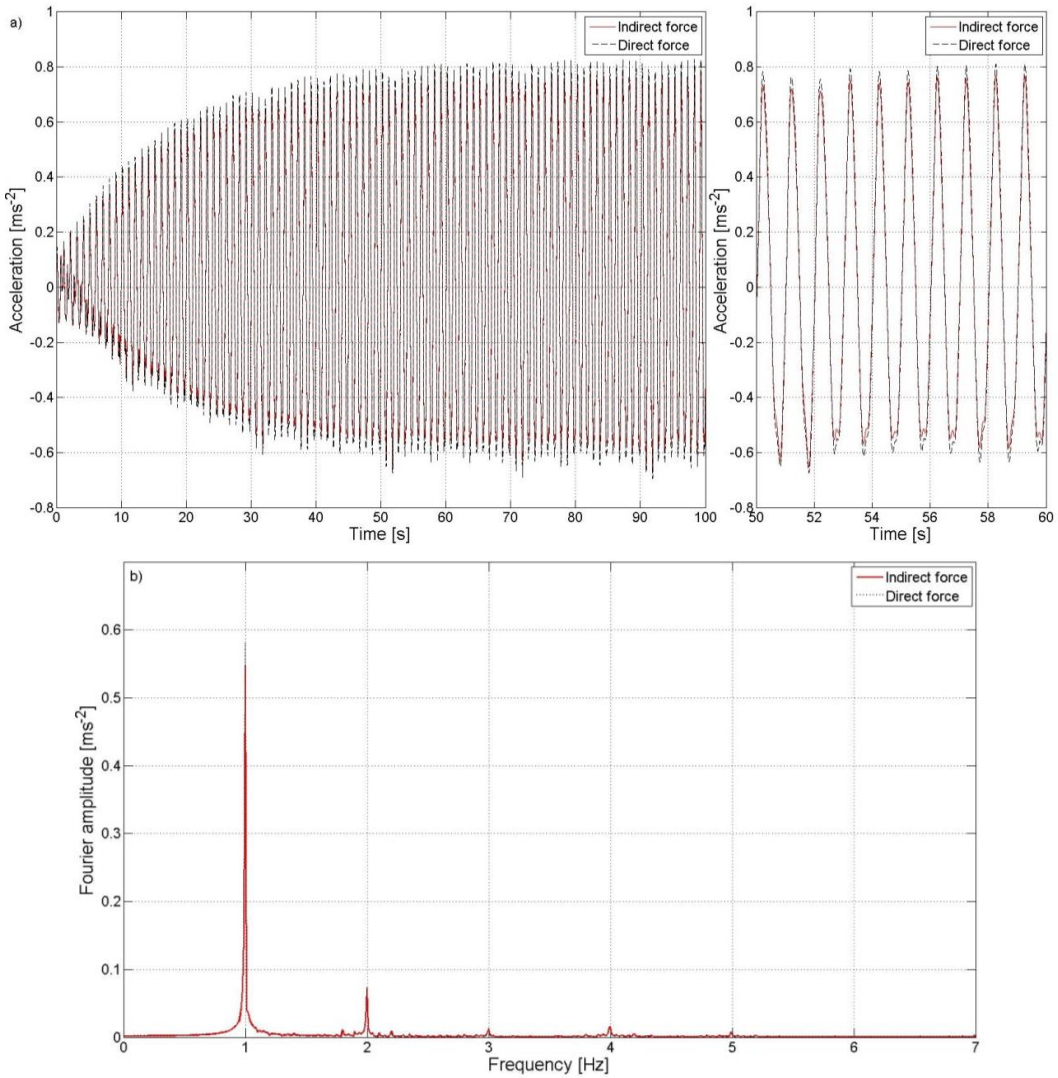

Figure 5.11 The structural accleration response in the a) t-domain (for 100s and 10s) and b) the f-domain, of a structure with f_n=1Hz and ζ=0.01, from TS4 jumping at 1Hz.

The modal masses from stand case studies were examined, values between 36,904kg and 290,830kg were reported by Jones et al. (2011a). Hence a conservative minimum estimate of

the modal mass of a stand is 35,000 kg. To incorporate this, the response values reported from the SDOF system should be divided by a mass factor m_f of 3.5.

The largest calculated structural acceleration is just over 6.07ms^{-2}. With the application of m_f this reduces to 1.73ms^{-1}, which is equivalent to 17.7% of g. This response occurred for a 2Hz system exposed to jumping at the same frequency. Large accelerations are also seen when the natural frequency matches the forcing frequency for a 3Hz system. When the 2nd and 3rd harmonics of the jumping force match the frequency of the structure the maximum accelerations are about half of those caused by the 1st harmonic. It should be noted that when jumping at 1Hz, the largest responses occur at 2Hz (Figure 5.12). This is consistent with 2nd harmonic dominance caused by the 1Hz jumping style as explained in Section 2.2.2.

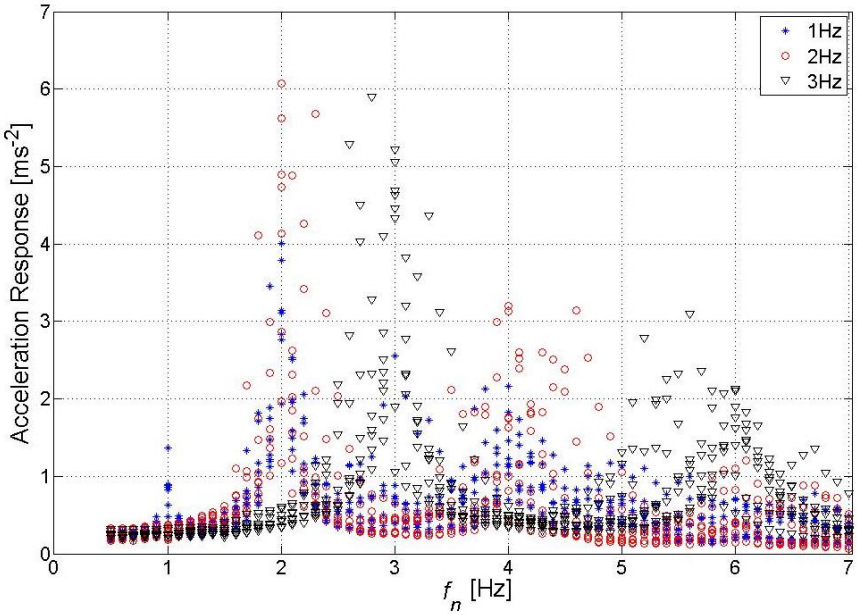

Figure 5.12 The peak acceleration response for SDOF systems exposed to jumping at different frequencies.

5.4.5.3 Response Ratio

The purpose of this section is to investigate how well the steady state accelerations of the SDOF systems due to the indirect force $A_{indirect}$, match the accelerations caused by the direct force A_{direct}. The effect of different structural natural frequencies and jumping frequencies is

examined. A ratio of the responses r_A is used to quantify the agreement between the responses and is calculated as:

$$\boldsymbol{r_A = \frac{A_{indirect}}{A_{direct}}} \quad 5.10$$

The subscripts $_t$ and $_f$ will be used to denote the ratio in the t- and f-domains, respectively. A r_A value of one implies complete agreement of the peak responses, r_A>1 that the indirect force overestimates the structural response, whereas r_A<1 implies that the response is underestimated. The response ratios are examined for each SDOF system and jumping frequency. This provides an insight into the range of f_n values where the greatest and least difference between the structural responses occurs.

Figure 5.13a shows the $r_{A,t}$ values from all the SDOF systems for jumping at 1Hz. Values of $r_{A,t}$ in the range of 0.9-1.1 are seen until approximately f_n= 2.5Hz. For f_n =2.5-5.0Hz the scatter increases gradually. However almost all the $r_{A,t}$ values remain in the range 1±0.2. This range is smaller than the range achieved in the crowd video tracking investigation (Mazzoleni and Zappa, 2012). For natural frequencies above 5Hz the spread in the data increases further. In these cases the direct force can be over or underestimated by up to a factor of two.

Figure 5.13b shows the $r_{A,t}$ values for jumping at 2Hz. As before, $r_{A,t}$ values in the range of 0.9-1.1 are seen for structures with a natural frequency f_n< 2.5Hz. However, when jumping at 2Hz the variation in $r_{A,t}$ values is greater between f_n = 2.5-5Hz than at 1Hz. Although the majority (85.9%) of the data points where the f_n<5Hz remain within 1±0.2, there is significant deviation caused by TS3. When the f_n exceeds 5Hz, the spread of the data increases further, suggesting that there is little correlation between the response from the direct and indirect forces in this frequency range.

The smallest spread in $r_{A,t}$ values over the range of natural frequencies can be seen for jumping at 3Hz, as shown in Figure 5.13c. If the worst performing TS is ignored, the majority (93.75%) of the $r_{A,t}$ values are within 0.9 and 1.2 for f_n≤7Hz. It should be noted that for jumping at 2Hz

and 3Hz, at higher natural frequencies the response is generally overestimated, which is preferable to underestimation.

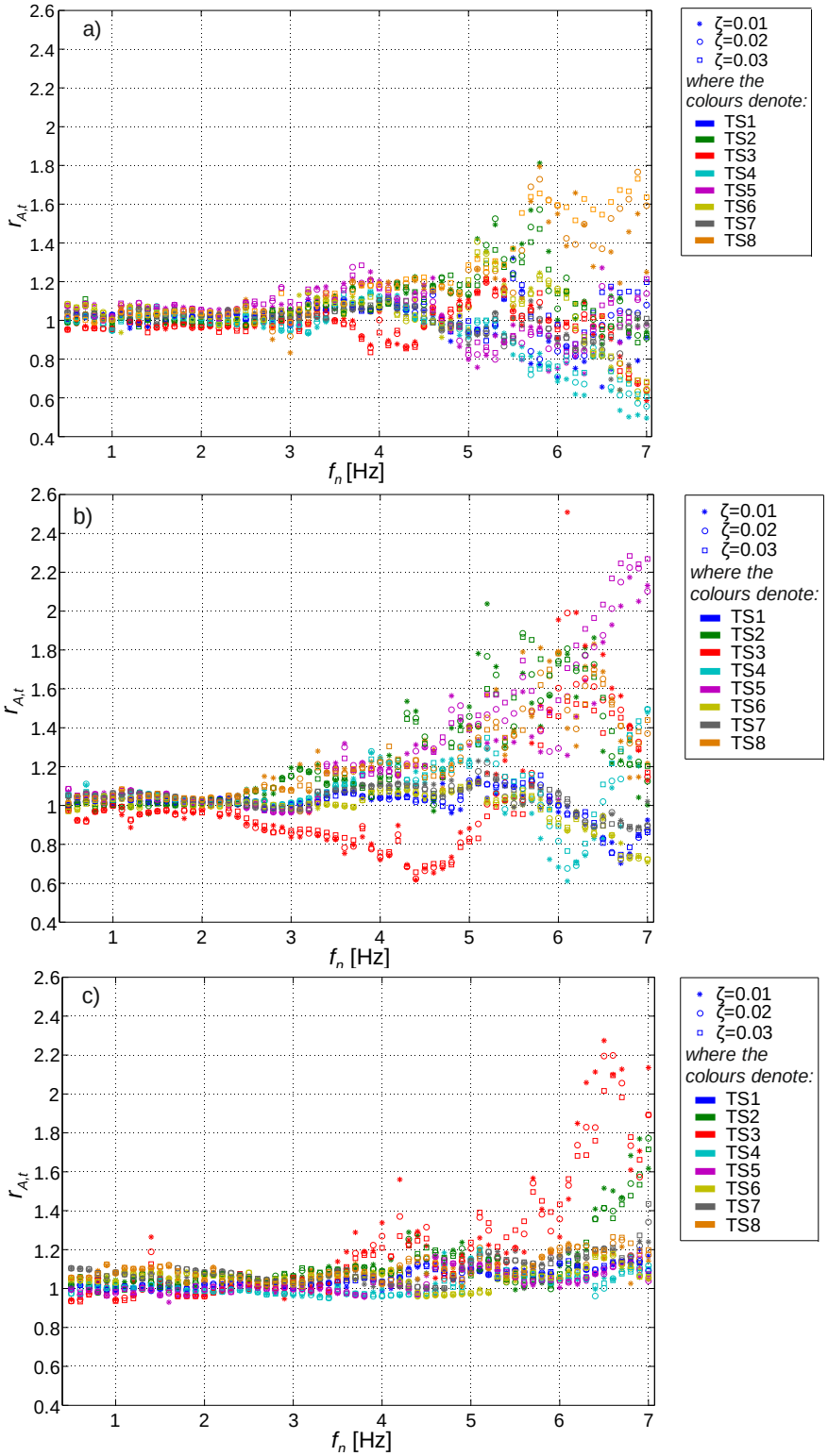

Figure 5.13 The B6 marker $r_{A,t}$ values for a range of SDOF systems due to jumping at a) 1Hz b) 2Hz and c) 3Hz.

These graphs suggest a very good agreement between the two responses for natural frequencies f_n<2.5Hz, good agreement for 2.5Hz ≤ f_n ≤ 5Hz, and poor agreement for f_n > 5Hz. An exception is jumping at 3Hz where the majority of the structural responses are well reproduced up to f_n =7Hz. This indicates that the ability of the indirect force to accurately generate the structural response is dependent on the jumping frequency and natural frequency.

Although in general the correspondence of the structural response is poor above 5Hz, the maximum response accelerations are lower at these natural frequencies (Figure 5.12). The maximum response after applying m_f when fn ≥ 5Hz is 0.88ms^{-2}, this value decreases to 0.52ms^{-2} for f_n > 6Hz. In addition the largest accelerations at frequencies above 5Hz are due to 3Hz jumping, where good consistency between the responses is seen. At f_n >5Hz the SDOF response due to jumping at 1 and 2Hz is likely to be small, therefore the inability to reproduce the response well at high values of f_n for these jumping frequencies is not critical.

There is little difference in the ratio of responses between SDOF systems with different damping ratios, therefore in further simulations the worst case scenario, a damping ratio of 0.01, is used. To compare the $r_{A,t}$ values at the harmonics of the jumping frequencies, the average $r_{A,t}$ values and the average $r_{A,t}$ ± 1STD are plotted against the structural frequencies normalised by jumping frequency (Figure 5.14).

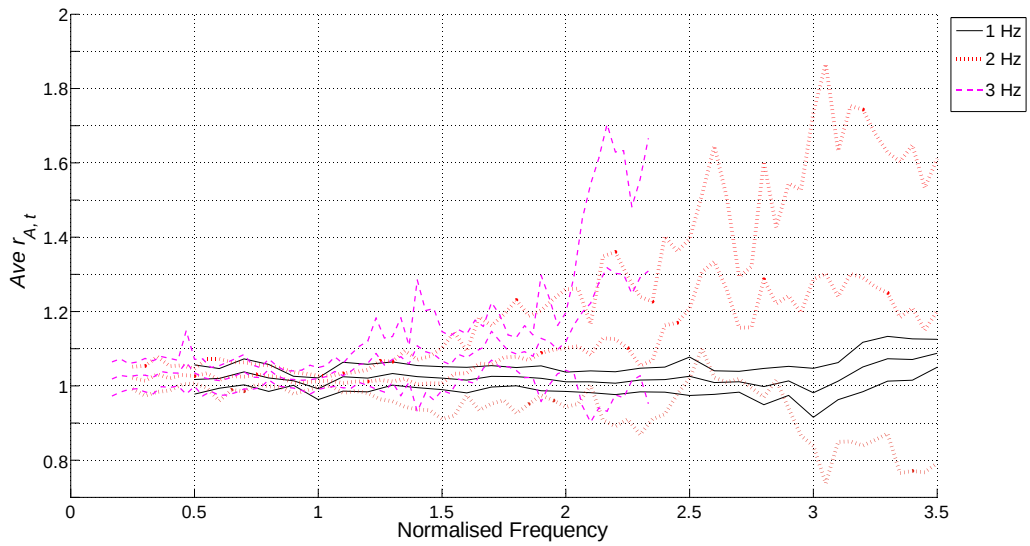

Figure 5.14 The average $r_{A,t}$ values for the B6 marker as a function of f_n normalised by the jumping frequency.

Figure 5.14 shows the average $r_{A,t}$ value of each jumping frequency is approximately one, and the STD within ±0.1, when the normalised frequency is less than or equal to 3, 1.5 and 1.0 for 1, 2 and 3 Hz jumping respectively. Therefore the average value of $r_{A,t}$ equals one for structures with $f_n \leq 3$Hz. The average values of $r_{A,t}$, for the different jumping frequencies are similar and near one at the 1st harmonic. The STDs at the 1st harmonic are small. This suggests that the structural responses are well reproduced at resonance conditions. The average $r_{A,t}$ values at the 2nd and 3rd harmonics of 1Hz jumping are also close to a value of one. This is not the case for jumping at 2Hz and 3Hz where increases in the average values and STDs are seen, however overall adequate responses are seen for all frequencies at the 2nd harmonics. Poor responses are apparent for 2Hz jumping at the 3rd harmonic. The greatest spread in the data occurs for jumping at 2Hz, which is consistent with observations in Section 5.4.4.

5.4.5.4 Force and Response Relationship

To quantify how the discrepancies between the frequency components of the direct and indirect forces will affect the structural acceleration response, a relationship was sought between the $r_{A,t}$ and $R^2_{F,f}$ values. $R^2_{F,f}$ values between the direct and indirect B6 marker force were recalculated to consider each main harmonic $R^2_{F,f\,harmonic}$ (1st, 2nd and 3rd) of the force ±

0.5Hz either side (Figure 5.15). It can be seen from Figure 5.15a that the structural response ratios associated with the 1st harmonic component of the force are very small, the majority of the $r_{A,t}$ values are between ±0.05. Figure 5.15b shows the $R^2_{F,f}$ and $r_{A,t}$ values closest to one for the 1st harmonic, a negative correlation is apparent.

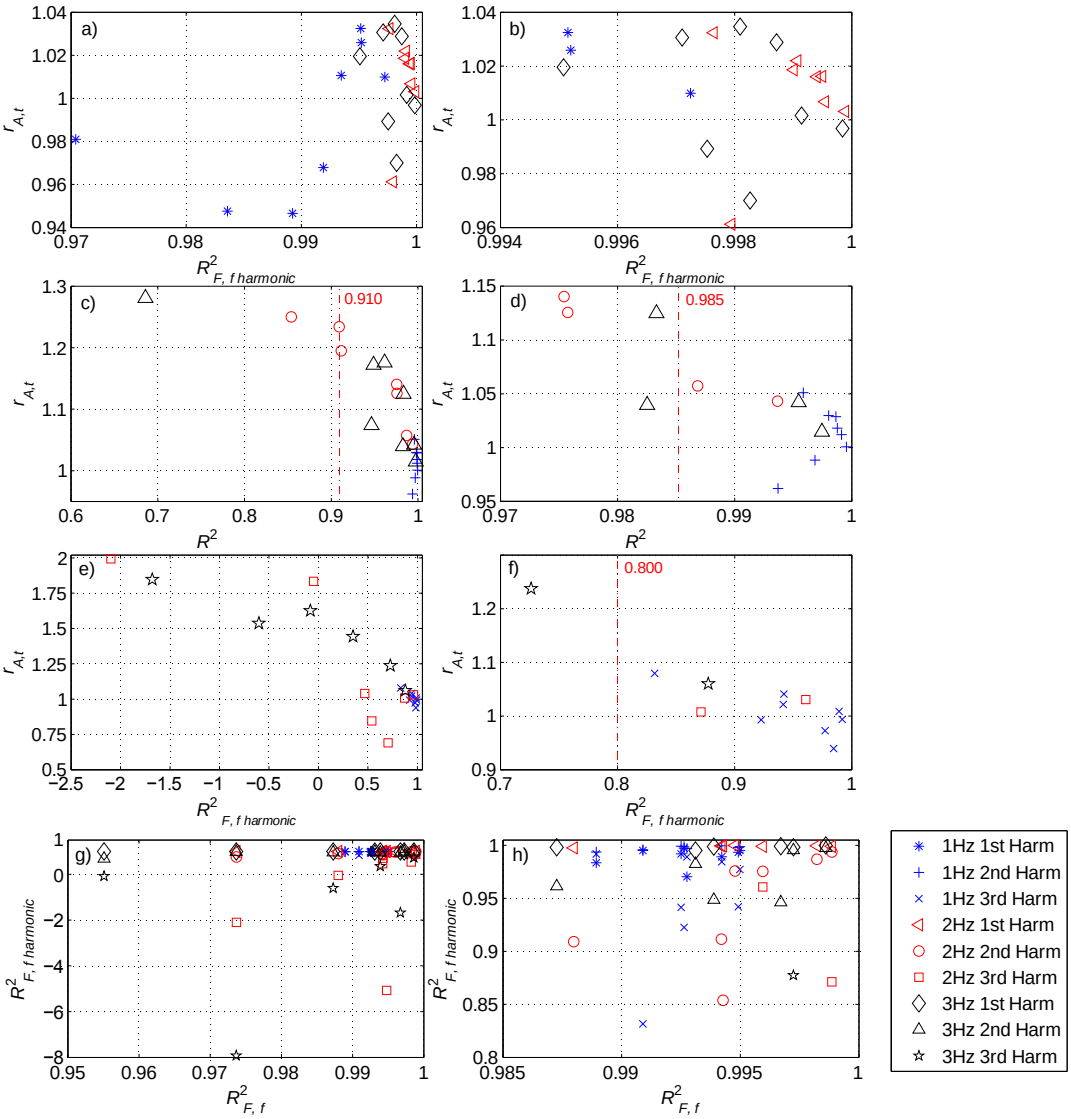

Figure 5.15 The $r_{A,t}$ values plotted against the $R^2_{F,f,harmonic}$ values at each harmonic of the force, for resonance due to the 1st (a & b), 2nd (c & d), and the 3rd (e & f) harmonic and all harmonics (g & h) where a,c, e & g) are an overview of the distribution and b, d, f & h) a zoomed section.

For the 2nd and 3rd harmonics the correlation is also negative (Figure 5.15 c-f), larger $r_{A,t}$ values occur for the jumping frequencies of 2 and 3Hz. To achieve a response ratio between 0.95 and 1.20 for resonance at the 2nd harmonic, an $R^2_{F,f\ harmonic}$ value of approximately greater or equal

to 0.91 (Figure 5.15c) is required, 83.3% of trials achieve this. For an $r_{A,\,t}$ value between 0.95 and 1.10 at the 2nd harmonic, an $R^2_{F,f\ harmonic}$ value of approximately 0.985 is needed (Figure 5.15d), 50% of trials achieve this (100% of 1Hz trials). When considering resonance at the 3rd harmonic, an $R^2_{F,\,f\ harmonic}$ value of greater or equal to approximately 0.80 will facilitate a response ratio of between than 1 ±0.10 (Figure 5.15 e and f), 45.8% of trials achieve this (100% of 1Hz trials).

Figures 4.15 g and h show the $R^2_{F,\,f\ harmonic}$ values plotted against the overall $R^2_{F,\,f}$ values. Excluding the 3rd harmonics of 2 and 3Hz jumping, 96.4% of forces with an $R^2_{F,\,f}$ value of 0.985 or greater have a response ratio between 0.8 and 1.10 at the main harmonics. 75% of trials using the B6 marker achieved this value or greater. The overall $R^2_{F,f}$ values of the 2 and 3Hz trials are less influenced by the higher harmonic components of the force. Therefore using the overall $R^2_{F,f}$ value to determine the response ratio at the 3rd harmonics of these jumping frequencies is inadequate.

It is also possible to use the ratio of direct and indirect peak forces at each harmonic in the f-domain $r_{F,f}$, and compare this to the structural response ratio at resonance of the harmonics in the t-domain $r_{A,t}$. This was carried out for resonance conditions as the largest structural responses occur. The jumping forces were applied to a subset of SDOF structures to excite them in resonance. The actual frequency of each jumping trial (which usually differs slightly from the jumping frequency targeted in the experiments) was investigated. The measured forces were applied to SDOF systems where the natural frequency matched either the 1st, 2nd or 3rd harmonic of the actual jumping frequency. To gauge whether $r_{A,\,t}$ was directly linked to the force ratio $r_{F,\,f}$ the variables were plotted against one another in Figure 5.16 for the first three harmonics.

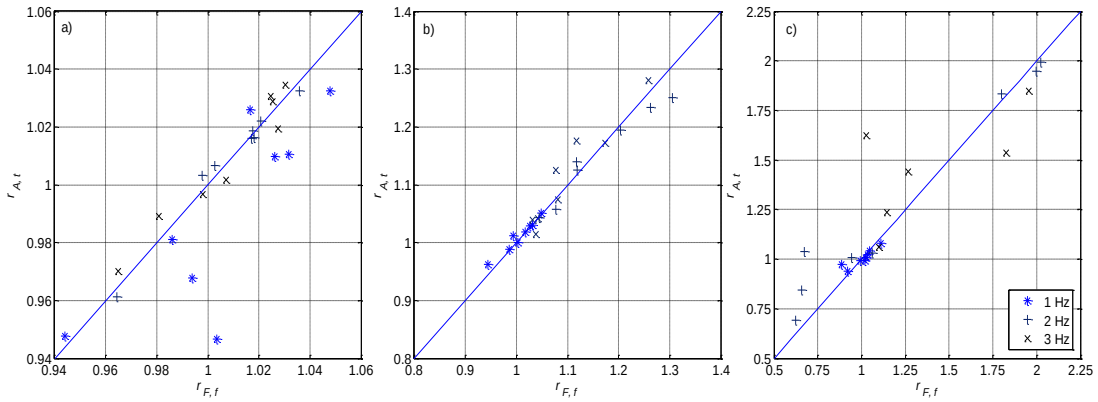

Figure 5.16 The structural response ratio in the t-domain against the peak force ratio in the f-domain, for resonance due to the a) 1st b) 2nd and c) 3rd harmonic component of the force.

A strong positive correlation which approximates to $r_{F,f} = r_{A,t}$ is present. This confirms that the ratio between the direct and indirect force in the f-domain is directly comparable to the structural response ratio in the t-domain. Therefore the PD of the force calculated in Section 5.4.4 can be used to estimate the PD in the structural response.

5.5 Discussion

In general the force measurement using a single marker was successful. The accuracy of the indirect force measurements is evaluated using R^2_F and the PD. Amongst the markers the B6 marker was the best marker for measuring the GRF. From Figure 5.9 97.5% of the $R^2_{F,f}$ values from the B6 marker are greater or equal to 0.963. Excluding the 3rd harmonics of 2 and 3Hz jumping, 96.4% of the resonance response ratios will be between 0.8 and 1.1 at the main harmonics, if the $R^2_{F,f}$ value is greater or equal to 0.985. The response ratio in the t-domain was found to be directly comparable to the peak force ratio in the f-domain for resonance conditions. Therefore, if the force measurement is satisfactory the predicted structural resonance response will also be satisfactory. Using the B6 marker accurate force measurements (average PDs of +2.34% -3.18%) and therefore accurate structural responses, for the first three harmonics are achieved if their harmonic frequency is less than or equal to 3Hz. The 2nd harmonic of the force (and the corresponding 2nd harmonic resonance response) can be measured satisfactorily between 3 and 6Hz inclusive (average PDs +12.55% and -

14.15%). Satisfactory measurement of the 3rd harmonic of the force (and the corresponding 3rd harmonic resonance response) is only possible at harmonic frequencies less than or equal to 3Hz. More accurate force measurements of the harmonics are apparent at 1Hz, and greater variation in the peak values are seen at 2Hz and 3Hz. This is due to a higher soft tissue artefact noise to signal ratio at the higher frequency components. It is therefore the harmonic frequency, not necessarily the harmonic number which is significant in dictating whether the force measurement will facilitate an accurate prediction of the response.

The F7 marker is highly visible, therefore quantifying its ability to replicate the direct force is useful. The PDs between the direct and indirect forces in the f-domain are calculated in Table 5.13 and are approximately equivalent to the PDs in the t-domain of the structural resonance response. Therefore, for the first three harmonics, if the frequency less than or equal to 3Hz, average PDs of +12.50% -23.04% are expected in the structural response. For 2nd harmonics with a frequencies between 3 and 6Hz average PDs of +31.28% occur. It is advised that the F7 marker is only used when considering resonance at the 1st harmonic, or resonance due to the 2nd and 3rd harmonics of 1Hz jumping. Caution should be practised when using the F7 marker as large errors in the response are likely, however if visibility is a priority the F7 marker could be used.

The discrepancies in the force may be caused by the inability of a single monitoring point to capture the whole body movement at the higher harmonics. Arm movements and other deviations from a 2D vertical jumping motion may cause the position of the body CoM to shift, hence introducing discrepancies in the force measurements. It is also likely that some of the discrepancies at the higher harmonic frequencies are caused by the inability of the indirect system to measure the higher frequency components of the force. The higher frequency components of the force are smaller and the influence of the noise due to soft tissue artefact is more significant, hence larger discrepancies occur. In addition, from Figure 5.10, the

frequencies of the harmonics are more variable at higher frequencies. Structures are most influenced by forcing frequencies which match their natural frequency. When the direct and indirect forces are applied to high frequency structures, large differences in response can occur. The harmonic frequencies may be mismatched and discrepancies may occur between the force measurements at higher frequencies (Figure 5.13).

Figure 5.8 revealed that the TSs at 1Hz created an additional bounce between jumps, spaced at 1s to aid their beat synchronisation (Yao et al., 2006). A consequence is the 2nd harmonic dominates the f-domain, and the principal activity frequency is 2Hz. This is likely the cause of the smaller PDs at the 2nd harmonic of 1Hz jumping, as this is the dominant harmonic. When jumping at 2 and 3Hz the 1st harmonic is dominant. The ability of the markers to successfully capture this intermittent bounce, bodes well for future use of this method to monitor bouncing TSs.

It is thought that soft tissue artefact would be more apparent in TSs with higher body fat and would cause noise and force discrepancies. A muscle wrap was used around the stomach in experiments and significantly reduced the soft tissue artefact, however the effect of body build on the $R^2_{F,f}$ value is investigated. To categorise body type the BMI (CDC, 2011) is calculated for each TS (Equation 5.4) and the results are presented in Table 5.1. Unfortunately the BMI is a ratio of weight to height^2 and therefore does not consider muscle density or fat content. TS1 has a high BMI index of 24.4, but had a muscular build, so a close approximation to the direct force is seen from the indirect force. Whereas TS3 has a similar BMI of 25.8 but higher body fat, and therefore there is more discrepancy between the forces. Although TS3 consistently performed the poorest, other TSs with high body fat and BMI indexes still achieved good $R^2_{F,f}$ values. Overall, there is insufficient evidence to link BMI and body fat to the $R^2_{F,f}$ and $r_{A,t}$. values. It is thought that body build will not significantly affect this work.

5.6 Conclusion

It was found that a single monitoring point can be used for the calculation of the dynamic force of a jumping TS. The most effective marker for the measurement of the force was the B6 marker located at the top of the back on the 7th cervical vertebra (C7/Vertebra Prominens). The first three harmonics of the force can be accurately measured if their harmonic frequency is less than or equal to 3Hz. Satisfactory force measurements can occur for the 2nd harmonic for frequencies between 3 and 6Hz. Reasonable measurements of the 3rd harmonic are only possible for jumping at 1Hz.

The B6 marker is located at the back of the individual and some logistical issues when monitoring the TSs may arise. If using the B6 marker is impractical within a particular test set up, an alternative is to use the F7 frontal marker which is located at the base of the neck. A greater range of structural response ratios are likely, but the F7 marker has the advantage of being highly visible. The indirect force using the F7 marker is unlikely to underestimate the direct force, therefore if a force underestimation is unacceptable the use of the F7 marker over the B6 marker is suggested.

These findings have the potential to facilitate future experimental determination of dynamic forces induced by crowd jumping at real-life stadium events. Monitoring of small to medium crowds using reflective markers is possible, and there is potential to expand to large crowds if the technique is adapted and combined with previous marker-less video techniques (Hoath et., al 2007).

6 Measuring Dynamic Force of a Bobbing Person by Monitoring their Body Kinematics

6.1 Introduction

Whilst jumping can produce large dynamic loads as seen in Chapter 4, the activity of bobbing (Section 2.3) requires less energy and is more commonly observed within crowds (NRC, 2006). Authors have noted greater degrees of coordination with the beat, and other individuals whilst bobbing (Parkhouse and Ewins, 2004), in addition a higher frequency range of activity is achievable (Sim et al., 2005). Therefore, accurate measures of bobbing forces are important.

Within this section the methodology presented in Chapter 5 is extended to consider remotely monitoring and measuring the dynamic forces of bobbing individuals. The ground reaction forces (GRF) from bobbing test subjects (TS) are measured directly from a force plate (known as the direct force), and indirectly using a motion capture system (known as the indirect force). The effect of marker position on force measurement is investigated. After which the percentage differences between the force spectra are analysed. To ensure the applicability of the measurement system the bobbing forces are applied to a single degree of freedom (SDOF) system and the responses examined.

The aim of these experiments is to deduce whether a single monitoring point can accurately measure the GRF of a bobbing individual, and to ascertain the best monitoring location.

6.2 Experimental Procedure

The experimental procedure is consistent with the methodology used in the jumping experiments in Chapter 5 and detailed in Section 5.3. The experiments took place within the Gait lab and eight individuals (the same individuals who took part in the jumping experiments) were asked to bob upon the force plate to a metronome beat. As noted in Section 2.3 a larger

frequency range of activity is possible whilst bobbing, therefore the activity frequencies were extended to 1, 2, 3 and 4Hz. The investigated marker positions were consistent with those used for the jumping experiments. Individuals were not coached in the bobbing style, this allowed them to choose whether they bounced or jounced to the metronome beat (Section 2.3). MATLAB R2011b (MathWorks, 2011) was used to process the bobbing data which was filtered as detailed in Section 5.3.

Due to the complex nature of the bobbing action which is comprised of an upward movement whilst maintaining contact with the floor, it is uncertain whether force measurement through the monitoring of one point is possible. The indirect force is calculated using the marker displacements which may have limited potential to convey the complex action. There is concern that the marker displacements will be similar to those of a jumping individual and hence overestimate the bobbing force.

6.3 Results and Analysis

The coefficient of determination R^2 (Draper and Smith, 1985) is used to quantify the agreement between the direct and indirect experimental forces. The subscripts $_F$, $_t$ and $_f$ will be used to denote the force, and the time- and frequency-domains of the force respectively. If a domain is not specified R^2_F refers to the R^2 values of the force in both domains. Hereafter the time- and frequency-domains will be referred to as the t- and f-domains respectively.

The experimental results from the markers will be examined by location group, starting with the hip group, followed by the front and back groups.

6.3.1 Hip Markers

For the hip group as a whole, the mean value and STD of $R^2_{F,t}$ are 0.877 and 0.122, and for $R^2_{F,f}$ the mean and STD are 0.912 and 0.120 (Table 6.1). The mean values are lower than the corresponding values when jumping ($R^2_{F,t}$ =0.945 and $R^2_{F,f}$ =0.960, Section 5.4.1) and the STDs

are higher ($R^2_{F,t,STD}$=0.027, $R^2_{F,t,STD}$ =0.024). From these comparisons it can be inferred that the indirect force measurement has a poorer agreement with the direct force and is less consistent when monitoring bobbing subjects, as predicted.

Table 6.1 The average R^2_F values for the hip markers.

	$R^2_{F,t}$						$R^2_{F,f}$					
	1Hz	**2Hz**	**3Hz**	**4Hz**	**Ave**	**STD**	**1Hz**	**2Hz**	**3Hz**	**4Hz**	**Ave**	**STD**
RH1	0.924	0.947	0.905	0.775	**0.888**	**0.110**	0.964	0.972	0.945	0.810	**0.923**	**0.107**
RH2	0.907	0.928	0.891	0.727	**0.863**	**0.129**	0.953	0.955	0.928	0.772	**0.902**	**0.123**
LH2	0.908	0.938	0.891	0.724	**0.865**	**0.126**	0.962	0.958	0.919	0.760	**0.900**	**0.131**
LH1	0.930	0.954	0.920	0.772	**0.894**	**0.119**	0.974	0.972	0.945	0.809	**0.925**	**0.115**
					0.877	**0.122**					**0.912**	**0.120**

Although the bobbing R^2_F values are lower than their jumping counterparts the mean values are still reasonably high and the STD relatively low. Consistent with the jumping experiments the hip group are on average the most consistent and successful at measuring the GRF.

The R^2_F values from the hip markers are very similar as they are in close proximity to one another. The markers in position 1 on the left and right hips have the highest R^2_F values (Table 6.2). Overall the LH1 marker has the highest mean values ($R^2_{F,t}$ =0.894 and $R^2_{F,f}$ =0.925) and therefore will be considered further from this group. For jumping the RH1 marker was the best performing marker, however there is very little difference in the R^2_F values between these two markers when bobbing. It is therefore the position and not the side of the body which is important for monitoring.

A comparison of the direct and indirect forces using the LH1 marker can be seen in Figure 6.1 for various bobbing frequencies. The indirect force generally matches the direct force well in both the t-and f-domains. However, there is always some degree of overestimation in the indirect force, with the greatest discrepancies occurring at 4Hz. The overestimations tend to increase at higher frequencies because the bobbing displacements become more similar to high frequency jumping displacements (Section 4.3.1). As the indirect force is calculated using the displacements, distinguishing the bobbing and jumping action becomes more difficult.

Contact is maintained with the ground during bobbing therefore the direct force is not as high as the jumping equivalent, this causes discrepancies between the direct and indirect forces.

It is worth noting that the bobbing GRFs are approximately half that of the corresponding jumping GRFs. The frequency components of the bobbing force are smaller than those from jumping, in Figure 6.1 none of the frequency components exceed a value of one.

Table 6.2 $R^2_{F,t}$ and $R^2_{F,f}$ values for the hip markers.

	TS	1	2	3	4	5	6	7	8	Ave	STD
$R^2_{F,t}$	RH1	0.835	0.969	0.904	0.962	0.922	0.902	0.969	0.925	**0.924**	**0.042**
1Hz	RH2	0.784	0.961	0.901	0.941	0.890	0.907	0.953	0.922	**0.907**	**0.052**
	LH2	0.822	0.971	0.945	0.943	0.908	0.821	0.935	0.923	**0.908**	**0.053**
	LH1	0.860	0.971	0.943	0.972	0.929	0.876	0.960	0.929	**0.930**	**0.039**
	RH1	0.866	0.986	0.968	0.975	0.953	0.979	0.878	0.973	**0.947**	**0.044**
2Hz	RH2	0.813	0.985	0.961	0.947	0.923	0.975	0.848	0.969	**0.928**	**0.059**
	LH2	0.864	0.987	0.976	0.948	0.916	0.972	0.866	0.971	**0.938**	**0.046**
	LH1	0.911	0.987	0.970	0.977	0.961	0.979	0.875	0.972	**0.954**	**0.037**
	RH1	0.798	0.975	0.922	0.923	0.805	0.932	0.950	0.939	**0.905**	**0.062**
3Hz	RH2	0.770	0.961	0.920	0.901	0.745	0.924	0.957	0.949	**0.891**	**0.079**
	LH2	0.853	0.958	0.933	0.884	0.726	0.952	0.936	0.882	**0.891**	**0.071**
	LH1	0.908	0.969	0.935	0.934	0.802	0.966	0.926	0.920	**0.920**	**0.049**
	RH1	0.903	0.860	0.842	0.853	0.395	0.798	0.728	0.822	**0.775**	**0.151**
4Hz	RH2	0.856	0.808	0.747	0.800	0.300	0.757	0.688	0.857	**0.727**	**0.170**
	LH2	0.710	0.780	0.887	0.761	0.326	0.846	0.740	0.742	**0.724**	**0.160**
	LH1	0.830	0.830	0.888	0.850	0.321	0.876	0.722	0.858	**0.772**	**0.177**
$R^2_{F,f}$	RH1	0.973	0.981	0.962	0.979	0.953	0.916	0.981	0.964	**0.964**	**0.020**
1Hz	RH2	0.948	0.978	0.956	0.961	0.927	0.924	0.966	0.965	**0.953**	**0.018**
	LH2	0.937	0.984	0.967	0.960	0.953	0.981	0.946	0.963	**0.962**	**0.015**
	LH1	0.966	0.982	0.968	0.985	0.968	0.986	0.969	0.964	**0.974**	**0.009**
	RH1	0.976	0.991	0.984	0.985	0.979	0.992	0.888	0.984	**0.972**	**0.032**
2Hz	RH2	0.941	0.990	0.977	0.960	0.949	0.987	0.856	0.979	**0.955**	**0.041**
	LH2	0.943	0.992	0.986	0.961	0.941	0.984	0.875	0.984	**0.958**	**0.037**
	LH1	0.972	0.993	0.981	0.989	0.982	0.992	0.882	0.986	**0.972**	**0.035**
	RH1	0.944	0.988	0.974	0.937	0.834	0.952	0.958	0.970	**0.945**	**0.045**
3Hz	RH2	0.900	0.977	0.973	0.912	0.777	0.949	0.966	0.975	**0.928**	**0.063**
	LH2	0.915	0.978	0.953	0.896	0.746	0.981	0.945	0.937	**0.919**	**0.071**
	LH1	0.954	0.984	0.961	0.951	0.824	0.988	0.933	0.969	**0.945**	**0.049**
	RH1	0.944	0.906	0.919	0.864	0.426	0.821	0.738	0.867	**0.810**	**0.157**
4Hz	RH2	0.896	0.862	0.881	0.812	0.337	0.783	0.698	0.905	**0.772**	**0.177**
	LH2	0.774	0.840	0.919	0.785	0.290	0.895	0.750	0.830	**0.760**	**0.186**
	LH1	0.881	0.877	0.911	0.874	0.364	0.902	0.742	0.921	**0.809**	**0.176**

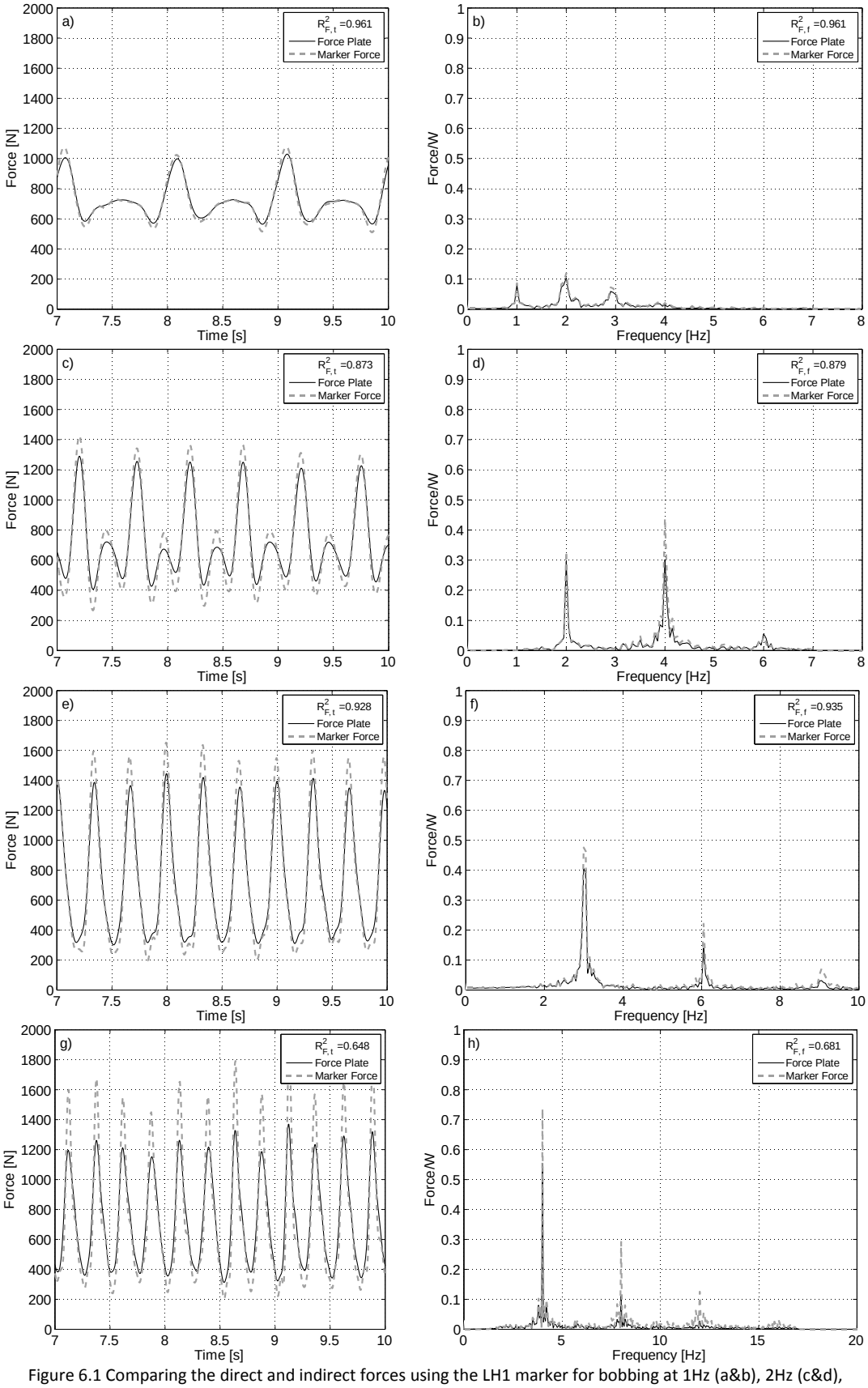

Figure 6.1 Comparing the direct and indirect forces using the LH1 marker for bobbing at 1Hz (a&b), 2Hz (c&d), 3Hz(e&f) and 4Hz (g&h), where a, c, e & g) are the t-domain, and b, d, f & h) the f-domain.

The distribution of the R^2_F values was investigated to find the range containing 95% of the data. As previously with the jumping experiments, each data record was split into three trials and new R^2_F values were calculated to increase the resolution of the R^2_F distribution. The newly split trials were approximately seven seconds in duration. The 95th percentiles were found by calculating the top and bottom 2.5% of R^2_F values within the data set, and hence defining the limits wherein 95% of the data lie. The 95th percentile R^2_F values for the LH1 marker and the hip group as a whole are calculated in Table 6.3 and shown in Figure 6.2. The percentile ranges across all bobbing frequencies and for each bobbing frequency are included.

Table 6.3 The average R^2_F and 95th percentiles for the hip markers.

	1Hz				2Hz				3Hz				4Hz			
	Ave	**95% Min**	**95% Max**	**Range**	**Ave**	**95% Min**	**95% Max**	**Range**	**Ave**	**95% Min**	**95% Max**	**Range**	**Ave**	**95% Min**	**95% Max**	**Range**
$R^2_{F,t}$																
RH1	0.924	0.826	0.978	0.152	0.947	0.843	0.987	0.145	0.905	0.772	0.975	0.204	0.775	0.351	0.921	0.569
RH2	0.907	0.763	0.965	0.202	0.928	0.786	0.987	0.201	0.891	0.730	0.962	0.232	0.727	0.237	0.879	0.641
LH2	0.908	0.804	0.972	0.168	0.938	0.843	0.987	0.144	0.891	0.724	0.960	0.236	0.741	0.337	0.892	0.555
LH1	0.930	0.848	0.983	0.135	0.954	0.865	0.988	0.123	0.920	0.800	0.971	0.171	0.769	0.276	0.906	0.630
Ave	0.917	0.801	0.977	0.176	0.942	0.825	0.989	0.164	0.902	0.735	0.974	0.239	0.753	0.230	0.918	0.687
$R^2_{F,f}$																
RH1	0.964	0.913	0.986	0.073	0.972	0.886	0.994	0.107	0.945	0.832	0.989	0.157	0.810	0.386	0.956	0.570
RH2	0.953	0.911	0.982	0.071	0.955	0.852	0.993	0.141	0.928	0.774	0.980	0.206	0.772	0.280	0.920	0.641
LH2	0.962	0.930	0.986	0.056	0.958	0.868	0.993	0.125	0.919	0.743	0.984	0.241	0.760	0.211	0.930	0.720
LH1	0.974	0.952	0.992	0.039	0.972	0.873	0.995	0.122	0.945	0.821	0.989	0.168	0.806	0.326	0.944	0.618
Ave	0.963	0.918	0.989	0.071	0.964	0.861	0.994	0.133	0.934	0.754	0.988	0.234	0.787	0.266	0.948	0.681

The majority of the lower limits for the LH1 marker are above 0.80, the lowest values are seen for bobbing at 4Hz (Table 6.3). The 95th percentile range increases with increasing frequency. The overall average $R^2_{F,f}$ value for all bobbing frequencies for the LH1 marker is 0.935 (Figure 6.2). The upper and lower $R^2_{F,f}$ limits are 0.993 and 0.542 respectively, demonstrating that 97.5% of the data have an $R^2_{F,f}$ value greater than 0.542.

The LH1 marker is unlikely to be visible within a crowd environment as it is low and potentially obstructed from view by other crowd members. Therefore using this marker to track movements within crowds is not recommended.

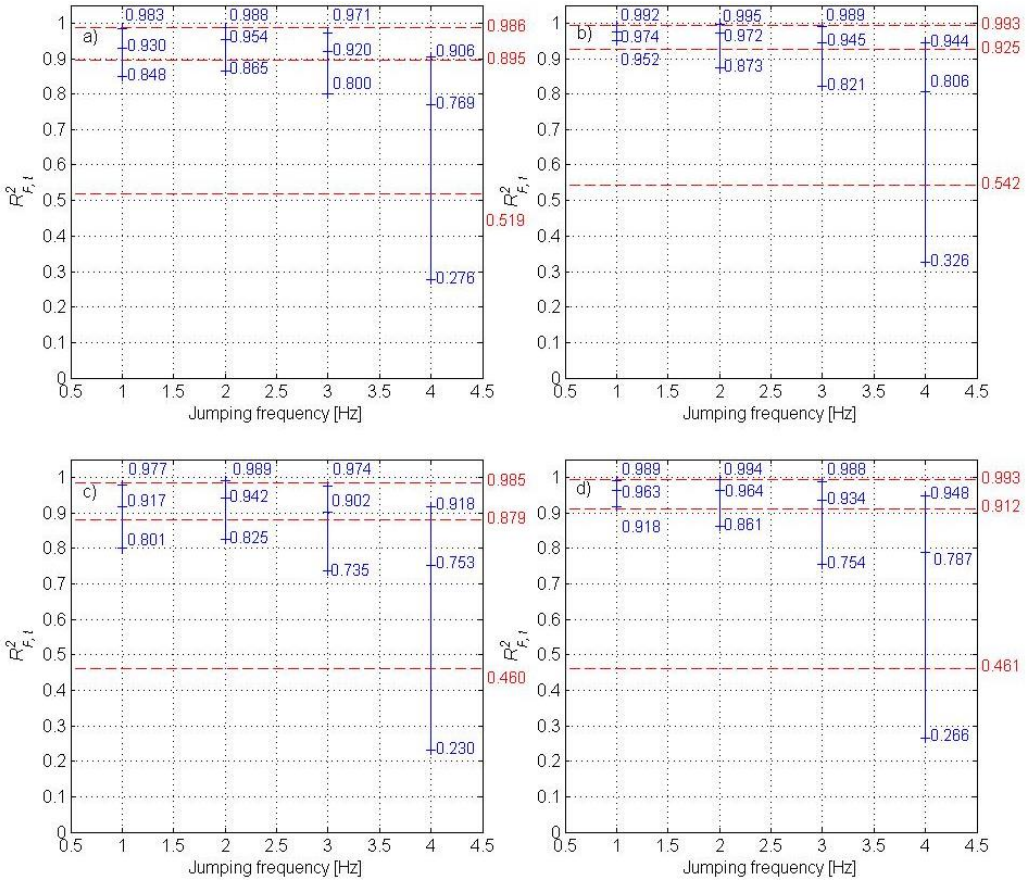

Figure 6.2 Average R^2_F values from the LH1 marker in the a) t-domain and b) f-domain and for the entire hip group in the c) t-domain and d) the f-domain. The mean values and 95th pecentiles for each frequency are marked as crosses, the dashed lines represent the mean and 95th percentile values across all the frequencies.

6.3.2 Front Markers

As a group, the front markers are not as good for force measurement as the hip and back markers. The reduced R^2_F values in Table 6.4 and Table 6.5 demonstrate this when compared to the hip R^2_F values in Table 6.1 and Table 6.2. The mean values are $R^2_{F,\,t}$ = 0.719 and $R^2_{F,\,f}$ = 0.754 (Table 6.4) which are smaller than the corresponding jumping values ($R^2_{F,\,t}$ =0.828 and $R^2_{F,\,f}$ = 0.857, Section 5.4.2). The STDs have increased from the values of $R^2_{F,\,t,\,STD}$=0.063, $R^2_{F,\,t,\,STD}$ =0.058 for the jumping experiments to $R^2_{F,\,t,\,STD=}$ 0.219 and $R^2_{F,\,f,\,STD}$= 0.200 for bobbing.

Table 6.4 The average R^2_F values for the front markers.

	$R^2_{F,t}$						$R^2_{F,f}$					
	1Hz	**2Hz**	**3Hz**	**4Hz**	**Ave**	**STD**	**1Hz**	**2Hz**	**3Hz**	**4Hz**	**Ave**	**STD**
F1	0.922	0.916	0.788	0.598	**0.816**	**0.180**	0.950	0.931	0.825	0.641	**0.846**	**0.164**
F2	0.888	0.880	0.696	0.577	**0.768**	**0.187**	0.915	0.897	0.743	0.616	**0.801**	**0.170**
F3	0.786	0.819	0.592	0.553	**0.698**	**0.218**	0.807	0.838	0.648	0.591	**0.732**	**0.198**
F4	0.788	0.816	0.567	0.458	**0.674**	**0.233**	0.809	0.835	0.626	0.497	**0.708**	**0.213**
F5	0.795	0.813	0.574	0.449	**0.668**	**0.241**	0.819	0.832	0.638	0.472	**0.701**	**0.227**
F6	0.736	0.809	0.630	0.482	**0.670**	**0.242**	0.787	0.834	0.690	0.544	**0.719**	**0.212**
F7	0.819	0.865	0.776	0.749	**0.804**	**0.160**	0.855	0.885	0.816	0.780	**0.836**	**0.144**
					0.719	**0.219**					**0.754**	**0.200**

The highest R^2_F values varied between the F1 and the F7 markers (Table 6.5). The F1 marker on average performs better, but the position of the F7 marker is more desirable and therefore will be considered further. The mean R^2_F values of the force using the F7 marker are $R^2_{F,\,t}$ =0.804 and $R^2_{F,\,f}$ = 0.836 (Table 6.4), which are reasonable. Figure 6.3 demonstrates the indirect force measurements using the F7 marker, which are similar to the direct force measurements. The biggest discrepancies between the force measurements occur at 4Hz.

The 95th percentiles of the F7 marker are shown in Figure 6.4 and demonstrate a dramatic increase in variability, compared to the LH1 marker. The range in percentiles (Table 6.6) and the larger STDs (Table 6.5) highlight the lack of consistency associated with the F7 marker. The R^2_F values decrease with increasing frequency. The F7 marker is the most visible of the markers. It is situated at the front of the body below the head, and should be visible within the crowded environment typical of grandstands. This marker could be used to calculate the force, but the accuracy of the force will be reduced when compared with the LH1 marker.

Table 6.5 $R^2_{F,t}$ and $R^2_{F,f}$ values for the front markers.

$R^2_{F,t}$	TS	1	2	3	4	5	6	7	8	Ave	STD
	F1	0.891	0.934	0.902	0.954	0.913	-	0.938	0.920	**0.922**	**0.020**
	F2	0.716	0.919	0.906	0.952	0.874	-	0.931	0.914	**0.888**	**0.073**
	F3	0.701	0.908	0.244	0.926	0.884	-	0.928	0.909	**0.786**	**0.233**
1Hz	**F4**	0.708	0.887	0.258	0.921	0.888	-	0.938	0.912	**0.788**	**0.228**
	F5	0.865	0.787	0.299	0.909	0.879	-	0.935	0.892	**0.795**	**0.207**
	F6	0.876	0.787	0.305	0.877	0.874	0.350	0.937	0.882	**0.736**	**0.239**
	F7	0.897	0.928	0.384	0.904	0.896	0.675	0.951	0.916	**0.819**	**0.183**
	F1	0.923	0.950	0.934	0.957	0.970	0.896	0.724	0.970	**0.916**	**0.076**
	F2	0.814	0.940	0.925	0.961	0.891	0.845	0.721	0.945	**0.880**	**0.077**
	F3	0.801	0.923	0.630	0.879	0.898	0.822	0.694	0.907	**0.819**	**0.100**
2Hz	**F4**	0.786	0.904	0.620	0.847	0.895	0.813	0.763	0.904	**0.816**	**0.090**
	F5	0.876	0.847	0.623	0.830	0.893	0.823	0.756	0.860	**0.813**	**0.082**
	F6	0.890	0.867	0.534	0.782	0.902	0.814	0.787	0.896	**0.809**	**0.114**
	F7	0.888	0.944	0.601	0.846	0.920	0.921	0.862	0.935	**0.865**	**0.105**
	F1	0.796	0.846	0.884	0.544	0.846	0.634	0.826	0.931	**0.788**	**0.123**
	F2	0.541	0.816	0.877	0.407	0.632	0.545	0.865	0.885	**0.696**	**0.175**
	F3	0.513	0.788	0.242	0.349	0.713	0.485	0.827	0.822	**0.592**	**0.212**
3Hz	**F4**	0.447	0.746	0.234	0.278	0.711	0.460	0.886	0.775	**0.567**	**0.229**
	F5	0.803	0.708	0.241	0.148	0.741	0.488	0.904	0.561	**0.574**	**0.252**
	F6	0.838	0.685	0.260	0.516	0.856	0.313	0.912	0.659	**0.630**	**0.231**
	F7	0.822	0.903	0.311	0.692	0.911	0.709	0.958	0.904	**0.776**	**0.198**
	F1	0.864	0.533	0.643	-	0.352	-	0.299	0.897	**0.598**	**0.230**
	F2	0.792	0.505	0.589	-	0.240	-	0.517	0.819	**0.577**	**0.195**
	F3	0.785	0.476	-	-	0.400	-	0.378	0.725	**0.553**	**0.169**
4Hz	**F4**	0.481	0.341	-	-	0.262	-	0.591	0.618	**0.458**	**0.139**
	F5	0.729	0.326	-	-	0.334	0.464	0.624	0.221	**0.449**	**0.178**
	F6	0.539	0.153	-	0.383	0.796	0.646	0.678	0.183	**0.482**	**0.231**
	F7	0.623	0.820	-	0.679	0.866	0.635	0.833	0.789	**0.749**	**0.093**
$R^2_{F,f}$	**F1**	0.922	0.946	0.958	0.971	0.944	-	0.953	0.954	**0.950**	**0.014**
	F2	0.753	0.932	0.963	0.968	0.895	-	0.948	0.949	**0.915**	**0.070**
	F3	0.737	0.922	0.254	0.937	0.903	-	0.945	0.950	**0.807**	**0.236**
1Hz	**F4**	0.743	0.905	0.268	0.932	0.907	-	0.955	0.955	**0.809**	**0.231**
	F5	0.887	0.823	0.309	0.920	0.896	-	0.948	0.948	**0.819**	**0.212**
	F6	0.906	0.832	0.398	0.889	0.897	0.470	0.950	0.954	**0.787**	**0.208**
	F7	0.919	0.948	0.464	0.916	0.919	0.744	0.963	0.969	**0.855**	**0.162**
	F1	0.950	0.957	0.950	0.973	0.979	0.911	0.742	0.983	**0.931**	**0.074**
	F2	0.848	0.949	0.948	0.976	0.899	0.861	0.738	0.957	**0.897**	**0.074**
	F3	0.835	0.933	0.674	0.888	0.906	0.837	0.710	0.920	**0.838**	**0.091**
2Hz	**F4**	0.817	0.913	0.662	0.856	0.903	0.830	0.781	0.917	**0.835**	**0.080**
	F5	0.898	0.863	0.664	0.840	0.902	0.844	0.767	0.875	**0.832**	**0.075**
	F6	0.916	0.884	0.593	0.799	0.914	0.850	0.799	0.915	**0.834**	**0.102**
	F7	0.917	0.952	0.659	0.859	0.931	0.938	0.875	0.949	**0.885**	**0.091**
	F1	0.835	0.867	0.911	0.636	0.855	0.690	0.843	0.963	**0.825**	**0.102**
	F2	0.632	0.839	0.901	0.534	0.649	0.612	0.877	0.899	**0.743**	**0.141**
	F3	0.603	0.813	0.344	0.478	0.725	0.554	0.840	0.830	**0.648**	**0.171**
3Hz	**F4**	0.555	0.767	0.326	0.422	0.724	0.531	0.898	0.784	**0.626**	**0.185**
	F5	0.853	0.736	0.331	0.337	0.757	0.565	0.914	0.609	**0.638**	**0.205**
	F6	0.874	0.745	0.324	0.634	0.900	0.433	0.920	0.693	**0.690**	**0.205**
	F7	0.859	0.917	0.380	0.791	0.945	0.752	0.964	0.917	**0.816**	**0.179**
	F1	0.877	0.574	0.672	-	0.394	-	0.399	0.932	**0.641**	**0.210**
	F2	0.834	0.548	0.622	-	0.287	-	0.577	0.830	**0.616**	**0.186**
	F3	0.827	0.519	-	-	0.432	-	0.443	0.731	**0.591**	**0.160**
4Hz	**F4**	0.537	0.387	-	-	0.297	-	0.640	0.626	**0.497**	**0.135**
	F5	0.744	0.306	-	-	0.388	0.486	0.684	0.226	**0.472**	**0.189**
	F6	0.575	0.251	-	0.449	0.821	0.671	0.717	0.324	**0.544**	**0.195**
	F7	0.637	0.853	-	0.741	0.895	0.665	0.860	0.807	**0.780**	**0.093**

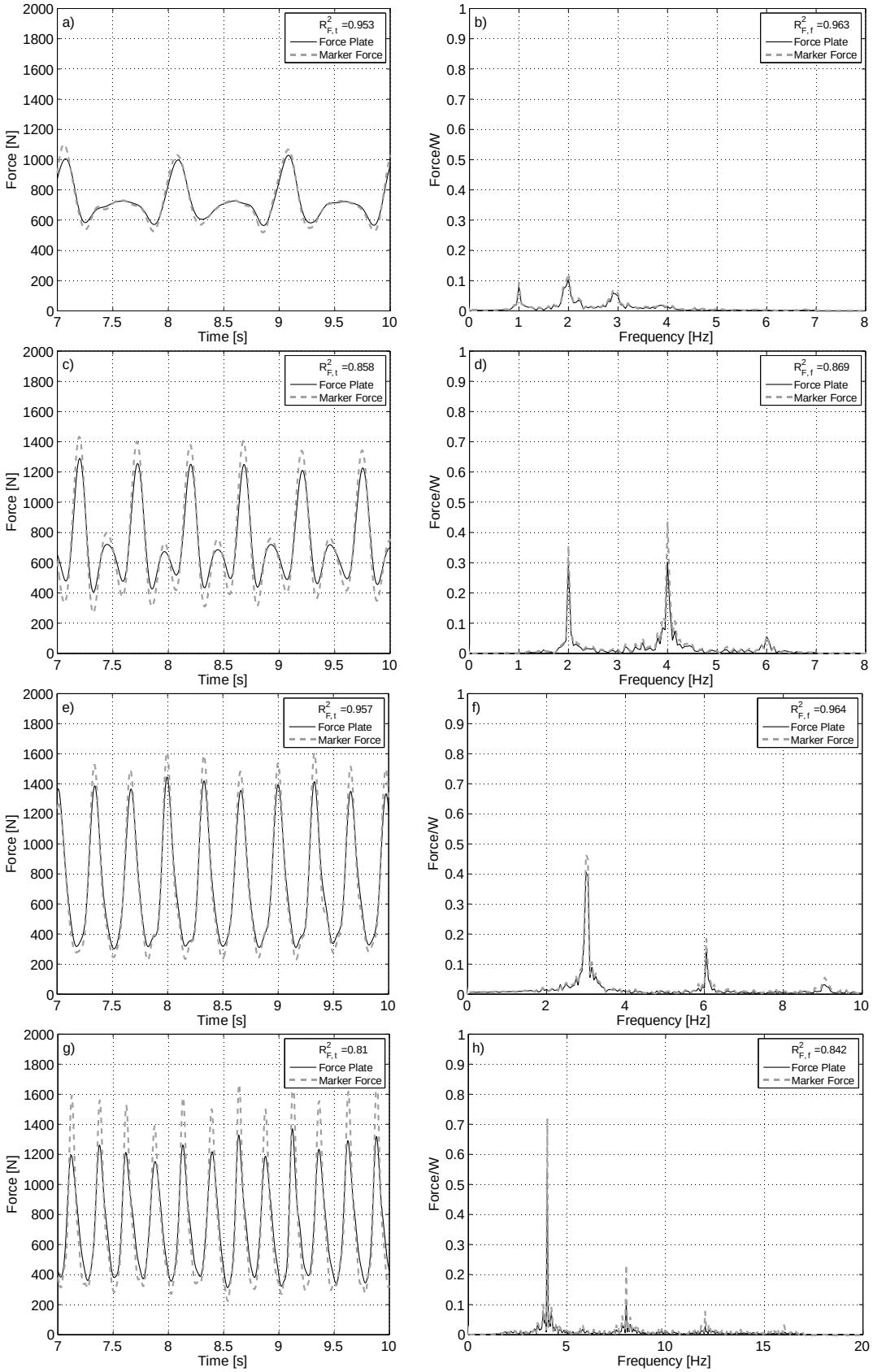

Figure 6.3 Comparing the direct and indirect forces using the F7 marker for bobbing 1Hz (a&b), 2Hz (c&d), 3Hz(e&f) and 4Hz (g&h), where a, c, e & g) are the t-domain, and b, d, f & h) the f-domain.

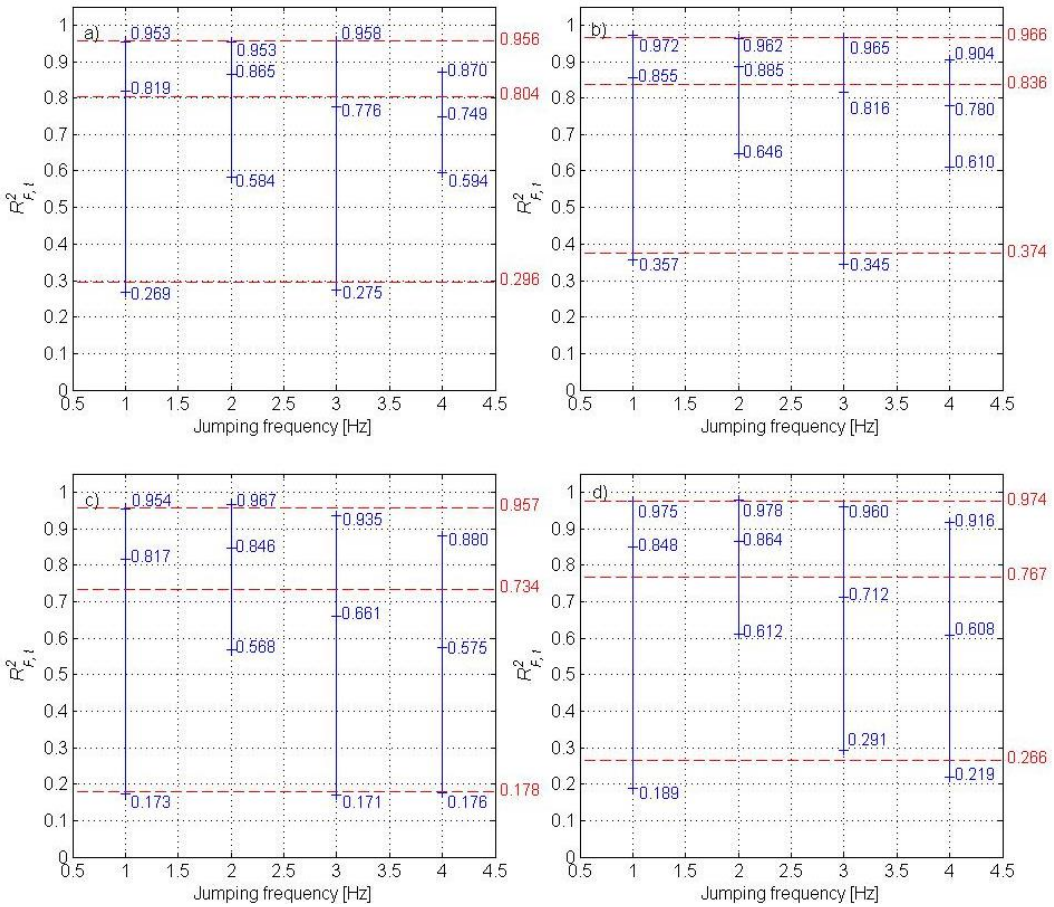

Figure 6.4 Average R^2_F values from the F7 marker in the a) t-domain and b) f-domain and for the entire front group in the c) t-domain and d) the f-domain. The mean values and 95th pecentiles for each frequency are marked as crosses, the dashed lines represent the mean and 95th percentile values across all the frequencies.

Table 6.6 The average R^2_F and 95th percentiles values for the front markers.

	1Hz				2Hz				3Hz				4Hz			
$R^2_{F,t}$	Ave	95% Min	95% Max	Range	Ave	95% Min	95% Max	Range	Ave	95% Min	95% Max	Range	Ave	95% Min	95% Max	Range
F1	0.950	0.919	0.977	0.058	0.931	0.725	0.986	0.261	0.825	0.600	0.970	0.370	0.641	0.328	0.941	0.614
F2	0.915	0.749	0.975	0.225	0.897	0.718	0.977	0.260	0.743	0.510	0.914	0.404	0.616	0.212	0.887	0.675
F3	0.807	0.137	0.961	0.824	0.838	0.639	0.935	0.296	0.648	0.330	0.853	0.522	0.591	0.370	0.864	0.494
F4	0.809	0.161	0.967	0.806	0.835	0.628	0.924	0.296	0.626	0.318	0.901	0.582	0.497	0.230	0.681	0.451
F5	0.819	0.204	0.958	0.755	0.832	0.628	0.908	0.280	0.638	0.282	0.916	0.634	0.487	0.150	0.777	0.628
F6	0.787	0.282	0.958	0.676	0.834	0.580	0.931	0.351	0.690	0.231	0.921	0.690	0.589	0.264	0.830	0.566
F7	0.855	0.357	0.972	0.614	0.885	0.646	0.962	0.316	0.816	0.345	0.965	0.621	0.780	0.610	0.904	0.294
Ave	0.817	0.173	0.954	0.781	0.846	0.568	0.967	0.398	0.661	0.171	0.935	0.764	0.575	0.176	0.880	0.704
$R^2_{F,f}$																
F1	0.922	0.883	0.964	0.081	0.916	0.705	0.979	0.274	0.788	0.520	0.940	0.420	0.598	0.244	0.908	0.664
F2	0.888	0.708	0.963	0.255	0.880	0.701	0.966	0.265	0.696	0.406	0.896	0.490	0.577	0.159	0.871	0.712
F3	0.786	0.131	0.942	0.811	0.819	0.589	0.925	0.336	0.592	0.220	0.842	0.622	0.553	0.327	0.840	0.513
F4	0.788	0.153	0.943	0.789	0.816	0.580	0.916	0.335	0.567	0.221	0.888	0.668	0.458	0.189	0.661	0.473
F5	0.795	0.196	0.936	0.740	0.813	0.582	0.896	0.314	0.574	0.136	0.905	0.769	0.488	0.207	0.769	0.562
F6	0.736	0.181	0.938	0.757	0.809	0.515	0.918	0.403	0.630	0.131	0.913	0.783	0.536	0.142	0.802	0.660
F7	0.819	0.269	0.953	0.684	0.865	0.584	0.953	0.370	0.776	0.275	0.958	0.683	0.749	0.594	0.870	0.276
Ave	0.848	0.189	0.975	0.786	0.864	0.612	0.978	0.366	0.712	0.291	0.960	0.670	0.608	0.219	0.916	0.697

6.3.3 Back Markers

The indirect force measurements using the back group of markers is reasonably successful. The mean value and STD of R^2_F for the back group as a whole are 0.851 and 0.162 in the t-domain, and 0.884 and 0.146 in the f-domain (Table 6.7). The mean values are smaller than the corresponding jumping values of $R^2_{F,\,t}$ =0.944 and $R^2_{F,\,f}$ = 0.954 (Section 5.4.3). The bobbing STDs are greater than the jumping values of $R^2_{F,\,t\,STD}$ =0.040 and $R^2_{F,\,f\,STD}$ = 0.046. This reiterates that the indirect force measurements are not as successful or as consistent when bobbing.

Table 6.7 The average R^2_F values for the back markers.

	$R^2_{F,t}$						$R^2_{F,f}$					
	1Hz	**2Hz**	**3Hz**	**4Hz**	**Ave**	**STD**	**1Hz**	**2Hz**	**3Hz**	**4Hz**	**Ave**	**STD**
B1	0.887	0.893	0.776	0.565	**0.788**	**0.204**	0.921	0.910	0.821	0.645	**0.831**	**0.165**
B2	0.880	0.891	0.827	0.505	**0.776**	**0.201**	0.916	0.909	0.864	0.570	**0.815**	**0.175**
B3	0.916	0.926	0.842	0.536	**0.805**	**0.199**	0.942	0.939	0.867	0.575	**0.831**	**0.194**
B4	0.930	0.962	0.922	0.790	**0.901**	**0.087**	0.958	0.973	0.941	0.819	**0.923**	**0.083**
B5	0.915	0.951	0.919	0.866	**0.913**	**0.065**	0.957	0.971	0.956	0.905	**0.947**	**0.052**
B6	0.924	0.960	0.929	0.902	**0.929**	**0.062**	0.968	0.982	0.964	0.944	**0.965**	**0.052**
					0.851	**0.162**					**0.884**	**0.146**

The R^2_F values for the back markers for all subjects are shown in Table 6.8. The highest R^2_F values from all markers are seen for the B6 marker, where the average value of $R^2_{F,\,t}$ is 0.929 and $R^2_{F,\,f}$ is 0.965 (Table 6.7). These values are smaller than the corresponding jumping values of $R^2_{F,\,t}$ =0.967 and $R^2_{F,\,f}$ =0.991 (Section 5.4.3). The STDs of the B6 marker are the smallest of all the markers when bobbing ($R^2_{F,\,t\,STD}$ =0.062 and $R^2_{F,\,f\,STD}$ =0.052) and are only slightly greater than the values when jumping ($R^2_{F,\,t\,STD}$ =0.04 and $R^2_{F,\,f\,STD}$ =0.046). The B6 marker is the most reliable marker, and the best at measuring the force, consistent with the previous jumping experiments. Figure 6.5 demonstrates that the B6 marker can effectively measure the direct force at different bobbing frequencies in both the t-and f-domains. The lowest R^2_F values are associated with bobbing at 4Hz.

The 95th percentiles and range of the R^2_F values for the B6 marker and the back group as a whole are shown in Figure 6.6. The range for the group as a whole is larger than for the B6 marker, the B6 marker's range of $R^2_{F,\,f}$ values is the smallest of all the markers. The largest

ranges between the percentiles are at 3Hz and 4Hz (Table 6.9). This indicates that the accuracy of the indirect force measurement reduces with bobbing frequency.

Table 6.8 $R^2_{F,t}$ and $R^2_{F,f}$ values for the back markers.

$R^2_{F,t}$	TS	1	2	3	4	5	6	7	8	Ave	STD
1Hz	B1	-	0.964	0.780	0.857	0.840	0.933	0.938	0.894	**0.887**	**0.060**
	B2	0.700	0.970	0.808	0.878	0.889	0.959	0.920	0.916	**0.880**	**0.083**
	B3	0.845	0.971	0.923	0.887	0.904	0.950	0.925	0.921	**0.916**	**0.036**
	B4	0.909	0.969	0.950	0.946	0.935	0.878	0.950	0.905	**0.930**	**0.028**
	B5	0.855	0.968	0.855	0.958	0.938	0.882	0.955	0.912	**0.915**	**0.044**
	B6	0.880	0.968	0.854	0.958	0.943	0.891	0.966	0.931	**0.924**	**0.040**
2Hz	B1	-	0.987	0.847	0.724	0.841	0.969	0.918	0.966	**0.893**	**0.088**
	B2	0.727	0.990	0.869	0.779	0.945	0.980	0.859	0.978	**0.891**	**0.093**
	B3	0.865	0.990	0.958	0.805	0.953	0.978	0.880	0.974	**0.926**	**0.063**
	B4	0.918	0.990	0.965	0.949	0.978	0.958	0.971	0.968	**0.962**	**0.020**
	B5	0.880	0.987	0.892	0.967	0.978	0.960	0.973	0.972	**0.951**	**0.038**
	B6	0.913	0.987	0.928	0.963	0.979	0.980	0.954	0.980	**0.960**	**0.026**
3Hz	B1	-	0.963	0.570	0.769	0.391	0.915	0.964	0.861	**0.776**	**0.203**
	B2	0.624	0.962	0.643	0.757	0.900	0.911	0.911	0.905	**0.827**	**0.124**
	B3	0.790	0.953	0.866	0.633	0.807	0.880	0.934	0.873	**0.842**	**0.094**
	B4	0.808	0.950	0.936	0.942	0.915	0.976	0.966	0.883	**0.922**	**0.051**
	B5	0.857	0.970	0.777	0.970	0.941	0.974	0.963	0.901	**0.919**	**0.066**
	B6	0.891	0.973	0.719	0.978	0.973	0.979	0.969	0.954	**0.929**	**0.084**
4Hz	B1	-	0.688	0.124	0.541	-	0.734	0.822	0.481	**0.565**	**0.228**
	B2	0.568	0.647	0.209	0.206	0.609	0.650	0.526	0.620	**0.505**	**0.176**
	B3	0.697	0.663	0.743	0.119	0.290	0.487	0.629	0.659	**0.536**	**0.208**
	B4	0.745	0.630	0.700	0.732	0.833	0.881	0.935	0.866	**0.790**	**0.097**
	B5	0.847	0.796	0.713	0.930	0.892	0.934	0.904	0.913	**0.866**	**0.072**
	B6	0.928	0.864	0.747	0.925	0.930	0.964	0.915	0.940	**0.902**	**0.064**
$R^2_{F,f}$	B1	-	0.981	0.852	0.877	0.866	0.975	0.950	0.945	**0.921**	**0.050**
1Hz	B2	0.801	0.982	0.869	0.893	0.909	0.982	0.931	0.963	**0.916**	**0.058**
	B3	0.908	0.980	0.959	0.905	0.927	0.973	0.936	0.951	**0.942**	**0.026**
	B4	0.938	0.979	0.961	0.960	0.966	0.962	0.962	0.940	**0.958**	**0.013**
	B5	0.942	0.983	0.917	0.974	0.969	0.958	0.968	0.947	**0.957**	**0.020**
	B6	0.963	0.985	0.927	0.974	0.971	0.980	0.980	0.967	**0.968**	**0.017**
2Hz	B1	-	0.991	0.889	0.740	0.870	0.980	0.927	0.976	**0.910**	**0.082**
	B2	0.785	0.994	0.904	0.790	0.954	0.992	0.862	0.988	**0.909**	**0.082**
	B3	0.899	0.994	0.981	0.814	0.962	0.991	0.885	0.983	**0.939**	**0.061**
	B4	0.932	0.994	0.973	0.959	0.987	0.970	0.983	0.985	**0.973**	**0.019**
	B5	0.937	0.993	0.916	0.981	0.988	0.972	0.991	0.987	**0.971**	**0.027**
	B6	0.968	0.993	0.950	0.978	0.988	0.994	0.994	0.991	**0.982**	**0.015**
3Hz	B1	-	0.977	0.728	0.779	0.421	0.949	0.980	0.909	**0.821**	**0.187**
	B2	0.686	0.974	0.767	0.774	0.907	0.942	0.921	0.942	**0.864**	**0.099**
	B3	0.820	0.964	0.929	0.661	0.814	0.916	0.947	0.886	**0.867**	**0.094**
	B4	0.831	0.961	0.952	0.966	0.932	0.991	0.994	0.904	**0.941**	**0.050**
	B5	0.979	0.982	0.831	0.989	0.958	0.989	0.995	0.923	**0.956**	**0.052**
	B6	0.988	0.987	0.775	0.995	0.996	0.995	0.998	0.977	**0.964**	**0.072**
4Hz	B1	-	0.740	0.425	0.567	-	0.769	0.826	0.543	**0.645**	**0.142**
	B2	0.585	0.699	0.496	0.231	0.634	0.671	0.567	0.674	**0.570**	**0.142**
	B3	0.710	0.714	0.853	0.169	0.312	0.515	0.645	0.680	**0.575**	**0.214**
	B4	0.756	0.685	0.712	0.756	0.853	0.916	0.950	0.921	**0.819**	**0.097**
	B5	0.900	0.850	0.754	0.966	0.918	0.955	0.941	0.956	**0.905**	**0.067**
	B6	0.963	0.913	0.781	0.965	0.985	0.991	0.977	0.980	**0.944**	**0.066**

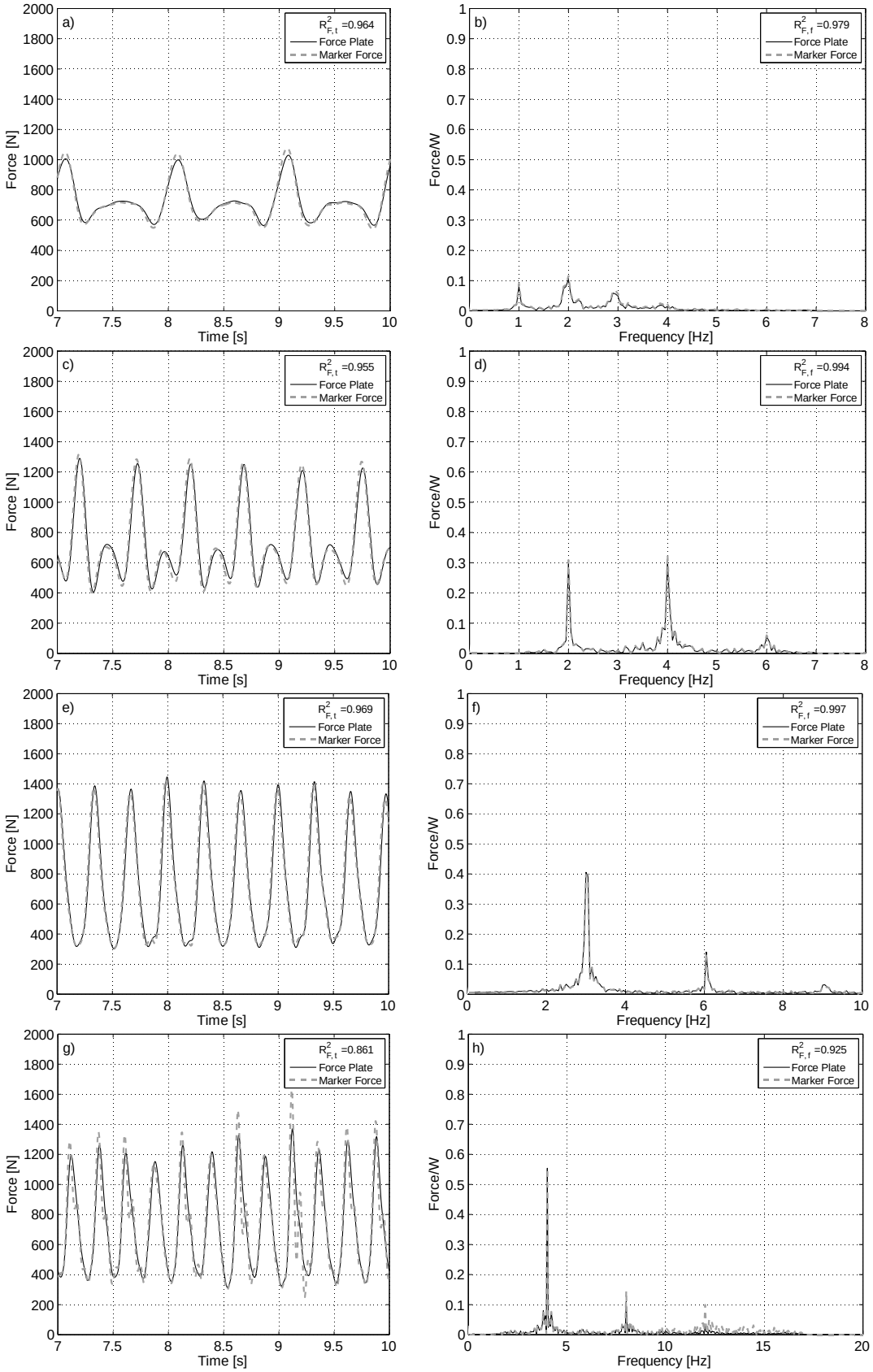

Figure 6.5 Comparing the direct and indirect forces using the B6 marker for bobbing 1Hz (a&b), 2Hz (c&d), 3Hz(e&f) and 4Hz (g&h), where a, c, e & g) are the t-domain, and b, d, f & h) the f-domain.

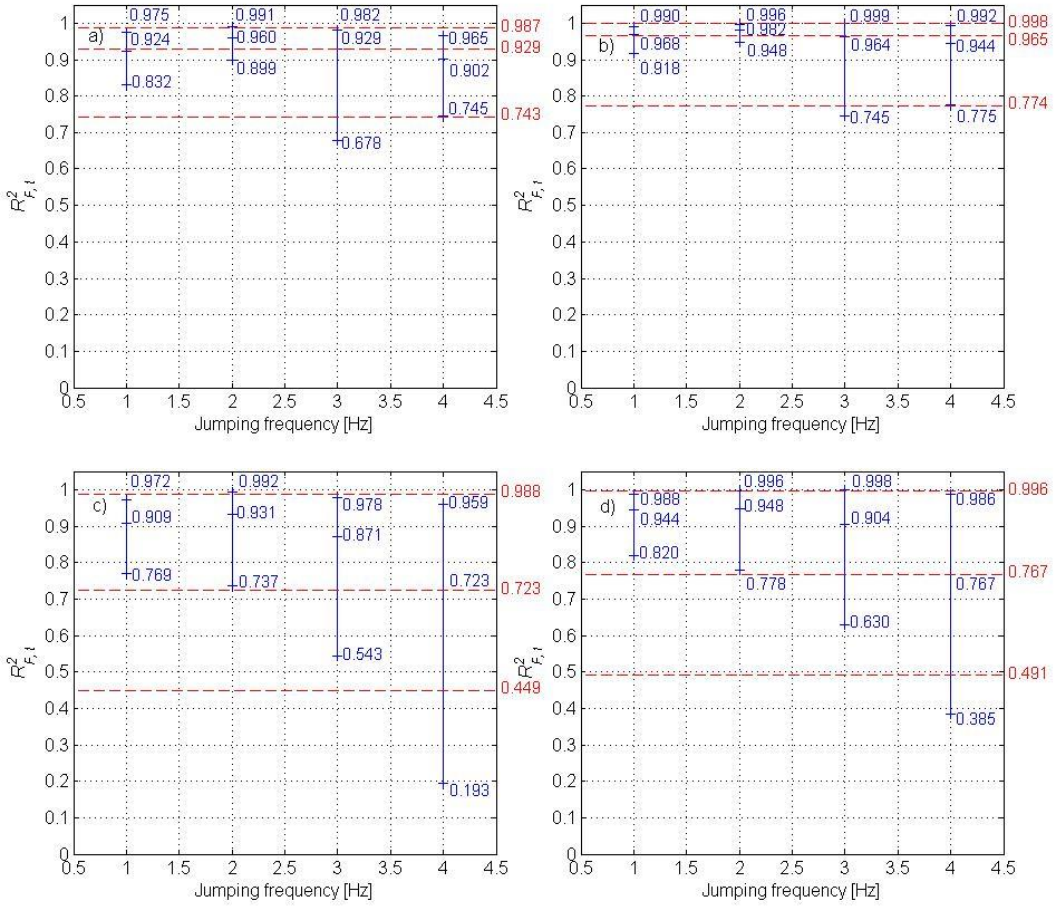

Figure 6.6 Average R^2_F values from the B6 marker in the a) t-domain and b) f-domain and for the entire back group in the c) t-domain and d) the f-domain. The mean values and 95th pecentiles for each frequency are marked as crosses, the dashed lines represent the mean and 95th percentile values across all the frequencies.

Table 6.9 The average R^2_F and 95th percentiles for the front markers.

	1Hz				2Hz				3Hz				4Hz			
$R^2_{F,t}$	Ave	95% Min	95% Max	Range	Ave	95% Min	95% Max	Range	Ave	95% Min	95% Max	Range	Ave	95% Min	95% Max	Range
B1	0.887	0.758	0.965	0.207	0.893	0.701	0.989	0.288	0.776	0.377	0.968	0.591	0.591	0.122	0.830	0.708
B2	0.880	0.660	0.971	0.311	0.891	0.706	0.991	0.285	0.827	0.589	0.964	0.375	0.532	0.198	0.719	0.522
B3	0.916	0.825	0.971	0.146	0.926	0.798	0.990	0.192	0.842	0.613	0.958	0.345	0.587	0.173	0.749	0.575
B4	0.930	0.862	0.969	0.107	0.962	0.911	0.991	0.080	0.922	0.800	0.977	0.177	0.790	0.608	0.938	0.329
B5	0.915	0.829	0.975	0.146	0.951	0.864	0.989	0.125	0.919	0.764	0.975	0.212	0.866	0.697	0.951	0.254
B6	0.924	0.832	0.975	0.144	0.960	0.899	0.991	0.092	0.929	0.678	0.982	0.304	0.902	0.745	0.965	0.219
Ave	0.909	0.769	0.972	0.203	0.931	0.737	0.992	0.255	0.871	0.543	0.978	0.435	0.723	0.193	0.959	0.765
$R^2_{F,f}$																
B1	0.921	0.810	0.982	0.173	0.910	0.718	0.993	0.275	0.821	0.411	0.981	0.570	0.645	0.410	0.833	0.423
B2	0.916	0.766	0.987	0.221	0.909	0.760	0.996	0.236	0.864	0.672	0.976	0.303	0.600	0.362	0.752	0.391
B3	0.942	0.890	0.981	0.091	0.939	0.809	0.995	0.186	0.867	0.641	0.968	0.327	0.626	0.209	0.862	0.653
B4	0.958	0.922	0.980	0.058	0.973	0.925	0.995	0.070	0.941	0.826	0.994	0.169	0.819	0.645	0.957	0.312
B5	0.957	0.906	0.985	0.078	0.971	0.912	0.994	0.082	0.956	0.820	0.996	0.176	0.905	0.739	0.976	0.237
B6	0.968	0.918	0.990	0.072	0.982	0.948	0.996	0.049	0.964	0.745	0.999	0.254	0.944	0.775	0.992	0.216
Ave	0.944	0.820	0.988	0.168	0.948	0.778	0.996	0.218	0.904	0.630	0.998	0.367	0.767	0.385	0.986	0.601

To conclude, the B6 marker is the best performing marker. However, as the marker is positioned on the back of the TS, monitoring the movement may be difficult in actual venues. In general the indirect force measurements from bobbing subjects are less accurate than from jumping subjects.

6.3.4 Actual Bobbing Frequency and Percentage Difference.

Within this section the actual bobbing frequency is compared to the target bobbing frequency. The indirect force is further analysed by calculating the percentage differences (PDs) of the peak indirect force relative to the peak direct force in the f-domain, for the B6 and F7 markers at each dominant harmonic. The bobbing trials are split into bouncing and jouncing to investigate whether force measurement of a specific action is easier.

The frequency and the PDs for the first three harmonics are calculated for the B6 marker in Table 6.10. Comparing the actual bobbing frequency to the target frequency, more TSs achieved a frequency of 1Hz when bobbing than jumping (Section 5.4.4). However, when bobbing at frequencies of 2Hz and above, a wider range in average actual bobbing frequencies and harmonics occurs. This contradicts previous work which found that bobbing at a specified frequency is easier than jumping (Sim et al., 2005). The style of bobbing used by the TSs is shown in Table 6.10. The TSs which bounced produced trials that are at, or very near the metronome beat. The frequency deviation is greater for the jouncing subjects, consistent with observations in Chapter 4. The majority of TSs are at, or very close to the target frequency when bobbing below 4Hz. The results are influenced by three jouncing TSs who missed the target frequencies significantly.

The PDs are sorted by over and under estimations of the force, mean values are calculated for each (Table 6.11). The PDs for each bobbing frequency and harmonic are plotted in Figure 6.7. A wider spread of PDs is seen compared to the corresponding jumping figure in Section 5.4.4.

For the 1st harmonic mean PDs values of +7.90% and -18.14% were found (Table 6.11). The largest PDs were at 1Hz, this is likely because the frequency components are small, and more affected by soft tissue artefact and variation in the CoM position.

Table 6.10 The B6 marker PDs at each harmonics for each TS.

	TS	1st Harm(%)	2nd Harm(%)	3rd Harm(%)	Freq 1st Harm (Hz)	Freq 2nd Harm (Hz)	Freq 3rd Harm (Hz)	Style	Heel contact
1Hz	1	-5.30	-1.43	-1.98	1.00	2.00	3.05	Jouncing	
	2	-8.09	-4.25	1.34	0.95	1.90	2.90	Jouncing	Yes
	3	-44.28	-19.33	-21.25	1.00	2.05	2.95	Jouncing	Yes
	4	9.55	17.17	12.41	1.00	2.00	2.95	Bouncing	Yes
	5	7.72	13.06	19.57	1.00	2.00	3.00	Bouncing	Yes
	6	-14.88	-6.82	-4.38	1.00	2.00	3.00	Jouncing	Yes
	7	11.27	10.76	13.69	1.00	2.00	2.90	Bouncing	Yes
	8	3.06	42.03	-5.81	1.00	2.00	3.00	Jouncing	Yes
	Overall Ave	-5.12	6.40	1.70	0.99	1.99	2.97		
	STD	17.15	17.54	12.31	0.02	0.04	0.04		
2Hz	1	0.08	-18.76	-19.22	2.00	4.00	6.00	Bouncing	
	2	-1.19	0.01	102.95	2.30	4.60	6.90	Jouncing	Yes
	3	-20.18	-16.17	47.26	2.25	4.45	6.40	Jouncing	Yes
	4	10.05	28.47	25.15	2.00	4.00	6.00	Bouncing	Yes
	5	4.46	28.54	70.65	2.00	4.05	6.05	Jouncing	Yes
	6	-3.42	11.78	7.74	2.50	4.95	6.95	Jouncing	No
	7	4.48	8.90	31.83	2.00	4.00	6.00	Bouncing	Yes
	8	2.65	25.64	58.75	2.00	4.05	6.05	Jouncing	Yes
	Overall Ave	-0.38	8.55	40.64	2.13	4.26	6.29		
	STD	8.42	17.78	35.60	0.19	0.35	0.39		
3Hz	1	-3.17	-14.78	-96.52	3.01	6.03	9.04	Bouncing	
	2	0.74	-1.29	77.67	2.55	5.05	7.70	Jouncing	Occasional
	3	-25.12	143.73	954.17	3.00	6.05	9.10	Jouncing	Yes
	4	-2.11	2.86	-8.26	3.00	6.00	9.00	Bouncing	Yes
	5	0.12	0.29	-5.56	3.03	6.07	9.10	Jouncing	Occasional
	6	0.79	-2.74	192.16	3.05	6.00	8.85	Jouncing	No
	7	-1.72	-1.55	26.78	3.00	6.05	9.05	Jouncing	Yes
	8	1.10	41.02	137.03	3.00	6.00	9.00	Jouncing	No
	Overall Ave	-3.67	20.94	159.68	2.96	5.91	8.86		
	STD	8.24	48.82	311.91	0.16	0.34	0.47		
4Hz	1	-15.03	21.62	497.20	4.00	7.75	11.85	Jouncing	
	2	8.43	113.44	788.55	3.45	6.76	10.06	Jouncing	No
	3	-33.75	117.98	213.77	3.60	7.10	10.65	Jouncing	Yes
	4	-2.60	29.14	263.68	4.00	8.00	12.00	Bouncing	Yes
	5	-1.11	-7.71	1549.63	4.00	8.00	12.00	Jouncing	No
	6	5.30	-33.43	675.99	3.85	7.70	11.55	Bouncing	Yes
	7	-0.26	31.40	260.12	4.00	8.00	12.00	Jouncing	Yes
	8	1.95	-0.06	48.45	3.55	7.10	10.65	Jouncing	No
	Overall Ave	-4.63	34.05	537.17	3.81	7.55	11.35		
	STD	12.77	51.23	447.79	0.22	0.49	0.75		

At the 2nd harmonic larger PDs occur, the mean PDs when ignoring one outlier are +28.85% and -11.06% (Table 6.11). The 2nd harmonic when bobbing at 4Hz had the largest PDs, this is

likely due to the higher soft tissue artefact noise to signal ratio at the high frequencies as described in Section 5.4.4. The mean PDs for the 2nd harmonic at 4Hz are +62.72% and -13.73%, these are unacceptably high.

Table 6.11 The PDs at the first three harmonics between the direct and indirect forces in the f-domain (B6 marker).

PD	Bobbing Frequency (Hz)	(+) Average overestimation	(-) Average underestimation	Overall Average	STD
1st Harmonic	1	7.90	-18.14	-5.12	17.15
	2	4.34	-8.26	-0.38	8.42
	3	0.69	-8.03	-3.67	8.24
	4	5.23	-10.55	-4.63	12.77
	All frequencies	4.54	-11.25	-3.45	12.34
2nd Harmonic	1	20.76	-7.96	6.40	17.54
	2	17.22	-17.47	8.55	17.78
	3	46.98	-5.09	20.94	48.82
	3 (without TS3)	14.72	-5.09	3.40	16.21
	4Hz	62.72	-13.73	34.05	51.23
	All frequencies	36.92	-11.06	17.49	39.12
	All frequencies without outliers	28.85	-11.06	13.10	32.39
3rd Harmonic	1	11.76	-8.36	1.70	12.31
	2	49.19	-19.22	40.64	35.60
	3	277.56	-36.78	159.68	311.91
	3Hz (without TS3)	108.41	-36.78	46.18	90.19
	4	537.17	0.00	537.17	447.79
	4 (without TS5)	392.54	0.00	392.54	248.60
	All frequencies	218.92	-16.09	184.80	345.81
	All frequencies without outliers	140.47	-16.09	120.26	201.67
All harmonics ≤ 4Hz		9.70	-11.25	0.41	14.87
2nd Harmonic > 4Hz		38.72	-9.41	18.72	50.47

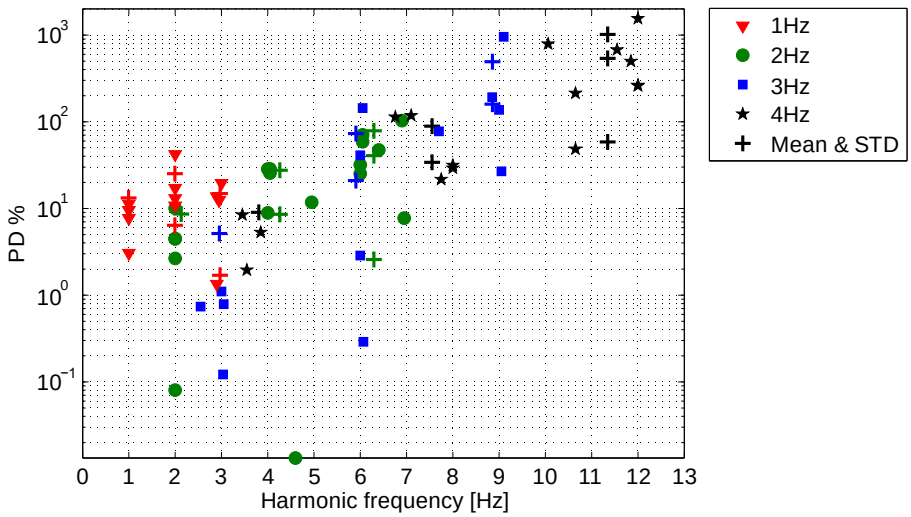

Figure 6.7 The positive PDs for the B6 marker for the dominant harmonics.

The average PDs at the 3rd harmonic (with the exclusion of two outliers) are +140.47% and -16.09% (Table 6.11). This demonstrates that measuring the 3rd harmonic component at higher frequencies is challenging, in addition it shows the tendency of the indirect force to overestimate the higher frequency components. It should be noted that the PDs at the 3rd harmonic of 1Hz bobbing are +11.76% and -8.26%, which are reasonably low.

In Table 6.12 the PDs from the B6 marker have been split into the different styles of bobbing to investigate whether the indirect force is more suited to measuring the force of a specific style. There appears to be more consistency in the force measurements between the bouncing TSs, demonstrated by the lower STDs highlighted in Table 6.12. At the 2nd and 3rd harmonics of 1Hz and the 1st harmonic of 2Hz the average values of PDs are lower for the jouncing TSs, whereas at higher frequencies the PDs from the bouncing TSs are smaller. In general the indirect force measurement shows better agreement with the direct force for the action of bouncing. However, fewer TSs chose to bounce and therefore these findings are based on a limited number of TSs.

Table 6.12 The Average PDs for bouncing and jouncing TS at the first three harmonics for the B6 marker.

PD at each Harmonic (%)	1Hz			2Hz			3Hz			4Hz		
	1st	2nd	3rd	1st	2nd	3rd	1st	2nd	3rd	1st	2nd	3rd
Bouncing Ave	9.51	13.66	15.22	4.87	6.20	12.59	-2.64	-5.96	-52.39	1.35	-2.15	469.84
Jouncing Ave	-13.90	2.04	-6.42	-3.54	9.96	57.47	-4.02	29.91	230.38	-6.63	46.11	559.62
Bouncing STD	1.45	2.65	3.12	4.08	19.38	22.66	0.53	8.82	44.13	3.95	31.29	206.16
Jouncing STD	16.24	20.91	7.80	8.77	16.59	31.05	9.48	53.21	330.27	14.01	50.90	501.17
Bouncing CoV	0.15	0.19	0.20	0.84	3.12	1.80	-0.20	-1.48	-0.84	2.93	-14.59	0.44
Jouncing CoV	-1.17	10.25	-1.22	-2.48	1.67	0.54	-2.36	1.78	1.43	-2.11	1.10	0.90

As the F7 marker is the most visible marker the PDs between the direct and indirect forces were also calculated and the average values presented in Figure 6.8. Significantly higher PDs (Table 6.13) are seen compared to those from the B6 marker, however very few underestimations of the force occurred. For harmonics with a frequency less than or equal to 4Hz the average values of PDs are -0.34 and +28.65. The 2nd harmonics which have a frequency value greater than 4Hz produce unacceptable average PDs (-45.80 and +64.90). For the 3rd

harmonic very large average PDs occur, except at 1Hz (-2.40 and + 26.33). Therefore using the F7 marker to measure frequency components above 4Hz will produce large overestimations of the force, however underestimations of the force are unlikely.

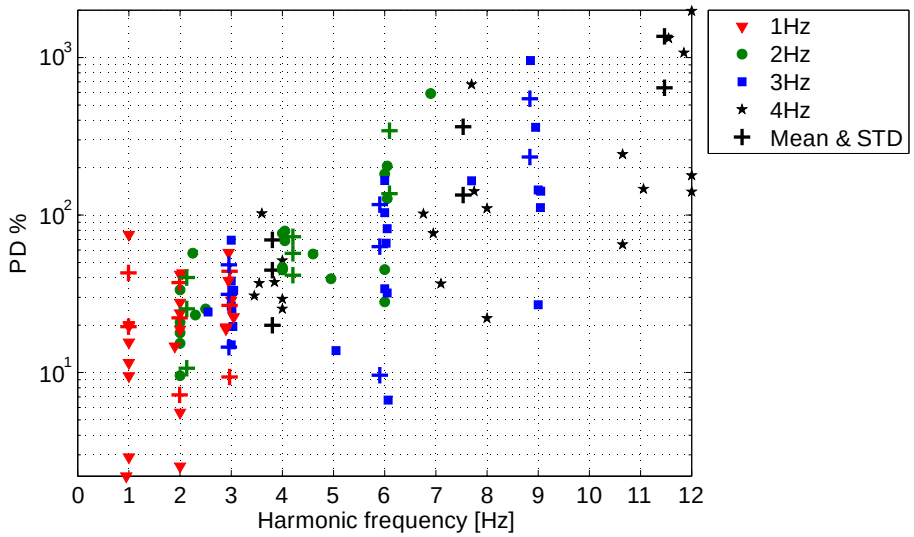

Figure 6.8 The positive PDs for the F7 marker for the dominant harmonics.

The values of PDs observed here are larger than those reported for the nine marker monitoring method (± 2% at the 1st harmonic, ± 4% at the 2nd harmonic and ± 7% at 3rd harmonic (Racic et al., 2010)). As the activity of bobbing is more complicated than jumping, the benefits from using multiple markers are more significant. However, it is worth noting that the nine marker methodology was only tested for 2TSs at frequencies between 1.4-2Hz.

It appears that the frequency of the harmonic affects the success of the force measurement. If the 1st and 2nd harmonics which are less than or equal to 6Hz are considered, as well as the 3rd harmonic of 1Hz, the average PDs from the B6 marker are +10.58 and -8.03 excluding outliers. The 95th percentiles for this data set are +34.78 and -20.72. The PDs between the higher frequency harmonic components of the direct and indirect force are large. The higher harmonics from the direct forces are very small and appear to diminish quicker than those from the indirect forces, this causes force overestimations at the higher harmonics. It is thought unlikely that these small frequency components will heavily influence the host

structure. Within the following section the bobbing forces will be applied to SDOF systems and the responses due to the higher harmonics investigated.

Table 6.13 The PDs at the first three harmonics between the direct and indirect forces in the f-domain (F7 marker).

PD	Bobbing Frequency	(+) Average overestimation	(-) Average underestimation	Overall Average	STD
1st Harmonic	1Hz	19.55	0.00	19.55	21.90
	1Hz (without TS3)	11.63	0.00	11.63	6.77
	2Hz	25.37	0.00	25.37	13.77
	2Hz (without TS3)	20.81	0.00	20.81	7.09
	3Hz	31.38	0.00	31.38	15.80
	3Hz (without TS3)	25.97	0.00	25.97	7.21
	4Hz	44.72	0.00	44.72	23.15
	4Hz (without TS3)	36.48	0.00	36.48	8.38
	All frequencies	30.25	0.00	30.25	21.24
	All frequencies without outliers	23.72	0.00	23.72	11.63
2nd Harmonic	1Hz	22.23	0.00	22.23	14.04
	2Hz	57.13	0.00	57.13	14.64
	3Hz	63.01	0.00	63.01	49.95
	3Hz (without TS6)	48.33	0.00	48.33	33.59
	4Hz	166.15	-91.60	133.93	214.97
	4Hz (without TS6)	81.47	-91.60	56.75	71.79
	All frequencies	77.13	-22.90	69.07	118.00
	All frequencies without outliers	52.29	-22.90	46.11	42.28
3rd Harmonic	1Hz	30.82	-2.40	26.67	16.18
	1Hz (without TS3)	26.33	-2.40	22.23	11.88
	2Hz	196.37	-41.93	136.79	192.71
	2Hz (without TS2)	117.50	-41.93	71.95	93.84
	3Hz	272.37	-37.27	233.67	293.90
	3Hz (without TS3 & TS6)	117.86	-37.27	92.00	72.86
	4Hz	643.30	0.00	643.30	673.94
	4Hz (without TS5)	453.00	0.00	453.00	478.92
	All frequencies	285.72	-20.40	260.11	445.87
	All frequencies without outliers	178.67	-20.40	159.79	305.24
All harmonics ≤ 4Hz		28.65	-0.34	28.07	17.61
2nd Harmonic > 4Hz		64.90	-45.80	52.54	56.20

6.3.5 Structural Response

To fully evaluate the success of the indirect force measurement the structural response to both the direct and indirect forces is examined and compared. A SDOF system was used to model the response from both the direct and indirect forces. The experimental procedure is consistent with the method used to apply jumping force histories to SDOFs in Section 5.4.5. A damping ratio of ζ=0.01 was used in the SDOF systems.

6.3.5.1 Response Magnitude

Within this section the magnitude of the structural response due to bobbing forces is investigated. This allows the quantification of the likely acceleration responses due to different bobbing and structural frequencies. Within Figure 6.9 the peak structural acceleration responses are plotted for SDOF systems with natural frequencies between 0.5 and 10Hz, for different bobbing frequencies. The maximum structural accelerations are compared to those from jumping forces in Figure 6.10.

From Figure 6.9 the resonance response values at 2Hz and 4Hz are approximately the same, indicating that the structural response is consistent for resonance conditions at these frequencies. The greatest resonance response occurs when bobbing at 3Hz, however the magnitude is not considerably bigger than at 2 and 4Hz. The resonance response at 1Hz is significantly smaller that at the other frequencies which is consistent with the structural responses from jumping forces.

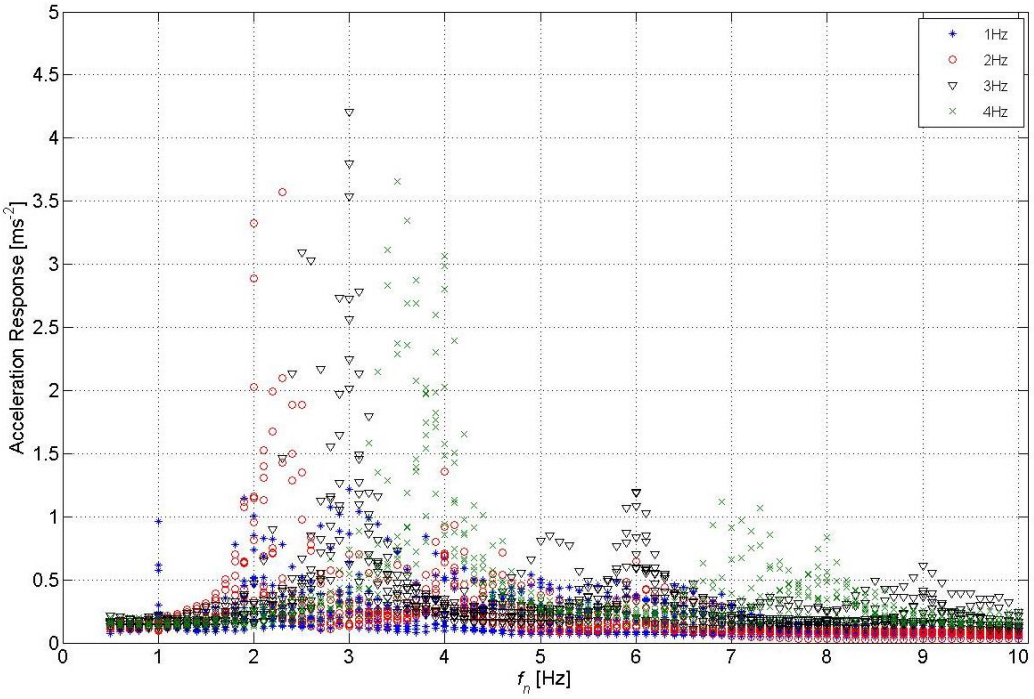

Figure 6.9 The peak acceleration response for SDOF systems exposed to bobbing at different frequencies.

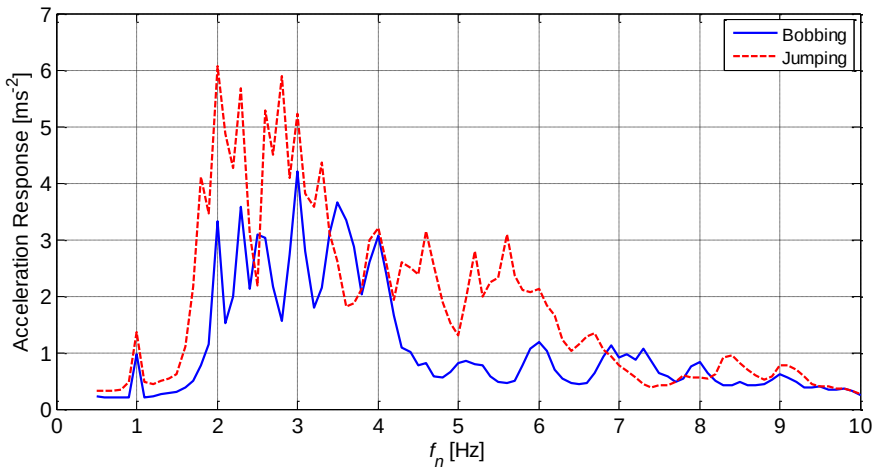

Figure 6.10 Comparison of the maximum structural responses for bobbing and jumping forces.

The maximum response due to bobbing (4.204ms^{-2}) is smaller than the maximum response when jumping (6.07ms^{-2} from Figure 6.10). Dividing the response by a mass factor m_f of 3.5 (a factor to reflect the mass of a stand) the maximum response reduces it to 1.20ms^{-2}, which is equivalent to 12.20% of g.

The SDOF responses due to the 2nd harmonics of the bobbing forces are smaller than the comparative jumping responses (Figure 6.10). The 2nd harmonic responses are approximately a quarter of the 1st harmonic value, compared to half when jumping. The responses due to bobbing at 1Hz are similar for the first three harmonics. This is consistent with previous observations of low frequency bobbing where the force spectra were not dominated by a specific harmonic (Sim et al., 2005).

For bobbing the largest response from a SDOF with a natural frequency greater or equal to 6Hz is 1.194 ms^{-2}, with the application of m_f this reduces to 0.341ms^{-2}. The comparative value when jumping is 0.629ms^{-2}. These structures ($f_n \geq$ 6Hz) are deemed to have a sufficiently high natural frequency and therefore not prone to crowd excitation (Section 5.2.1).

It is worth noting from Figure 6.10 that there are occasions when the response from the bobbing force is larger than from jumping. This occurs between 3-4Hz and the corresponding

2nd harmonic when bobbing subjects were attempting to move at 4Hz but achieved a lower frequency. At f_n= 8Hz which matches the 2nd harmonic of 4Hz, the bobbing response is larger than the jumping response. However several jumping harmonics occur after this point with a larger magnitude. It is suggested that the responses from the 3rd harmonics of jumping are larger than those from the 2nd harmonics of bobbing. The response due to 2nd and 3rd harmonic of bobbing is far smaller than for jumping, diminishing more rapidly. Although it may be possible for bobbing forces to reach harmonics of a greater frequency, the magnitudes at these harmonics are small. At the frequencies investigated jumping is the more extreme force. It is therefore not critical that the higher frequency harmonics of bobbing were poorly measured by the indirect force.

6.3.5.2 Response Ratio

The purpose of this section is to investigate how well the steady state accelerations of the SDOF systems due to the indirect force $A_{indirect}$, match the accelerations caused by the direct force A_{direct}. The effect of different structural natural frequencies and bobbing frequencies is examined. A ratio of the response r_A, introduced in Section 5.4.5 is used to quantify the variation between the responses (Equation 5.6). The response ratio will only be considered in the t-domain.

Within Figure 6.11 the response ratio is plotted against the natural frequency of the SDOF for different bobbing frequencies. A comparison between this figure and the corresponding figure in Section 5.4.5 reveals that a greater spread of r_A values is apparent for the activity of bobbing. This highlights that there are more discrepancies between the responses due to the indirect and direct force when bobbing compared to jumping.

Figure 6.11a shows the response ratios from the 1Hz bobbing forces have the largest spread of r_A values at lower frequencies. The values remain within approximately 1± 0.2 until f_n=5Hz where greater spread in the r_A values is seen. There is less spread in the r_A values at lower

frequencies in Figure 6.11b -d where 2Hz, 3Hz and 4Hz bobbing forces are applied. These graphs follow a similar pattern, the majority of r_A values are within 1± 0.2 at the low frequencies. When the f_n is near to the bobbing frequencies the r_A values closest to one are seen. This can also be seen at the 1st harmonic in Figure 6.12 where the mean and the mean ±1STD of the response are plotted against the normalised bobbing frequency. For f_n values larger than 4Hz a greater range of r_A values occur for 2 and 3Hz bobbing, this value is shifted to 4.5Hz for 4Hz bobbing (Figure 6.11b –d). From these figures TS3 is shown to have consistently different r_A values to the other TSs.

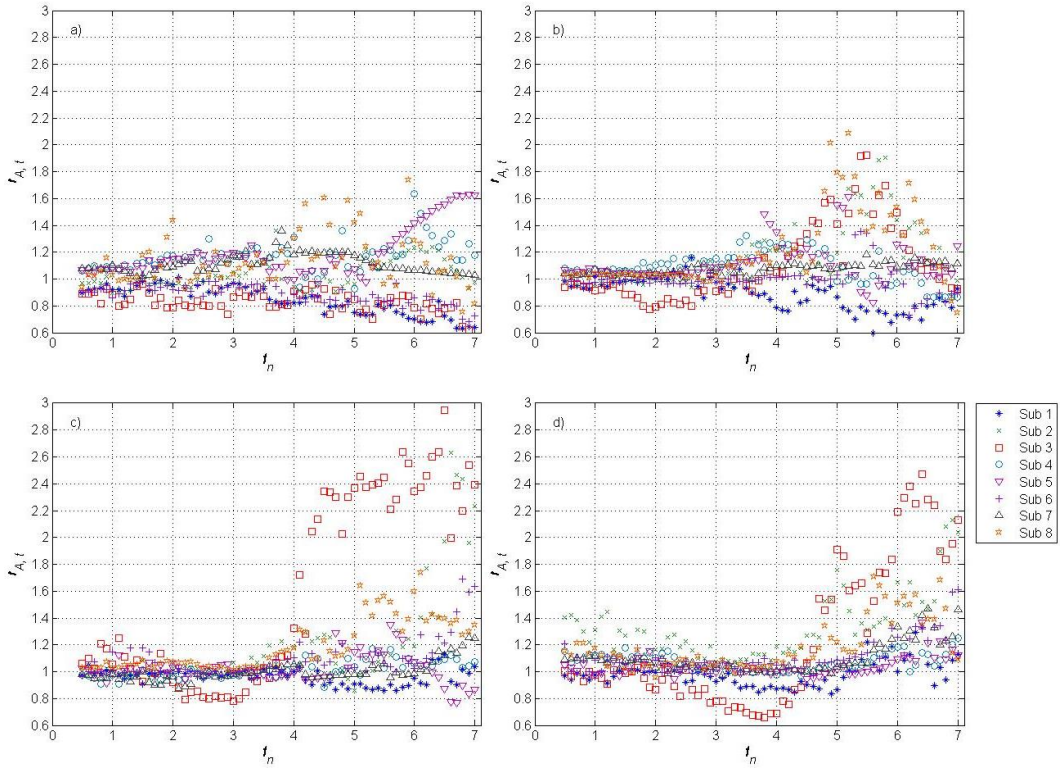

Figure 6.11 The B6 marker $r_{A,t}$ values for a range of SDOF systems due to bobbing at a)1Hz b)2Hz and c)3Hz d)4Hz.

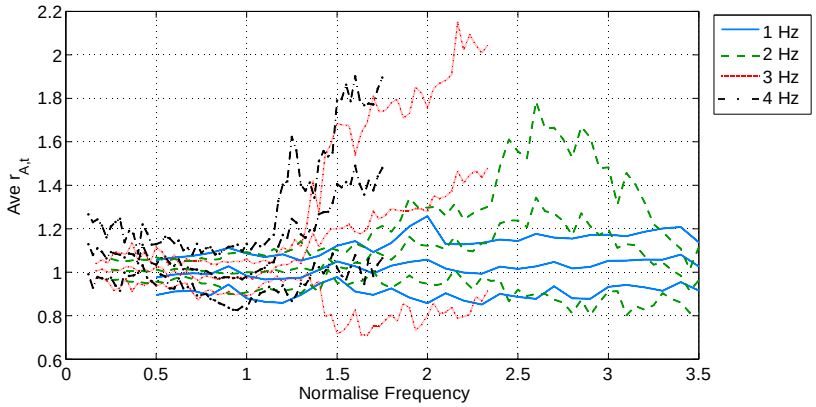

Figure 6.12 The average $r_{A,t}$ values for the B6 marker as a function of f_n normalised by the bob frequency.

6.3.5.3 Quantification of the r_A values for the B6 and F7 markers.

A relationship was sought between the structural ratio and the $R^2_{F,f}$ value of the force, to understand how differences in the f-domain of the direct and indirect forces propagate to the structural accelerations. $R^2_{F,f}$ values were recalculated to consider the main harmonics $R^2_{F,f\ harmonic}$ ($_{1st,\ 2nd}$ & $_{3rd}$) of the force ± 0.5Hz. Figure 6.13 a and b show the $R^2_{F,f\ 1st}$ and $r_{A,t}$ values for resonance at the 1st harmonic. If $R^2_{F,f\ 1st} \geq 0.970$, 94.7% of the structural ratios are between 1 ± 0.10. Of the B6 markers trials 81.3% have a $R^2_{F,f\ 1st}$ value ≥ 0.970. To reduce to the structural ratios to 1± 0.05 an $R^2_{F,f\ 1st}$ value ≥ 0.995 should be sought, this applies to 59.4% of B6 trials.

For resonance due to the 2nd harmonic of the force (Figure 6.13 c and d) a negative correlation can be observed between the two variables. To obtain an $r_{A,t}$ value between 1 ± 0.20 an $R^2_{F,f\ 2nd}$ value of ≥ 0.950 is advised (the case for 37.5% of trials), to achieve a reduced $r_{A,t}$ value of 1 ± 0.10 an $R^2_{F,f\ 2nd}$ value of ≥ 0.980 is needed (the case for 21.9% of trials). A negative correlation between $R^2_{F,f\ 3rd}$ and $r_{A,t}$ at resonance of the 3rd harmonic can be seen in Figure 6.13 e and f. For a structural ratio between 1 ± 0.20 an $R^2_{F,f\ 3rd}$ value of 0.900 is recommended (the case for 34.4% of trials).

All the $R^2_{F,f\ harmonic}$ values are plotted against the overall $R^2_{F,f}$ values for each trial (Figure 6.13 g and h), in general the overall $R^2_{F,f}$ value appears to have very little effect on the 2nd and 3rd

harmonic $R^2_{F,f\,harmonic}$ values. The 1st harmonic dominants the overall $R^2_{F,f}$ value. However, this is not the case at 1Hz where a weak positive correlation can be observed at each of the harmonics, this is consistent with the non-dominant harmonic observations in Section 6.3.5.1. Using the $R^2_{F,f}$ value to predict the response due to the 2nd or 3rd harmonic component of a bobbing force, with a frequency greater than 1Hz is likely to lead to large discrepancies in the response.

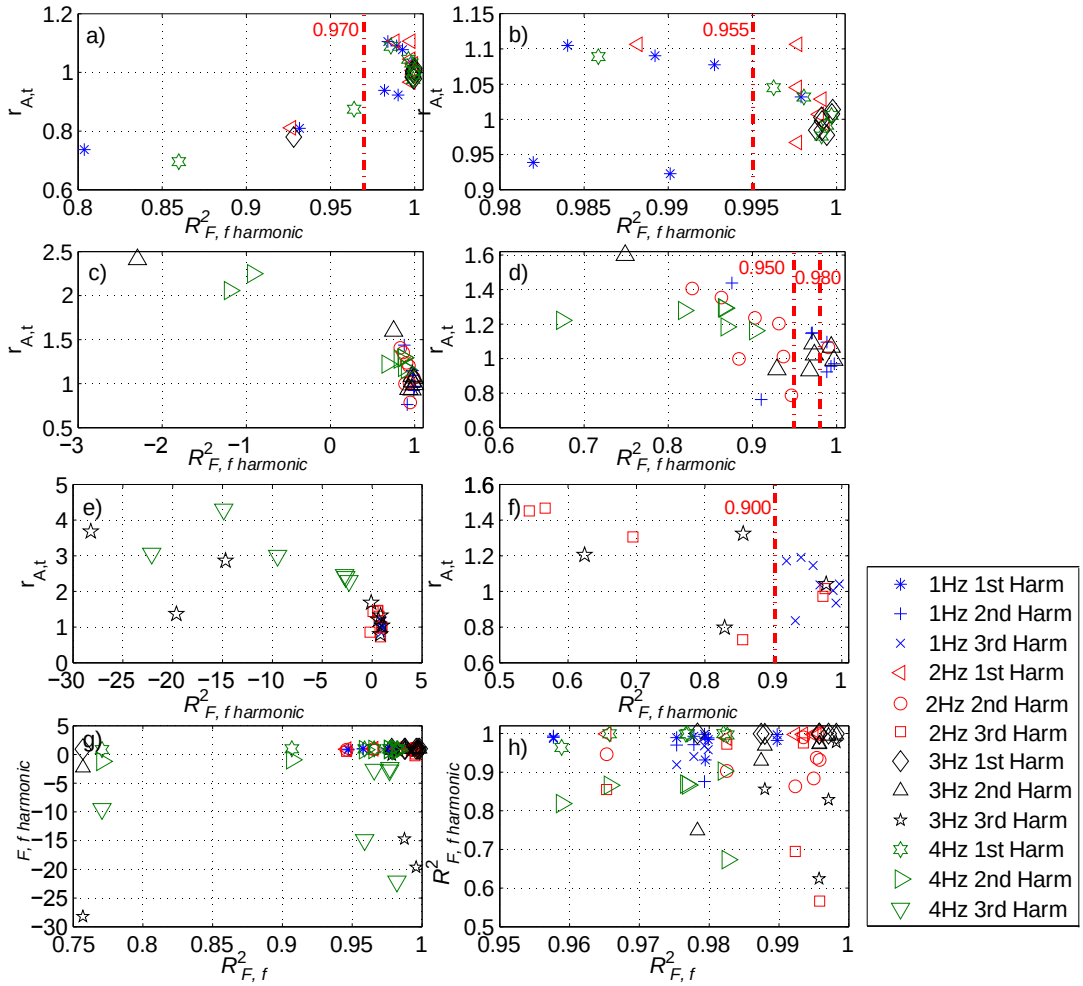

Figure 6.13 The $r_{A,t}$ values plotted against the $R^2_{F,f,harmonic}$ values at each harmonic of the force, for resonance due to the 1st (a & b), 2nd (c & d) and 3rd (e & f) harmonic and all harmonics (g & h) where a,c, e & g) are an overview of the distribution and b, d, f & h) a zoomed section.

For further comparison between the structural response and the force, the ratio of direct and indirect force at each harmonic in the f-domain $r_{F,f}$, is compared to the structural response ratio in the t-domain $r_{A,t}$. The actual frequency of each bobbing trial was found, and the trial

applied to a SDOF system with the corresponding natural frequency (or the 2nd or 3rd multiple of it). The relationship between $r_{F,f}$ and $r_{A,t}$ can be seen in Figure 6.14 for the domain harmonics. Strong positive correlations occur and both variables are approximately equal to one another. Therefore the PD in the structural response can be approximated to the PD between the direct and indirect force found in Section 6.3.4. The average PDs of the force and therefore the corresponding resonance responses for the 1st and 2nd harmonics which are less than or equal to 6Hz, as well as the 3rd harmonic of 1Hz are +10.58 and -8.03 excluding outliers. The PDs at the 3rd harmonic are unsuitably large, with the exception of bobbing at 1Hz. It appears that the frequency of the harmonic affects the success of the force measurement.

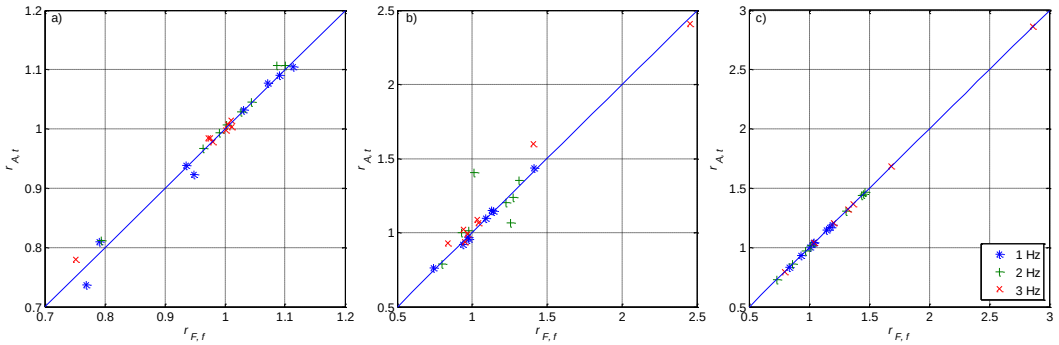

Figure 6.14 The structural response ratio in the t-domain against the peak force ratio in the f-domain, for resonance due to the a) 1st b) 2nd and c) 3rd harmonic component of the force.

6.4 Conclusion

It is possible to measure the bobbing force indirectly using the B6 marker, placed at the top of the back. If an underestimation is unacceptable the F7 marker could be used to measure the force, although greater errors in the response are likely. These findings are consistent with the jumping experiments detailed in Chapter 5. However, a larger error in the force is present when measuring bobbing. Greater PDs occur between the indirect and direct force at the harmonics when bobbing, especially at the high frequency harmonics. This is because bobbing

is a more complex activity and therefore more difficult to quantify using measurements from one point of the body only.

Smaller and more consistent PDs are seen when TSs chose to bounce rather than jounce, indicating that one marker monitoring is better suited for bouncing. In addition there is better correspondence between the actual bobbing frequency and the target frequency.

The response ratio in the t-domain was shown to be approximately equivalent to the peak force ratio in the f-domain, and therefore the PDs from the force can be used to estimate the equivalent PDs in the response.

Although bobbing can take place at a higher frequency the force and frequency components from bobbing are smaller than for jumping. The effect of the harmonics of bobbing on the structural response is smaller than from the corresponding jumping harmonics (Figure 6.10). Hence the large PDs between the direct and indirect bobbing forces at high harmonics are not critical. Jumping is the more severe activity likely to adversely affect structures and will be studied further within later experiments investigating synchronisation.

7 Group and Individual Synchronisation using a Range of External Stimuli

7.1 Introduction

It is not uncommon when groups of people assemble at events such as concerts, sports matches and club nights for their actions to become synchronised. The presence of a beat from a source such as music often acts to further coordinate and encourage movement at a specific frequency. Visual and tactile stimuli can also encourage the crowd to move in a specific rhythm. Varying the beat frequency and stimulus can affect the synchronisation of the individuals with each other and the beat, as discussed in Chapter 2.4. Due to differences in rhythmic ability and enthusiasm, it is unlikely an entire crowd would be able to regulate their activity to coordinate perfectly with one another. Identifying the levels of coordination with the beat and with one another, in response to different stimuli, beat frequencies and group sizes is important for economic yet safe structural design.

Within this chapter individual and group synchronisation with a beat is investigated with the use of two audial stimuli and one visual stimulus. The effects of the frequency of the stimuli, group size and position within the group will be considered. As seen in Chapters 5 and 6 jumping is deemed the most severe activity and therefore will be the focus of this study. The use of a single marker on the $C7^{th}$ vertebrae to calculate the ground reaction force (GRF) whilst jumping is presented in Chapters 5 and applied to groups of two, four and eight test subjects (TS) jumping.

The response of single degree of freedom (SDOF) systems to GRFs from different group sizes, stimulus and target frequency are examined and compared to responses from periodic signals. In addition the structural responses from the experimental forces which are measured on rigid

ground, are compared to the responses from a flexible bridge. Charts are presented detailing the levels of resonance response likely for each stimulus and group size.

7.2 Background

Previous authors have found that jumping in a group can increase an individual's synchronisation with a beat. Better beat synchronisation was observed from individuals jumping in a pair compared to those jumping alone (Sim, 2006; Ebrahimpour and Fitts, 1996). However, this crowd effect is limited by group size (Kasperski and Niemann, 1993; Ellis and Ji). From experiments in a stadium, good coordination whilst jumping was achieved within groups of up to 20 individuals (Kasperski and Niemann, 1993). For groups larger than 20 a linear decrease in coordination was observed. Other authors have noted a reduction and large scatter in the dynamic load factors (DLF) with increased group size (Ellis and Ji, 2002). The extent of the group coordination varies depending on the age of the group and the enthusiasm levels (Kasperski and Niemann, 1993), and on the frequency and song choice (Littler, 2003).

There is conflicting information regarding the frequency range groups can coordinate their actions across. The BS 6399 (BSI, 1996) recommends a frequency range of 1.5-2.8Hz for large groups, as they consider high frequency coordination unlikely within groups. An alternative suggestion is a reduced range of 1.8-2.3Hz (Ginty et al., 2001), however, good individual synchronisation with a beat has been noted at 3Hz (Sim et al., 2008). Furthermore, crowd synchronisation has been noted in stadia and dance floor environments up to frequencies of 3.11Hz (Littler, 2003).

There is also disagreement on the effect of different types of stimuli on synchronisation. Individual jumping experiments where the stimulus was varied between a visual and audio metronome saw worse beat synchronisation when using the visual metronome (Parkhouse and Ewins, 2006). Jumping at 1.5Hz was an exception where better synchronisation occurred using the visual metronome. From these experiments it was concluded that the effects of

visual stimuli were minimal. Therefore, increased synchronisation due to individuals within a crowd observing one another was considered unlikely. Other experiments used audio, visual and tactile cues on pairs jumping (Noormohammadi et al., 2011). It was found that although better individual synchronisation with the beat occurred when using an audio signal, the synchronisation within the pairs was better when using the visual cue. It is possible that group synchronisation is dominant over individual synchronisation with a beat. It should be noted that at times the variability between pairs was large. From group experiments it has been suggested that visual cues and the presence of other individuals were a more effective stimuli for short term synchronisation than audio cues (Comer et al., 2007). From further experiments with pairs jumping it was found that the best group synchronisation occurred when the individuals were facing one another, holding hands and using an audio metronome (Racic et al., 2013). The variability of results from different authors, the limited number of test groups and the limited group sizes, highlights the need for a larger study of group stimuli experiments.

Most group experiments have focused on a small number of individuals (Sim, 2006; Ebrahimpour and Fitts, 1996). The synchronisation results from small groups have been extrapolated to predict the synchronisation levels for larger groups (Ginty et al., 2001). However, as seen from experiments, the degree of synchronisation varies with group size. Other experiments have measured the structural response from larger groups and back calculated the DLFs, however, the quantification of the group synchronisation is often neglected (Kasperski and Niemann, 1993; Ellis and Ji, 2002). Other authors have overlapped individual time histories to recreate a group and then calculated the synchronisation between the members (Parkhouse and Ewins, 2006; Kasperski and Agu, 2005). This method neglects the increased synchronisation as a result of the group interaction. There is a real lack of group synchronisation experiments. This lack, coupled with the varying information regarding group size, frequency range and effect of stimuli from different authors, demonstrates a clear need for more group synchronisation experiments that consider these factors.

7.3 Experimental Procedure

The purpose of these experiments is to investigate the effect of group size, stimulus, and target frequency on the synchronisation of individuals and groups. Previous synchronisation experiments have either studied medium sized groups (15TSs) and maintained a constant external stimuli (Comer et al., 2007), or varied the external stimuli but limited group size to two individuals (Racic et al., 2013). Unlike the previous experiments the external stimuli and the group size were varied to include up to 8TSs. The GRF from each TS will be measured simultaneously allowing the synchronisation to be quantified directly. Three different group sizes will be investigated, as well as six target frequencies and three different stimuli.

The synchronisation experiments took place inside the Gait lab at the University of Warwick. In total 60 TSs, 43 male and 17 female, were involved in the experiments. The TSs' ages ranged between 18 and 42, the average was 23. Most TSs were undergraduate or postgraduate students, and therefore representative of a young adult concert or sports event audience.

All TSs were deemed fit and able to partake in the experiments through the use of a physical activity readiness questionnaire (Appendix A). The TSs were encouraged to warm up prior to the trials and stretch between trials and at the end. Scheduled opportunities to rest were given every six trials. However the subjects were made aware that they could have a break at any time, and if necessary leave the experiment. The experiments were approved by the Biomedical & Scientific Research Ethics Committee at the University of Warwick on the 24th September 2012. A risk assessment was completed and TS consent forms collected from each TS prior to the experiments, the risk assessment and consent form are available in Appendix A.

The main focus of the experiments was the effect of group size and external stimuli on individual and group synchronisation. Group sizes of 2, 4 and 8 TSs were investigated. There were 25 different groups in total, 11 groups of 2TSs, 10 groups of 4TSs, and 4 groups of 8TSs. Each TS was involved in up to three different groups, each of a different size.

The experiments were split into three sessions each with a different external stimulus. Two different types of audial and one visual stimulus were used in the experiments to aid group coordination. The majority of the previous synchronisation experiments utilise an audio metronome, which is solely a beat at a specific frequency. Music however, is a more complex stimulus, involving different sounds and beats and is more common in a crowd environment. Both stimuli were used within these experiments. A comparison of the audial results will indicate whether previous authors are justified in extrapolating experimental results found using a metronome, to music based situations. In addition to the visual stimulus provided by the other group members, a visual metronome comprising of an animated box in simple harmonic motion was used to investigate the importance of visual stimuli on synchronisation.

Reflective markers were placed on the C7th vertebrae (Figure 7.1) and were tracked by 12 infra-red VICON cameras (Oxford Metrics Group, 2007) sampling at a rate of 200Hz (Figure 7.2). Nexus software (Oxford Metrics Group, 2008) was used to process the data (Figure 7.3). The infra-red cameras were arranged to optimise marker capture in the test space, ensuring at least two cameras could track each marker (Figure 7.4). Two digital video cameras and a high speed camera were also used to record the groups.

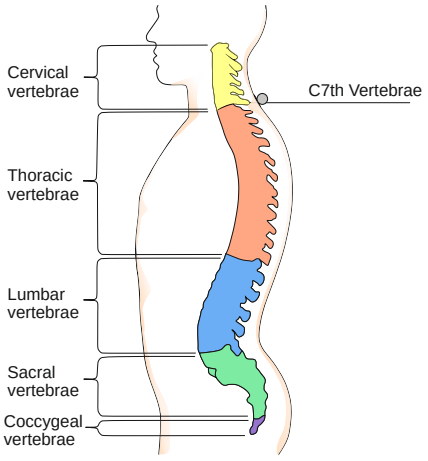

Figure 7.1 The human spine showing vertebrae and the C7th marker placement.

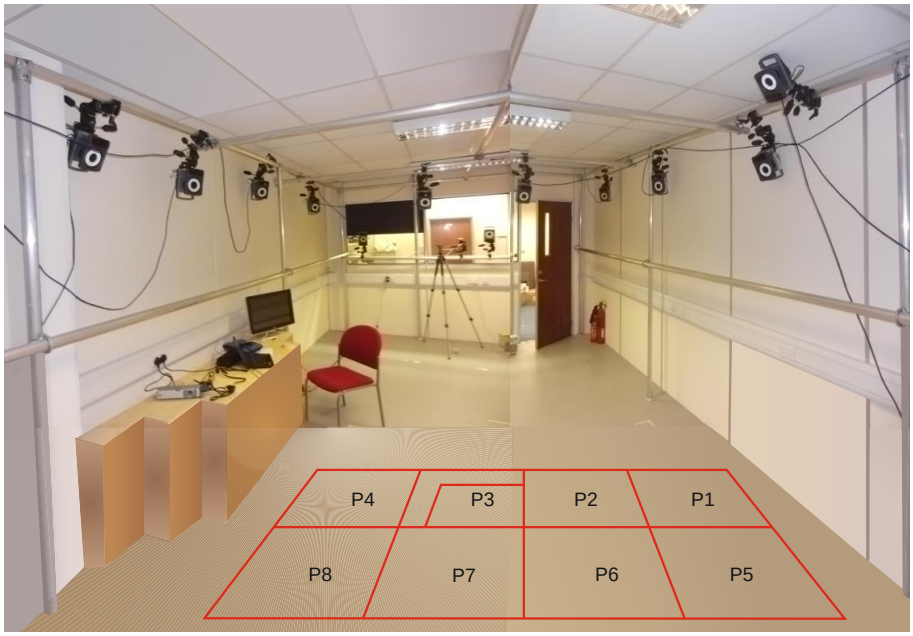

Figure 7.2 The Gait lab experimental setup for the synchronisation experiments.

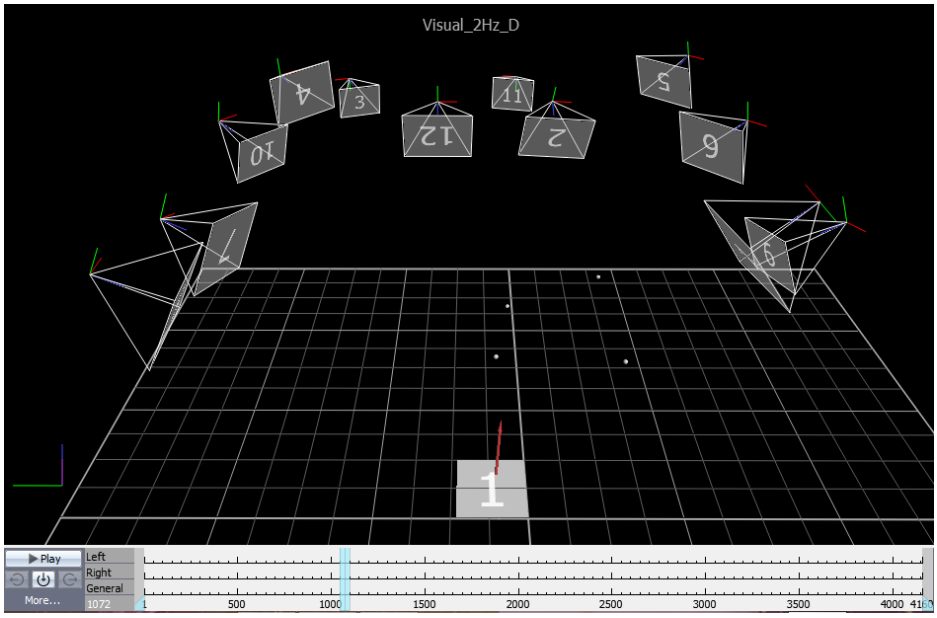

Figure 7.3 Camera layout and force plate and markers from the Nexus software (Oxford Metrics Group, 2008).

A grid was taped in the middle of the gait lab separating the test area into eight 0.60 by 0.70m rectangles. Each TS was allocated a standing area of 0.42 m^2 in accordance to the current UK recommendations of 2-3 people/m^2 (UK Working Group, 2008) and the limited gait lab space. The data processing was made easier as the horizontal displacements of the TSs were restricted, similar to a stadium environment. Furthermore the ownership of each marker was

easier to identify. The TSs layout was arranged according to group size (Figure 7.5). All TSs faced towards the projector screen at the back of the room. Where possible, two rows of TSs were formed to simulate a stadium layout. A further advantage of this layout is the possible comparison of the synchronisation between the TSs in the rows. The TSs in the back row have the additional visual stimulus of the TSs in the front row. An AMTI Biomechanics Force Platform OR6 (AMTI, 2007) with a sampling rate of 1000Hz was placed in position 3 in the TS layout. This was used as a check of the force calculations.

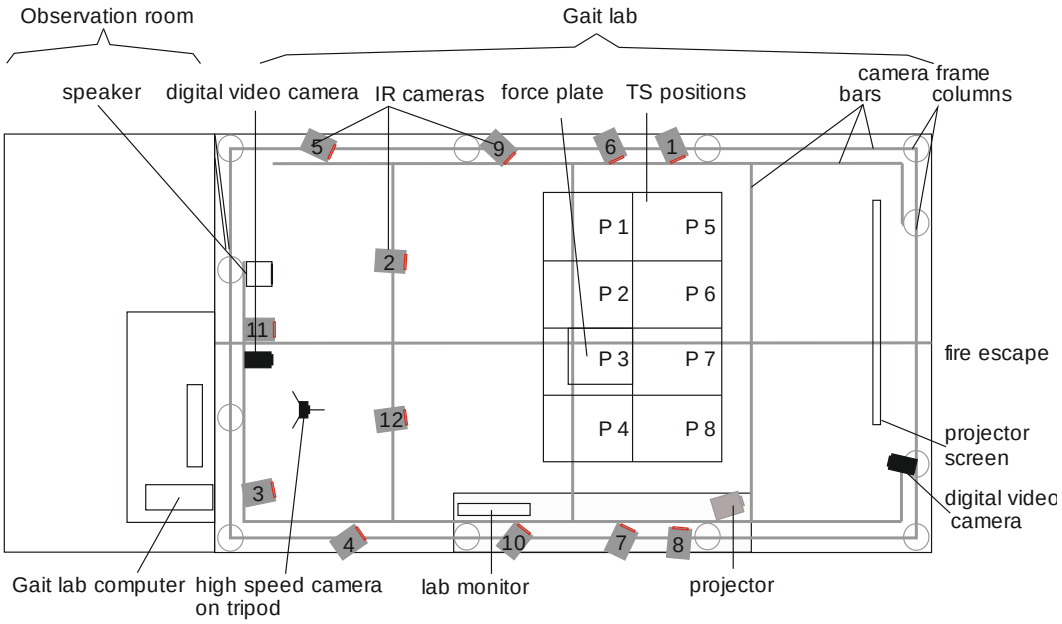

Figure 7.4 Experimental setup of the gait lab and observation room. The camera layout is optimised for group experiments.

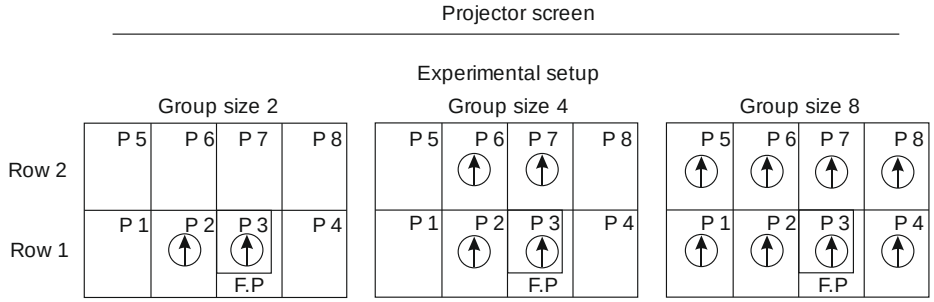

Figure 7.5 TS layout for different group sizes, where P is the position, the arrow dictates the direction the TSs are facing and F.P is the force plate.

The groups of TSs were exposed to stimuli at frequencies of 1.5Hz, 1.75Hz, 2Hz, 2.67Hz, 3Hz and 3.5Hz. These frequencies were chosen to allow a high enough resoultion to effectively

map the effect of frequency on synchronisation in different group sizes. The highest frequency of the quoted synchronisation range has varied between authors. The largest of these values, 3.5 (Littler, 2003) has been used as our maximum frequency. The minimum frequency of 1.5Hz was chosen as Parkhouse and Ewins (2006) observed superior beat synchronisation at this frequency using a visual metronome, compared to an audial metronome. The middle frequency values, 2Hz and 2.67Hz, were chosen as good beat and group synchronisation have been seen at these frequencies (Sim, 2006; Racic et al., 2013).

Once the TSs were assembled in the appropriate layout for the group size the stimulus was played and the TSs asked as a group to jump in time to the beat. An aclimitisation period of 5s was allowed to familise the TSs with the rhythm, 20 seconds of data were then recorded. Three trials were recorded for each frequency, the order of the frequencies was randomised to prevent over familarisation.

The first session of each experiment featured an audial metronome as the stimulus (Figure 7.6a). The stimuli used in the second session were a selection of songs with the same beat as one of the experimental target frequencies (Table 7.1). Two different songs were found to match the beat for each of the target frequencies, to prevent over familiarisation with a specific song. The 1st song was repeated for the 3rd trial. The frequency range of the music stimulus was reduced due to difficulty obtaining songs with a 3.5Hz beat. Due to limited 2.67Hz song avaliablity, songs with a beat frequency of 2.6Hz and 2.65Hz were used. A group of 4TSs jumping to a music stimulus can be seen in (Figure 7.6b).

The final session of the experiments used a visual cue projected onto a screen (Figure 7.6c). A range of on–off style metronomes were experimented with, including flashing colours and a number trigger, however TSs struggled to relate them to a jumping motion. To combat this an animated box in simple harmonic motion (Figure 7.7) was used (Pasman, 2012). The motion of the box was easier to translate into a physical action and was more reminiscent of the real

stimulus likely at group events. To encourage TSs to use the visual metronome rather than the sound of footfall, ear protectors were used to nullify noise (Figure 7.6c).

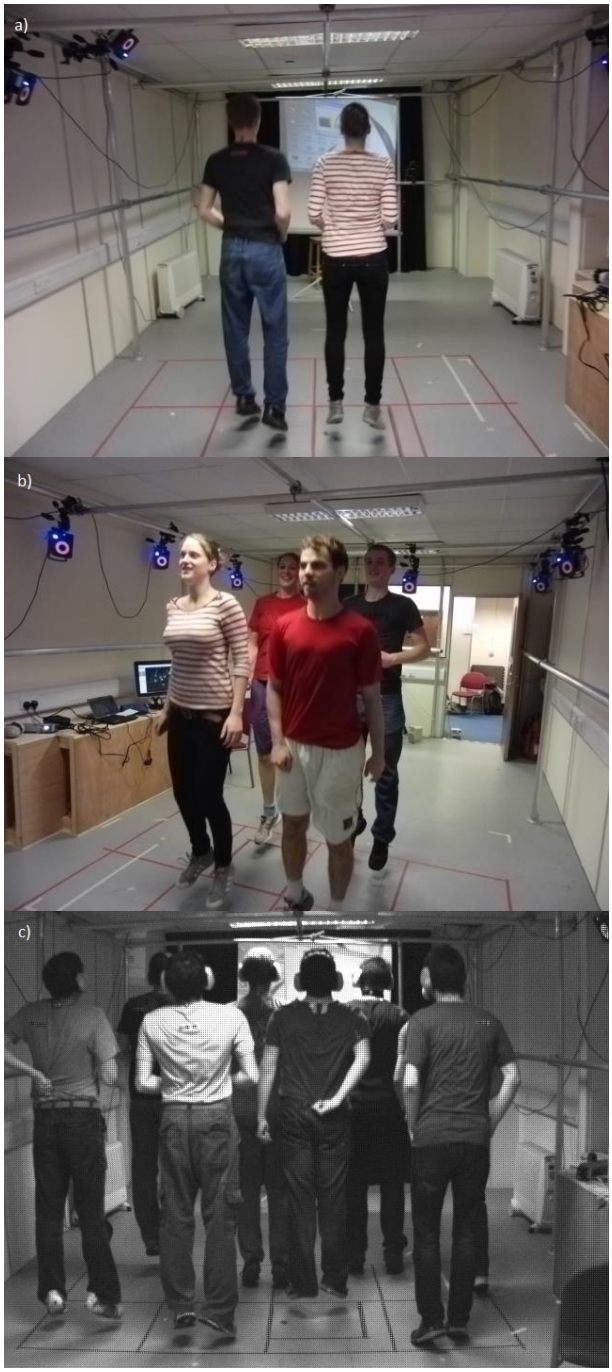

Figure 7.6 a) A group of 2 TSs jumping to an audial metronome beat, b) a group of 4 TSs jumping to music, c) a group of 8 TSs jumping to a visual metronome.

Table 7.1 The music stimulus songs.

Song 1			Song 2		
Frequency (Hz)	**Title**	**Artist**	**Frequency (Hz)**	**Title**	**Artist**
1.5Hz	'I'm Like a Bird'	Nelly Furtado	**1.5Hz**	'Hurt'	Johnny Cash
1.75Hz	'Rolling in the Deep'	Adele	**1.75Hz**	'The Real Slim Shady'	Eminem
2Hz	'Avaliable'	Flo Rida feat Akon	**2Hz**	'Don't Stop Believin'	Journey
2.65Hz	'Hey Ya!'	OutKast	**2.6Hz**	'Don't Stop Me Now'	Queen
3Hz	'Hurts Like Heaven'	Coldplay	**3Hz**	'In Da Club'	50 Cent

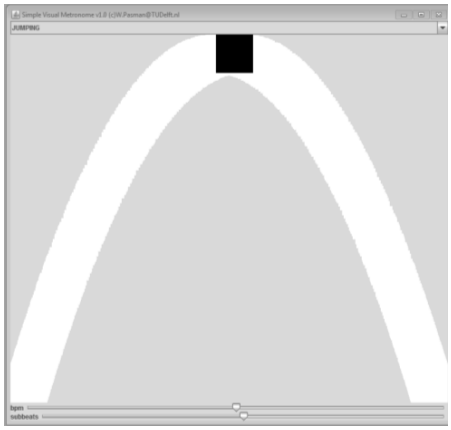

Figure 7.7 The visual metronome, simple harmonic motion of an animated box (Pasman, 2012).

The data was processed using MATLAB R2012b (MathWorks, 2012) in acccordance to the procedure outlined in Chapter 5. The marker trajectories were filtered using a fifth order Butterworth filter where the cut-off frequency of the filter was either 4.5 times the frequency of the target force or 7Hz, whichever was the larger. Examination of the first four harmonics was possible, however as stated in Chapter 5 the one marker method should in general only be used for force calculations up to the 2nd harmonic. The GRF force was calculated as detailed in Chapter 5.

All the forces and summed group forces from the trials were cut to complete cycles, starting and returning to zero, to avoid spectral leakage. In consequence some trials were shorter than 20s. However all trials were zero padded before and after the signal to a total duration of 100s, increasing the resolution of the frequency spectrum from 0.05 to 0.01Hz.

In total 1,275 trials of different sized groups were recorded and 4,794 individual GRFs. This is possibly the most extensive database of individual and group GRFs in response to different stimuli and group sizes.

7.4 Individual Synchronisation

This section focuses on how group size and stimuli affect individual synchronisation. Individual synchronisation can be broken down into two areas, synchronisation with the target beat and individual self-synchronisation. Synchronisation with the beat is a reflection on how well each individual matches the target frequency dictated by the stimulus. Self-synchronisation considers how consistent an individual is within their own action irrespective of the target frequency. An individual may jump consistently at a frequency other than the target frequency, displaying high self-synchronisation and low intra subject variability (IASV), but poor beat synchronisation.

7.4.1 Synchronisation Calculation Methodology

To measure both types of synchronisation a previous methodology for calculating synchronisation factor (Parkhouse and Ewins, 2006) was adapted. For both factors the power spectral density *p* (PSD) of the force time histories were calculated:

$$\boldsymbol{p = \frac{1}{2}\frac{a^2}{\Delta f}} \qquad 7.1$$

where *a* is the amplitude of the force component at each frequency which occupies a bandwidth *Δf.* The PSDs were split into the harmonics of interest using a bandwidth filter.

The beat synchronisation factor was defined as the ratio of the power of the force component coordinated with the beat, and the total power of the signal within each harmonic section (Figure 7.8). The total power was calculated as the area under the PSD. The beat component corresponds to the area of the PSD (which has resolution *Δf*=0.01Hz) at the activity frequency. The self-synchronisation factor was defined as the ratio of the area of the largest frequency

component within a harmonic section over the total power of that harmonic (Figure 7.8). A synchronisation factor of one equates to perfect beat, or self-synchronisation.

When calculating the beat synchronisation the bandwidth filter was centred around the target frequency, or twice the target frequency for the 2nd harmonic. To ensure the actual harmonics of the signal were targeted when calculating the self-synchronisation factor and the DLF values, a flexible bandwidth filter midpoint was instigated. The dominant frequency of the signal was found by identifying the maximum peak in the PSD. This was attributed to either the 1st or 2nd harmonic by determining if the frequency was greater than the target frequency*1.5 (2nd harmonic dominance) or less than the target frequency*1.5 (1st harmonic dominance). This allowed for the possibility of 2nd harmonic dominance which is common at lower jumping frequencies. The frequency of the dominant harmonic (or half the dominant frequency for 2nd harmonic dominance), multiplied by the harmonic number was used as the midpoint for the bandwidth filter.

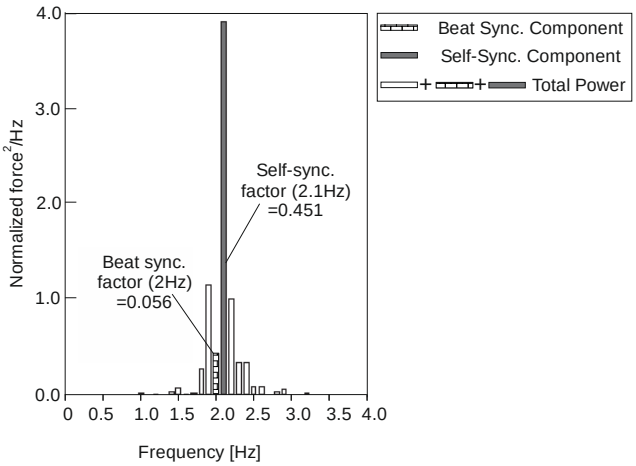

Figure 7.8 The calculation of the beat and self-synchronisation factor.

All the frequency components contributing to each harmonic should be included in the bandwidth filters. However, non-relevant frequency components such as background noise, or frequency components belonging to another harmonic should be excluded. A target frequency dependant bandwidth was proposed as frequency spread is more common at higher

frequencies than mid-range frequencies (Section 4.2.1). This frequency spread will propagate further at the higher harmonics.

The sensitivity of both synchronisation factors and the harmonic DLFs to the frequency range was tested to ensure a bandwidth of adequate but not excessive size was used. Average values of the synchronisation factors and DLFs are shown in Figure 7.9 for a sample of TSs when different frequency bandwidths (% target frequency) were applied. It is worth noting that the total bandwidth is twice the size of the frequency band as it is applied to both sides of the midpoint. A bandwidth filter of ±30% of the target frequency was chosen as stable values of synchronisation factors and DLFs were seen in this range.

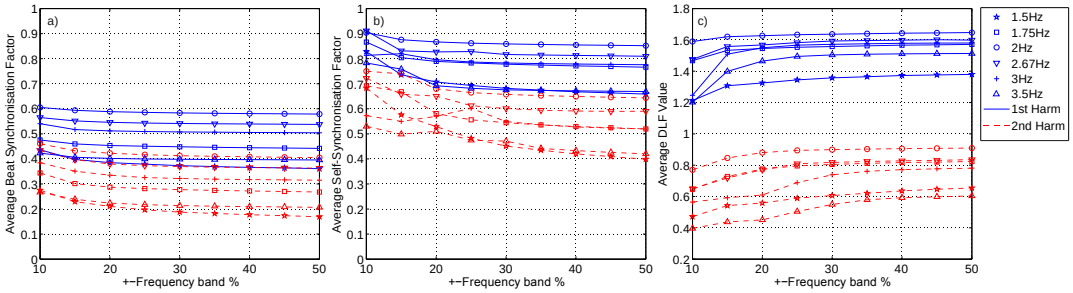

Figure 7.9 The average values of a) beat synchronisation factor, b) self synchronisation factor and c) DLF for different frequency bands centered around the flexible harmonic midpoint frequency as a percentage of the target frequency.

From observations of PSD plots a ±30% band is narrow enough to avoid the inclusion of irrelevant frequency components. However, it was noted that as a smaller range of values are included at the lower jumping frequencies, some relevant frequency components were excluded from these spectra. A lower limit on the bandwidth range was proposed. From observations of the bandwidths at which the synchronisation factors and DLFs stabilised at other jumping frequencies (Figure 7.10), and PSD plots of 1.5Hz and 1.75Hz, a minimum range of ±0.6Hz was suggested. An example time history and frequency spectra relating to the first two harmonics and filtered as detailed above is shown in Figure 7.11 a and b.

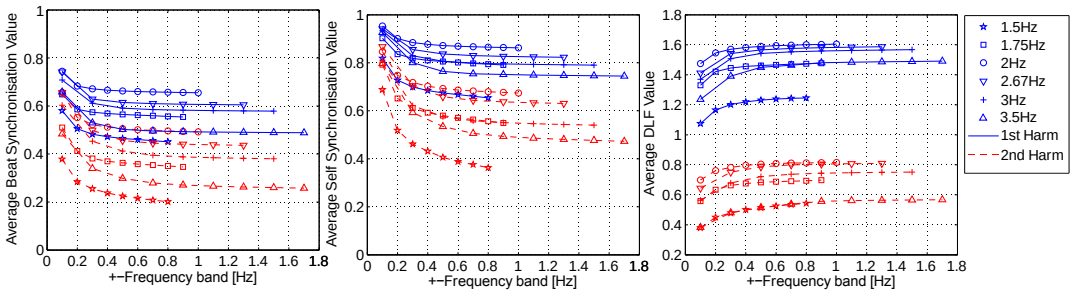

Figure 7.10 The average values of a) beat synchronisation factor, b) self synchronisation factor and c) DLF for different frequency bands (Hz) centered around the flexible harmonic midpoint frequency.

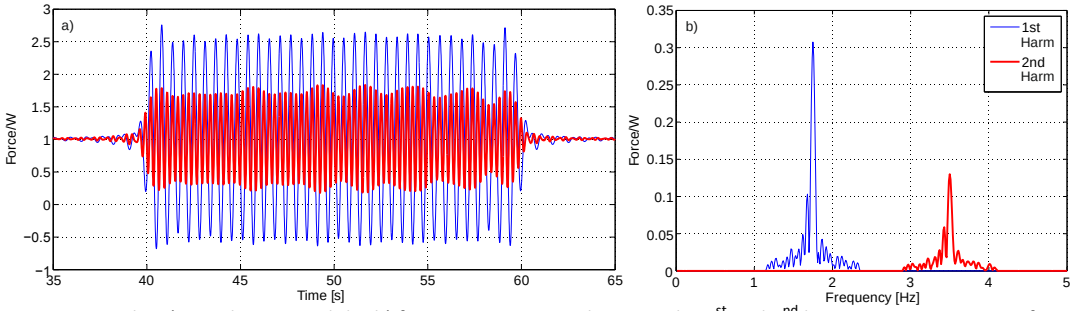

Figure 7.11 The a) time history and the b) frequency spectra relating to the 1st and 2nd harmonic components of an individual TS jumping at 1.75Hz. Some of the zero padding can be seen in figure a) and the 0.6*2 bandwidth filter is demonstrated in figure b).

To ensure the stability of the PSD spectrum, the variation of self-synchronisation factors were investigated with regard to the number of cycles within the signal. Previous work has suggested that a minimum of 30 cycles are required for spectrum stability (Parkhouse and Ewins, 2006). However regardless of the number of cycles, oscillation of the synchronisation factors was observed if the resolution of the frequency spectrum was not adequately high to pick up the peak values. To counteract this, the signals were zero padded to 100 seconds to improve the resolution of the frequency spectrum (Figure 7.11a). The inclusion of additional zeroes reduced the overall power of the signal. In addition the increased resolution reduced the area of the synchronised component in relation to the total area of the spectrum. A zero padding factor equal to the total signal length/original signal length was applied to all synchronisation values, this counteracted the reduced power and synchronisation factor due to the zero padding. Having applied the appropriate zero padding factor the stability of the synchronisation factor could be assessed (Figure 7.12). The 3Hz metronome trials were used

because of the large number of cycles. The trials were sampled in increments of six cycles between 6 to 54. The self-synchronisation factor of 67.4% of trials stabilised at or before 30 cycles and 84.0% of the trial stabilised by 40 cycles. Within this experiment the minimum cycle number is 30 for the 1.5Hz trials. A sample of 300 trials using a 1.5Hz metronome beat were tested for sensitivity between 3 and 27 cycles in increments of 3 cycles (Figure 7.13). 83.3% of trials stabilise before 27 cycles. The majority of the self-synchronisation values are stable and the high number of force time histories should reduce the significance of any anomalies in the data. From this investigation it was confirmed that approximately 30 cycles are required for synchronisation factor stability, and, in addition the duration of the signal has to be adequately long to include the frequency peaks. Zero padding with the inclusion of a zero padding factor is an appropriate method to extend the signal without influencing the original signal. It is recommended that trials are zero padded to 100s, however there is little variability in the synchronisation factor over 50s (Figure 7.14). This confirms that stability is reached within the majority of trials for all the frequencies investigated in this body of work.

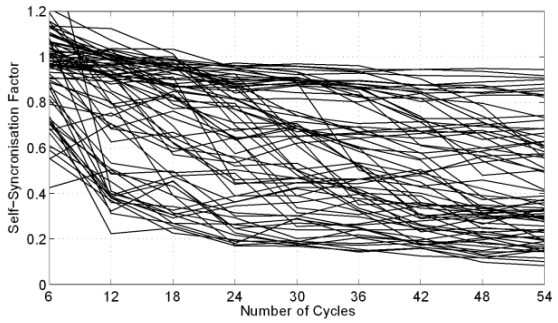

Figure 7.12 The variation in self-synchronisation factor with number of cycles for a sample of TSs jumping at 3Hz.

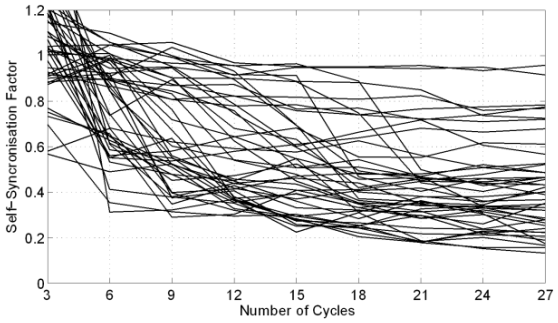

Figure 7.13 The variation in self-synchronisation factor with number of cycles for a sample of TSs jumping at 1.5Hz.

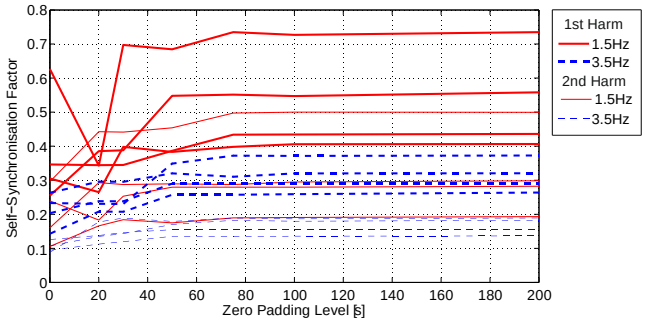

Figure 7.14 The sensitivity of self-synchronisation factor to the length of the trials, where zero padding was used, this example demonstrates a sample of 1.5Hz and 3.5Hz trials.

7.4.2 Individual Synchronisation Results

The beat and self-synchronisation factors were calculated for each individual within each group and separated into stimulus, group size and frequency. To ensure the synchronisation factors were representative, the values for each individual were averaged across the three trials for each frequency and stimuli.

7.4.2.1 Individual Beat Synchronisation Factors

The beat synchronisation factors were tested for normality using a 5% Anderson-Darling test (AD test). Considering the 1st harmonic of all jumping frequencies and stimuli, only 5.9% passed the AD test, 27.5% passed at the 2nd harmonic. The results considering the stimuli separately are shown in Table 7.2.

Table 7.2 AD test pass rate for beat synchronisation factors.

AD Test pass rate	Metronome	Music	Visual	All
1st Harmonic	5.6%	0.0%	11.1%	5.9%
2nd Harmonic	0.0%	46.7%	38.9%	27.5%
All Harmonic	2.8%	23.3%	25%	16.7%

The skewness and kurtosis of the beat synchronisation factors were calculated and compared to twice the standard error of skewness (SES) and twice the standard error of kurtosis (SEK) respectively in Table 7.3. Values less than 2*SES and 2*SEK are consistent with a normal distribution. The results were inconsistent for both skewness and kurtosis. Considering these and the AD test results it is unlikely that the beat synchronisation factors are consistently

normally distributed, hence the 95th percentiles will be used to quantify data spread. The mean (filled markers) and the 95th percentiles (hollow markers) of the synchronisation factors are plotted for each stimulus, group size and frequency in Figure 7.15, Figure 7.16 and Figure 7.17.

Table 7.3 Skewness and kurtosis values for beat synchronisation below 2*SES and 2*SEK respectively.

Skew pass rate	Metronome	Music	Visual	All
1st Harmonic	61.1%	33.3%	33.3%	43.1%
2nd Harmonic	72.2%	60.0%	72.2%	68.6%
All Harmonic	66.7%	46.7%	52.8%	55.9%
Kurtosis pass rate				
1st Harmonic	66.7%	60.0%	61.1%	62.7%
2nd Harmonic	83.3%	86.7%	77.8%	82.4%
All Harmonic	75.0%	73.3%%	69.4%	72.5%

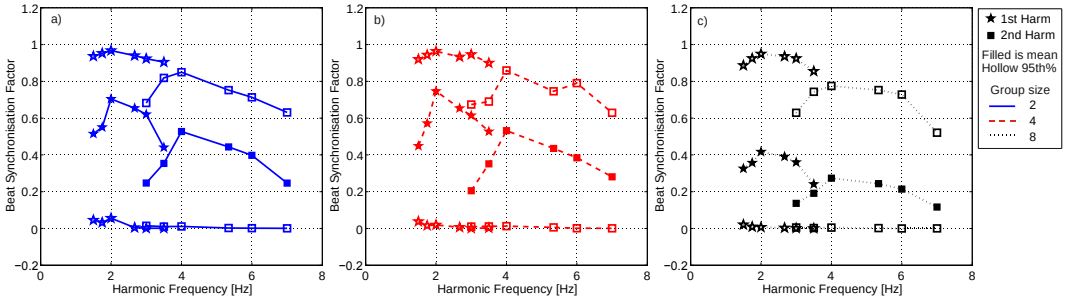

Figure 7.15 Mean and 95th percentiles of metronome beat synchronisation factors for group sizes of a) 2, b) 4 and c) 8.

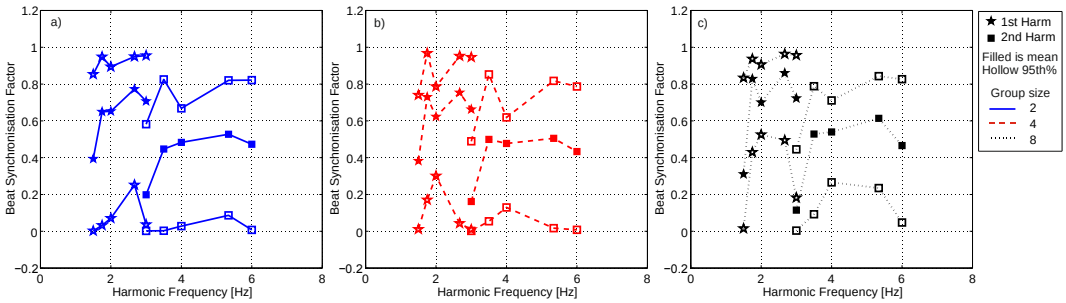

Figure 7.16 Mean and 95th percentiles of music beat synchronisation factors for group sizes of a) 2, b) 4 and c) 8.

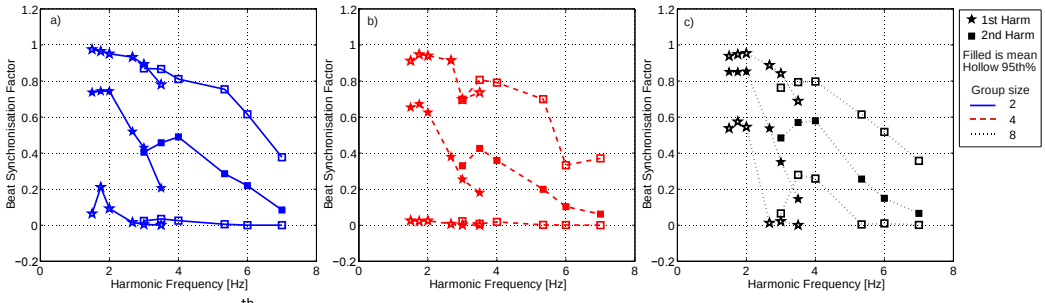

Figure 7.17 Mean and 95th percentiles of visual beat synchronisation factors for group sizes of a) 2, b) 4 and c) 8.

Mean values of beat synchronisation between 0.2 and 0.8 are seen for the 1st harmonic of most jumping frequencies. The largest values are highlighted for each stimulus, group size, frequency and harmonic in Table 7.4. The greatest average beat synchronisation factors are seen for groups of 8TSs jumping at 2.67Hz to music (0.86) and jumping between 1.5-2Hz using a visual stimulus (0.85).

Table 7.4 Mean individual beat synchronisation factors.

Stimulus	**Metronome**						**Music**						**Visual**					
Group Size	**2**		**4**		**8**		**2**		**4**		**8**		**2**		**4**		**8**	
Harmonic	**1st**	**2nd**	**1st**	**2nd**	**1st**	**2nd**	**1st**	**2nd**	**1st**	**2nd**	**1st**	**2nd**	**1st**	**2nd**	**1st**	**2nd**	**1st**	**2nd**
1.5Hz	0.52	0.25	0.45	0.21	0.33	0.14	0.39	0.20	0.38	0.16	0.31	0.11	0.74	0.41	0.65	0.33	0.85	0.48
1.75Hz	0.55	0.35	0.57	0.35	0.36	0.19	0.65	0.45	0.73	0.50	0.83	0.53	0.74	0.46	0.67	0.43	0.85	0.57
2Hz	0.70	0.53	0.75	0.53	0.42	0.27	0.65	0.48	0.62	0.48	0.70	0.54	0.74	0.49	0.63	0.36	0.85	0.58
2.67Hz	0.65	0.44	0.65	0.44	0.39	0.24	0.77	0.53	0.75	0.51	0.86	0.61	0.52	0.29	0.38	0.20	0.54	0.26
3Hz	0.62	0.40	0.61	0.38	0.36	0.21	0.71	0.47	0.66	0.43	0.72	0.47	0.43	0.22	0.25	0.10	0.35	0.15
3.5Hz	0.44	0.25	0.53	0.28	0.24	0.12							0.21	0.08	0.18	0.06	0.15	0.07

The lowest beat synchronisation factors were expected at 3.5Hz consistent with the poor synchronisation found by previous authors (Sim et al., 2005; Parkhouse and Ewins, 2004). This was the case when using a visual metronome. However, the beat synchronisation factors at 3.5Hz, when using an audial metronome were not significantly different from the factors at other frequencies. Individual beat synchronisation should be considered possible at all the frequencies studied here.

The 95th percentile boundaries show the potential range of beat synchronisation factors. Beat synchronisation factors as high as 0.98 are possible at the 1st harmonic, indicating near perfect beat synchronisation. In addition near-zero values are possible at all harmonics, stimuli and group sizes. This is an indicator of the large scatter in the beat synchronisation from individual jumpers.

The mean beat synchronisation factors for all group sizes are plotted in Figure 7.18 a, b and c for each stimuli. The peak values of mean beat synchronisation are similar for the different stimuli for groups of 2 and 4 TSs. The beat synchronisation increased slightly when using either

the visual or music stimuli in a group of 8TSs. Excluding the metronome stimulus, the presence of a group encouraged synchronisation, as previously seen (Comer et al., 2007). The peak mean beat synchronisation factors increase from a value of 0.63 to 0.85 for 2Hz jumping with a visual stimulus, and from 0.75 to 0.86 at 2.67Hz using music (Table 7.4).

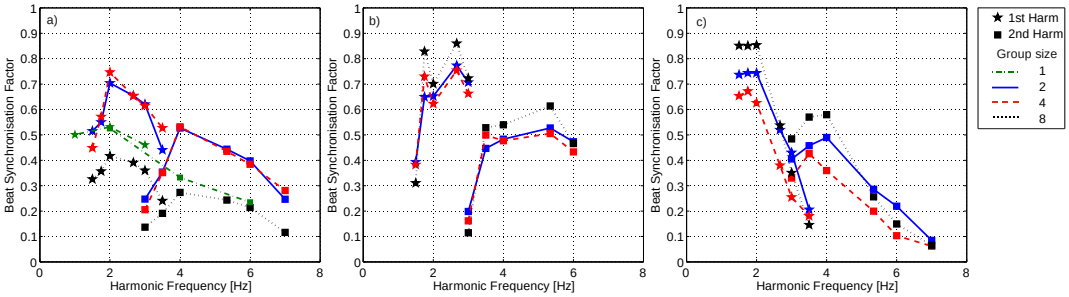

Figure 7.18 Mean values of beat synchronisation factors for all group sizes for a) metronome, b) music and c) visual stimuli.

For groups of 8TSs the metronome beat synchronisation factors are significantly smaller than those seen using the visual or music cues. The levels of synchronisation for different excitation frequencies gathered from previous metronome stimulus experiments (Sim et al., 2005; Parkhouse and Ewins, 2004), are not directly transferrable to other more varied stimuli.

The beat synchronisation factors were also calculated for the eight individual TSs (1TS) who jumped to a metronome in Chapter 5. This enabled a comparison of the beat synchronisation between individuals within a group, and individuals jumping alone for a metronome stimulus (Figure 7.18a). The values of beat synchronisation from 1TS were in general smaller than those from TSs in groups of 2 and 4. The beat synchronisation factors from 1TS were greater than those seen in groups of 8TSs. However, the 8TSs factors from the metronome were smaller than those from other stimuli, the 1TS values are generally smaller than the 8TSs values for music and visual stimuli.

Three TSs who participated in the individual experiments, also took part in an experiment of every group size. Their beat synchronisation factors were averaged and plotted against group size for 2 and 3Hz in Figure 7.19. The beat synchronisation factors increased in groups for both

investigated harmonics and frequencies. Between 1 and 8TSs the average increase in beat synchronisation at the first harmonic was 0.35. This is an average increase in beat synchronisation of 82.0%. As only a metronome was used within the 1TS experiments conclusions about other stimuli cannot be drawn, however inclusion within a group clearly affects beat synchronisation. Individual GRFs combined to make a group force (Parkhouse and Ewins, 2006) are unlikely to be equivalent to the GRFs from a corresponding real life crowd.

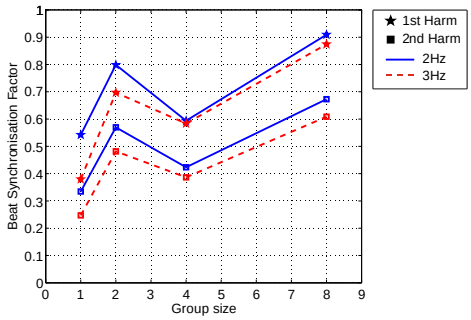

Figure 7.19 The average beat synchronisation factors from 3 TSs who took part in experiments of all group sizes.

From observing Figure 7.18 it is apparent that each stimulus favours beat synchronisation at different jumping frequencies. The largest beat synchronisation factors are seen at the middle frequencies (2-3Hz) when using a metronome (Table 7.4). Jumping at frequencies of 1.75, 2.67 and 3Hz produce the highest beat synchronisation when using music as a cue. Lower values occur at 2Hz than at the adjacent frequencies indicating that TSs struggled to maintain the specific beat at this frequency. In addition, poor beat synchronisation is seen at 1.5Hz.

Beat synchronisation using a visual cue is best at low frequencies between 1.5-2Hz (Table 7.4). The ability of the TSs to match the lower beat frequencies indicates that visual cues are significant. However, at higher frequencies the TSs are unable to follow the beat as the visual metronome moves too fast for the individuals to interpret the visual stimulus into movement.

7.4.2.2 Individual Self-Synchronisation Factors

Beat synchronisation factors are only concerned with the synchronisation at the target frequency. Self-synchronisation factors take into account other frequencies, and therefore are a better indicator of maximum individual synchronisation.

The self-synchronisation factors were processed as above, and their distribution tested for normality using a 5% AD test, and the skewness and kurtosis of the data. The AD test pass rates (Table 7.5) were higher than those for beat synchronisation, however the values in general indicate a non-normal distribution at the 1st harmonic.

Table 7.5 AD test pass rate for self-synchronisation factors.

	Metronome	Music	Visual	All
1st Harmonic	16.7%	13.3%	50.0%	27.5%
2nd Harmonic	83.3%	73.3%	55.6%	70.6%
All Harmonic	50.0%	43.3%	52.8%	49.0%

The majority of the kurtosis values were less than 2*SEK, the skewness results however were more varied (Table 7.6). Considering these factors it is unlikely that the self-synchronisation factors are consistently normally distributed, and therefore the 95th percentiles will be used as an indicator of spread.

Table 7.6 Skewness and kurtosis values for self-synchronisation below 2*SES and 2*SEK respectively.

Skew pass rate	Metronome	Music	Visual	All
1st Harmonic	44.4%	26.7%	55.6%	43.1%
2nd Harmonic	88.9%	86.7%	83.35	86.3%
All Harmonic	66.7%	56.7%	69.4%	64.7%
Kurtosis pass rate				
1st Harmonic	66.7%	73.3%	77.8%	72.5%
2nd Harmonic	100.0%	86.7%	94.4%	94.1%
All Harmonic	83.3%	80%	86.1%	83.3%

The mean self-synchronisation factors (filled markers) and 95th percentiles (hollow markers) are plotted for stimulus, group size, frequency and harmonic in Figure 7.20, Figure 7.21 and Figure 7.22. The self-synchronisation factors reflect the largest frequency component within the specified area of the PSD spectrum and are therefore higher (or equal to) the beat synchronisation factors. Mean self-synchronisation factors between 0.6 and 0.9 are seen for

the 1st harmonic for most jumping frequencies. The largest values are highlighted for each stimulus, group size, frequency and harmonic in Table 7.7. The greatest average self-synchronisation factors are seen for groups of 8TSs jumping at 1.75Hz to music (0.90) and to a visual stimulus (0.89).

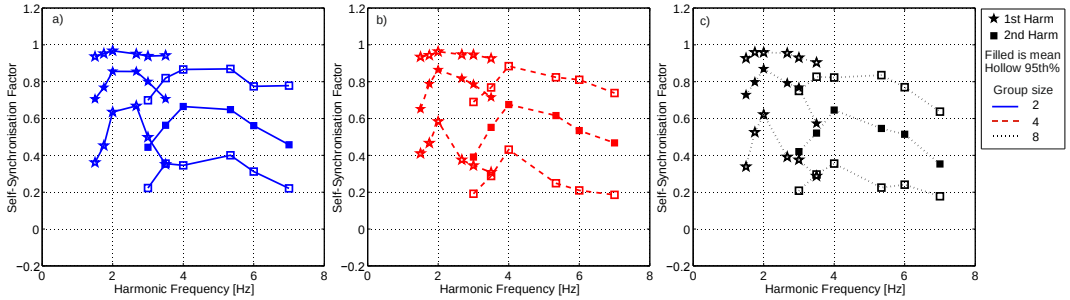

Figure 7.20 Mean and 95th percentiles of metronome self-synchronisation factors for group sizes of a) 2, b) 4 and c) 8.

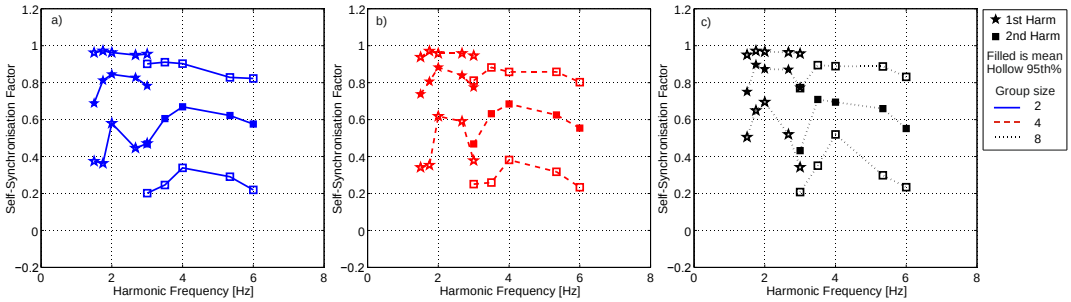

Figure 7.21 Mean and 95th percentiles of music self-synchronisation factors for group sizes of a) 2, b) 4 and c) 8.

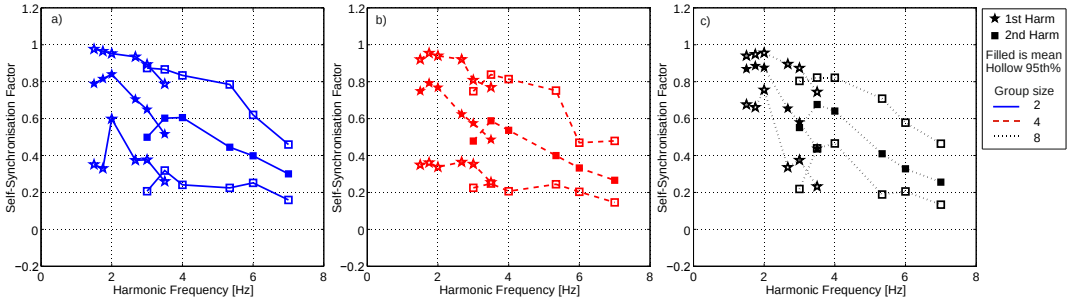

Figure 7.22 Mean and 95th percentiles of visual self-synchronisation factors for group sizes of a) 2, b) 4 and c) 8.

The lowest self-synchronisation factors occur when using a visual stimulus to jump at 3.5Hz. However, the equivalent 3.5Hz self-synchronisation factors when using a metronome are not significantly lower than the synchronisation factors at other frequencies, except in groups of 8TSs. It is thought that self-synchronisation is possible over all the frequencies examined here.

These experiments support previous recommendation to raise the frequency range of comfortable jumping to 3.5Hz (Littler, 2003).

Table 7.7 Mean individual self-synchronisation factors.

Stimulus	Metronome						Music						Visual					
Group Size	2		4		8		2		4		8		2		4		8	
Harmonic	1st	2nd	1st	2nd	1st	2nd	1st	2nd	1st	2nd	1st	2nd	1st	2nd	1st	2nd	1st	2nd
1.5Hz	0.71	0.44	0.65	0.39	0.73	0.42	0.69	0.47	0.74	0.47	0.75	0.43	0.79	0.50	0.75	0.48	0.87	0.55
1.75Hz	0.77	0.56	0.79	0.55	0.80	0.52	0.81	0.61	0.81	0.63	0.90	0.71	0.82	0.60	0.79	0.59	0.89	0.68
2Hz	0.86	0.67	0.86	0.68	0.87	0.65	0.85	0.67	0.88	0.68	0.87	0.69	0.84	0.61	0.77	0.54	0.88	0.64
2.67Hz	0.86	0.65	0.82	0.62	0.79	0.55	0.83	0.62	0.84	0.62	0.87	0.66	0.70	0.45	0.62	0.40	0.65	0.41
3Hz	0.80	0.56	0.79	0.53	0.77	0.51	0.78	0.58	0.78	0.55	0.77	0.55	0.65	0.40	0.58	0.33	0.58	0.33
3.5Hz	0.71	0.46	0.72	0.47	0.57	0.35							0.52	0.30	0.49	0.27	0.44	0.26

The 95th percentile boundaries show the range of self-synchronisation factors and is smaller than the equivalent beat synchronisation range. Synchronisation values as high as 0.98 are possible at the 1st harmonic, indicating near perfect self-synchronisation. The lower 95th percentile values are higher than those from beat synchronisation, and do not approach zero.

The self-synchronisation for each stimulus improves slightly within groups of 8TSs (Figure 7.23) consistent with previous findings (Comer et al., 2007). However, the difference in self-synchronisation is not as significant as the increased beat-synchronisation factors for visual and music cues in larger groups. An exception is jumping at 3.5Hz to a metronome where self-synchronisation is reduced in groups of 8TSs. The high speed stimulus is difficult to jump to, and it is likely that each individual tries to accommodate the metronome beat and the movement of other group members confusing the jumping pattern and increasing the IASV.

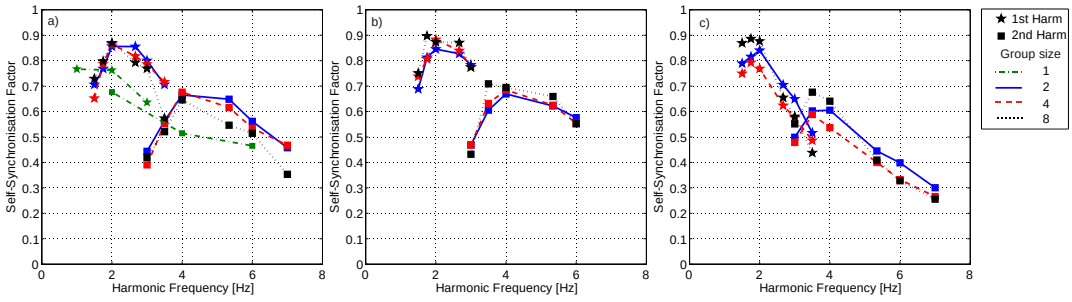

Figure 7.23 Mean values of self-synchronisation factors for all group sizes for a) metronome, b) music and c) visual stimuli.

The self-synchronisation factors calculated from the individuals jumping alone detailed in Chapter 5 are also presented in Figure 7.23. The self-synchronisation factors from the 1TS are considerably lower than those within a group.

The self-synchronisation values were averaged over the three TSs which participated in all group sizes throughout the experimental program (Figure 7.24). The self-synchronisation factors increased in groups but not as significantly as for the beat synchronisation (Figure 7.19). Inclusion within a group improves an individual's self-synchronisation reducing the IASV of the period.

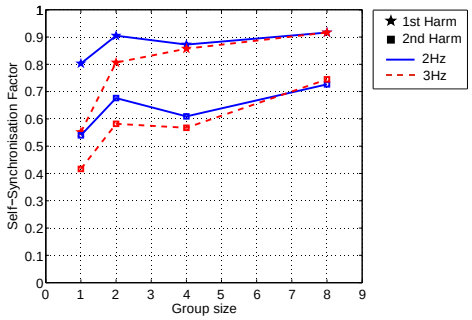

Figure 7.24 The average beat synchronisation factors from 3 TSs who took part in experiments of all group sizes.

The audial and visual cues aid self-synchronisation at different frequencies. Consistent with beat synchronisation, good visual self-synchronisation occurs at low jumping frequencies (1.5-2Hz). Both audial cues produce the highest self-synchronisation factors at target frequencies of 2-2.67Hz. This highlights that individual synchronisation frequency ranges should take into consideration the type of stimulus involved.

The self (hollow markers) and beat (filled markers) synchronisation factors are compared in Figure 7.25. When using a metronome as the stimulus the average self-synchronisation factors are consistently higher than the beat synchronisation factors at all harmonics (Figure 7.25a). This indicates that individuals struggled to translate the sound signals into a matching jumping action and are using the other group members to set their jumping frequency. The largest difference between the factors occurs when jumping in a group of 8TSs. The self-

synchronisation is high whereas the beat synchronisation is low, this suggests that the group effect is more significant to individual synchronisation than the metronome cue. This was postulated in Section 7.2 based on previous findings (Noormohammadi et al., 2011).

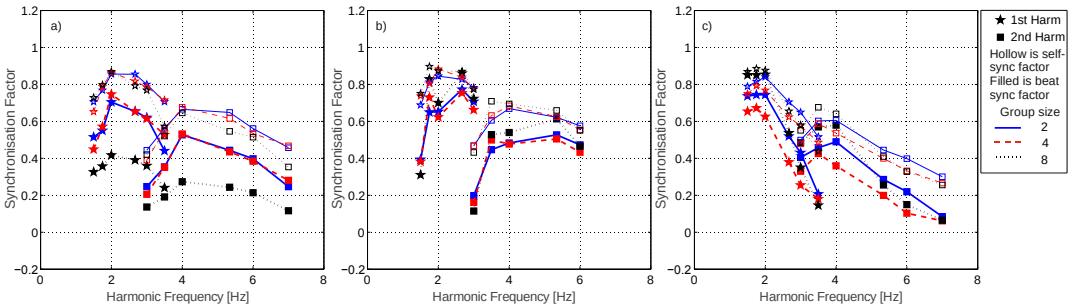

Figure 7.25 Comparision of mean self-synchronisation and beat synchronisation factors for all group sizes stimuli for a) metronome, b) music and c) visual stimuli.

The differences between the types of synchronisation are less consistent when using a music stimulus. At 1.5Hz and 2Hz there are significant differences between the two factors, here TSs struggled to achieve the target frequencies, but jumped consistently and had low IASV values. Both synchronisation factors from the groups of 8TSs are similar to one another, unlike the metronome stimulus. This suggests that TSs are using both the music cue and the other group members to stay in time to the beat.

Between 1.5 and 2Hz the visual beat and self-synchronisation factors are very similar to one another. The difference between the two types of synchronisations is smallest within groups of 8TSs, here the presence of the group aids self-synchronisation without distracting the TSs from the target frequency. The difference between the factors increase at frequencies greater than or equal to 2.67Hz. The TSs are able to use the visual metronome to match the beat at the lower frequency, however at higher frequencies, they are unable to interpret the movement fast enough to translate it to the equivalent body motion.

7.5 Group Synchronisation

Both the self and beat synchronisation of the whole group are quantified in this section using the PSD method described in Section 7.4. The group beat synchronisation factor reflects how well the group as a whole achieves the target frequency. The group self-synchronisation factor quantifies how synchronised the members of the group are with one another. The force time histories from each individual within the group are summed together to create a group time history. The group time history is then processed according to the procedure outlined in Section 7.4. The group beat and self-synchronisation factors are calculated for each harmonic. The factors are averaged across the three trials recorded for each stimulus and frequency. The mean group synchronisation factors are then found for each group size, stimulus, frequency and harmonic.

7.5.1 Group Beat Synchronisation Factors

The group beat synchronisation factors are discussed first and are shown in Figure 7.26. Mean values of group beat synchronisation between 0.2 and 1 are seen for the 1st harmonic for all jumping frequencies. The largest values are highlighted for each group size, stimulus, frequency and harmonic in Table 7.8. The greatest average group beat synchronisation factors are seen for groups of 8TSs jumping at 2.67Hz to music (0.96) and jumping between 1.5-2Hz for visual stimulus (0.93-0.94). Values as high as 0.98 were seen for some groups of 8TSs jumping to music at 2.67Hz.

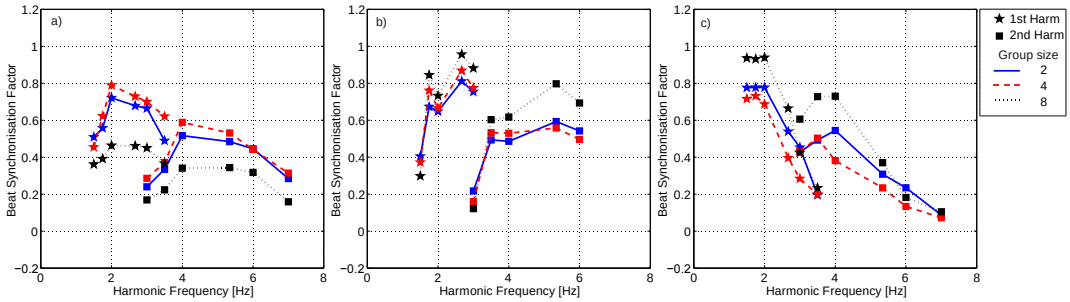

Figure 7.26 Mean values of group beat synchronisation factors for all group sizes for a) metronome, b) music and c) visual stimuli.

The beat synchronisation at different frequencies is dependent on the stimulus. The lowest 1st harmonic group beat synchronisation factors occur when using a visual stimulus to jump at 3.5Hz. However, the values of beat synchronisation at 3.5Hz when using a metronome are not significantly different from those at low frequencies. Poor group beat synchronisation is also seen when using a music stimulus at 1.5Hz. The lowest and highest synchronisation factors are consistent with the individual beat synchronisation factors. It is thought that group beat synchronisation is possible to some degree over all the frequencies examined here.

Table 7.8 Mean group beat synchronisation factors.

Stimuli	**Metronome**						**Music**						**Visual**					
Group Size	**2**		**4**		**8**		**2**		**4**		**8**		**2**		**4**		**8**	
Harmonic	**1st**	**2nd**	**1st**	**2nd**	**1st**	**2nd**	**1st**	**2nd**	**1st**	**2nd**	**1st**	**2nd**	**1st**	**2nd**	**1st**	**2nd**	**1st**	**2nd**
1.5Hz	0.51	0.24	0.45	0.29	0.36	0.17	0.40	0.22	0.37	0.16	0.30	0.12	0.78	0.43	0.72	0.43	0.94	0.61
1.75Hz	0.56	0.33	0.62	0.37	0.39	0.22	0.67	0.49	0.76	0.53	0.84	0.60	0.78	0.49	0.73	0.50	0.93	0.73
2Hz	0.72	0.52	0.79	0.59	0.46	0.34	0.65	0.49	0.67	0.53	0.73	0.62	0.78	0.54	0.69	0.38	0.94	0.73
2.67Hz	0.68	0.48	0.73	0.53	0.46	0.34	0.81	0.59	0.87	0.56	0.96	0.80	0.54	0.31	0.40	0.23	0.66	0.37
3Hz	0.66	0.45	0.70	0.44	0.45	0.32	0.75	0.54	0.77	0.50	0.88	0.69	0.45	0.23	0.28	0.13	0.42	0.18
3.5Hz	0.49	0.28	0.62	0.31	0.37	0.16							0.20	0.09	0.20	0.07	0.23	0.10

Similar beat synchronisation factors are seen for groups of 2 and 4 TSs, for all stimuli. The factors from the audial stimuli (metronome and music), from groups of 4TSs are slightly larger than those from groups of 2TSs. Most significantly the beat synchronisation factors are larger for groups of 8TSs when using a music or visual cue (Figure 7.26 b, c). This phenomenon also occurs at the 2nd harmonic and is consistent with observations from individual beat synchronisation factors. In certain situations group size can increase group beat synchronisation. As this effect is opposite to what occurs when using a metronome stimulus (Figure 7.26a), extrapolation of metronome data to larger groups with diverse stimuli is not justifiable as it may lead to underestimations of a crowd's capacity for beat synchronisation. A consequence of this is an underestimation of the crowd loading and the potential for resonance.

7.5.2 Group Self-Synchronisation Factors

The group self-synchronisation factors are based on the largest PSD frequency component of each harmonic range. They are therefore greater or equal to the group beat synchronisation factors. The mean group self-synchronisation factors are plotted in Figure 7.27.

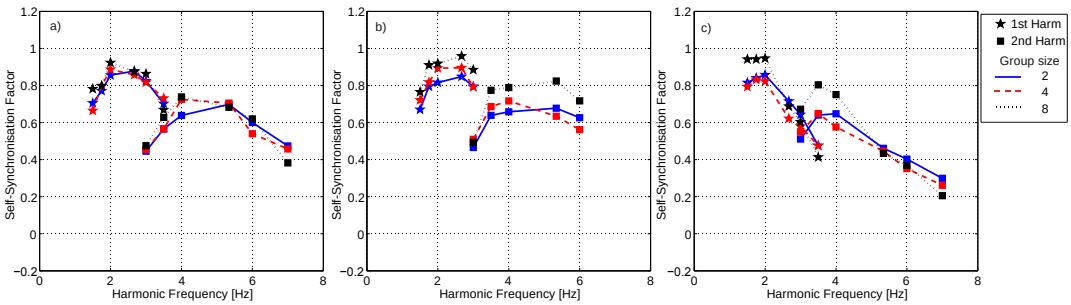

Figure 7.27 Mean values of group self-synchronisation factors for all group sizes for a) metronome, b) music and c) visual stimuli.

The mean 1st harmonic group self-synchronisation factors are between 0.4 and 1 for all frequencies. As seen previously synchronisation is easier at certain frequencies with the use of specific stimuli. The maximum mean group self-synchronisation values occur for groups of 8TSs using a music cue at 2.67Hz (0.96, Table 7.9), values as high as 0.98 were found for a group of 8TSs. High factors were also seen between 1.5-2Hz for visual stimulus (0.94-0.95). The lowest group self-synchronisation occurs at 3.5Hz when using a visual stimulus. The group self-synchronisation factors are largest in groups of 8TSs, where the presence of the crowd has improved synchronisation.

Table 7.9 Mean group self-synchronisation factors.

Stimuli	**Metronome**						**Music**						**Visual**					
Group Size	**2**		**4**		**8**		**2**		**4**		**8**		**2**		**4**		**8**	
Harmonic	**1st**	**2nd**	**1st**	**2nd**	**1st**	**2nd**	**1st**	**2nd**	**1st**	**2nd**	**1st**	**2nd**	**1st**	**2nd**	**1st**	**2nd**	**1st**	**2nd**
1.5Hz	0.70	0.45	0.66	0.45	0.78	0.48	0.67	0.47	0.72	0.51	0.77	0.49	0.82	0.51	0.79	0.55	0.94	0.67
1.75Hz	0.77	0.57	0.80	0.57	0.80	0.63	0.79	0.64	0.82	0.69	0.91	0.77	0.84	0.64	0.83	0.65	0.94	0.80
2Hz	0.86	0.64	0.89	0.73	0.92	0.74	0.82	0.66	0.89	0.72	0.92	0.79	0.86	0.65	0.82	0.58	0.95	0.75
2.67Hz	0.88	0.70	0.86	0.70	0.87	0.68	0.85	0.68	0.90	0.63	0.96	0.82	0.72	0.46	0.62	0.45	0.69	0.43
3Hz	0.82	0.60	0.82	0.54	0.86	0.62	0.79	0.63	0.79	0.56	0.88	0.72	0.64	0.40	0.58	0.35	0.60	0.37
3.5Hz	0.70	0.47	0.73	0.46	0.67	0.38							0.48	0.30	0.48	0.26	0.41	0.21

Values of group self-synchronisation above 0.67 are possible for groups of 8TSs at all frequencies examined here and therefore frequencies between 1.5 and 3.5Hz should be considered to have crowd synchronisation potential.

The group self-synchronisation factors give an indication of how well a group of TSs are able to replicate a jumping period relative to each other. A high group self-synchronisation factor is indicative of consistent periods and lower time lags between TSs. The initial period timing for each TS and jump was plotted in Figure 7.28 for a trial with high (0.97) and low (0.47) group self-synchronisation factor for 8TSs jumping at 2Hz to music. Each colour represents the timing of an individual TS. There is very little spread in the initial timing of each jump in Figure 7.28a, whereas in Figure 7.28b there is a wide variation in TS jump timings, as would be expected.

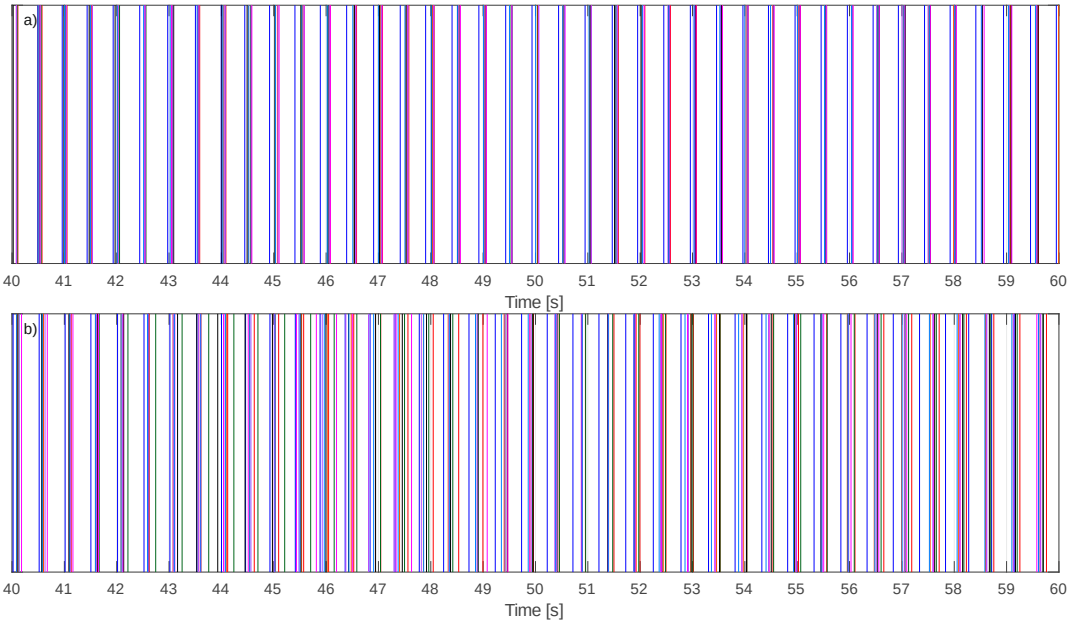

Figure 7.28 The initial time of each period for a) a high group self-synchronisation factor (0.97) and b) a low group self-synchronisation factor (0.47) for a group of 8TSs jumping at 2Hz to music.

The group beat (filled markers) and self (hollow markers) synchronisation factors are compared to one another in Figure 7.29. There is a noticeable difference between the group beat and self-synchronisation factors when using a metronome. Groups of individuals are able to keep time with one another but not at the prescribed metronome frequency. The values of

beat and group self-synchronisation factor are more similar when using music or visual stimuli. The only significant difference between the factors for a music stimulus is at 2Hz where TSs struggled to maintain the target frequency, but were well synchronised with one another. At frequencies above 2Hz the group beat synchronisation factors for the visual stimulus become substantially smaller than the group self-synchronisation factors. Individuals are unable to keep in time to the visual stimulus but maintain some semblance of synchronisation with one another. The difference between the synchronisation factors increases at the 2nd harmonic.

The environment and the stimulus frequency should be examined when deciding the level of crowd synchronisation to design against. Groups of 8TSs were able to achieve mean self-synchronisation factors of 0.96 in certain conditions. This is potentially 0.96*8*dynamic load of one individual. Individuals within groups of up to 8TSs have the potential for near perfect synchronisation with one another.

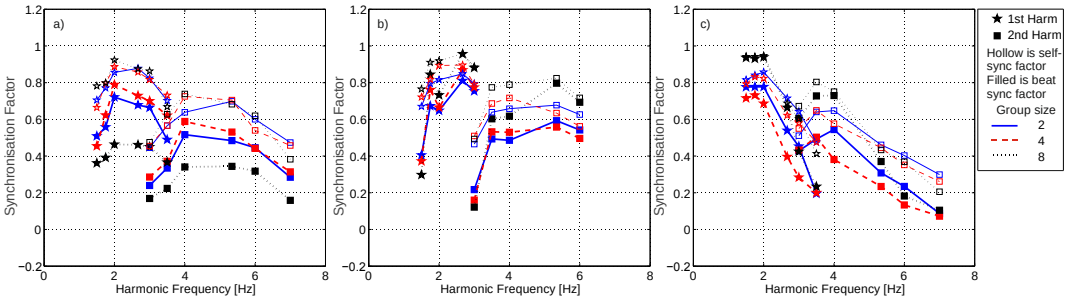

Figure 7.29 Mean values of group beat and group self-synchronisation factors for all group sizes for a) metronome, b) music and c) visual stimuli.

The group self-synchronisation factors demonstrate the crowd's ability to synchronise with one another and therefore should be consulted when considering an action within a given frequency range. However, if a certain jumping frequency is expected and of particular concern, for example to avoid structural resonance, the values of beat synchronisation should be referenced.

7.5.3 Synchronisation Factors of the Rows

As noted the two rows of TSs are subjected to different stimuli. The back row of TSs (row 1) has the advantage of an additional visual stimulus in the form of the movements of the front row (row 2). The two rows can be analysed separately to investigate the effect of row position in groups of 4 and 8 TSs. The row synchronisation factors are processed as outlined above to create row beat synchronisation factors and row self-synchronisation factors (Figure 7.30, Figure 7.31).

From Figure 7.30 there appears to be little difference between the row beat synchronisation factors from row 1 (filled markers) and row 2 (hollow markers). The same observation is true for the row self-synchronisation factors in Figure 7.31. The addition of individuals in front does not necessarily improve the synchronisation of the row behind. Being within a crowd improves synchronisation, however the position of an individual within the crowd appears insignificant.

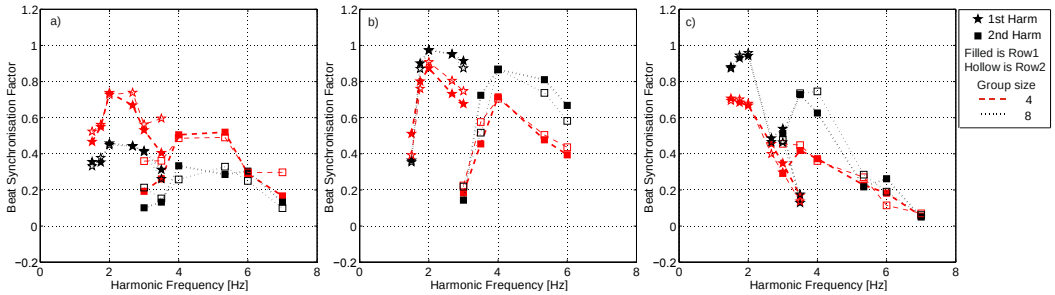

Figure 7.30 Mean values of row 1 and row 2 beat synchronisation factors for groups of 4 and 8 TSs for a) metronome, b) music and c) visual stimuli.

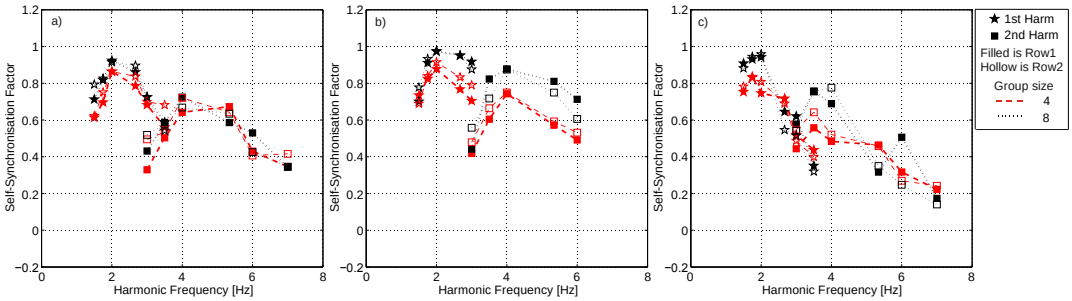

Figure 7.31 Mean values of row 1 and row 2 self-synchronisation factors for groups of 4 and 8 TSs for a) metronome, b) music and c) visual stimuli.

7.6 Structural Response

7.6.1 Response to Experimental Forces

The response of a SDOF system was used to demonstrate the implications of crowd synchronisation on a structure with reference to different crowd sizes and stimuli. To illustrate the effect SDOF structures were simulated in Matlab (MathWorks, 2012) with a modal mass of 35000kg and varying damping ratios ζ of 1%, 2%, 3%. These values with the application of a mass factor m_f are in keeping with those considered in Section 5.4.5 and are typical stadia values. To ensure the simulations reflect the likely structural natural frequencies, the frequency of the SDOF system f_n is varied in steps of 0.05Hz from 0.5Hz to 7Hz, or 2.5*target frequency, whichever is the larger. This ensures the vulnerable frequencies under 6Hz (UK Working Group, 2008) are considered and the response to the first two harmonics of the force is captured. The purpose of these simulations was not to give firm response values but to reflect likely values using a simplified model.

The 20s duration forces from groups of 2, 4 and 8TSs were filtered as described in Section 7.3 and cut to ensure the signal started and ended at zero. The group forces were then applied to single point on the simulated SDOF structures, the maximum response for each structural frequency and damping ratio were recorded, as highlighted by asterisks in Figure 7.32. In some cases due to the combination of several force time histories and the length of the trials the steady state response was not reached, an example of this is Figure 7.32h. The response for 8TSs is less like the conventional resonance response seen in Figure 7.32 d and f for 2 and 4TSs. These trials used the metronome stimulus and therefore the slight spread of frequencies in Figure 7.32g is consistent with the lower synchronisation factors associated with these conditions.

The maximum responses for each SDOF structure were averaged across the three trials, then for each target frequency, stimulus and group size. For ease of viewing the envelope of

maximum mean response including all frequencies, and the maximum 90th and 10th percentile bands are plotted against structural f_n in Figure 7.33, Figure 7.34 and Figure 7.35. Charts of the mean, 90th and 10th percentile bands of the maximum response for each specific target frequency are shown in Appendix B.

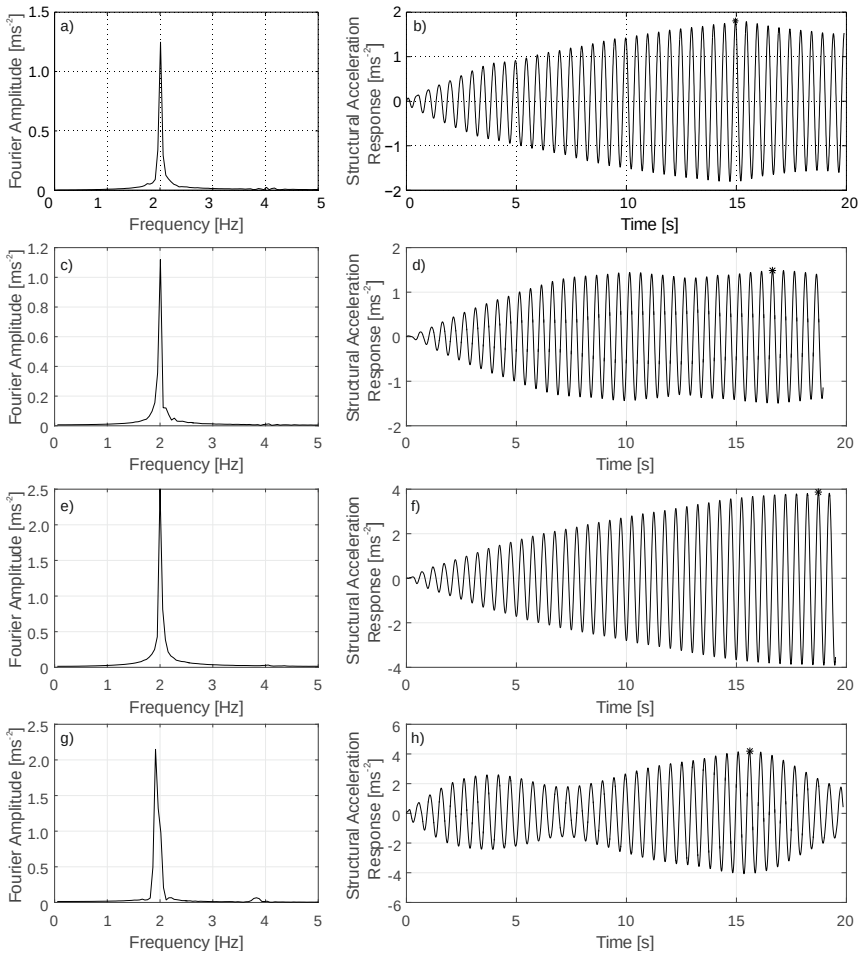

Figure 7.32 The frequency spectra and the time histories of the acceleration structural response for SDOFs with 1% damping and an f_n of 2Hz, subjected to a and b)1TS, c and d) 2TSs, e and f) 4TSs and g and h) 8TSs jumping at 2Hz. The value of maximum response is marked for each time history.

Figure 7.33, Figure 7.34 and Figure 7.35 can be used to predict the response to 1, 2, 4 and 8 TSs jumping on a structure with natural frequency between 0.5 and 7Hz and damping ratio of 1%, 2%, or 3%. The responses can be applied to structures of different modal masses M by multiplying the responses by a factor of 35,000/M.

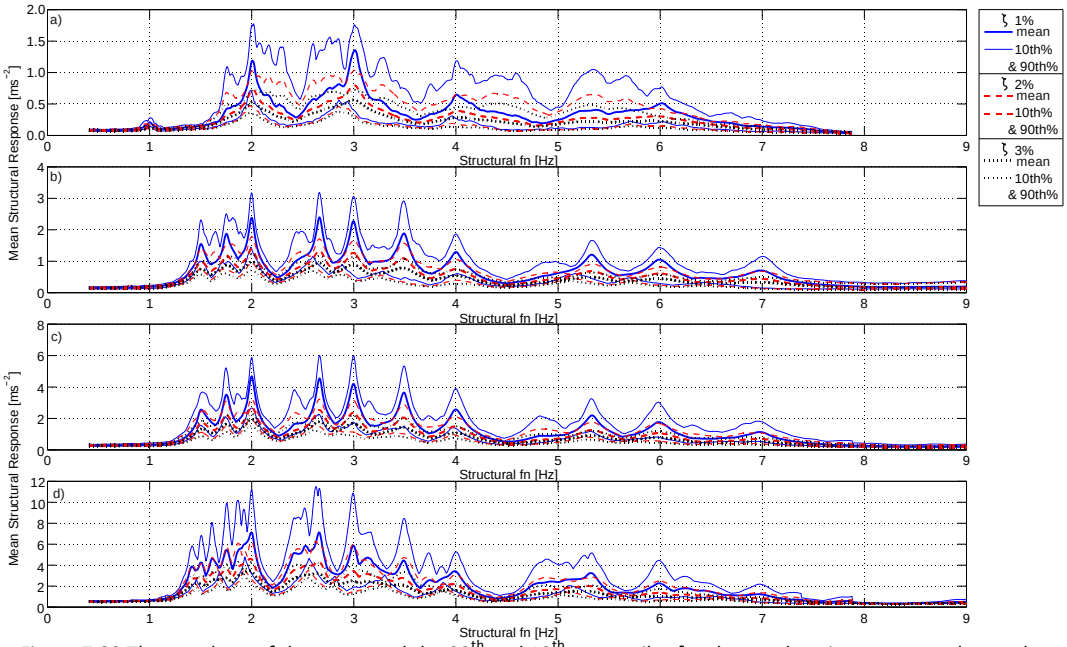

Figure 7.33 The envelope of the mean and the 90th and 10th percentiles for the acceleration response due to the metronome stimulus, considering the largest mean response (or 90th and 10th percentile) value found for all frequencies for each structural frequency and damping ratio. a) 1TS, b) 2TSs, c) 4TSs and d) 8TSs.

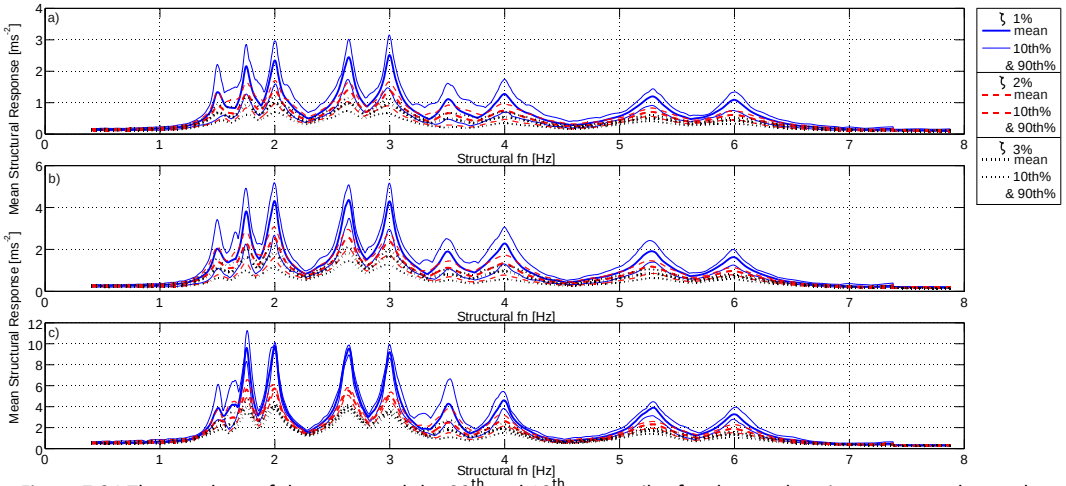

Figure 7.34 The envelope of the mean and the 90th and 10th percentiles for the acceleration response due to the music stimulus, considering the largest mean response (or 90th and 10th percentile) value found for all frequencies for each specific structural frequency and damping ratio. a) 1TS, b) 2TSs, c) 4TSs and d) 8TSs.

The widest spread of response values, where the TSs either varied their jumping frequencies, or different groups and TSs achieved different overall frequencies were seen for groups of 1 and 8TSs for the metronome stimulus. This is consistent with the lowest beat and group beat synchronisation factors for these experimental conditions. The response peaks from the metronome stimulus were wider than for the other stimuli. More pronounced response peaks

were seen in Figure 7.34 for the music stimulus and in Figure 7.35 for visual stimulus, indicating high consistency within and between the groups, causing structural resonance.

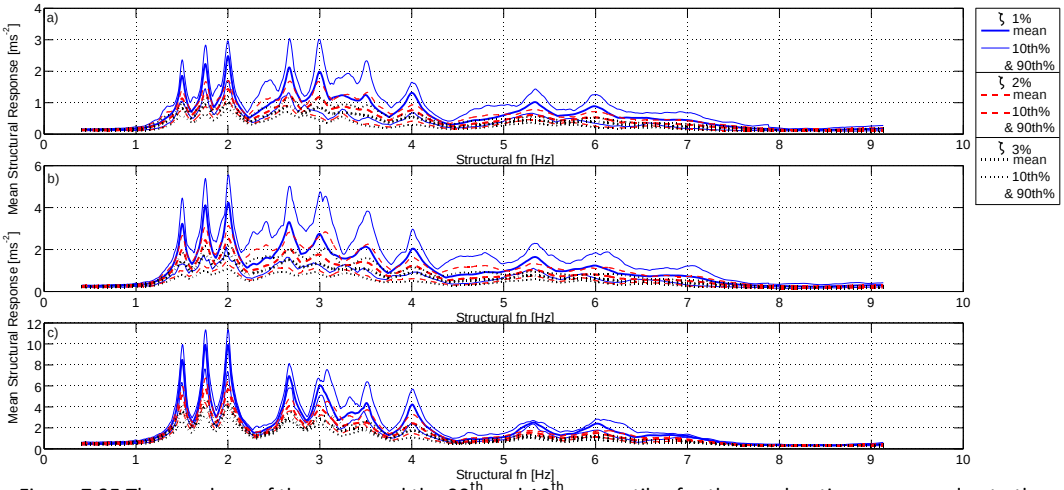

Figure 7.35 The envelope of the mean and the 90th and 10th percentiles for the acceleration response due to the visual stimulus, considering the largest mean response (or 90th and 10th percentile) value found for all frequencies for each specific structural frequency and damping ratio. a) 1TS, b) 2TSs, c) 4TSs and d) 8TSs.

7.6.2 Comparison with the Response to an Equivalent Half-Sine Force

The maximum responses to periodic half-sine forces of each target frequency are plotted in Figure 7.36, Figure 7.37 and Figure 7.38. The magnitude of the force is equal to the average DLF value from the summed force and average group weight (Table 7.10) for each group size, stimulus, frequency and harmonic. In addition the maximum responses when using the 90th percentile of the DLFs values and of the group weight are also plotted.

Comparing Figure 7.33 and Figure 7.36 the structural responses to the mean experimental data and the periodic equivalent for the metronome stimulus for groups of 1, 2 and 4TSs are in agreement for resonance at 2, 2.67Hz and 3Hz. At the other target frequencies and especially at the 2nd harmonic of the forces, the responses from the periodic forces are larger than from the experimental data. In groups of 8TSs the response from the periodic force overestimates the experimental data responses at all frequencies. Occasionally the 90th percentile response from the experimental data is marginally larger than the equivalent periodic response.

The responses to the experimental data and the equivalent periodic force from the music stimulus are shown in Figure 7.34 and Figure 7.37. For all group sizes the two responses are in agreement for resonance at 1.75Hz to 3Hz. At 1.5Hz and the 2nd harmonics the periodic response overestimates the experimental data response.

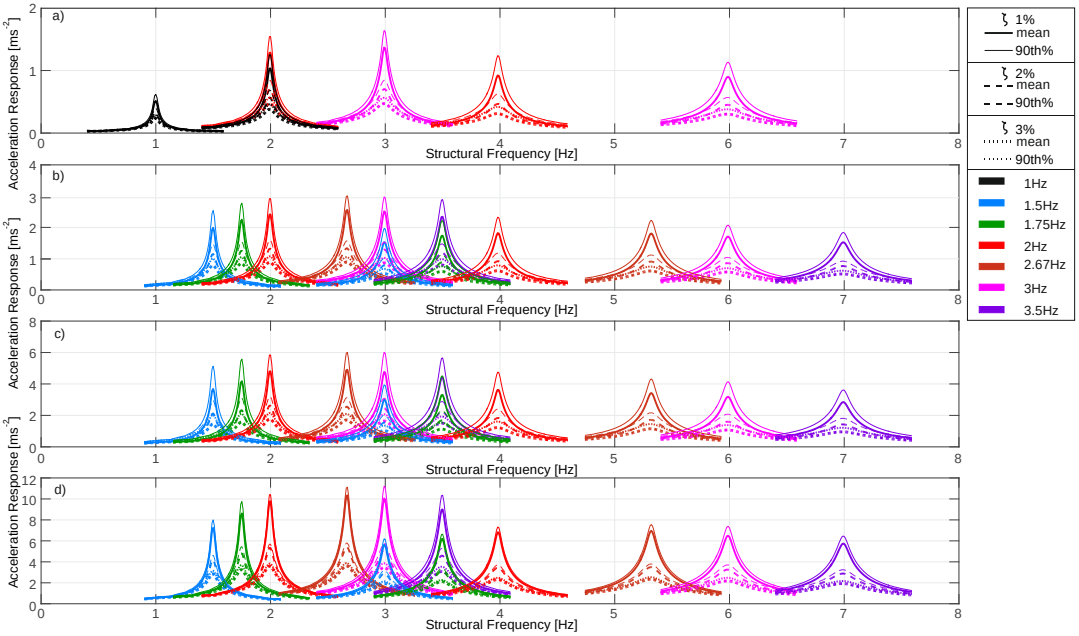

Figure 7.36 The acceleration response to a periodic half-sine force of each target frequency, with magnitude equal to the average DLF value from the metronome stimulus for group sizes of a)1TS, b) 2TSs, c) 4TSs and d)8TSs.

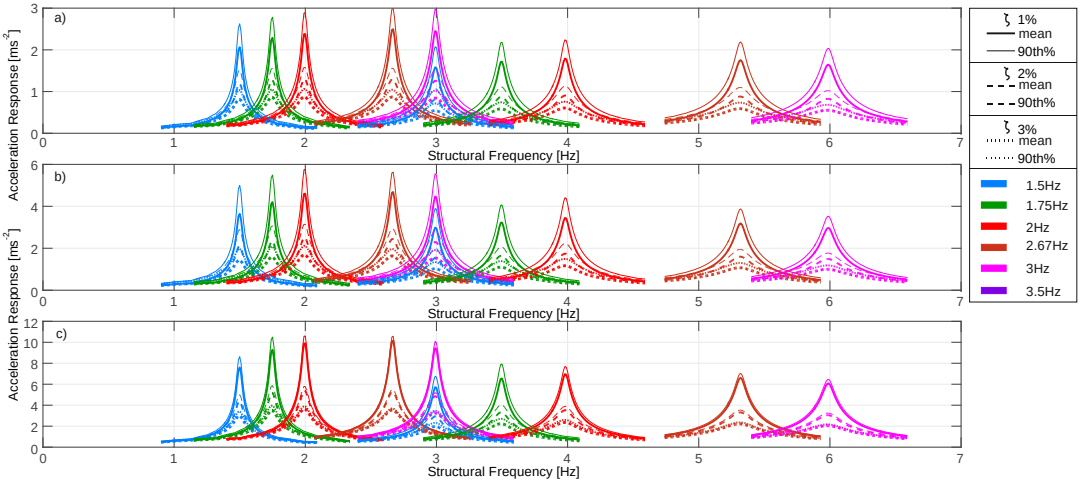

Figure 7.37 The acceleration response to a periodic half-sine force of each target frequency, with magnitude equal to the average DLF value from the music stimulus for group sizes of a)2TS, b) 4TSs, and c) 8TSs.

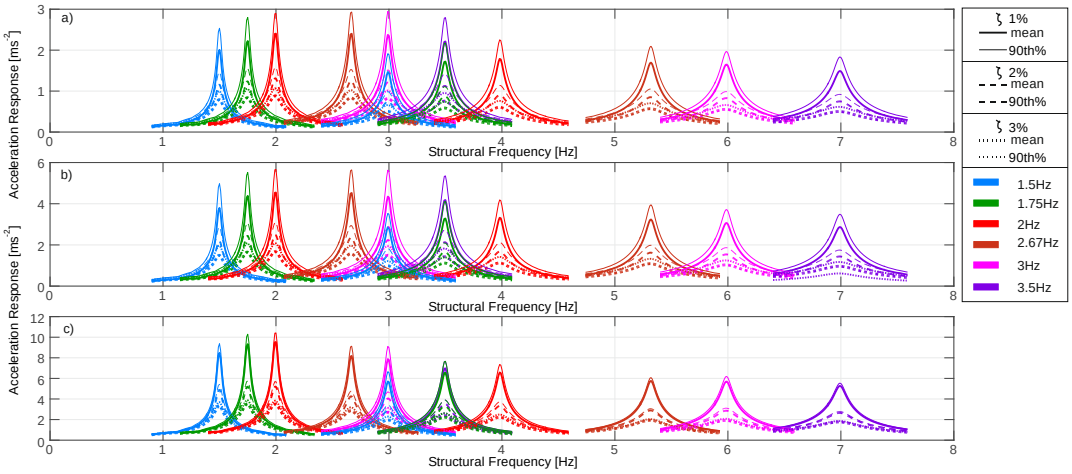

Figure 7.38 The acceleration response to a periodic half-sine force of each target frequency, with magnitude equal to the average DLF value from the visual stimulus for group sizes of a)2TS, b) 4TSs, and c) 8TSs.

Table 7.10 The mean, 10th and 90th percentiles of the TS's weight and the DLF values for each group size and stimulus.

			1st Harmonic DLF							2nd Harmonic DLF						
		W(kg)	1Hz	1.5Hz	1.75Hz	2Hz	2.67Hz	3Hz	3.5Hz	1Hz	1.5Hz	1.75Hz	2Hz	2.67Hz	3Hz	3.5Hz
Metronome																
1TS	Mean	74.13	0.27			1.49		1.47		1.00			0.64		0.59	
	90%	84.40	0.35			1.63		1.60		1.13			0.93		0.75	
2TS	Mean	69.48		1.21	1.38	1.50	1.50	1.42	1.24		0.48	0.66	0.72	0.70	0.61	0.43
	90%	78.55		1.50	1.60	1.67	1.60	1.54	1.44		0.68	0.87	0.95	0.85	0.72	0.53
4TS	Mean	70.99		1.00	1.17	1.43	1.35	1.25	1.07		0.42	0.54	0.68	0.58	0.47	0.31
	90%	79.44		1.49	1.59	1.64	1.57	1.54	1.36		0.66	0.89	0.97	0.78	0.70	0.49
8TS	Mean	73.47		0.90	1.16	1.39	1.39	1.29	1.03		0.29	0.40	0.53	0.55	0.44	0.28
	90%	76.13		1.03	1.36	1.46	1.48	1.47	1.26		0.36	0.45	0.58	0.62	0.58	0.38
Music																
2TS	Mean	69.48		1.29	1.43	1.46	1.44	1.36			0.53	0.64	0.70	0.65	0.55	
	90%	78.55		1.58	1.61	1.64	1.59	1.54			0.77	0.84	0.88	0.82	0.69	
4TS	Mean	70.99		0.98	1.18	1.33	1.24	1.11			0.41	0.51	0.60	0.47	0.37	
	90%	79.44		1.43	1.55	1.60	1.41	1.34			0.64	0.70	0.83	0.59	0.45	
8TS	Mean	73.47		1.00	1.33	1.42	1.35	1.16			0.30	0.48	0.56	0.47	0.35	
	90%	76.13		1.19	1.54	1.50	1.36	1.22			0.49	0.73	0.66	0.51	0.39	
Visual																
2TS	Mean	69.48		1.23	1.36	1.48	1.35	1.29	1.11		0.42	0.64	0.69	0.59	0.55	0.40
	90%	78.55		1.49	1.63	1.65	1.54	1.52	1.36		0.63	0.84	0.89	0.74	0.64	0.52
4TS	Mean	70.99		1.06	1.28	1.30	1.17	1.05	0.95		0.35	0.53	0.54	0.49	0.41	0.32
	90%	79.44		1.42	1.56	1.56	1.42	1.38	1.24		0.49	0.72	0.73	0.62	0.53	0.43
8TS	Mean	73.47		1.23	1.34	1.33	0.89	0.80	0.57		0.30	0.48	0.47	0.28	0.27	0.17
	90%	76.13		1.38	1.49	1.46	1.04	1.00	0.67		0.47	0.67	0.59	0.30	0.33	0.19

For the visual stimulus (Figure 7.35 and Figure 7.38) good agreement between the periodic and experimental data responses are seen for resonance at 1.5 to 2Hz for all group sizes. The resonance response due to other jumping frequencies and the 2nd harmonics of the forces are overestimated by the periodic equivalent force. In general the 90th percentiles of the response

from the periodic forces are greater or equal to those from the experimental data. However, occasionally the 90th percentiles from the experimental data are marginally larger than from the periodic force.

The responses to periodic forces with a magnitude equal to the 10th percentiles of group weight and DLF values (Table 7.10) are shown in Figure 7.39, Figure 7.40 and Figure 7.41. They are compared to the 10% percentile responses from the experimental forces. For the metronome stimulus (Figure 7.39) the periodic response overestimates the experimental data 10th percentile response. The responses are most similar at 2Hz resonance. The responses correspond well for all group sizes at the 1st harmonics of 1.75 to 3Hz for the music stimulus (Figure 7.40). The periodic response estimation for the visual stimulus is better than for the metronome, the responses are best matched for groups of 8TSs, except at 3.5Hz. The responses at the 2nd harmonics are overestimated for all stimuli and group sizes.

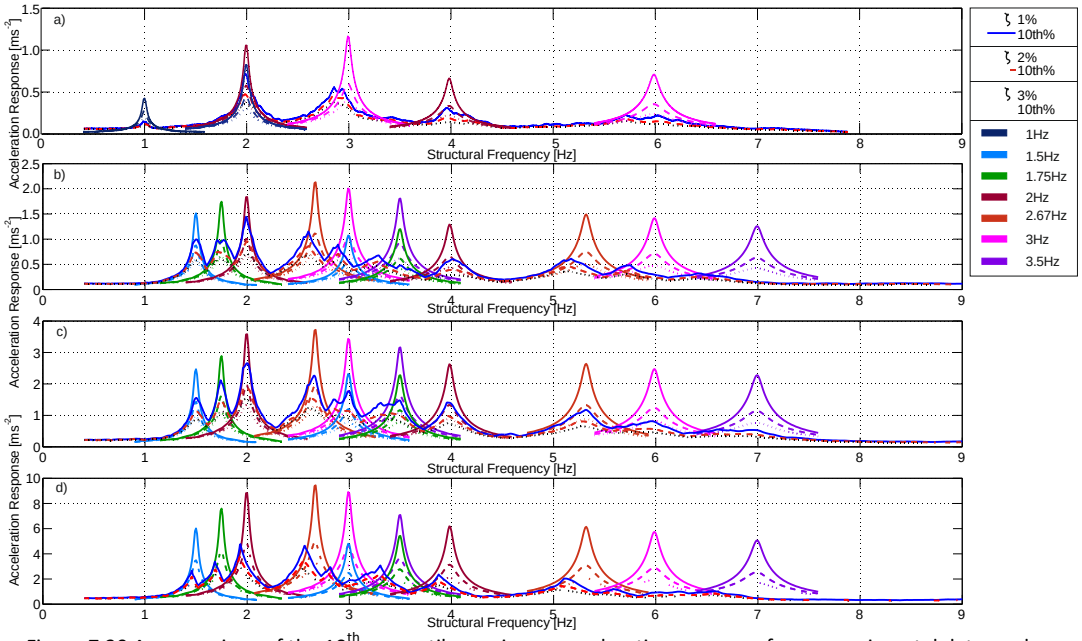

Figure 7.39 A comparison of the 10th percentile maximum acceleration response from experimental data, and an equivalent periodic half-sine force of each target frequency, with magnitude equal to the 10th percentile DLF value from the metronome stimulus for group sizes of a)1TS, b) 2TSs, c) 4TSs and d) 8TSs.

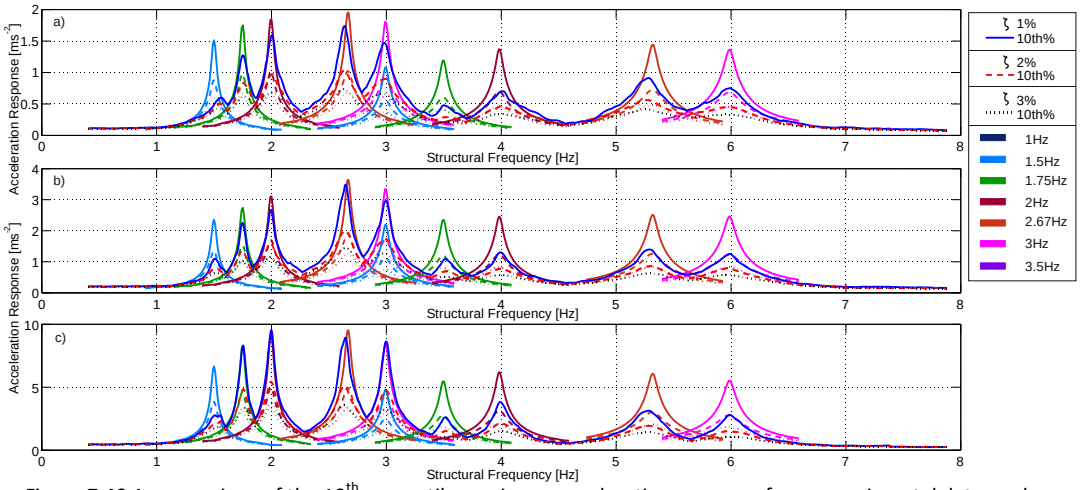

Figure 7.40 A comparison of the 10th percentile maximum acceleration response from experimental data, and an equivalent periodic half-sine force of each target frequency, with magnitude equal to the 10th percentile DLF value from the music stimulus for group sizes of a)2TS, b) 4TSs, and c) 8TSs.

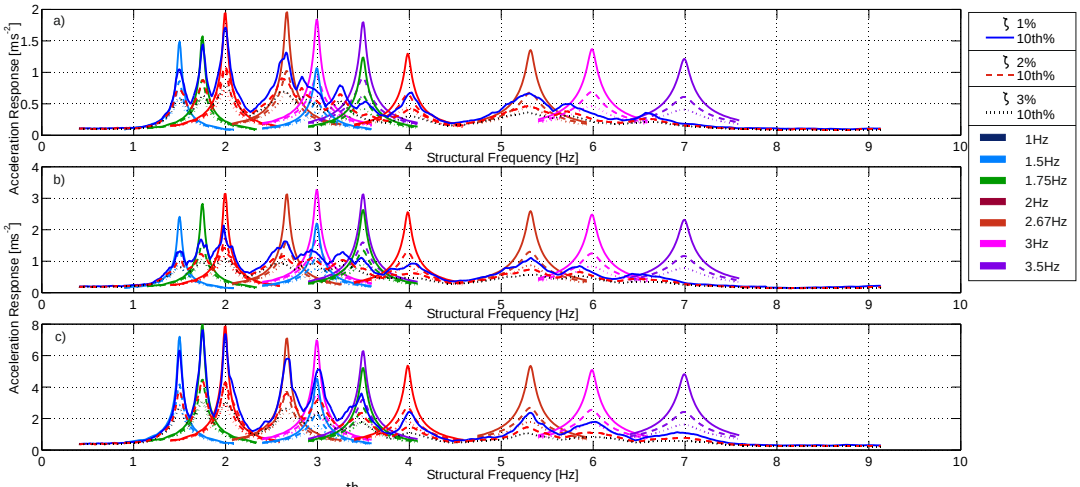

Figure 7.41 A comparison of the 10th percentile maximum acceleration response from experimental data, and an equivalent periodic half-sine force of each target frequency, with magnitude equal to the 10th percentile DLF value from the visual stimulus for group sizes of a)2TS, b) 4TSs, and c) 8TSs.

Considering all stimuli good agreement between the periodic and experimental force SDOF resonance responses was seen for the 1st harmonics of 1.5 to 3.5Hz jumping for all group sizes. Therefore there is potential for a half-sine function of adequate DLF and group weight to model loading for groups of 1, 2, 4 and 8TSs when jumping between 1.5 and 3Hz. The response due to the 2nd harmonics of the experimental forces were overestimated when using a periodic jumping force, therefore the use of a periodic force to model the 2nd harmonic is not recommended. It is worth noting that by using a periodic model additional frequency

components within the experimental forces are ignored and the corresponding response is potentially overlooked at non-resonance frequencies.

Examining the values of structural response in Figure 7.33, Figure 7.34 and Figure 7.35, it is possible for a lightly damped structure (ζ=1%) having a modal mass of 35000kg to be excited to extremely high structural accelerations when the TS's frequency matches that of the structure. Especially high values of mean acceleration occurred for 8TSs for visual (9.91ms^{-2}) and music (9.79ms^{-2}) stimuli. In addition the 90th percentiles reach 11.35ms^{-2} for the visual stimulus and 10.13ms^{-2} for the music stimulus. As there is potential for the structural accelerations to exceed gravity, occupants may be thrown from the structure.

7.6.3 Comparison with the Response of a Flexible Bridge

Previous authors argued that TSs were unable to continually perform an activity at the natural frequency of the structure when exposed to already large accelerations (Yao et al., 2006). TSs are unlikely to maintain their synchronised force, and therefore such high structural accelerations are unlikely to be reached. Reductions in the GRFs have been seen at resonance, known as force drop out (Yao et al., 2006). However these maximum peak accelerations should not be over looked as accelerations of 11.28ms^{-2} have been recorded on the Valladolid Science Museum Bridge in Spain (Figure 7.42a) due to pairs jumping at resonance.

The response accelerations in Figure 7.33 to Figure 7.38 include group effect but no human structure interaction (HSI). As seen in Section 3.2.2 the GRFs measured on flexible surfaces are different from those on rigid surfaces (Dougill et al., 2006; Yao et al., 2006). Experiments were conducted on the 2nd span of the Valladolid Museum Bridge (Figure 7.42b) which is noted for being lively with extreme responses (Casado et al., 2011). The 1st bending mode of the span has a natural frequency of 3.5Hz which can be easily excited by the 2nd harmonic of pedestrian traffic, or individuals or groups jumping at 3.5Hz. The span of the bridge is lightly damped (ζ=0.7%) and has a modal mass M of 18,500kg. An accelerometer was placed in the middle of

the span and recorded the structural accelerations at 600Hz. A Pair of individuals jumped in the middle of the span for three minutes at frequencies between 1.5 to 3.75Hz to a metronome beat. Three pairs participated in the experiments.

The acceleration responses were filtered in accordance to the experimental procedure in Section 7.3. The maximum acceleration response was found for each pair of TSs for frequencies of 1.5, 1.75, 2 and 3.5Hz and plotted in Figure 7.43. The 2TS experimental forces measured on a rigid surface using a metronome were applied to an equivalent SDOF system to investigate any differences in the response. The mean maximum response values and the 10th and 90th percentiles are marked on Figure 7.43.

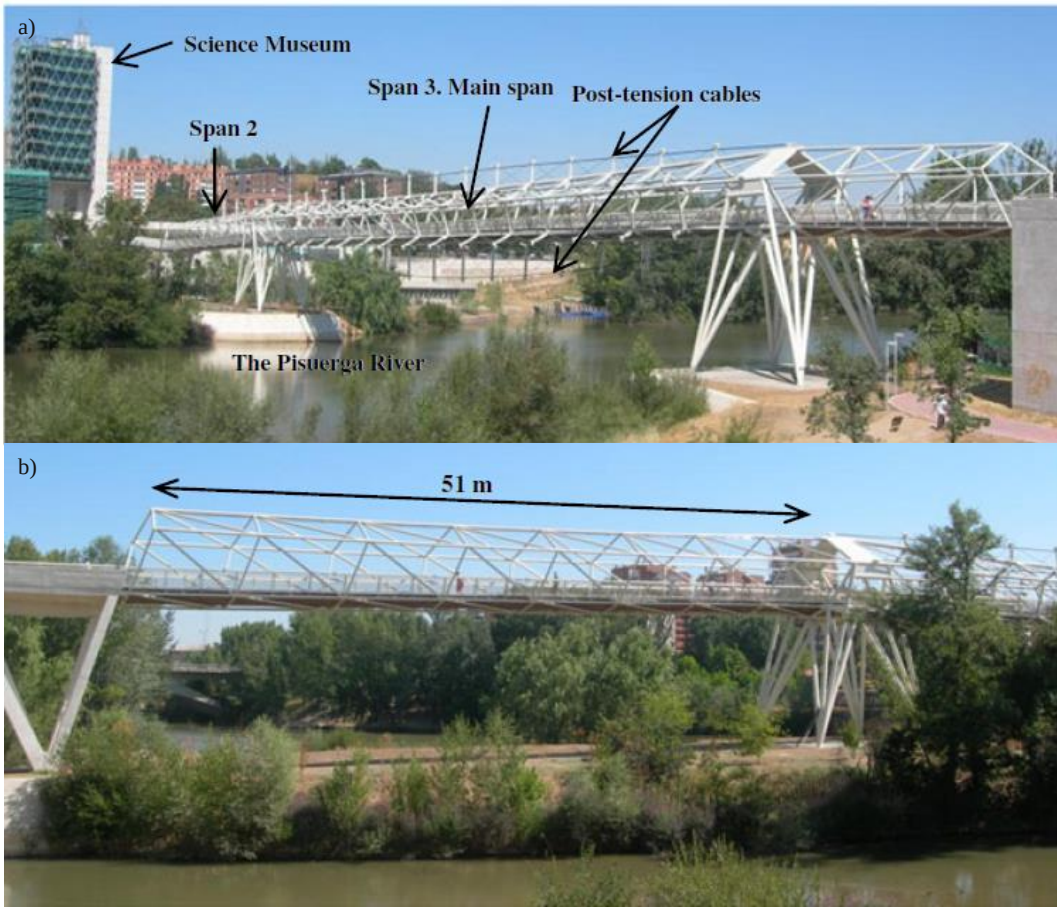

Figure 7.42 The Valladolid Science Museum Footbridge, in Spain a) the whole structure, b) span 2.

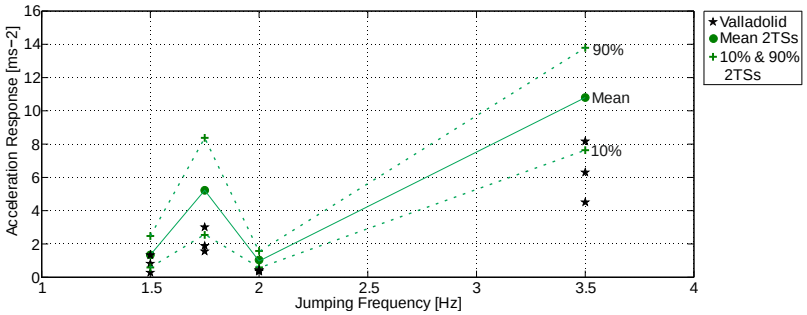

Figure 7.43 A comparision of the maximum acceleration response from pairs jumping on the flexible Valladolid Museum bridge and an equivalent SDOF system with experimental 2TSs metronome forces measured on rigid surfaces.

The responses from the 2TS forces measured on a rigid surface were larger than the bridge responses (Figure 7.43). Outside of resonance the 90th percentiles are on average within 1.14ms^{-2} of the bridge's response. The 10th percentiles are a conservative estimate of the minimum response value (Figure 7.43). At resonance due to the 1st harmonic of 3.5Hz and the 2nd harmonic of 1.75Hz the difference between the bridge responses and the 2TS responses increased. This is potential caused by force drop out (Yao et al., 2006). The 10th percentiles are however a good approximation of the bridge responses at resonance. It is suggested that outside of resonance the 10th percentile to mean of the rigid forces are a conservative approximation of the range of forces on flexible surfaces. At resonance it is suggested that the 10th percentile approximates the flexible forces. This should prevent large overestimations in the response. However these findings are only based on a limited number of experiments using a metronome stimulus and should be verified for other stimuli. Further experiments on flexible surfaces are recommended as only three pairs of TSs jumped on a single bridge with a natural frequency of 3.5Hz within this work.

7.6.4 Response Envelopes for Excitation in Resonance

Using the prominent response peaks from experimental and periodic data, charts (Figure 7.44, Figure 7.45 and Figure 7.46) have been created to give an indication of the levels of accelerations expected for resonance for different structural frequencies, damping ratios and

stimuli. The 10th and 90th percentiles of the response have been included for both the periodic and experimental data.

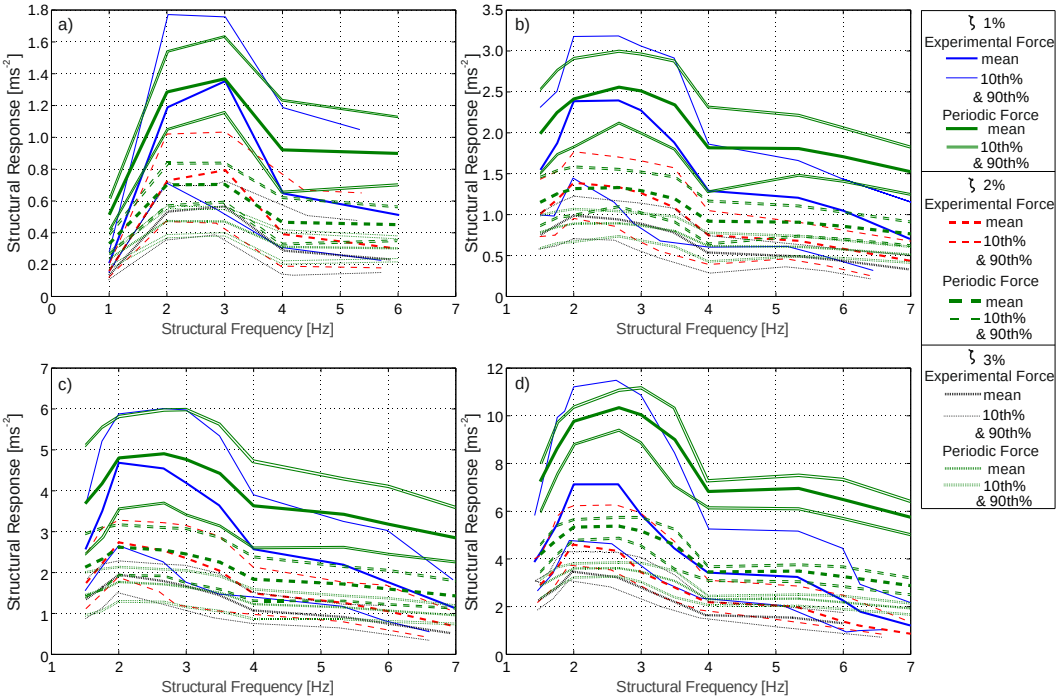

Figure 7.44 The expected structural resonance response for different structural frequencies for the metronome experimental data and the equivalent periodic signal, for a)1TS, b) 2TSs, c) 4TSs and d) 8TSs.

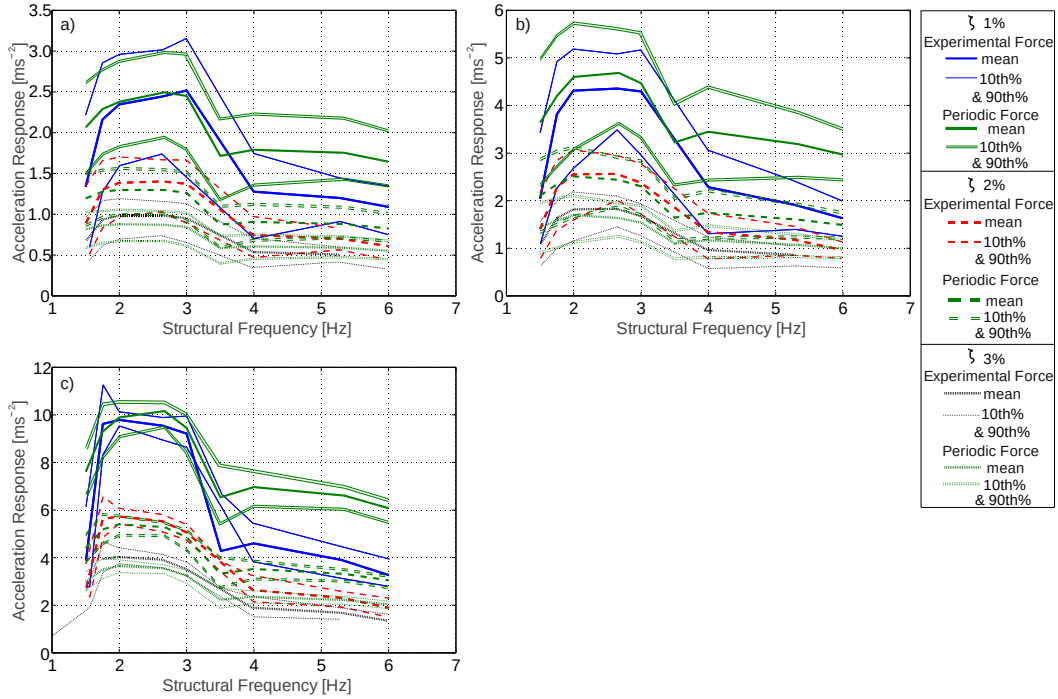

Figure 7.45 The expected structural resonance response for different structural frequencies for the music experimental data and the equivalent periodic signal, for a)2TSs, b) 4TSs, and c) 8TSs.

In public event space design for groups of 2, 4 and 8 synchronised individuals jumping, both the charts for music (Figure 7.45) and visual (Figure 7.46) stimuli should be consulted for the resonance response. For low frequency structures (≤2Hz), the focus should be on the visual stimulus (Figure 7.46), and mid frequency structures (1.75-3Hz) the music stimulus (Figure 7.45). For the over lapping frequencies (1.75-2Hz) both music and visual charts should be consulted equally or the chart most appropriate for the end use.

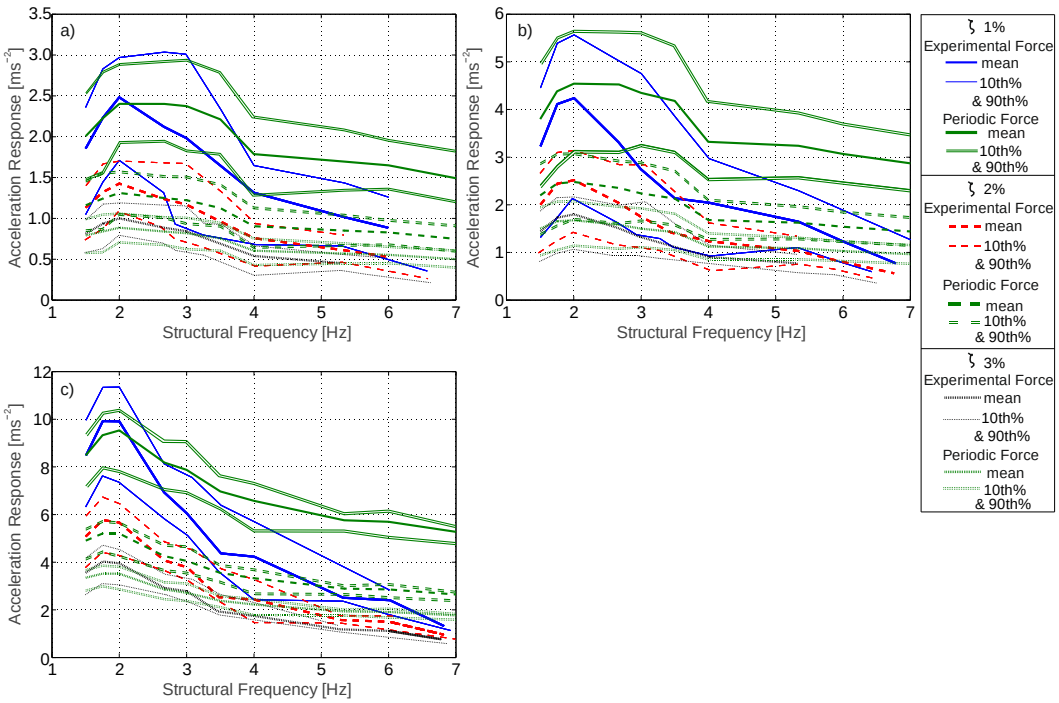

Figure 7.46 The expected structural resonance response for different structural frequencies for the visual experimental data and the equivalent periodic signal, for a)2TSs, b) 4TSs, and c) 8TSs.

The periodic responses are a good approximation of the mean, 10th and 90th percentiles for the 1st harmonic of the experimental responses. The two responses are most comparable for the visual stimulus at low frequencies (1.5-2Hz), and the mid-frequencies for music stimulus (1.75-3Hz). The underestimations from the periodic response in Figure 7.45a and c and Figure 7.46a and c are likely caused by transient responses as the steady state response was not reached by some group jumping forces. As the steady state response is of greatest concern (Section 5.4.5) the effect of these underestimations is unlikely to be critical. The use of the periodic curves is

recommended as adaption for different TS weights and DLF values is simple. Considering the findings in Section 7.6.3 for jumping on a flexible surface using a metronome, the mean and 10th percentile curves may produce the most realistic values of the response of flexible structures. A factor of 35,000/M should be applied to the responses for different modal masses. For the effects of the 2nd harmonics the experimental data curves should be used to avoid significant overestimations of the structural response.

7.6.5 The Structural Response and the Group Synchronisation Factors

The synchronisation factors discussed in 7.4 and 7.5 are a measure of synchronisation of, and between individuals, not necessarily the synchronisation with the structure. However, it is thought high group synchronisation should translate to high levels of structural synchronisation. For each stimulus, group size, frequency and harmonic the group self-synchronisation factors are compared to the mean maximum structural response from all the structural frequencies investigated for 1, 2 and 3% damping (Figure 7.47). The structural frequency where the response is largest should correspond to the largest PSD component representing the group self-synchronisation factor. In addition, the group self-synchronisation factors and the 10th percentiles of the maximum responses are compared (Figure 7.48).

There is a positive correlation between the 1st harmonic group self-synchronisation factors and the mean and 10th percentiles of the maximum structural responses, as seen in Figure 7.47a, c and e, and Figure 7.48a, c and e. The correlation is strongest in groups of 8TSs. The relationship varies depending on the group size and damping ratio, but stimulus does not appear to affect it. The gradient of the relationships at the 10th percentiles are shallower than for the mean values, indicating that the effect of group self-synchronisation on the response is less. The relationships in Figure 7.47a, c and e, and in Figure 7.48 a, c and e can be used to estimate the maximum structural response (having applied 35000/M) caused by an assumed degree of synchronisation. As seen in Section 7.6.3 the 10th percentile of response may be a more

realistic approximation of the response of a flexible structure at resonance. At the 2nd harmonic of the force there is no correlation between the group self-synchronisation factors and the responses, Figure 7.47b, d and f Figure 7.48b, d and f.

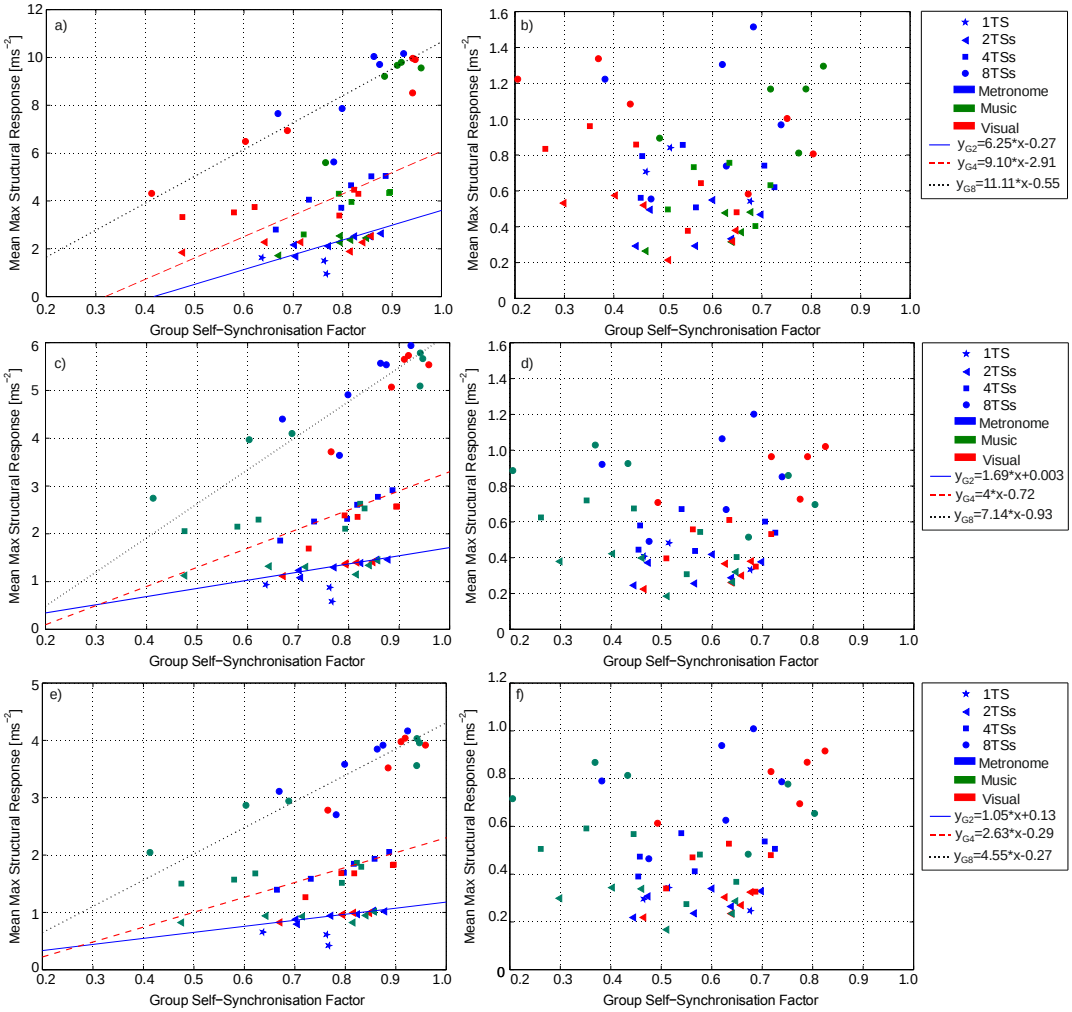

Figure 7.47 The relationship between the group self-synchronisation factors and the mean maximum structural response for 1% (a &b), 2% (c &d) and 3%(e &f) damping, where a, c &e are the 1st harmonic and b, d &f the 2nd harmonic.

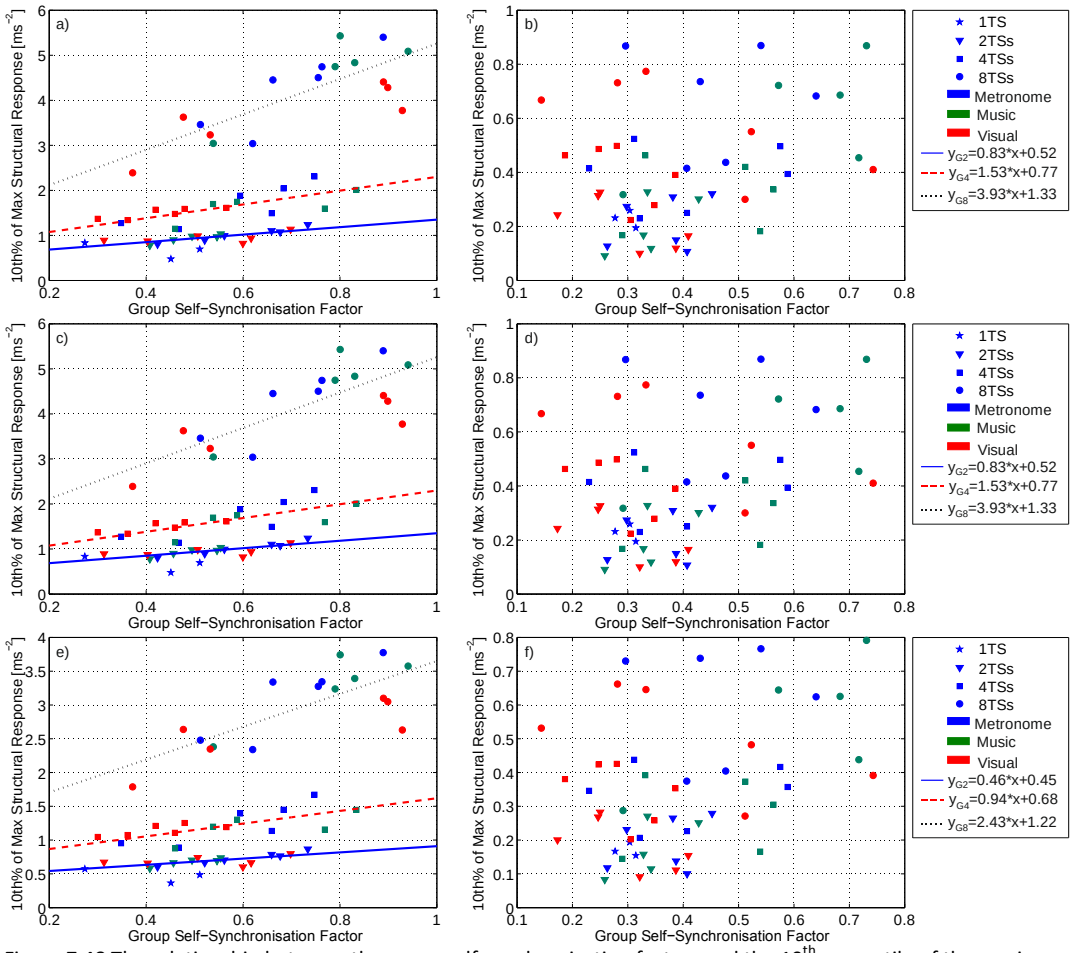

Figure 7.48 The relationship between the group self-synchronisation factors and the 10th percentile of the maximum structural response for 1% (a &b), 2% (c &d) and 3%(e &f) damping, where a, c &e are the 1st harmonic and b, d &f the 2nd harmonic.

7.7 Conclusions

This work has provided an in-depth study into the effect of stimuli and group size on synchronisation and quantified group synchronisation for 2, 4 and 8 TSs. Synchronisation with one's self and other TSs, and synchronisation with a beat has been investigated.

Individual beat and self-synchronisation is possible between 1.5 to 3.5Hz, the degree of this depends on the external stimulus. A visual stimulus encourages high average values of beat (≥0.63, Table 7.4) and self-synchronisation (≥0.75, Table 7.7) factors at low frequencies (1.5-2Hz). However, the average synchronisation at high target frequencies (2.67-3.5Hz) is poor (beat ≥0.15, self ≥0.44). In general the highest average beat (≥0.62) and self-synchronisation

(≥0.79) factors for audial stimuli are seen at the mid frequencies (2Hz-2.67Hz), however good mean self-synchronisation is possible between 1.5-3.5Hz (≥0.71).

The mean individual beat synchronisation factors are between 0.2 and 0.8 at the 1st harmonic and vary with group size, target frequency and stimulus (Figure 7.18). However, synchronisation factors as high as 0.98 can occur (Figure 7.15, Figure 7.16, Figure 7.17). The mean self-synchronisation factors are between 0.6-0.9 and vary with group size, target frequency and stimulus (Figure 7.23) However self-synchronisation factors as high as 0.98 are possible (Figure 7.20, Figure 7.21, Figure 7.22).

The beat and self-synchronisation factors calculated for eight solitary individual TSs were found to be significantly smaller than those from individuals within groups. If combining solitary individual GRFs (Parkhouse and Ewins, 2006) the improved synchronisation due to the crowd effect is ignored and therefore the equivalent crowd force will be underestimated. It is recommended that solitary individual force time histories are not extrapolated to create group loading.

Inclusion within a group improves the beat synchronisation of individuals considerably in most cases, supporting conclusions about crowd effect made by previous authors (Sim, 2006; Ebrahimpour and Fitts, 1996; Comer et al., 2007). An exception is the metronome stimulus, where the other group members become a stronger stimulus than the beat itself, encouraging synchronisation within the group. This highlights that stimuli affect synchronisation in different ways. Inclusion within a group also moderately improves an individual's self-synchronisation reducing the IASV of the period.

For examining individual synchronisation, the self-synchronisation factors in Figure 7.23 are recommended as mean values. However, if knowledge of synchronisation at a specific frequency is required the mean beat synchronisation factors in Figure 7.18 should be used.

Group beat and self-synchronisation factors were calculated using the total group time histories. Mean group beat synchronisation factors between 0.2 and 1 occur (Figure 7.26), which are dependent on the stimulus, target frequency and group size. The lowest synchronisation was seen for music stimulus at 1.5Hz and visual stimulus between 3 and 3.5Hz. The group beat synchronisation factors were largest for groups of 8TSs for the majority of frequencies, when using visual (max value 0.94, Table 7.8) or music cues (max value 0.96) Figure 7.26 b, and c. Hence, in certain situations group size can increase beat synchronisation. As this affect is not linked to the metronome stimulus, extrapolation of metronome data (Dougill et al., 2006; Sim et al., 2008) to larger groups with diverse stimuli may lead to underestimations of a crowd's capacity for beat synchronisation, and consequentially underestimate the load and the potential for resonance.

Group self-synchronisation factors give an indication of the consistency of the periods and the values of the time lags between individuals (Figure 7.28). A high level of mean group self-synchronisation (≥0.67, Table 7.9) is possible between at least 1.5 and 3.5Hz for all group sizes depending on the stimulus. The mean group self-synchronisation factors are between 0.4 and 1 and are dependent on target frequency, group size and stimulus. The best group self-synchronisation was seen in for 8TSs using a music cue at 2.67Hz (0.96, Table 7.9) and between 1.5-2Hz for visual stimulus (0.94-0.95). The worst synchronisation occurred at 3 and 3.5Hz when using a visual stimulus. The group self-synchronisation factors were largest in groups of 8TSs, where the presence of a crowd has improved synchronisation. For the metronome stimulus the group self-synchronisation factors from 8TS (0.67-0.92, Table 7.9) were significantly larger than the group beat synchronisation factors (0.36-0.46, Table 7.8). This indicates that synchronisation with other group members is dominant over synchronisation with a beat for a metronome stimulus.

The environment and the stimulus frequency and type should be examined when deciding the level of synchronisation to design against. Groups of 8TSs were able to achieve mean self-synchronisation factors of 0.96 in certain conditions. In some cases group self-synchronisation factors as high as 0.98 were seen. Individuals within groups of 8TSs have the potential for near perfect synchronisation with one another.

The group self-synchronisation factors in Figure 7.27 demonstrate the crowd's ability to synchronise with one another regardless of whether the target frequency was achieved. The level of synchronisation is not only dependant on the frequency but on group size and stimulus. The group self-synchronisation factors should be consulted when considering jumping within a given frequency range. However, if a certain jumping frequency is expected and of particular concern, for example to avoid structural resonance, the values of beat synchronisation in Figure 7.26 should be referenced.

The high synchronisation potential when using visual stimulus, especially at low frequencies was demonstrated with in this work. This challenges statements made by previous authors where the synchronisation potential from visual stimulus was disregarded (Parkhouse and Ewins, 2006). From this study it is advised that both visual and audial stimuli should be considered to have the potential to cause synchronisation. In addition individual and group synchronisation frequency ranges should take into consideration the type of stimulus involved.

The effect of position within a crowd was investigated and it was found that the addition of individuals in front does not necessarily improve the synchronisation of the row behind. Being within a crowd improves synchronisation however the position of an individual within the crowd appears insignificant.

The group forces and equivalent half-sine periodic forces were applied to SDOF systems of various natural frequencies and damping ratios. For lightly damped structures accelerations above gravity were possible. However it is unlikely that groups will continue applying a

synchronised force when exposed to such large accelerations (Yao et al., 2006). Considering all stimuli, good agreement between the SDOF resonance responses to periodic and experimental forces at the 1st harmonic of 1.5 to 3Hz were possible for all group sizes. Therefore there is potential for a half-sine function of adequate DLF and group weight to model group loading for 1, 2, 4 and 8TSs when jumping between 1.5 and 3Hz.

As seen by previous authors (Dougill et al., 2006; Yao et al., 2006) rigid and flexible GRFs may not be comparable. Real acceleration responses from pairs of individuals jumping on a bridge were compared to the responses of an equivalent SDOF system using experimental data from groups of 2TSs on rigid surfaces. The responses from forces measured on rigid surfaces were in general larger than those from a flexible surface (bridge), especially at resonance. It is suggested that outside of resonance the 10th percentiles and mean values of the response from the forces measured on rigid surfaces can be used to approximate the response to flexible forces. At resonance there is potential for the 10th percentiles to be used to prevent response overestimations. Charts were created to inform designers of the values of resonance response likely for different structural properties, group sizes and stimuli, Figure 7.44, Figure 7.45 and Figure 7.46. Positive correlation was found between the group self-synchronisation factors and the maximum structural responses (Figure 7.47, Figure 7.48). The relationships can be used to estimate the structural response from different values of group self-synchronisation.

This body of work set out to investigate the effect of group size, target frequency and external stimulus on individual and group synchronisation. Group and individual synchronisation factors have been calculated for group sizes of 2, 4 and 8 TSs. These synchronisation factors can be used in conjunction with current crowd and individual jumping models (Chapter 3) to simulate crowd or individual dynamic loading, with reference to the frequency and type of stimulus

expected. Ideally further experiments would be conducted with larger group sizes to investigate the applicability of these factors to larger group sizes.

Further experiments are recommended using this method and different stimuli on flexible grandstand structures to understand further the differences between rigid and flexible GRFs. In addition these experiments can be used to determine if crowd synchronisation on flexible surfaces is the same as on rigid surfaces.

It is suggested that the use of metronomes be discontinued as a stimulus for synchronisation experiments. The variation between the metronome beat synchronisation factors for both individuals and groups, for 8TSs, compared to other stimulus was significant.

The effect of position within a group was briefly studied within this chapter. Further experiments with additional rows would be of benefit to validate those conclusions drawn on the TS position within this work.

8 Conclusions and Recommendations for Further Work

8.1 Conclusions

Within this work the properties of jumping and bobbing activities have been examined for 8 test subjects (TS) over a range of frequencies, and relationships sought between them (Chapter 4). Thought was given to the physical characteristics of the TSs and the potential influence on the properties investigated. The properties of interest for jumping, observed on a jump-by-jump basis, were frequency, peak force, dynamic load factor (DLF), impulse, contact ratio and displacement. For bobbing the properties of interest were frequency, peak force, DLF and displacement observed on a bob-by-bob basis. The intra-subject variation (IASV), the inter-subject variation (IESV) and the inter-intra-subject variation (EIASV) were examined and quantified.

For jumping it was observed that male TSs generated larger normalised peak forces than female TSs, however this distinction was lost at 3Hz. TS weight influenced the normalised peak forces at 1-2Hz, however at 3Hz TS height was the dominant influence. The effect of TS height on the maximum displacement was investigated and for the jumping frequencies of 2 and 3Hz taller TS's were found to have larger displacements. At 1Hz TS height appeared to have little influence on the maximum displacement. Unlike jumping, the normalised bobbing force was unaffected by TSs weight and height, and no correlation was observed between TS height and maximum displacements.

There is an inverse relationship between contact ratio and peak force, which varies with jumping frequency. Contact ratios are not necessarily specific to a jumping frequency. However, very high contact ratios are mostly associated with low frequency jumping, and very low contact ratios with jumping at frequencies around 2Hz.

The TS's frequency variation was most similar to one another at 2Hz (EIASV, mean CoV=0.035, Table 4.2) and most varied at 1Hz (EIASV, mean CoV=0.043). Overall the normalised peak forces of the TSs were most consistent with one another at 3Hz (IESV, CoV=0.07, Table 4.4) and least consistent at 2Hz (IESV, CoV=0.14). For jumping a significant portion of the properties were found to have the largest IESV at a frequency of 2Hz, suggesting high diversity of jumping properties between TSs. For bobbing displacement the EIASV values were smallest at 1Hz (mean CoV=0.202, Table 4.17) and largest at 4Hz (mean CoV=0.444). In general the bobbing DLF values were most consistent between the TSs at the 1st harmonic, more IESV occurred at the higher harmonics (3 and above). The IESV and EIASV values in general were smaller for jumping than for bobbing, indicating that jumping TSs are more consistent with each other. This is likely due to the wider variety of styles and force profiles possible when bobbing.

For the activity of bobbing the force profiles of two different styles, bouncing and jouncing were examined and characterised. In general the forces were larger from jouncing TSs. A high variety of profile shapes were possible for both styles, the variety reduced with increased bobbing frequency. At high frequencies the bouncing and jouncing force profiles became more similar, tending towards a single force peak comparable to jumping force profiles.

This study into the variation of jumping and bobbing properties provides a greater understanding of how the actions change on a cycle-by-cycle basis, and between people. These variations can be used to improve current jumping and bobbing models (Chapter 3) facilitating more realistic characteristics.

To tackle the difficulty of crowd force measurements a novel approach was developed (Chapters 5 & 6) from existing motion capture techniques. The use of a single monitoring point was proposed to increase ease of multiple subject tracking. This could be used indirectly to calculate the ground reaction force (GRF). To achieve this, the movement of the centre of mass (CoM) was required. 17 locations with the potential to track the CoM movements were

proposed on the front, back and hips of the eight participating TSs. A metronome dictating target frequencies of 1, 2 and 3Hz was used for jumping, 4Hz was used in addition for bobbing. After comparing the indirect (motion capture) force measurement for each potential location to the direct force simultaneously measured by a force plate, an adequate location on the back (C7th vertebrae) of the TSs was found. The first three harmonics of a jumping force can be accurately measured if their harmonic frequency is less than or equal to 3Hz. The average percentage differences (PD) between the direct and indirect force in the f-domain for frequencies less than or equal to 3Hz were +2.34% -3.18% (Table 5.12). Satisfactory jumping force measurements can occur for the 2nd harmonic for frequencies between 3 and 6Hz (average PDs +12.55% and -14.15%). Reasonable measurements of the 3rd harmonic are only possible at 1Hz (average PDs +2.53% and -3.72%). For the activity of bobbing the average PDs for the 1st and 2nd harmonics which are less than or equal to 6Hz, as well as the 3rd harmonic of 1Hz are +10.58 and -8.03 excluding outliers. The PDs at the 3rd harmonic are unsuitably large, with the exception of bobbing at 1Hz. The higher error is because bobbing is a more complex activity and therefore more difficult to quantify using measurements from one point of the body only.

The indirect and direct forces were applied to a selection of SDOF systems. The response ratio in the t-domain was shown to be approximately equal to the peak force ratio in the f-domain, therefore the PDs from the force can be used to estimate the equivalent PDs in the response. These findings have the potential to allow experimental determination of dynamic forces induced by jumping and bobbing crowds at real-life stadium events. There is potential for the C7th vertebra location to be used in crowd monitoring, future developments may allow its use in marker-less video monitoring.

Although bobbing can take place at a higher frequency the DLF values from bobbing are on average between 1.7 and 2.3 times smaller than jumping at the 1st harmonic and between 2.68

and 4.5 times at the 2nd harmonic. Jumping is the more critical activity likely to adversely affect structures and it therefore was focus of the synchronisation experiments.

Having found a suitable crowd monitoring technique the synchronisation of groups of 2, 4 and 8 TSs jumping were investigated over six different target frequencies using different audial and visual cues (Chapter 7). In total 1,275 trials of different sized groups were recorded and 4,794 individual GRFs. This is possibly the most extensive database of individual and group GRFs for jumping in response to different stimuli and group sizes.

The individual TS synchronisation was first investigated. Both the synchronisation with the beat (beat-synchronisation) and how consistently they maintained their rhythm irrespective of the target frequency (self-synchronisation) was considered.

Individual beat and self-synchronisation is possible between 1.5 to 3.5Hz, the degree of this depends on the external stimulus. A visual stimulus encourages high average values of beat (≥0.63, Table 7.4) and self-synchronisation (≥0.75, Table 7.7) factors at low frequencies (1.5-2Hz). However, the average synchronisation at high target frequencies (2.67-3.5Hz) is poor (beat ≥0.15, self ≥0.44). In general the highest average beat (≥0.62) and self-synchronisation (≥0.79) factors for audial stimuli are seen at the mid frequencies (2Hz-2.67Hz), however good self-synchronisation is possible between 1.5-3.5Hz (≥0.71). The highest beat synchronisation values were seen for groups of 8TSs (0.86), with an exception of the metronome stimulus where the average 8TS beat synchronisation factors were between 0.24-0.42, Table 7.4. The other group members became a stronger stimulus than the metronome beat itself, encouraging synchronisation with one another not the beat. This highlights that stimuli affect synchronisation in different ways. Inclusion within a larger group (8TSs) moderately improves an individual's self-synchronisation as well.

The beat and self-synchronisation factors calculated for eight solitary individual TSs were found to be significantly smaller than those from individuals within groups. Inclusion within a

group improves the beat synchronisation of individuals considerably in most cases, supporting conclusions about crowd effect made by previous authors (Sim, 2006; Ebrahimpour and Fitts, 1996; Comer et al., 2007). If combining GRFs from solitary individuals (Parkhouse and Ewins, 2006) the improved synchronisation due to the crowd effect is ignored and therefore the equivalent crowd force may be underestimated. Hence it is recommended that solitary individual force time histories are not extrapolated to create group loading.

Group beat and group self-synchronisation factors were also calculated to determine how well the groups as a whole managed to maintain the target frequency, and how synchronised they were with one another. The group beat synchronisation factors were largest for groups of 8TSs for the majority of frequencies, when using visual (max value 0.94, Table 7.8) or music cues (max value 0.96). Hence, in certain situations group size can increase beat synchronisation. As this effect is not linked to the metronome stimulus, extrapolation of metronome data (Dougill et al., 2006; Sim et al., 2008) to larger groups with diverse stimuli may lead to underestimations of a crowd's capacity for beat synchronisation, and consequentially underestimate the load and the potential for resonance.

A high level of average group self-synchronisation (≥0.67, Table 7.9) is possible between at least 1.5 and 3.5Hz for all group sizes depending on the stimulus. The group self-synchronisation factors were largest in groups of 8TSs (max value 0.96, Table 7.8), where the presence of the crowd improved synchronisation. For the metronome stimulus the group self-synchronisation factors from 8TSs (0.67-0.92) were significantly larger than the group beat synchronisation factors (0.36-0.46). This indicates that synchronisation with other group members is dominant over synchronisation with a beat for a metronome stimulus.

The environment and the stimulus frequency and type should be examined when deciding the level of synchronisation to design against. Individuals within groups of 8TSs have the potential for near perfect synchronisation with one another. From this study it is advised that both

visual and audial stimuli should be considered to have the potential to cause synchronisation. In addition individual and group synchronisation frequency ranges should take into consideration the type of stimulus involved.

For examining synchronisation, the self-synchronisation factors in Figure 7.23 and Figure 7.27 for individuals and for groups are recommended as mean values. However, if a certain jumping frequency is expected and of particular concern, the values of beat synchronisation factors in Figure 7.18 and Figure 7.26 should be referenced.

The effect of position within a crowd was investigated and it was found that individuals in front do not necessarily improve the synchronisation of the row behind, the position of an individual within the crowd appears insignificant.

The measured group forces and equivalent half-sine periodic forces were applied to SDOF systems of various natural frequencies and damping ratios. Considering all stimuli good agreement between the SDOF resonance responses to periodic and experimental forces at the 1^{st} harmonic of 1.5 to 3Hz were possible for all group sizes. There is potential for a half-sine function of adequate DLF and group weight to model group loading for 1, 2, 4 and 8TSs when jumping between 1.5 and 3Hz. However, the response outside of resonance maybe underestimated due to additional frequency components in the real forces.

Real acceleration responses from pairs of individuals jumping on a bridge were compared to the responses of an equivalent SDOF system using experimental data from 2TSs on rigid surfaces. The responses from the forces measured on rigid ground were larger, especially at resonance. There is potential for the 10^{th} percentile of the response from the forces measured on rigid ground to be used to approximate the resonance response from flexible forces. Charts were created to inform designers of the values of resonance response likely for different structural properties, group sizes and stimuli, Figure 7.44, Figure 7.45 and Figure 7.46.

8.2 Recommendations for Further work

The indirect force measurement technique presented in this thesis provides potential for in-situ crowd observations. However the use of the IR cameras currently limits the method to mostly lab environments. In addition, the application of markers to a crowd is difficult from a resources and logistics perspective. If the technique is adapted and combined with previous marker-less video techniques which use digital cameras (Hoath et al., 2007) there is potential to track the C7th vertebrae without using an external marker. This would allow large in-situ crowds to be monitored with less equipment restraints.

The characteristics of jumping and bobbing individuals have been studied within this body of work, it is recommended that this study be extended to include individuals who are part of a group and groups as a whole. This would allow further investigation into the crowd effect on jumping and bobbing time histories.

An aim from this body of work was to investigate the effect of group size, target frequency and external stimulus on individual and group synchronisation. Group and individual synchronisation factors have been calculated for group sizes of 2, 4 and 8 TSs. Ideally further experiments would be conducted with larger group sizes to investigate the applicability of these factors. These synchronisation factors can be used in conjunction with current crowd and individual jumping models (Chapter 3) and the individual jumping and bobbing characterisations in Chapter 4 to simulate crowd or individual dynamic loading. It would be possible to reflect the frequency and type of stimulus within the model.

Further experiments are recommended using the indirect method and a variety of stimuli on flexible grandstand structures to investigate the differences between rigid and flexible GRFs. In addition these experiments can be used to determine if crowd synchronisation on flexible surfaces is the same as on rigid surfaces.

The effect of position within a group was briefly studied in Chapter 7, further experiments with additional rows would be of benefit to validate those conclusions drawn on the TS position within this work.

References

ALLEN, D. E. 1990. Floor vibrations from aerobics. *Canadian Journal of Civil Engineering,* 17**,** 771-787.

ALLEN, D. E., RAINER, J. H. & PERNICA, G. 1985. Vibration criteria for assembly occupancies. *Canadian Journal of Civil Engineering,* 12**,** 617-623.

AMTI 2007. Force Plate Manual - Model OR6-7. *In:* Advanced Mechanical Technology INC (ed.). Watertown, Massachusetts, USA.

ANDERSON, J. C. & NAEIM, F. 2012. *Basic Structural Dynamics*, Wiley.

BACHMANN, H. & AMMANN, W. 1987. *Vibrations in Structures: Induced by man and machines,* Zurich, International Association for Bridge and Structural Engineering.

BAUMANN, K. & BACHMANN, H. 1987. Dynamic loading by persons and its effect on beam structures. *In:* Institution of Structural Engineering, S. F. (ed.). Zurich: Inst. of Techn.

BBC. 1999. Safety concerns over Manics gig. *BBC News, Wales*.

BBC. 2013. Seattle Seahawks football fans 'caused minor earthquake'. *BBC News*.

BRE 1997. The response of structures to dynamic crowd loads. *BRE Digest 426.* Building Research Establishment.

BRE 2004. The response of structures to dynamic crowd loads -2004 edition. *BRE Digest 426.* Building Research Establishment.

BROWNJOHN, J. M. W., PAVIC, A. & OMENZETTER, P. 2004. A spectral density approach for modelling continuous vertical forces on pedestrian structures due to walking. *Canadian Journal of Civil Engineering,* 31**,** 65-77.

BSI 1996. BS 6399. *Part 1: Loading for buildings.* London: British Standards Institution.

CASADO, C., DIAZ, I., SEBASTIAN, J., PONCELA, A. & LORENZANA, A. 2011. Implementation of passive and active vibration control on an in-service footbridge. *Structural Control and Health Monitoring*.

CDC. 2011. Body Mass Index: Considerations for practitioners. Available: http://www.cdc.gov/obesity/downloads/bmiforpactitioners.pdf.

COMER, A. J., BLAKEBOROUGH, A. & WILLIAMS, M. S. 2013. Rhythmic crowd bobbing on a grandstand simulator. *Journal of Sound and Vibration,* 332**,** 442-454.

COMER, A. J., WILLIAMS, M. S. & BLAKEBOROUGH, A. 2007. Experimental determination of crowd load and coherency when jumping on a rigid raked grandstand. *2007 IMAC-XXV: Conference & Exposition on Structural Dynamics.*

CROSS, R. 1999. Standing, walking, running, and jumping on a force plate. *American Journal of Physics,* 67**,** 304.

DE LEVA, P. 1996. Adjustments to Zatsiorsky-Seluyanov's segment inertia parameters. *Journal of Biomechanics,* 29**,** 1223-1230.

DOUGILL, J. W., WRIGHT, J. R., PARKHOUSE, J. G. & HARRISON, R. E. 2006. Human structure interaction during rhythmic bobbing. *The Structural Engineer,* 84**,** 32-39.

DRAPER, N. & SMITH, H. 1985. *Applied regression analysis,* New York, John Wiley & Sons, Inc.

EBRAHIMPOUR, A. & FITTS, L. 1996. Measuring coherency of human-induced rhythmic loads using force plates. *Journal of Structural Engineering,* 122**,** 829-831.

EBRAHIMPOUR, A. & SACK, R. L. 1989. Modeling dynamic occupant loads. *Journal of Structural Engineering,* 115**,** 1476-1496.

EBRAHIMPOUR, A. & SACK, R. L. 1992. Design live loads for coherent crowd harmonic movements. *Journal of Structural Engineering,* 118**,** 1121-1136.

EBRAHIMPOUR, A., SACK, R. L., SAUL, W. E. & THINNESS, G. L. 1986. Measuring dynamic occupant loads by microcomputer. Electronic Computation (1986), ASCE, 328-338.

ELLIS, B. R. & JI, T. 1994. Floor vibrations induced by dance-type loads: Verification. *The Structural Engineer,* 72**,** 45-50.

ELLIS, B. R. & JI, T. 1997. Human-structure interaction in vertical vibrations. *Proceedings of the ICE - Structures and Buildings,* 122**,** 1-9.

ELLIS, B. R. & JI, T. 2002. *Loads generated by jumping crowds: experimental assessment*, Taylor & Francis Group.

ELLIS, B. R. & JI, T. 2004. Loads generated by jumping crowds: numerical modelling. *The Structural Engineer,* 82**,** 35-40.

FOREMAN & LASER JOCK. 2008. *Billboard Hot 100, including song length* [Online]. The 100 Hour Board. Available: http://theboard.byu.edu/questions/44286/ [Accessed 07/2013].

GINTY, D., DERWENT, J. M. & JI, T. 2001. The frequency ranges of dance-type loads. *The Structural Engineer,* 79**,** 27-31.

HANSEN, S. O. & SØRENSEN, J. D. 2002. Dynamic loads due to synchronized movements of people. *Structural Dynamics: EURODYN 2002.* Munich, Germany: Taylor & Francis.

HARRISON, R. E., WRIGHT, J. R. & DOUGILL, J. W. 2006. Video monitoring of human-structure interaction for bouncing on a flexible structure. 2006 IMAC-XXIV: Conference & Exposition on Structural Dynamics, 2006. Society for Experimental Mechanics (SEM).

HARRISON, R. E., YAO, S., WRIGHT, J. R., PAVIC, A. & REYNOLDS, P. 2008. Human jumping and bobbing forces on flexible structures: Effect of structural properties. *Journal of Engineering Mechanics,* 134**,** 663-675.

HOATH, R. M., BLAKEBOROUGH, A. & WILLIAMS, M. S. 2007. Using video tracking to estimate the loads applied to grandstands by large crowds. *2007 IMAC-XXV: Conference & Exposition on Structural Dynamics***,** 19-22.

HOMAN, S. W., BOASE, A. J., RAIDER, C. J., JENSEN, H., MATTHEWS, H. W., SMITH, G. B. & C.H., W. 1932. Horizontal forces produced by movements of the occupants of a grandstand. *American Standards Association Bulletin,* 3**,** 123-126.

ISO 2007. ISO 10137:2007. *Bases for design of structures- Serviceability of buildings and walkways against vibrations.* International Organization for Standardization.

JI, T. & ELLIS, B. R. 1994. Floor Vibration. Floor vibration induced by dance-type loads: theory. *The Structural Engineer,* 72**,** 37-44.

JI, T. & WANG, D. 2001. A supplementary condition for calculating periodical vibrations. *Journal of Sound and Vibration,* 241**,** 920-924.

JONES, C. A., PAVIC, A., REYNOLDS, P. & HARRISON, R. E. 2011a. Verification of equivalent mass–spring–damper models for crowd–structure vibration response prediction. *Canadian Journal of Civil Engineering,* 38**,** 1122-1135.

JONES, C. A., REYNOLDS, P. & PAVIC, A. 2011b. Vibration serviceability of stadia structures subjected to dynamic crowd loads: A literature review. *Journal of Sound and Vibration,* 330**,** 1531-1566.

KASPERSKI, M. & AGU, E. 2005. Prediction of crowd-induced vibrations via simulation. *2005 IMAC-XXIII: Conference & Exposition on Structural Dynamics.*

KASPERSKI, M. & NIEMANN, H. 1993. Man induced vibrations of a stand structure. *Structural Dynamics: EURODYN 1993.* Balkema.

LINTHORNE, N. P. 2001. Analysis of standing vertical jumps using a force platform. *American Journal of Physics,* 69**,** 1198-1204.

LITTLER, J. D. 2002. Measured phase shifts in the dynamic response of a large permanent cantilever grandstand to human loading. *Structural Dynamics: EURODYN 2002.* Munich, Germany: Taylor & Francis.

LITTLER, J. D. 2003. Frequencies of synchronised human loading from jumping and stamping. *The Structural Engineer,* 81**,** 27-35.

LYNN, P. A. & FUERST, W. 2000. *Introductory digital signal processing with computer applications, sampling and analog-to-digital coversion*, John Wiley & Sons.

MANCHESTEREVENINGNEWS. 2007. Robbie fans in danger at cricket ground gig. *Manchester-Evening-News*, 17th Feb 2007.

MATHWORKS 2011. MATLAB R2011b. MATLAB. MathWorks.

MATHWORKS 2012. MATLAB R2012b. *MATLAB.* MathWorks.

MATSUMOTO, Y. & GRIFFIN, M. J. 2003. Mathematical models for the apparent masses of standing subjects exposed to vertical whole-body vibration. *Journal of Sound and Vibration,* 260**,** 431-451.

MAZZOLENI, P. & ZAPPA, E. 2012. Vision-based estimation of vertical dynamic loading induced by jumping and bobbing crowds on civil structures. *Mechanical Systems and Signal Processing,* 33**,** 1-12.

MCDONALD, M. G. & ZIVANOVIC, S. 2013. Measuring dynamic force of a jumping person by monitoring their body kinematics. *RASD 2013.* Pisa: University of Southampton OCS (beta).

MEGHDARI, A. & ARYANPOUR, M. 2003. Dynamic modeling and analysis of the human jumping Process. *Journal of Intelligent and Robotic Systems,* 37**,** 97-115.

MORELAND, R. 1905. The weight of a crowd. *Engineering,* 79**,** 551.

NHLEKO, S., ZINGONI, A. & MOYO, P. 2008. A variable mass model for describing load impulses due to periodic jumping. *Engineering Structures,* 30**,** 1760-1769.

NOORMOHAMMADI, N., BROWNJOHN, J. M. W., WING, A., RACIC, V., JOHANNSEN, L. & ELLIOTT, M. T. 2011. Effect of different cues on spectators' synchronisation, a vibration engineering approach. *Structural Dynamics: EURODYN 2011.* Leuven, Belgium,: Eurodyn.

NRC 2006. Canadian commission on building and fire codes. User's Guide-NBC 2005: Structural Commentaries (Part 4 of Division B),. Institute for Research in Construction, Ottwa: National Research Council of Canada.

OXFORD METRICS GROUP 2007. Vicon MX Hardware: System Reference. Oxford Metrics Group,.

OXFORD METRICS GROUP 2008. Vicon Nexus Revesion 1.4.1.: Oxford Metrics Group,.

PARKHOUSE, J. G. & EWINS, D. J. 2004. Vertical dynamic loading produced by people moving to a beat. ISMA International Conference on Noise and Vibration Engineering, Sept 20-22, 2004 Belgium. Katholieke Universiteit Leuven, 821-836.

PARKHOUSE, J. G. & EWINS, D. J. 2006. Crowd-induced rhythmic loading. *Proceedings of the ICE - Structures and Buildings*, 159, 247-259.

PARKHOUSE, J. G. & WARD, I. 2010. Design charts for the assessment of grandstands subject to dynamic crowd action. *The Structural Engineer,* 88**,** 27-34.

PASMAN, W. 2012. Simple visual metronome v.10. Softpedia.

PERNICA, G. 1990. Dynamic load factors for pedestrian movements and rhythmic exercises. *Canadian Acoustics,* 18**,** 3.

RACIC, V. 2009. *Experimental measurement and mathematical modelling of near periodic human-induced dynamic force signals.* Degree of Doctor of Philosophy in Engineering, The University of Sheffield.

RACIC, V., BROWNJOHN, J. M. W. & PAVIC, A. 2010. Reproduction and application of human bouncing and jumping forces from visual marker data. *Journal of Sound and Vibration,* 329**,** 3397-3416.

RACIC, V., BROWNJOHN, J. M. W., WANG, S., ELLIOT, M. T. & WING, A. 2013. Effect of sensory stimuli on dynamic loading induced by people bouncing. *Topics in Dynamics of Civil Structures, Volume 4*. Springer.

RACIC, V. & PAVIC, A. 2010. Stochastic approach to modelling of near-periodic jumping loads. *Mechanical Systems and Signal Processing,* 24**,** 3037-3059.

RACIC, V., PAVIC, A. & BROWNJOHN, J. M. W. 2009. Number of successive cycles necessary to achieve stability of selected ground reaction force variables during continuous jumping. *Journal of Sports Science and Medicine,* 8**,** 639-47.

RAINER, J. H., PERNICA, G. & ALLEN, D. E. 1988. Dynamic loading and response of footbridges. *Canadian Journal of Civil Engineering,* 15.

REID, W. M., DICKIE, J. F. & WRIGHT, J. R. 1997. Stadium structures: are they excited? *The Structural Engineer,* 75**,** 383-8.

ROGERS, D. & THOMPSON, R. 2000. Liverpool stand gets a red card. *Construction News*, 10 Aug 2000.

SACHSE, R., PAVIC, A. & REYNOLDS, P. 2002. The influence of a group of humans on modal properties of a structure. *Structural Dynamics: EURODYN 2002.* Munich, Germany: Taylor & Francis.

SAKKA, S. & YOKOI, K. 2005. Humanoid vertical jumping based on force feedback and inertial forces optimization. *ICRA: International Conference on Robotics and Automation 2005* IEEE.

SALYARDS, K. A. & HANAGAN, L. M. 2007. Analysis of coordinated crowd vibration levels in a stadium structure. *2007 IMAC-XXV: Conference & Exposition on Structural Dynamics.* Orlando, FL.

SAUL, W. & TUAN, C. 1986. Review of live loads due to human movements. *Journal of Structural Engineering,* 112**,** 995-1004.

SAZAK, H. O., CATBAS, F. N. & GUL, M. 2011. Structural health monitoring and evaluating structural performance of a stadium. *In:* PROULX, T. (ed.) *Civil Engineering Topics, Volume 4.* Springer New York.

SETAREH, M. 2011. Vibration studies of a cantilevered structure subjected to human activities using a remote monitoring system. *Journal of Performance of Constructed Facilities,* 25**,** 87-97.

SIM, J. H. 2006. *Human-structure interaction in cantilever grandstands.* Doctor of Philosophy, The University of Oxford.

SIM, J. H., BLAKEBOROUGH, A. & WILLIAMS, M. S. 2005. Dynamic loads due to rhythmic jumping and bobbing. *In:* Schueller, C. S. G. I. (ed.) *Structural Dynamics: EURODYN 2005.* Paris, France.

SIM, J. H., BLAKEBOROUGH, A. & WILLIAMS, M. S. 2007. Modelling of joint crowd-structure system using equivalent reduced-DOF system. *Shock and Vibration,* 14**,** 261-270.

SIM, J. H., BLAKEBOROUGH, A., WILLIAMS, M. S. & PARKHOUSE, J. G. 2008. Statistical model of crowd jumping loads. *Journal of Structural Engineering,* 134**,** 1852-1861.

THORNTON-TRUMP, A. B. & DAHER, R. 1975. The prediction of reaction forces from gait data. *Journal of biomechanics,* 8**,** 173-178.

TILDEN, C. J. 1913. *Kinetic effects of crowds*.

TUAN, C. & SAUL, W. 1985. Loads due to spectator movements. *Journal of Structural Engineering,* 111**,** 418-434.

UK WORKING GROUP 2008. Dynamic performance requirements for permanent grandstands subject to crowd action. *In:* The Insititution of Structural Engineers , The Department for Communities and Local Governement & The Department for Culture Media and Sport (eds.). The Institution of Stuctural Engineers.

WEI, L. & GRIFFIN, M. J. 1998. Mathematical models for the apparent mass of the seated human body exposed to vertical vibration. *Journal of Sound and Vibration,* 212**,** 855-874.

WILFORD, M. 2001. An investigation into crowd-induced vertical dynamic loads using available measurements. *The Structural Engineer,* 79**,** 21-5.

WYATT, T. A. 1985. Floor excitation by rhythmic vertical jumping. *Engineering Structures,* 7**,** 208-210.

YAO, S., WRIGHT, J. R., PAVIC, A. & REYNOLDS, P. 2002. Forces generated when bouncing or jumping on a flexible structure. *ISMA International Conference on Noise and Vibration Engineering.* Katholieke Universiteit Leuven.

YAO, S., WRIGHT, J. R., PAVIC, A. & REYNOLDS, P. 2004. Experimental study of human-induced dynamic forces due to bouncing on a perceptibly moving structure. *Canadian Journal of Civil Engineering,* 31**,** 1109-1118.

YAO, S., WRIGHT, J. R., PAVIC, A. & REYNOLDS, P. 2006. Experimental study of human-induced dynamic forces due to jumping on a perceptibly moving structure. *Journal of Sound and Vibration,* 296**,** 150-165.

ZATSIORSKY, V. M., SELUYANOV, V. N. & CHUGUNOVA, L. G. 1990. The mass and inertia characteristics of the main segments of the human body. *In:* G., C. & S.A., R. (eds.) *Contemporary Problems of Biomechanics.* Massachusetts: CRC Press.

ZIVANOVIC, S., MCDONALD, M. G. & DANG, H. V. 2016. Characterising randomness in human actions on civil engineering structures *IMAC 2016.*

A. Appendix: Experimental Documents

<u>Project title</u>: Experimental Identification of Dynamic Forces Produced by Individuals and Groups
<u>Investigators</u>: Miss M G McDonald and Dr Stana Zivanovic

CONSENT & APPLICATION FORM

1. I, the undersigned, voluntarily agree to take part in the study above.
2. I have read and understood the *Project Information Sheet* dated 25/06/2012. I have been given a full explanation by the investigators of the nature, purpose, location, and likely duration of the study, and of what I will be expected to do. I have been given the opportunity to ask questions on all aspects of the study and have understood the advice and information provided. I am aware that I can take rest at any time during the study.
3. I have completed the *Physical Activity Readiness Questionnaire* and have been able to answer "NO" to all questions.
4. I agree to comply with any instructions given to me during the study and to co-operate fully with the investigators.
5. I understand that all personal data relating to volunteers are held and processed in the strictest confidence, and in accordance with the Data Protection Act (1998). I agree that I will not seek to restrict the use of the results of the study on the understanding that my anonymity is preserved.
6. I agree that photographs and video records in which I feature can be taken during experiments. I am aware that they will be used for the quality assurance and data analysis purposes only.
7. I do/do not (*delete as appropriate*) give permission for video records and photographs in which I feature to be used in seminars, publications, for conference presentations and in other forms of publicity of this research.
8. I would/would not (*delete as appropriate*) like to take part in experiments in which I will be blindfolded.
9. I would/would not (*delete as appropriate*) like to take part in experiments within a group.
10. I understand that I am free to withdraw from the study at any time without needing to justify my decision. I agree that in case of withdrawal the data that have already been collected can be used in the research.
11. I understand that the University of Warwick holds insurance that cover claims for injury or deterioration in health, which arise directly from participation in clinical trials, but that it applies only in those situations where the University can be shown to be legally liable.
12. I confirm that I have read and understood the information above and freely consent to participating in this study. I have been given adequate time to consider my participation and agree to comply with the instructions and restrictions of the study.

Details to be completed by applicant: Please **PRINT** clearly

Full name:		
Email address:	Contact no:	
Signature:.....Date:..... *For admin use only:*		TS#

University of Warwick

School of Engineering
Civil Research Group

Project title: **Experimental Identification of Dynamic Forces Produced by Individuals and Groups**

Investigators: Miss M G McDonald and Dr Stana Zivanovic

PHYSICAL ACTIVITY READINESS QUESTIONNAIRE

We are asking you to complete this questionnaire to check whether you are suited for the kind of physical activity you will be asked to engage in. The activity will not be physically strenuous and the levels of fitness we are looking for are normal levels. However, before you participate in any experiment we would like to identify a small number of people for whom even this level of activity might be inappropriate. To enable us to do this, we need you to answer the questions below.

Please read the following questions carefully and answer them to the best of your knowledge by ticking the appropriate boxes. This form will be kept securely by the investigators who will respect its confidentiality. The form will be shred no later than six months after completing the experiments.

	Yes (Initial)	No (Initial)
1. Has your doctor ever said you have a heart condition and recommended only medically supervised physical activity?		
2. Do you have chest pain brought on by physical activity?		
3. Have you developed chest pain within the last month?		
4. Do you lose consciousness or fall over as a result of dizziness?		
5. Do you have a difficulty in balancing whilst walking, jumping, bouncing, stamping?		
6. Has a doctor ever recommended medication for your blood pressure or a heart condition?		
7. Are you currently on any medication that could affect your health when exposed to physical activity?		
8. Are you aware, through your own experience or a doctor's advice, of any reason why you should not exercise without medical supervision?		
9. Have you consumed excessive amount of alcohol or any other substance in the last 24h that could compromise your balance and alertness?		
10. Has your doctor ever said you have a heart condition and recommended only medically supervised physical activity?		

I have completed this questionnaire truthfully to the best of my knowledge.

Signature:.....Date: .....

Name (BLOCK CAPITALS):.....

University of Warwick

School of Engineering
Civil Research Group

Project title: **Experimental Identification of Dynamic Forces Produced by Individuals and Groups**
Investigators: Miss M G McDonald and Dr Stana Zivanovic

PARTICIPANT DATA, To be filled in by the Investigator.

Coded name:		Age:	
Gender:	☐ Male ☐ Female	Preferred hand:	☐ Left ☐ Right
Height [m]:		Preferred leg (if known):	☐ Left ☐ Right
Body mass [kg]:		Preferred eye (if known):	☐ Left ☐ Right
Permission to use photos/videos granted:		Yes / No	
Participant agreed to take part in the tests involving blindfolding? *(Note: This info is for additional experiments which will run only if there are volunteers)*		Yes / No	
Participant agreed to take part in the tests in groups?		Yes / No	
Marker Positions			

Date:

Risk Assessment

Individual Jumping and Bobbing Experiments

Procedure

The experimental procedure is detailed in Chapter 5 and Chapter 6.

Risks and Control Measures

The expected risks and measures put in place to combat the risks are detailed in Table A.1.

Table A.1 The risk assement and control measures for the indivdual jumping and bobbing experiments.

Risk	Control measures
Trip hazards	The Gait lab was scouted for trip hazards and any loose cables were taped to the floor.
TS becoming dehydrated	Provide water if required and ensure the room temperature is appropriate.
TS's personal details being stolen	All paper copies of data relating to TSs are locked in a secure filing cabinet. Any electronic data is stored in a password protected area on a University desktop PC.
Fire	The TSs were made aware of the fire alarm procedure and the location of the nearest fire exit.

Group Synchronisation Experiments

Procedure

The experimental procedure is detailed in Chapter 7.

Risks and Control Measures

The additional expected risks, and measures put in place to combat the risks for the group synchronisation experiments are detailed in Table A.2 and were used in addition to Table A.1.

Table A.2 The risk assement and control measures for the group synchronisation experiments.

Risk	Control measures
TS becoming hot and dehydrated due to the number of TS involved	Use the air conditioning system to maintain an acceptable temperature and provide water when required.
TS bumping into one another	Allocate an adequate space allowance per TS which is marked out on the floor.
TS's personal details being stolen	All paper copies of data relating to TSs are locked in a secure filing cabinet. Any electronic data is stored in a password protected area on a University desktop PC.

B. Appendix: Response Graphs

The mean, 10th and 90th percentiles of maximum acceleration responses of SDOF structures excited by groups of 1, 2, 4 and 8 TSs jumping at different target frequencies.

Metronome Stimulus

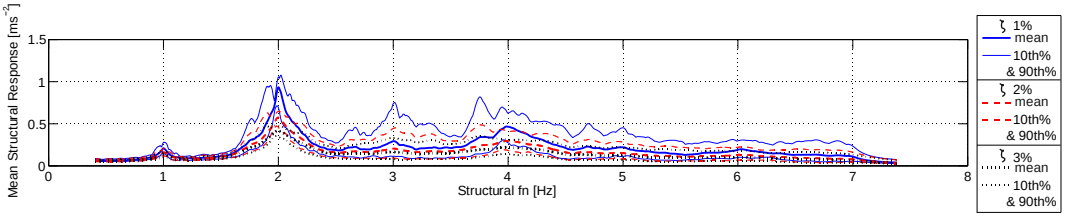

Figure B.1 Structural responses to 1TS jumping at 1Hz to a metronome.

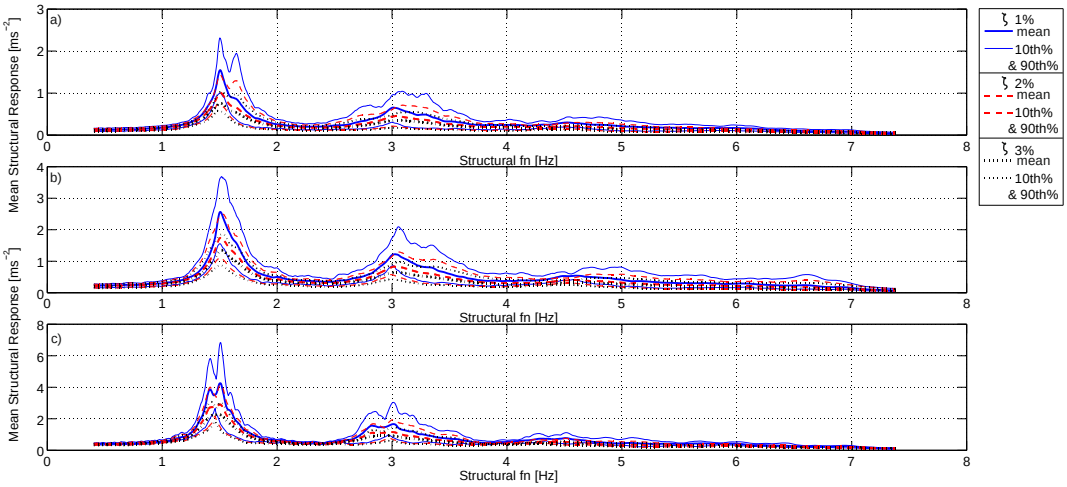

Figure B.2 Structural responses to a)2TSs, b) 4TSs and c) 8TSs jumping at 1.5Hz to a metronome.

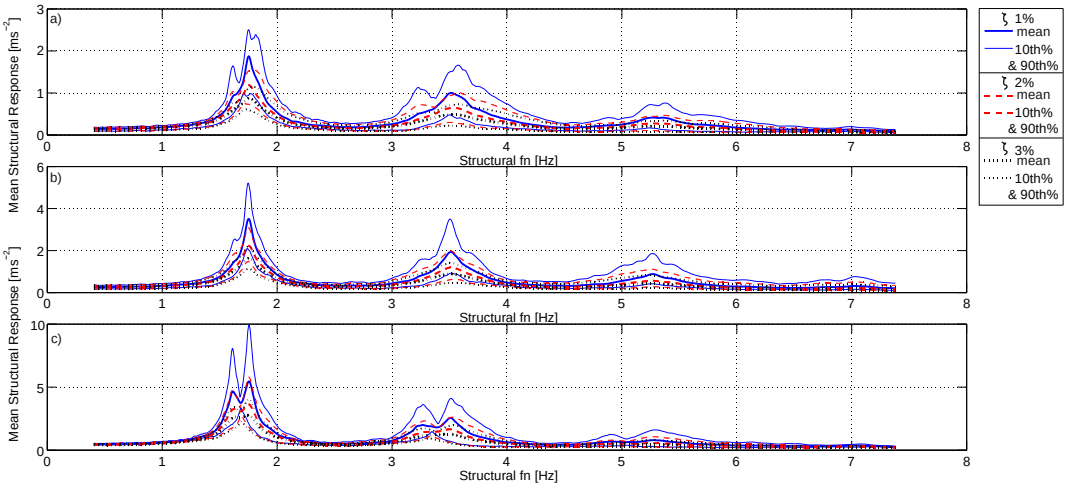

Figure B.3 Structural responses to a)2TSs, b) 4TSs and c) 8TSs jumping at 1.75Hz to a metronome.

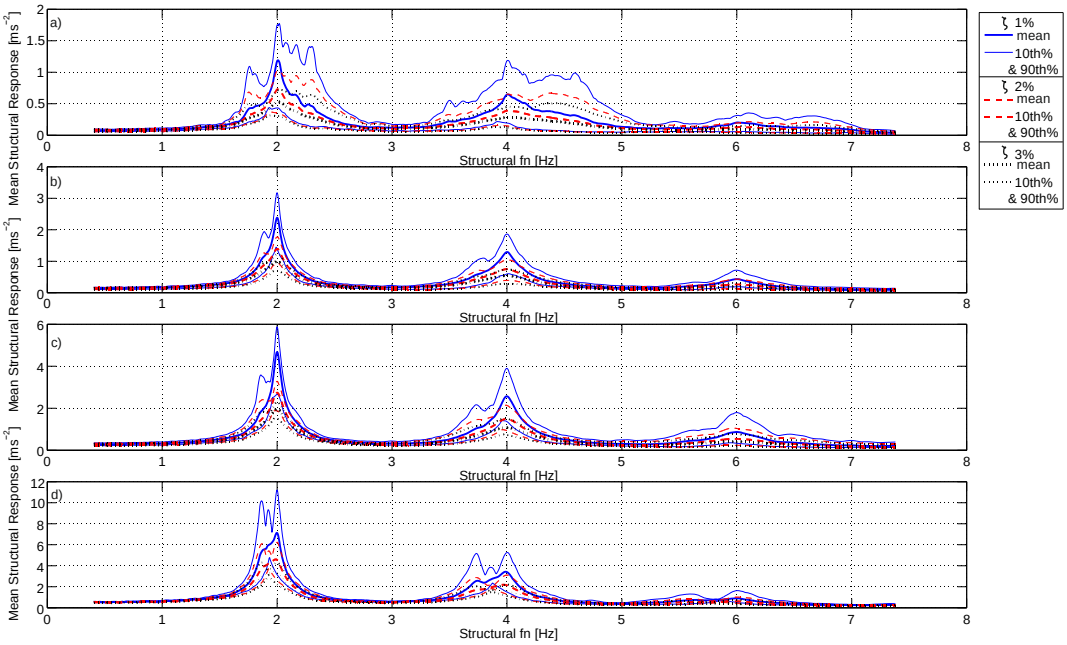

Figure B.4 Structural responses to a)1TS, b)2TSs, c) 4TSs and d) 8TSs jumping at 2Hz to a metronome.

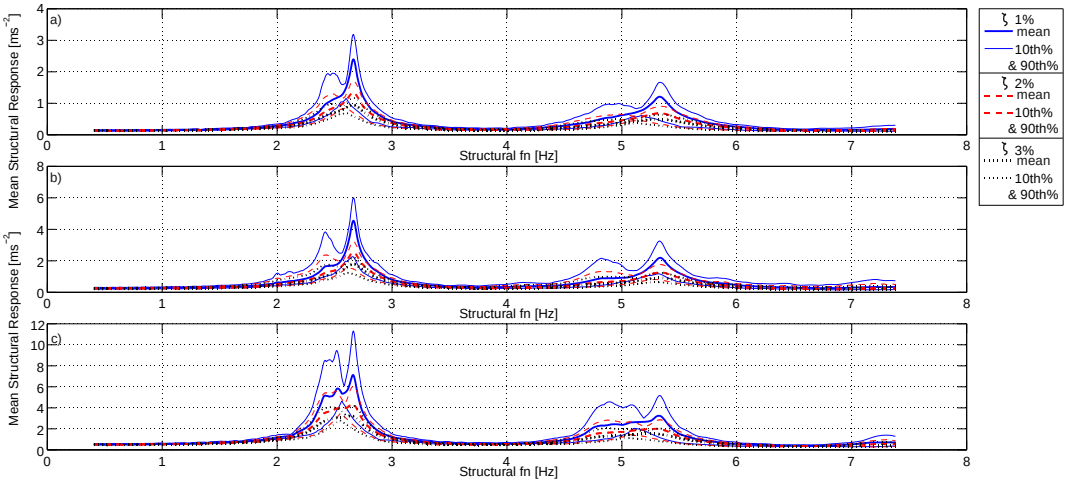

Figure B.5 Structural responses to a)2TSs, b) 4TSs and c) 8TSs jumping at 2.67Hz to a metronome.

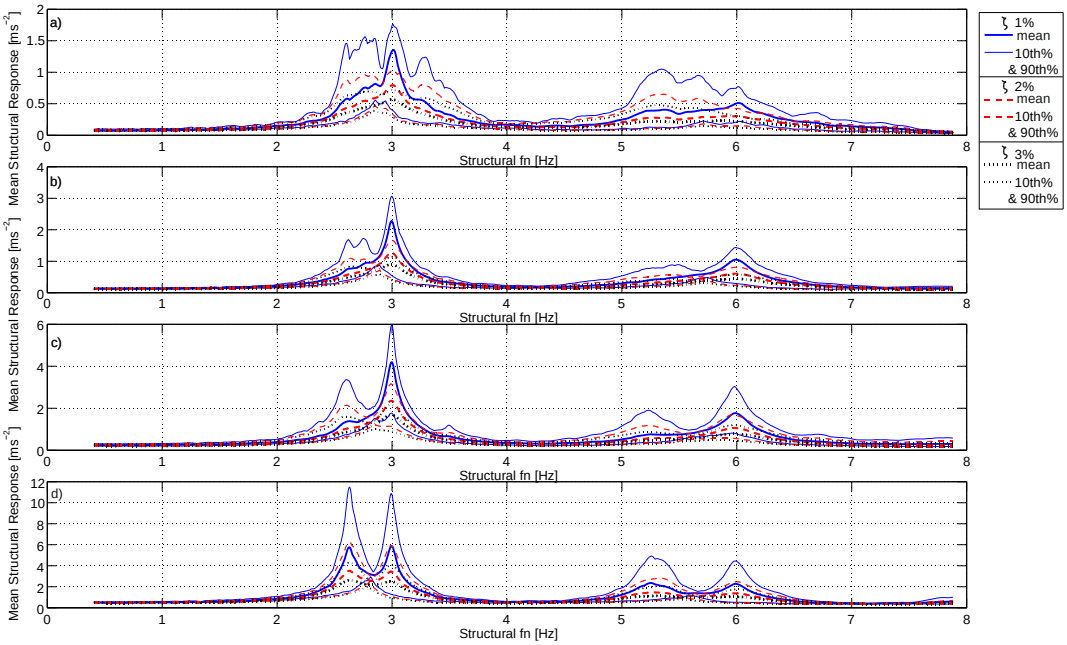

Figure B.6 Structural responses to a)1TS, b)2TSs, c) 4TSs and d) 8TSs jumping at 3Hz to a metronome.

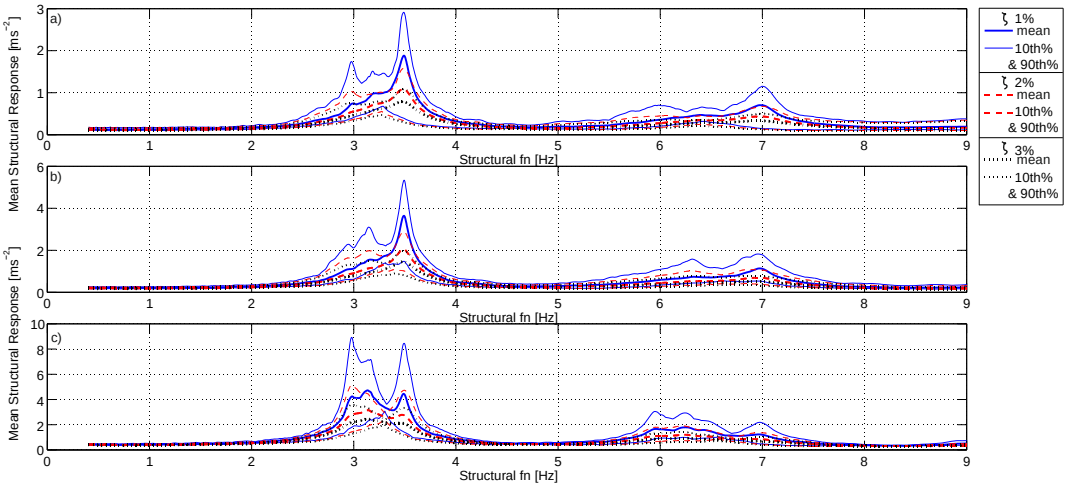

Figure B.7 Structural responses to a)2TSs, b) 4TSs and c) 8TSs jumping at 3.5Hz to a metronome.

Music Stimulus

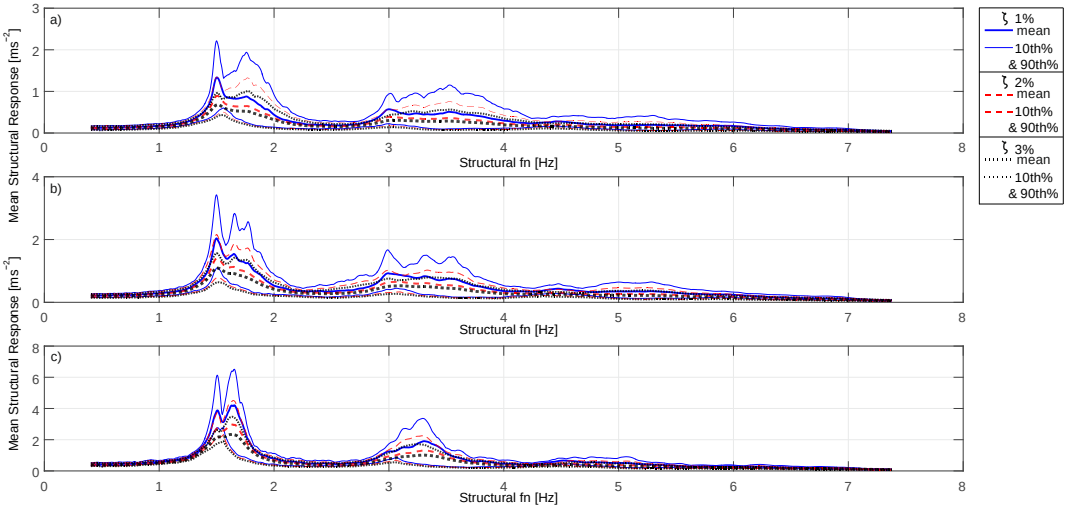

Figure B.8 Structural responses to a)2TSs, b) 4TSs and c) 8TSs jumping at 1.5Hz to music.

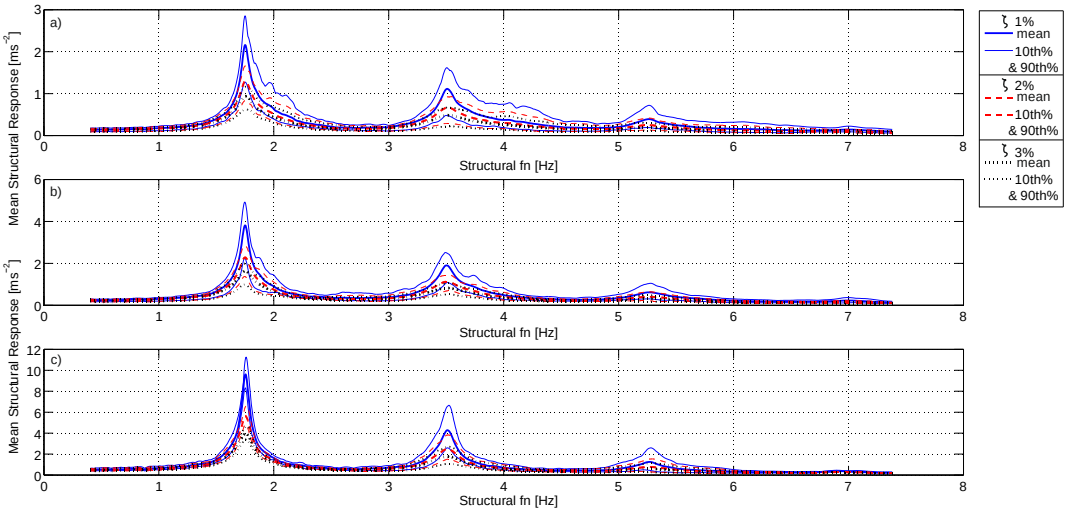

Figure B.9 Structural responses to a)2TSs, b) 4TSs and c) 8TSs jumping at 1.75Hz to music.

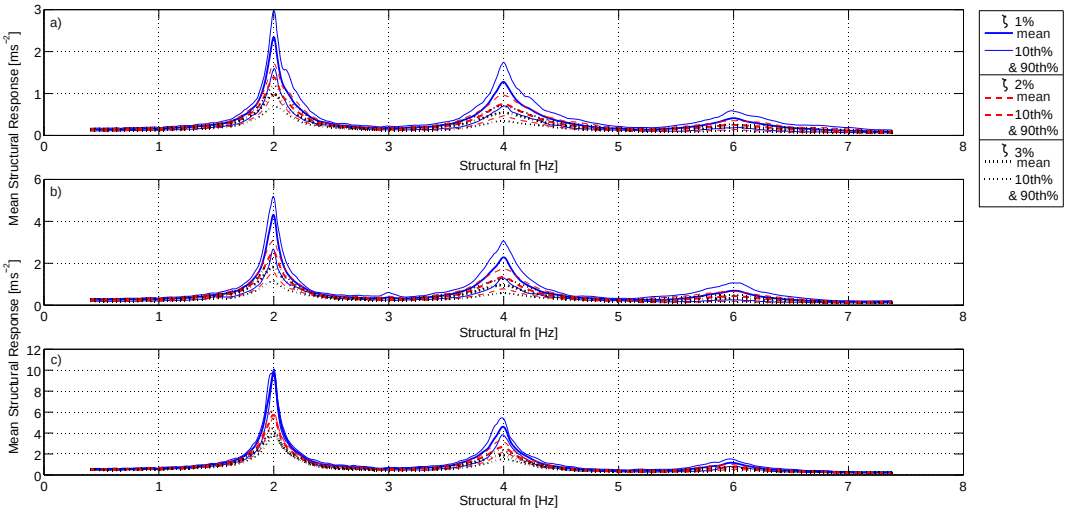

Figure B.10 Structural responses to a)2TSs, b) 4TSs and c) 8TSs jumping at 2Hz to music.

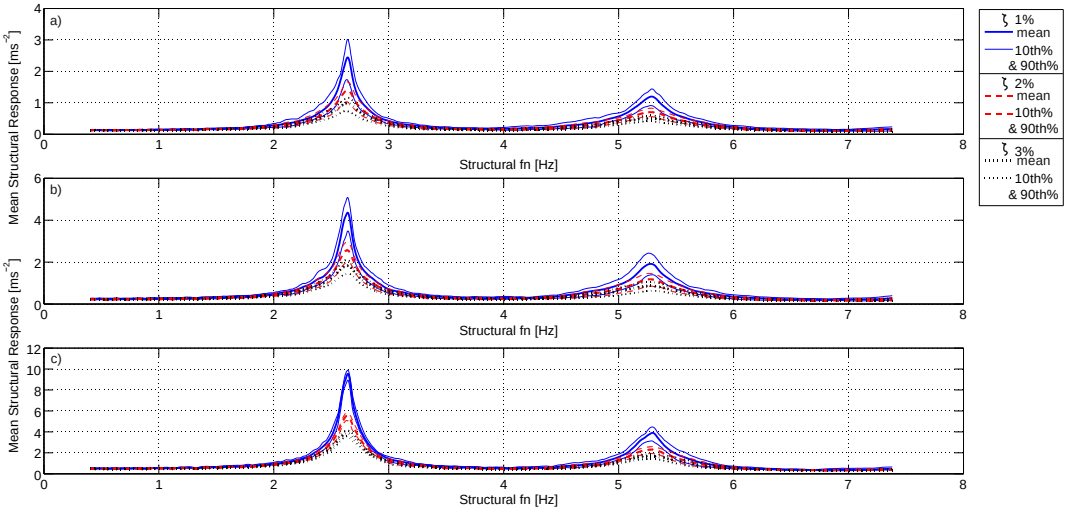

Figure B.11 Structural responses to a)2TSs, b) 4TSs and c) 8TSs jumping at 2.67Hz to music.

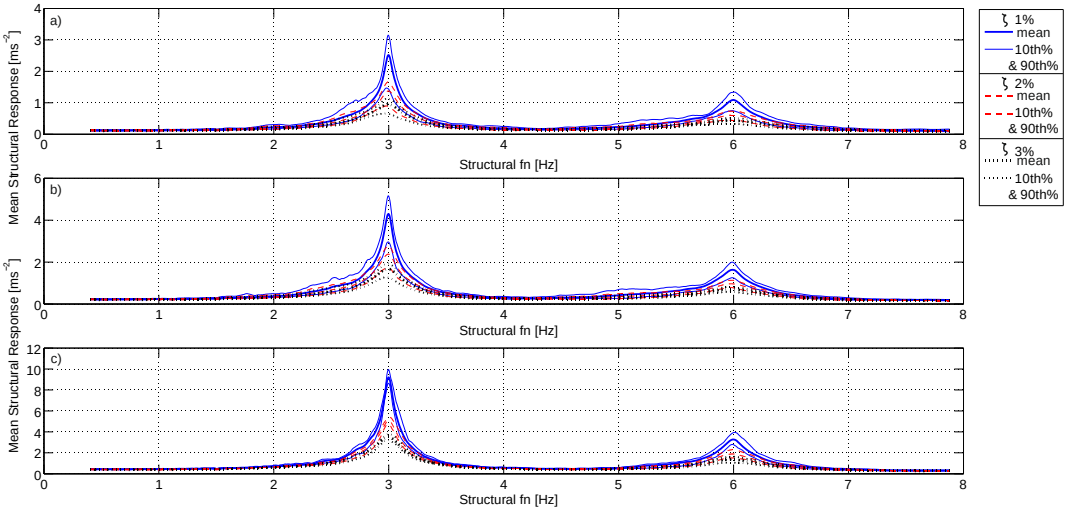

Figure B.12 Structural responses to a)2TSs, b) 4TSs and c) 8TSs jumping at 3Hz to music.

Visual Stimulus

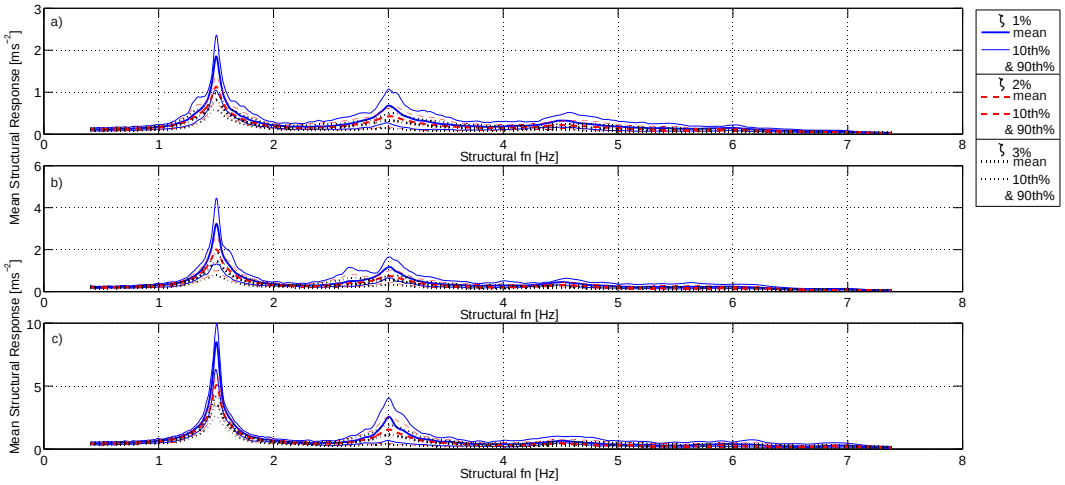

Figure B.13 Structural responses to a)2TSs, b) 4TSs and c) 8TSs jumping at 1.5Hz to visual stimulus.

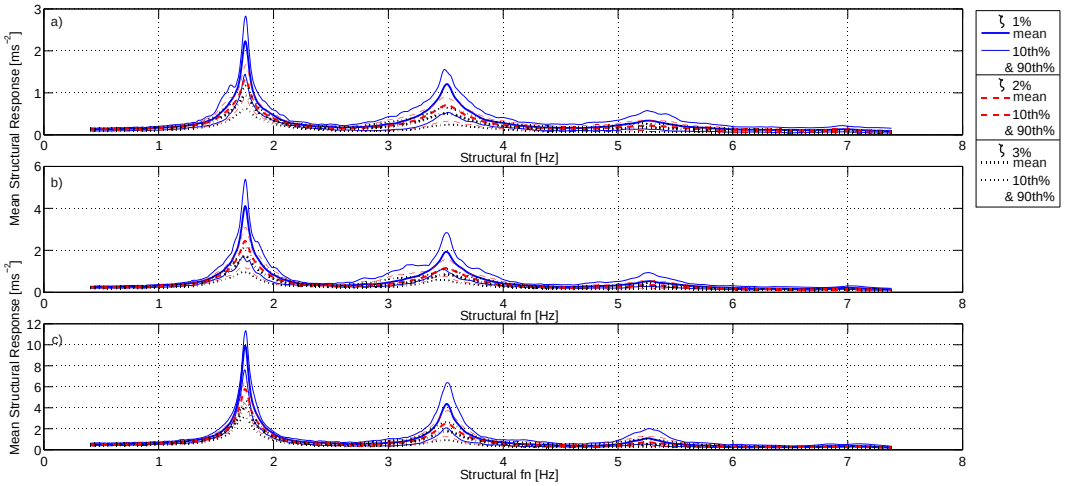

Figure B.14 Structural responses to a)2TSs, b) 4TSs and c) 8TSs jumping at 1.75Hz to visual stimulus.

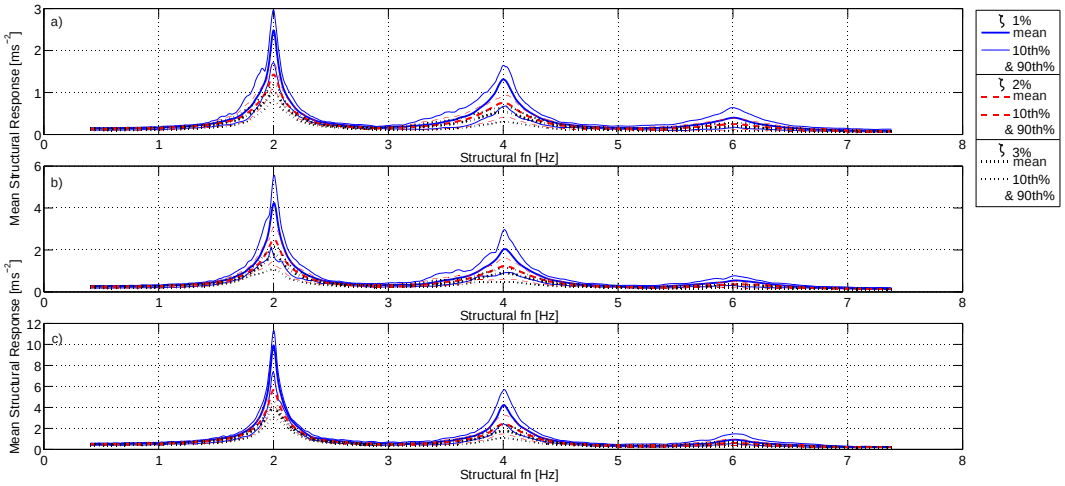

Figure B.15 Structural responses to a)2TSs, b) 4TSs and c) 8TSs jumping at 2Hz to visual stimulus.

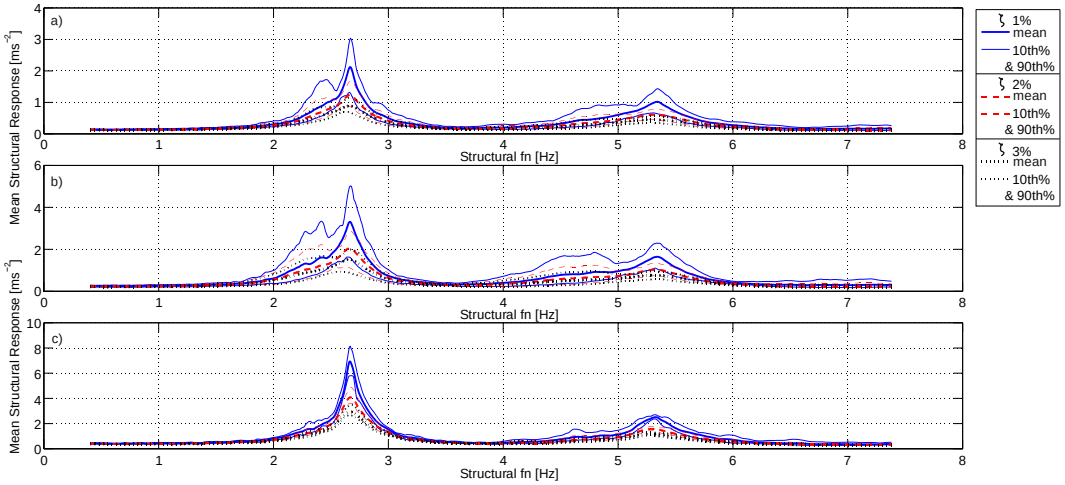

Figure B.16 Structural responses to a)2TSs, b) 4TSs and c) 8TSs jumping at 2.67Hz to visual stimulus.

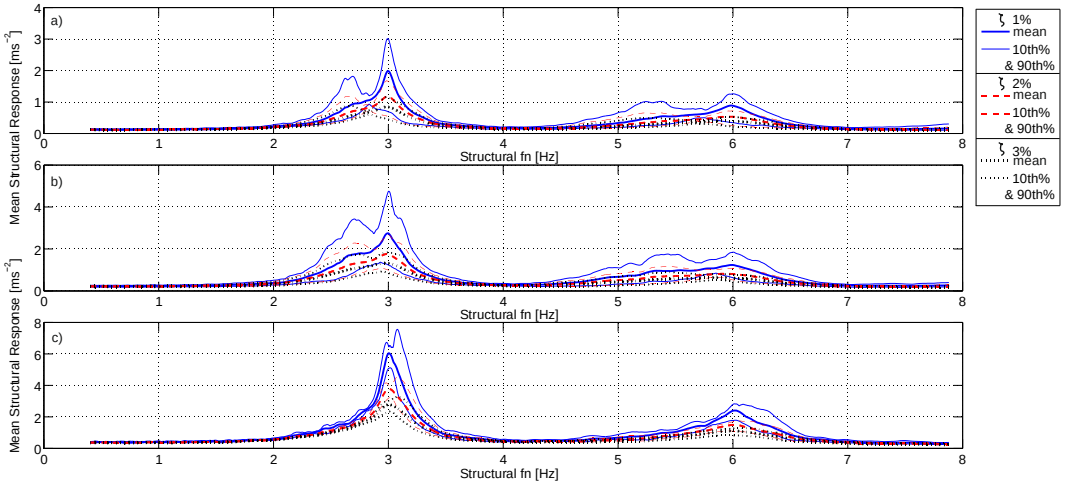

Figure B.17 Structural responses to a)2TSs, b) 4TSs and c) 8TSs jumping at 3Hz to visual stimulus.

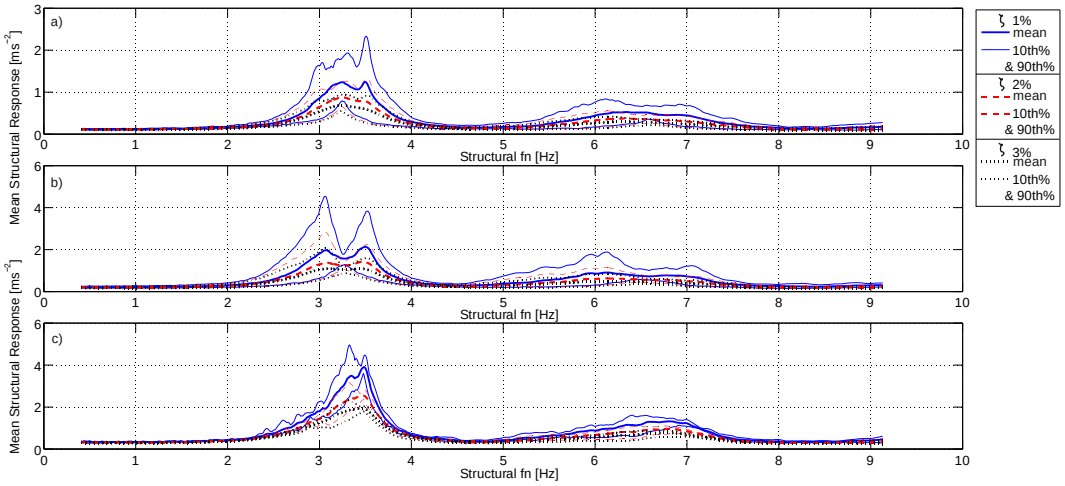

Figure B.18 Structural responses to a)2TSs, b) 4TSs and c) 8TSs jumping at 3.5Hz to visual stimulus.